DHI

Comprehensive Hydrological Study of the Lee County Southeastern Density Reduction / Groundwater Resource (DR/GR) Area

Final Report of the MIKE SHE Model Development and Results

Lee County – Division of Natural Resources
Ft. Myers, FL 33901

MIKE SHE

dynamic modelling system for integrated groundwater and surface water resources

September 2009

Comprehensive Hydrological Study of the Lee County Southeastern Density Reduction / Groundwater Resource (DR/GR) Area.
Final Report of the MIKE SHE Model Development and Results

100 Second Ave. South,
Suite 302 North
Saint Petersburg, FL 33701

Tel: (813) 831-4700
Fax: (813) 831-4774
e-mail: thz@dhi.us
Web: www.dhi.us

Client	Client's representative
Dover Kohl and Associates on behalf of Lee County	Jason King

Project	Project No
Lee County DR/GR Model Study	4021.604

Authors	Date
Marcelo Lago, PhD Kevin Vought, PE Tim Hazlett, PhD	September 10, 2009
	Approved by Tim Hazlett, PhD

Revision	Description	By	Checked	Approved	Date

Key words	Classification
Lee County Water Resources DR/GR Land use changes	☐ Open ☐ Internal ☒ Proprietary

Distribution	No of copies
Client DHI US	

Table of Contents

Acronyms and abbreviations

BC: Boundary condition
BCB: Big Cypress Basin
BLM: Base Line Model
DBHYDRO: South Florida Water Management District's corporate environmental database
DET: (spatially) distributed ET
DR/GR: Density Reduction/Groundwater Resources
DSS: Domestic self supply
ECM: Existing Conditions Model
ECWCD: East County Water Control District
EIC: Estero-Imperial River
ERP: Environmental Resource Permit
ET: Evapotranspiration
ETp: Potential Evapotranspiration
FAS: Floridan Aquifer System
FCM: Future Conditions Model
FCRB: Freshwater Caloosahatchee River Basin
FLUCCS: Florida Land Use, Land Cover Classification System
ft: feet
GSE: Ground surface elevation
IAS: Intermediate Aquifer System
ICA: Irrigation command area
KLECE: Kevin L. Erwin Consulting Ecologist, Inc.
LC: Lee County
LE: Lake evaporation
LIDAR: Light Detection and Ranging
LS: Local scale
MAE: Mean absolute error
ME: Mean error
MIKE 11: Hydraulic component in MIKE SHE
MIKE SHE: Dynamic modeling system for integrated groundwater and surface water
    resources
NEXRAD: Next-Generation Radar
NRD: Natural Resources Division
NSM: Natural System Model
PET: potential ET
PL: Performance level
R: Correlation coefficient
RET: reference ET
RMSE: Root mean square error
SAS: Surficial Aquifer System
SET: station-based ET
SFWMD: South Florida Water Management District

SWFFS: Southwest Florida Feasibility Study
TCRB: Tidal Caloosahatchee River Basin
USGS: United States Geological Survey
WTE: Water table elevation
WTP: Water treatment plant

List of Tables

List of Figures

Executive Summary

The Lee County Density Reduction/Groundwater Resource (DR/GR) Area was designated as an area of limited land development to protect sustainable ground-water resources. This study evaluates the effects of land use changes (*e.g.,* urban, agricultural, wetlands, mining, etc.) on the storage and availability of water resources in the area.

In order to understand how land use changes affect the water resource distribution, a comprehensive hydrologic model has been developed to simulate hydrologic and hydraulic conditions for several land use conditions. The MIKE SHE model, developed by DHI, integrates all major hydrologic processes such as rainfall, evapotranspiration (ET), surface water runoff, infiltration, ground-water recharge, ground-water flow, and surface flow through canals. MIKE SHE has been widely used by government agencies and local governments in Florida for water resource management studies and has been identified by Lee County as the best tool available for evaluating the effects of land use change on ground-water resources.

The goal of the Lee County MIKE SHE modeling is to provide the County with a valuable planning aid which quantifies the potential outcomes of water resource balancing efforts. Furthermore, the model results can serve as input for site-specific models for evaluating mining permit applications.

The general approach implemented for this study consisted of developing several MIKE SHE models that simulate the hydrologic and hydraulic response to different land use development conditions in the DR/GR area. The land use conditions evaluated are the conditions that exist today and several future land-use alternatives. A comparative analysis of the results from these models provides quantitative insights into the benefits or stresses caused by specific land use changes on Lee County's water resources.

The Existing Conditions Model (ECM) is a baseline model to which the results of land use alternatives are compared. This model was developed using the most current data available to represent the existing land use conditions. Two scales of models were developed: 1. a large sub-regional scale model covers the entire Lee County area and additional areas to the north, south, and east that are hydraulically connected to the County; and 2. a local-scale model at a higher resolution focusing on the DR/GR area.

Two versions of the ECM were developed as part of this study. The first version is an intermediate version that was immediately updated with more accurate data that became available following its completion. The second version is the update to version one, and serves as the baseline for comparison of land use alternatives.

Observation data for the Existing Conditions Model was obtained from the South Florida Water Management District (SFWMD), Lee County, and the USGS. Some of the initial model development originated from a previously developed MIKE SHE model of the

Southwest Florida Feasibility Study (SWFFS) area. Updates to the SWFFS model input data for the Lee County model include meteorological, land use, irrigation and ground-water withdrawal, and topography.

The Lee County Model represents all the major hydrologic processes in a fully integrated and spatially distributed manner. The surface water model includes an extensive network of primary and secondary canals with many hydraulic structures, natural sloughs, rivers, and lakes. The ground-water model includes the Water Table, Lower Tamiami, and Sandstone aquifers and the Bonita Springs Marl and Upper Peace River confining units. The model simulates distributed irrigation and ground-water withdrawals based on actual well locations and land use maps and estimated rates based on permit data and other information.

As part of the model development, considerable effort was spent improving the representation of certain important features in the model, such as the mining pits and flow ways in the DR/GR area. Furthermore, a number of model parameters, such as overland flow roughness coefficients, hydraulic conductivities and storage parameters of the geologic layers, and subsurface drainage parameters, were tested and varied in order to produce a closer match between model results to observed data.

As part of the calibration process, the Existing Conditions Model results were compared with measured ground-water and surface water data. Since this study focuses on ground-water resources in the DR/GR area, the calibration efforts were prioritized accordingly. Thus, the highest calibration priority was given to the ground-water stations south of the Caloosahatchee River.

The determination of wetland hydroperiods has been an important indicator used in this study. For this evaluation, wetland hydroperiod is defined as the period during which water is above the ground surface. The hydroperiod output of the model, together with the water table elevation and the water balance computation, provides useful insight into the impact of the land use changes on wetland areas.

In order to evaluate the hydrological effects of land use changes in the DR/GR area, four Future Conditions Models (FCMs) were developed. The results of these models were analyzed by using relative measures, such as differences in hydroperiod, water table elevations, and overall water budget.

A natural systems model (NSM) was constructed using the intermediate ECM. The revised topography changed the hydroperiod prediction significantly and the NSM based on that intermediate step was not accurate enough to be useful in the analyses presented in this final report. As such, hydroperiod maps developed by KLECE corresponding to years 1953 and 2007 were used to evaluate how the present developments in the DR/GR Area have affected the water resources, and to evaluate at what extent the model predictions for the future conditions scenarios are going to impact them in the direction of the historical conditions.

The future land use modeling scenarios consist of four alternatives in the DR/GR Area that were provided by Lee County. The land use changes consist of three types: creation of urban areas, expansion or creation of mining pits, and restoration of agricultural lands into wetlands:

- Land use alternative 1 (FCM1) is conceptually similar to Scenario 1 in "Prospects for Southeast Lee County" [Dover, Kohl & Partners, July 2008]. Mining would be limited to already-approved mining pits plus some new pits north of Alico Road near the airport (but with fewer pits than in Scenario 1). A broad westerly flow way to Corkscrew Swamp would be restored southward from the Imperial Marsh.

- Land use alternative 2 (FCM2) is conceptually similar to Scenario 2 in the Dover Kohl report. Mining would be limited to already-approved pits plus a major expansion to the Green Meadows Mine. A broad flow way to Corkscrew Swamp would be restored southward from the east end of Corkscrew Road in Lee County.

- Land use alternative 3 (FCM3) is conceptually similar to Scenario 3 in the Dover Kohl report. Mining would be limited to already-approved pits plus proposed new pits that were in the application process in September 2007, including pits along Corkscrew Road east of the Flint Pen Strand. Both flow ways to Corkscrew Swamp would be restored to whatever extent is still possible after significant portions of each were mined.

- Land use alternative 4 (FCM4) is conceptually similar to an alternative scenario that emerged favorably during public meetings after release of the Dover Kohl report. Mining would be limited to already-approved pits plus a moderate expansion to the Green Meadows Mine. Both flow ways to Corkscrew Swamp would be restored in full.

The extent of the restored areas in all scenarios is less than originally proposed in the Dover Kohl report but would still be a major long-term undertaking for which funding is not currently available. The new urban areas added in the future conditions land use map were exactly the same in all four alternatives. The increase of new mining areas from smallest to largest is: FCM1, FCM4, FCM2, and FCM3. The new mining areas in FCM3 are nearly double the amount of mining areas than in FCM1. The total amount of newly restored areas increases in the order FCM1, FCM2, FCM3 and FCM4.

All land use based parameters in the model were modified to correspond to the new land use types. The irrigation setup in the future conditions model was modified to reflect future land use changes. For example, irrigation areas were removed in areas where the land use was converted from urban or agricultural to mining or wetland areas. The well field configuration of the ECM remained the same in the FCMs, i.e., no wells were added or removed. The ground-water withdrawal rates for public water supply in the last year of available data were repeated for every year in the simulation period for the four future conditions scenarios. The domestic self-supply rates vary according to land use changes.

In order to evaluate the effects of land use changes in the water resources of the DR/GR area, various types of results were generated and compared between the ECM and four future conditions alternatives. Water table elevation maps were created for all land use alternatives for two times of the year: at the end of the dry season (end of May) and at the end of the wet season (end of September). Additionally, water table levels at specific locations (where changes in land use occur) were generated to observe the changes in fluctuations throughout the five-year simulation period. Water budget calculations were extracted for the entire DR/GR to determine which hydrologic components were affected by the different alternatives. Finally, hydroperiod maps and maps of the mean water depth during the hydroperiod were also produced.

From the perspective of water table elevation and hydroperiod, the different scenarios produce changes that in some cases are quite notably distinct from one FCM to another. All of the future condition scenarios show areas where the water level and hydroperiod would decrease with respect to the existing conditions in some areas, while increasing in others. Decreases represent potentially negative impacts to the wetland ecosystems in those areas. The cause of the lower water table level and hydroperiod is the flattening effect of proposed single large mining pits or the combined flattening effect from several mining pits that have a high hydrological connectivity (i.e. via the ground-water).

The model results from the different land use scenarios indicate several concepts that may be useful during the planning process.

- Wetland areas converted from agricultural areas in the future condition alternatives help to increase the water table elevations during the dry season and to extend the period of time that those areas are wet (hydroperiod).

- The conversion of natural and agricultural areas to urban development slightly lowers the water table during the wet season due to the new urban drainage system. The water table in the new urban areas is typically higher at the end of the dry season compared to the existing conditions, which is likely related to a reduction in the ET losses.

- The water budget in all mines and lakes around the DR/GR Area suggests that the annual net rainfall (rainfall minus evaporation) is about zero on average. This is a consequence of the open water evaporation rate, which is commonly higher than the annual ET rate in pre-mined conditions. The model also predicts that the drainage system around some mines produces a positive net surface water outflow from the mines. As a result, the aquifers need to supply water to the mining pits (negative net groundwater recharge) in about the amount that is lost through the drainage system.

- This modeling has indicated, in general, that the annual averaged ET rates from the DR/GR Area would be higher with greater areal coverage of mining pits. The surface water outflow rate (runoff) from the DR/GR Area was lower in all the scenarios compared to the ECM, which is likely related to the greater mining pit coverage.

These results are expected due to the higher ET losses and the lower runoff from mining pits and its effect on the surface water flow in neighboring areas.

- Mining pits cause a flattening in the water table that affects the pre-developed water table gradient. This often implies a decrease in the water table elevation on the up-gradient side of the pits and an increase on the down-gradient side. On the down gradient side, there may also be a decrease in some situations. The most pronounced flattening effect is seen towards the end of the dry season. This also has an effect on the hydroperiod by shortening the up-gradient hydroperiod and increasing (or sometimes also decreasing) the down-gradient hydroperiod. The flattening effect of mine development on the water table is larger in areas with steeper water table gradients, in larger mine pits, and in the case of a number of mining pits that are closer and therefore more hydrologically connected (i.e. via groundwater).

Water budgets, hydroperiod maps, and water elevation maps resulting from the modeling were analyzed for all four FCMs. These maps and numbers were compared to the local scale existing conditions model (LS ECM) results, and the scenarios were ranked according to their impact on natural areas in the DR/GR Area. This comparison revealed that scenarios with higher proportions of restored land areas than mining areas had less negative impact on the overall DR/GR Area. In cases where the areal extent of newly restored land area exceeded the areal extent of new mining areas, there was an overall benefit to the water resources in the DR/GR Area. The scenario that minimizes stress on the current water resources within the DR/GR Area is FCM4. This is followed, from second best to worst, by FCM1, FCM2, and FCM3.

Introduction

The Lee County Density Reduction/Groundwater Resource (DR/GR) Area was designated as an area of limited land development in an effort to provide a sustainable use of groundwater resources for the County. This study evaluates through the use of a computer model the effect of the land use changes (*e.g.,* urban, agricultural, wetlands, mining, etc.) on the storage and availability of water resources in the area. In order to understand how land use changes affect the water resources distribution, a comprehensive hydrologic model has been developed to simulate hydrologic and hydraulic conditions for several land use conditions. The MIKE SHE model, developed by DHI, is capable of fully integrating all major hydrological processes including: rainfall, evapotranspiration (ET), surface water runoff, infiltration, groundwater recharge, groundwater flow, and surface flow through canals. MIKE SHE has been widely used by government agencies and local governments in Florida for water resources management studies and has been identified by Lee County as a suitable tool for evaluating the effects of land use change on groundwater resources. The goal of the Lee County MIKE SHE modeling is to provide the County with a valuable planning tool which aides in the understanding of the potential outcomes of water resource balancing efforts. Furthermore, the model will generate results that may serve as input for site-specific models for evaluating permit applications.

The general approach implemented for this study consisted of developing several MIKE SHE models that describe the hydrologic and hydraulic response to different land use development conditions in the DR/GR Area. The models represent all the major hydrologic processes in a fully integrated and spatially distributed manner. The land use conditions evaluated are existing and several future alternatives. A comparative analysis of the results from these models is intended to provide a quantitative insight into the benefits or stresses caused by specific land use changes on Lee County's water resources.

This report describes the development and calibration of two Existing Conditions Models (ECMs), one regional (ECM) and one local scale (LS ECM), and the development of four Future Conditions Models (FCMs) based on the LS ECM.

Development of the LS ECM was a multi-step process. The ECM was developed first, which has a resolution of 1500 ft and contains the entire Lee County area. This model was used to extract the LS ECM for the DR/GR Area at a 750-ft resolution and to establish its boundary conditions. The calibration process had been completed early in the development of the LS ECM when much more accurate topographic data became available. The County decided it was in their best interest to utilize the high resolution topographic data to generate a more accurate model, which also included the redefinition of the flow ways. This initially calibrated intermediate step in the development of the final LS ECM is referred to in places as LS ECM V1 in the report. Details about the calibration process for this intermediate model can be found in Appendix J. Results from LS ECM V1 are presented in some discussions regarding the calibration of the final model to demonstrate the sensitivity of the model to the refined topography and flow ways, and to highlight the importance these improvements had in

the ultimate model performance. The final LS ECM is referred to in some graphs and figures as LS ECM V2, but it is otherwise referred to as LS ECM throughout the report.

Another significant change that was implemented in the LS ECM following the introduction of the high resolution topography in the model was the introduction of distributed evapotranspiration (ET) data instead of station based data. Similar to the occasional presentation of output from LS ECM V1, output from other intermediate model development steps is presented to show the sensitivity of the model to the distributed ET data.

This report is organized as follows. The data sources for the model are presented, as well as descriptions of how the data are used by the various model components. Plots that compare the observed data and ECM results for the DR/GR Area are included in the report. The changes in land use for the future scenarios are described in relation to the existing land use, as well as the components of the model that were altered to represent these changes. The final part of the report includes the results that show the effects of the land use changes, i.e., the hydrologic/hydraulic evaluation of the future condition scenarios. Finally, the limitations of the model are stated, as well as recommendations that may improve the accuracy of the results. Several appendices are included which provide more detailed results and additional information on the modeling.

Objectives

The main objective of this study is to quantitatively analyze the benefits or stresses caused by specific land use changes on Lee County's water resources to help the County during the planning process. The land use includes creating new urban areas, wetland areas and mining pits in the DR/GR Area. The effects are evaluated specifically on water balance components, water table elevations and hydroperiods. The study is expected to reveal generalities about the effect of the land use changes, and produce a ranking of the different future condition scenarios tested from a water resources perspective.

Existing Conditions Model

The Existing Conditions Model (ECM) is the base model to which the results of several land use alternatives will be compared. The model was developed using the most current data available to represent the existing land use conditions. The input data for the Existing Conditions Model was obtained from the South Florida Water Management District (SFWMD), the United States Geological Survey (USGS), and from Lee County. Two model scales were developed: 1. a larger scale 1500-ft grid model (ECM) that covers the entire Lee County area and additional areas to the north, south, and east that are hydraulically connected to the County; and 2. a local-scale model (LS ECM) that is a higher resolution model (750-ft grid) focused on the DR/GR Area. The purpose of the larger model is to generate representative boundary conditions at the sub-regional level for the local scale model. All the future land use alternatives were developed at the local scale level using the same boundary conditions and the LS ECM.

Baseline Model

Some of the initial model development originated from a previously developed MIKE SHE model of the Southwest Florida Feasibility Study (SWFFS) area. The SWFFS area consists of four major basins (Tidal Caloosahatchee River, Freshwater Caloosahatchee River, Estero River, and the Big Cypress Basin) and forms part of five counties (Charlotte, Glades, Lee, Henry, and Collier). Figure 1 shows the SWFFS model, ECM, and LS ECM areas. Since the SWFFS model simulates the period of 1995 to 1999, much of the data required updating for use in the Lee County Existing Conditions Model period of 9/1/2002 to 11/1/2007. The SWFFS model hydraulic features are limited to those critical canals, creeks, rivers and sloughs necessary to accurately route surface water flows at a regional scale. Thus, considerable hydraulic detail was added when developing the ECM and LS ECM from other modeling efforts at the sub-regional scale level within the SWFFS area.
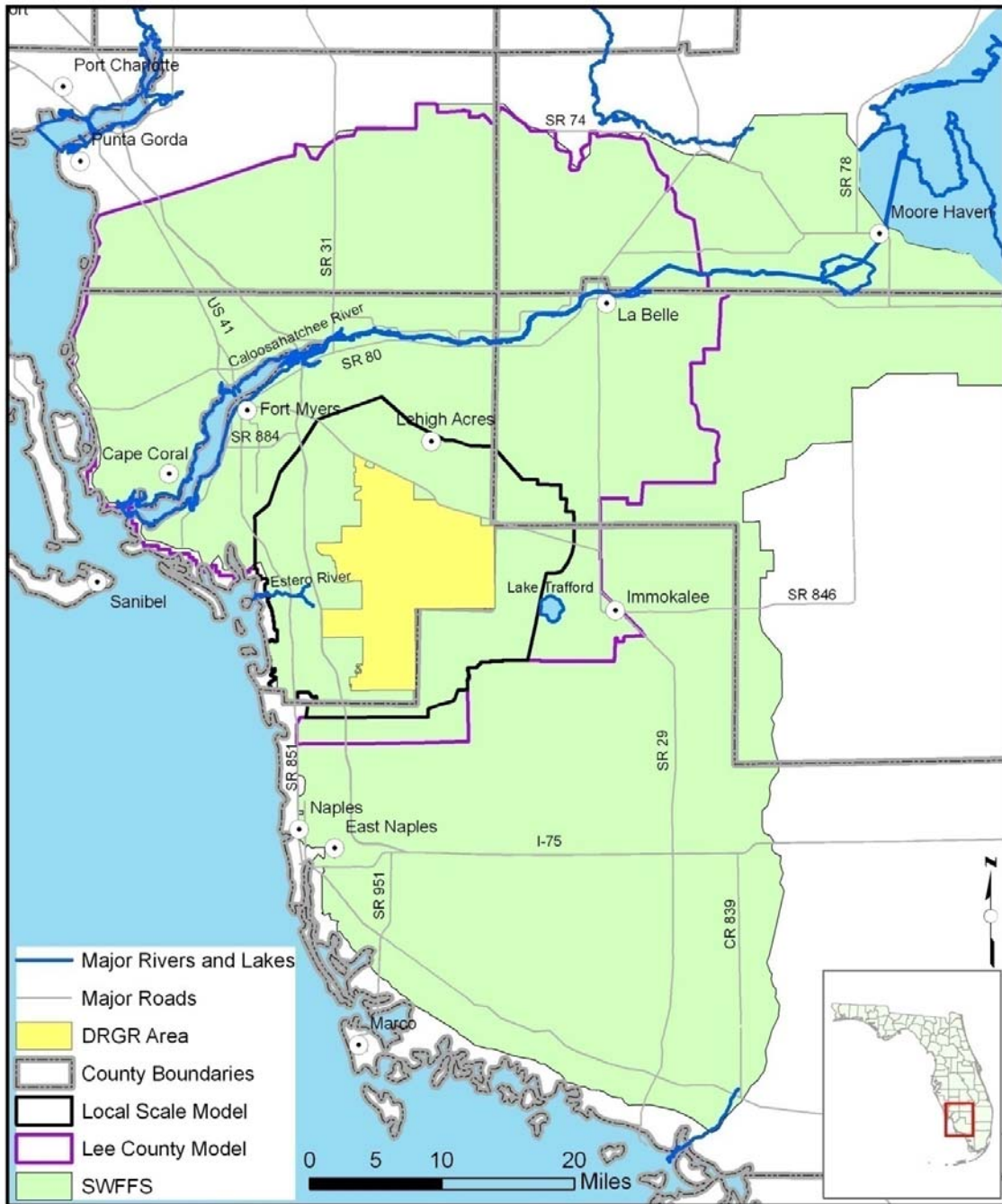
Figure 1. Model Domain Areas.

A preliminary comparison of the ECM and the SWFFS model was performed before any updates or improvements were made to the model. This preliminary model is referred to as Lee County Baseline Model (LCBLM). The differences between the SWFFS and the LCBLM are the size of the model domain, canals and structures added or modified from the

Estero-Imperial River (EIC), Big Cypress Basin (BCB), and Tidal Caloosahatchee River Basin (TCRB) sub-regional models, and the boundary conditions. Results of this comparison for two stations, one at Corkscrew and the other at Imperial River, are shown in **Figure 2**. The locations of these stations are shown in **Figure 3**. In general, both models produce similar results for stations within or close to the DR/GR Area. The differences between the simulated and the observed data are addressed during the development and the refinement of the existing conditions model (ECM). The modifications made to the ECM include: update of time-varying data for the period of 2002-2007, extension of the model area further to the south for better boundary representation, and improvements for better calibration performance.
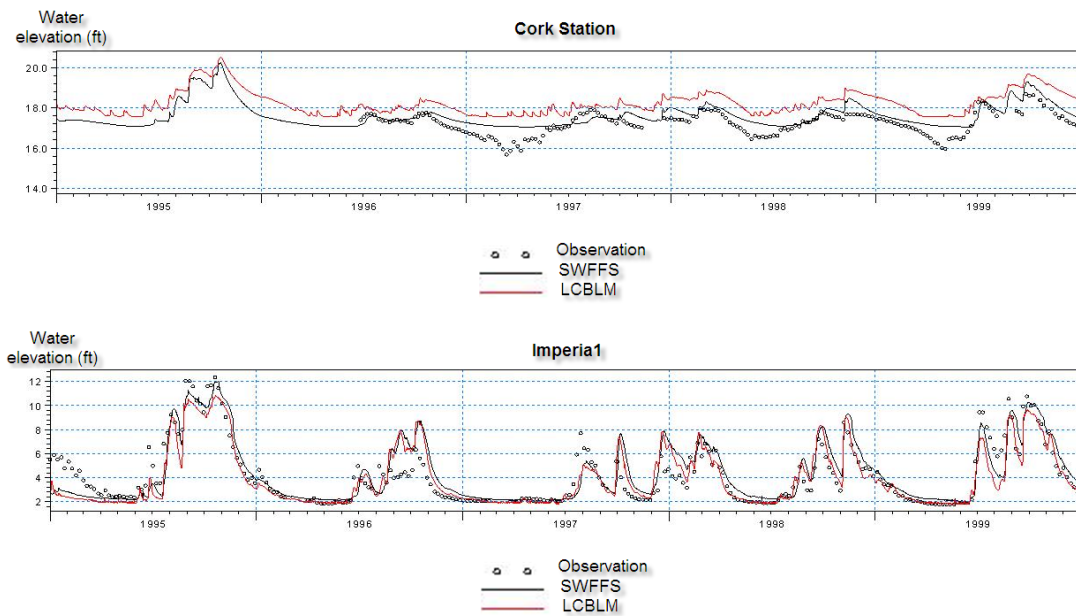
Figure 2. Comparison of the SWFFS model, LCBLM, and measured stages.
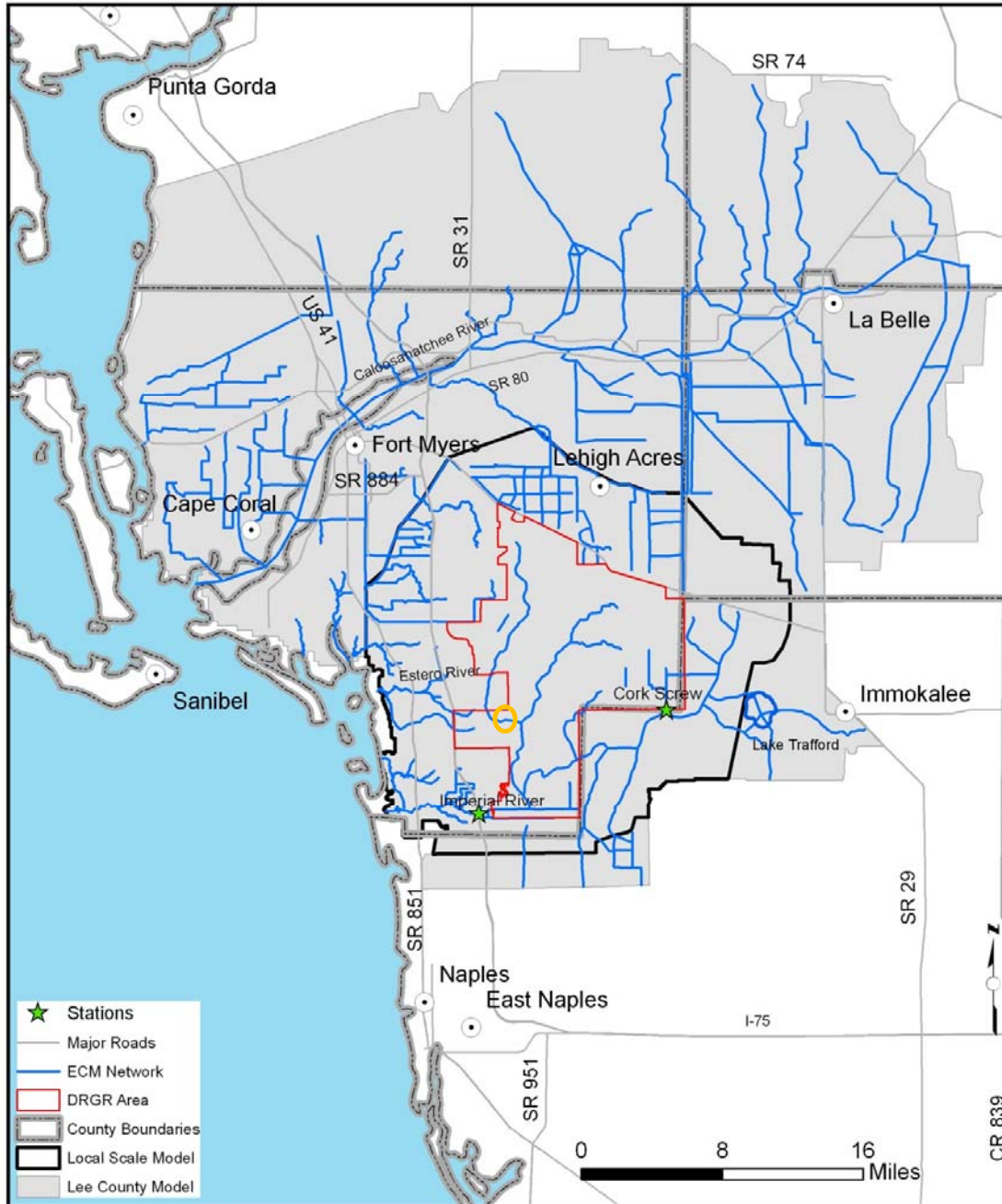
Figure 3. Location of stations that were used to compare SWFFS model to the LCBLM.
Note: the connection marked in the southern part of the DR/GR in the figure with the orange circle was adopted from the SWFFS model. However, as shown in the model results (Figure 40), there is not significant flow in that connection on a yearly averaged basis. The water flowing south from the western branch is diverted into the overland flow and collected by the branches that discharge in the Gulf of Mexico. This conceptualization of the surface water flow was improved in additional work described later in this report.

Local Scale Model

As previously mentioned, a Local Scale Existing Conditions Model (LS ECM) was derived from the Lee County ECM. The purpose of the LS ECM is to zoom into the DR/GR Area at a higher resolution. The LS ECM domain area is shown in previous figures. It covers a somewhat larger extent than the DR/GR Area (approximately 2-6 miles of surrounding area) in order to include all the features modified in future conditions scenarios and to avoid boundary condition effects. The LS ECM has a grid cell size of 750 feet, which is half the size of the original ECM grid size. The total number of grid cells remains approximately the same in both models. The vertical resolution was also increased by splitting the computational layer 3 in the ECM into 2 computational layers. Thus, the LS ECM has four computational layers in total.

The river network for the LS ECM was initially obtained from the ECM network portion that is in the local scale model boundary. A constant head boundary condition is applied by using the time series stage results of the ECM. The time series water levels applied as boundary conditions for the groundwater layers are also extracted from the ECM.

While the initial river network was obtained from the ECM, several significant modifications to the network were made. These modifications are discussed in detail in the Surface Water Model section. Other modifications made to the LS ECM are included in following sections.

The changes introduced in the local scale model make the use of initial conditions extracted from the ECM inappropriate. Thus, a preliminary run of the LS ECM was performed in order to extract the initial conditions from the model results. The model was then initialized using the results of September 1st, 2004 from the previous run. The LS ECM simulation period is from September 1st, 2001 to November 1st 2007.

Climate Data

The climate data input to the model consists of rainfall and potential evapotranspiration data.

Rainfall

The rainfall input data was obtained from high resolution radar (NEXRAD) data. The SFWMD provided 15-minute radar rainfall data sets from January 2002 to October 2007. This data set has a spatial resolution of approximately 1.9 km (1.2 miles). The radar rainfall grid in the model domain area is shown in **Figure 4**. Individual time series data for the period from 2005 to 2007 were also provided to correct the data values for some of the pixels.

During the NEXRAD processing, the original data was replaced with the corrected values for the specified pixel locations. The 15-min data was added to obtain daily rainfall values. Finally, the ASCII data was converted to a time varying dfs2 file, the two-dimensional grid format of MIKE SHE. The resulting dfs2 file has a spatial resolution of 1,500 ft and covers the ECM domain area.

The NEXRAD rainfall data was compared to rainfall gage data located around the DR/GR Area. The locations of the stations with available rainfall data in DBHYDRO are also shown on Figure 4. Total daily radar data does not exactly match the daily values measured at the observation stations. The differences are reasonable because the two data sets have a different error range and represent different spatial extents, i.e., radar rainfall data are spatial averaged values from indirect estimations and station data are more exact measurements at a specific location. Thus, the higher error in NEXRAD rainfall data estimation is compensated by capturing the high spatial variability of the rainfall, which is critical when the distance between rainfall stations is large.
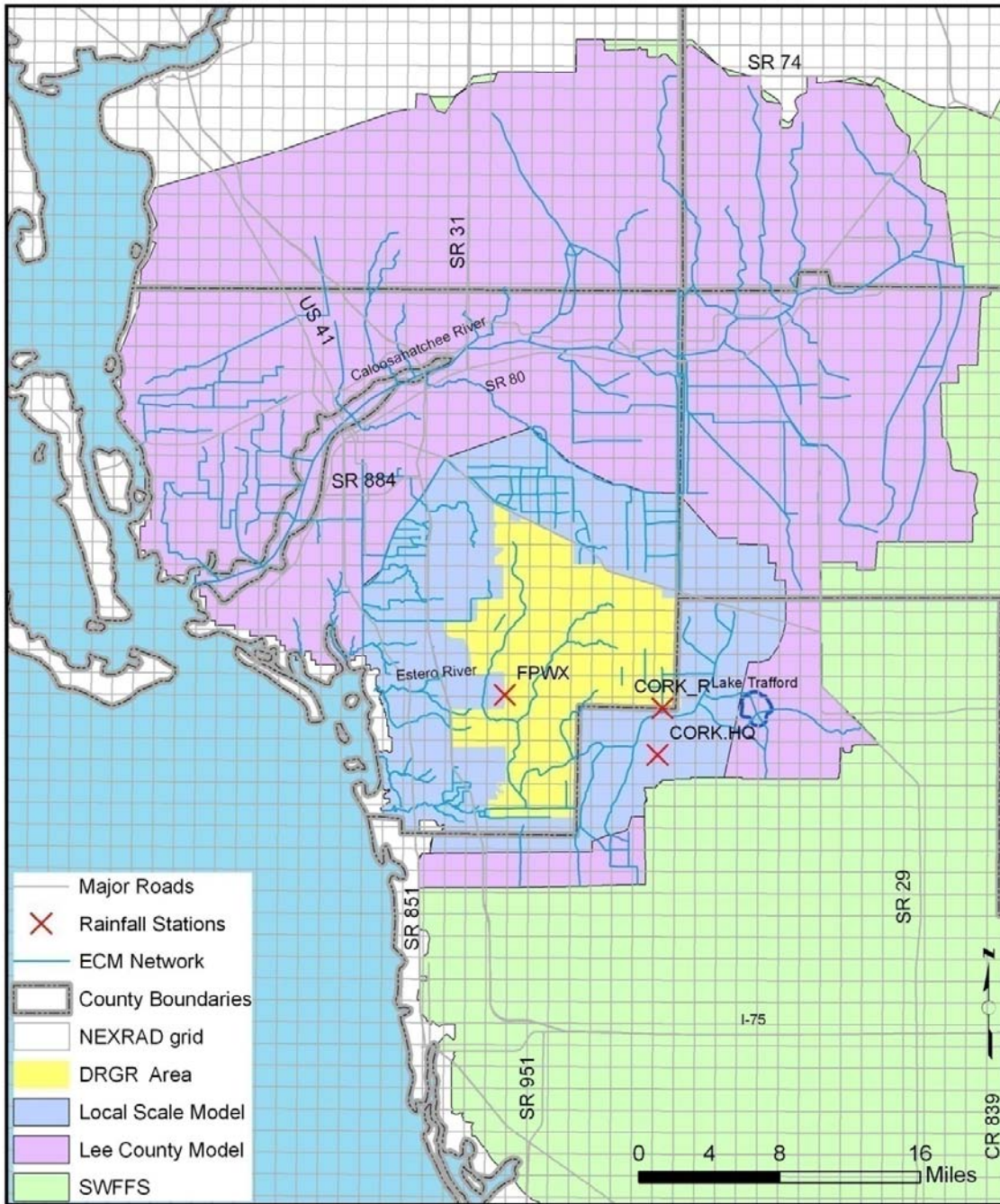
Figure 4. Rainfall Stations and NEXRAD Grid.

The differences between NEXRAD and station data sets decrease as the daily values are averaged over a longer period. The relatively good match between monthly cumulative rainfall values from both methods is shown in **Figure 5** at the CORK.HQ station.
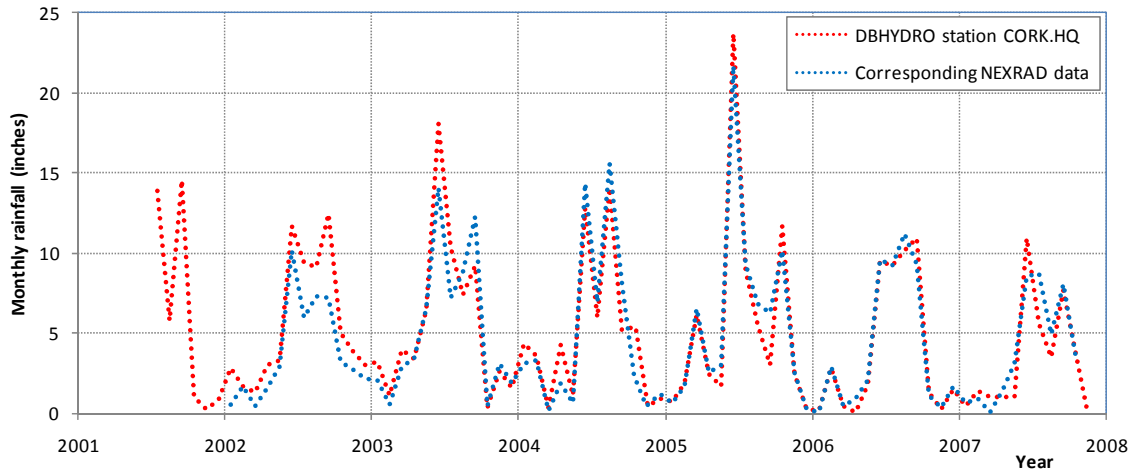
Figure 5. Comparison of monthly values between the daily rainfall of a DBHYDRO station and the radar rainfall data at the same location.

Evapotranspiration

The following sections discuss how this and other ET parameters were used in the ECM and the LS ECM.

Evapotranspiration in the ECM

The SFWMD defines potential evapotranspiration (ETp) as "actual evaporation for lakes, wetlands, and any feature that is wet year-round" (Abtew, 2005). It uses the following equation to estimate ETp rates:

$$ET = K_1 \frac{Rs}{\lambda}$$

where ET is daily evapotranspiration from wetland or shallow open water (mm/d), Rs is solar radiation (MJ/m^2·d), λ is the latent heat of vaporization (MJ/kg), and K_1 is an empirical coefficient equal to 0.53 mm·m^2/kg (Abtew, 2005).

ETp is a time-varying and spatially distributed input to the MIKE SHE model, like rainfall.

Potential ET rate data from three stations within or near Lee County were extracted from the SFWMD DBHYDRO database. The station data period and locations are presented in **Table 1**. The observed daily ET rates were distributed across the model domain by using a

Thiessen polygon network, as shown in **Figure 6**. A more refined distributed ET was used in the LS ECM as described in the next section.

Table 1. DBHYDRO stations with potential ET data for the ECM.

Dbkey	Station	Start Date	End Date	County
OH520	FPWX	1-Jan-01	31-Dec-07	LEE
RW483	S78W	22-Oct-92	31-Dec-07	GLA
RW482	SILVER	6-Dec-00	31-Dec-07	COL

In MIKE SHE, actual evapotranspiration (ETa) is calculated for every cell of the model using several factors. The calculation of ETa uses meteorological and vegetative data to predict the total evapotranspiration and net rainfall after interception of rainfall by the canopy, drainage from the canopy to the soil surface, evaporation from the canopy surface, evaporation from the soil surface, and transpiration, based on soil moisture in the unsaturated root zone (DHI 2008).

The ET processes are split up and modeled in the following order (DHI 2008):

1. a proportion of the rainfall is intercepted by the vegetation canopy, from which part of the water evaporates;
2. the remaining water reaches the soil surface, producing either surface water runoff or percolating to the unsaturated zone;
3. part of the water standing on the soil surface is evaporated;
4. part of the infiltrating water is evaporated from the upper part of the root zone or transpired by the plant roots; and
5. the remainder of the infiltrating water recharges the groundwater in the saturated zone.
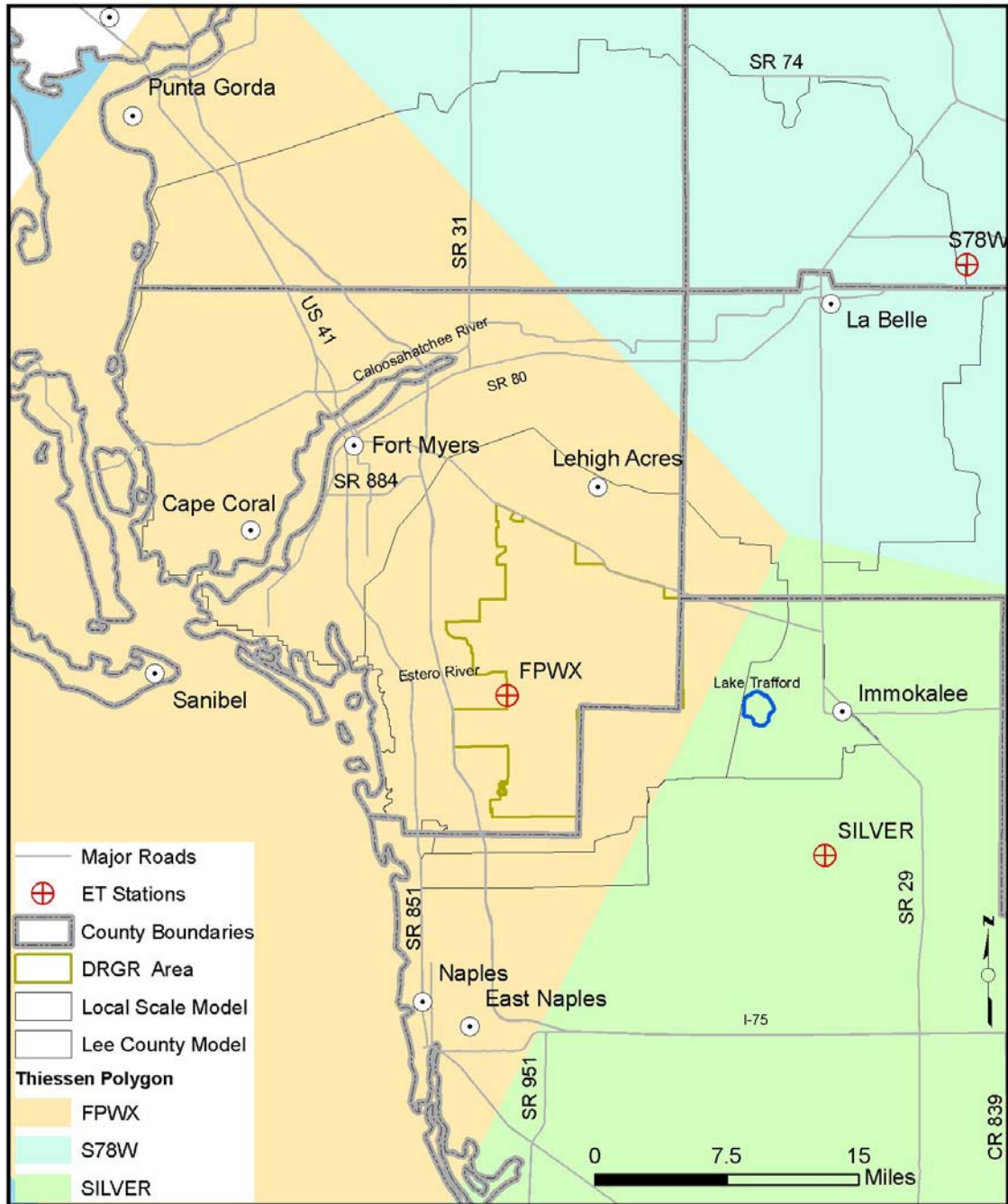
Figure 6. Potential Evapotranspiration Stations and Thiessen Polygons.

The ET parameters were divided into two groups: one for land use independent parameters (see **Table 2**) and the other for land use dependent parameters (see **Table 3**) such as leaf area index (LAI) and root depth (Rd).

Table 2. Constant ET Parameters.

Parameter	value
Canopy interception storage capacity	5 mm
Growth cycle	one year
Crop coefficient (Kc)	1
empirical parameter C1	0.2
Kristensen and Jensen empirical parameter C2	0.3
Kristensen and Jensen empirical parameter C3	20 mm/day
Kristensen and Jensen Root mass distribution parameter (Aroot)	0.25 m^{-1}

Table 3. Land use dependent ET Parameters.

Land Use/Vegetation	LAI	Rd (m)
Citrus	4.5	1.25
Pasture	3 - 4	0.75
Sugar Cane & Sod	1 - 6	0.5 – 1.5
Truck (Row) Crops	1.5 – 4.5	0.15 – 0.75
Golf Course	3	0.75
Bare Ground	0	0
Mesic Flatwood	1.5 - 3	1.219
Mesic Hammock	2.5 - 4	1.219
Xeric Flatwood	1 - 2	1.219
Xeric Hammock	2 - 3	1.219
Hydric Flatwood	1.5 - 3	1.219
Hydric Hammock	2.5 - 4	1.219
Wet Prairie	1.5 - 3	0.75
Dwarf Cypress	1 - 2	0.75
Marsh	2 - 4	0.75
Cypress	2 - 4	1.524
Swamp Forest	3 - 5	1.524
Mangrove	3 - 4	1.824
Water	4	2.3
Urban Low Density	2.5	0.6
Urban Medium Density	2	0.6
Urban High Density	2	0.5

Note: LAI = Leaf Area Index, Rd = root depth

Refined Evapotranspiration in the LS ECM

The USGS recently released spatially distributed ET data for the same 2-km grid as the rainfall distributed data introduced in the model (see grid in **Figure 7**), so this was used to define the ET rates for the model.
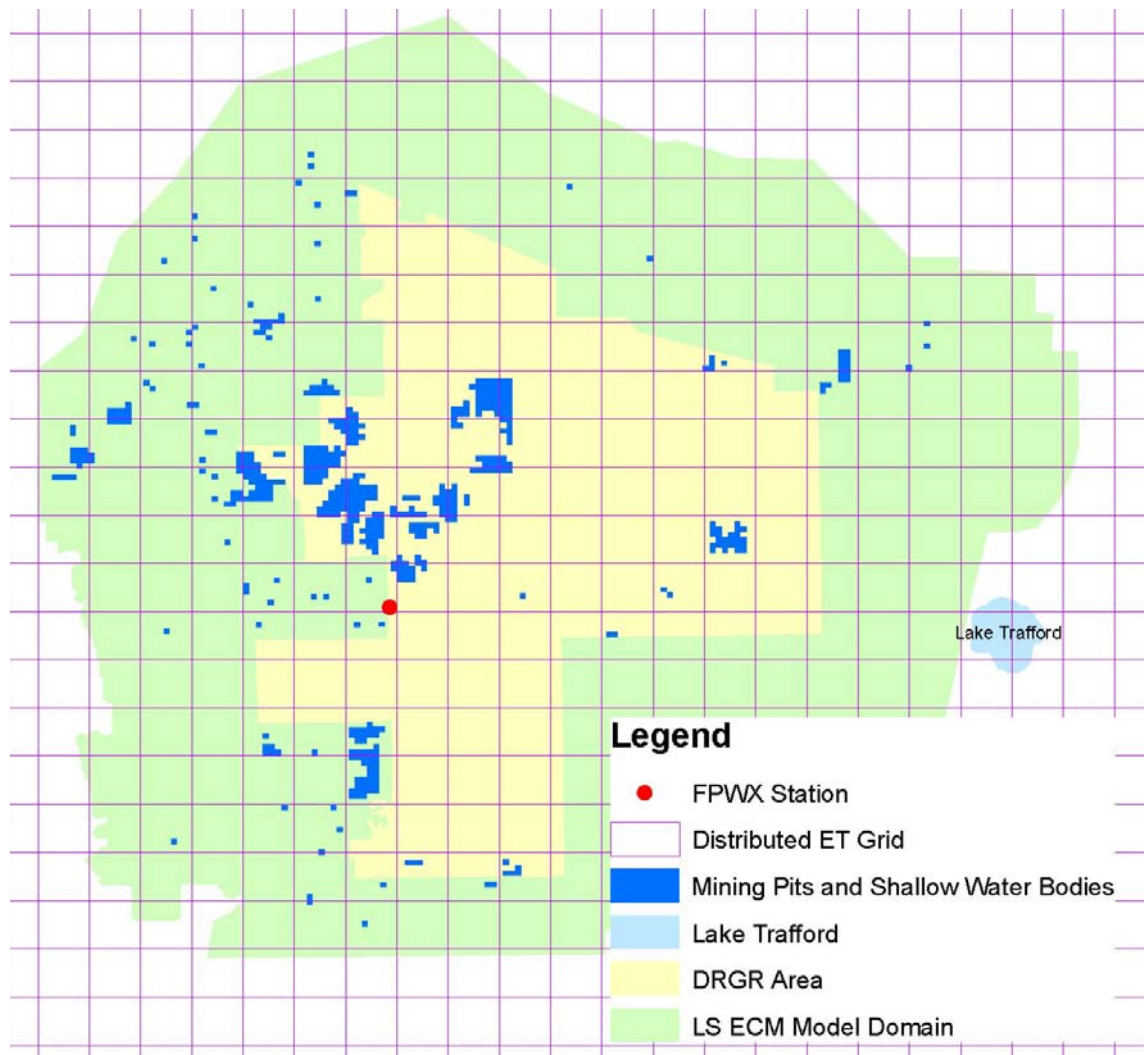
Figure 7. Distributed ET grid around the model domain area.

The distributed ET data may have uncertainties since air temperature, relative humidity, and wind speed are interpolated from weather stations [D. Sumner, USGS, personal communication]. The comparison of the distributed ET data and the ET data at station FPWX is presented in Appendix E. The RET approximately reproduce the ET station data on a daily and annual basis.

The value of RET + 8.2% was found to provide the best estimate for the lake evaporation in mining pits and other shallow water bodies in the model domain. Additional details are provided in Appendix E. The lake evaporation is considered in the model by assigning a crop coefficient (Kc) of 1.082 in the land use classified as water.

The actual evapotranspiration (ETa) is calculated for every cell of the model in the same manor as for the ECM.

The ET parameters were divided into two groups: one for land use independent parameters (see Table 2) and the other for land use dependent parameters (see **Table 4**) such as leaf area index (LAI) and root depth (Rd). Numbers in bold in Table 4 were modified in the LS ECM compared to those used in the ECM.

Table 4. Land use dependent ET Parameters.

Land Use/Vegetation	LAI	Rd (m)
Citrus	4.5	1.25
Pasture	3 - 4	0.75
Sugar Cane & Sod	1 - 6	0.5 – 1.5
Truck (Row) Crops	1.5 – 4.5	0.15 – 0.75
Golf Course	3	0.75
Bare Ground	0	**100**
Mesic Flatwood	1.5 - 3	1.219
Mesic Hammock	2.5 - 4	1.219
Xeric Flatwood	1 - 2	1.219
Xeric Hammock	2 - 3	1.219
Hydric Flatwood	1.5 - 3	1.219
Hydric Hammock	2.5 - 4	1.219
Wet Prairie	1.5 - 3	0.75
Dwarf Cypress	1 - 2	0.75
Marsh	2 - 4	0.75
Cypress	2 - 4	1.524
Swamp Forest	3 - 5	1.524
Mangrove	3 - 4	1.824
Water	**0**	2.3
Urban Low Density	2.5	0.6
Urban Medium Density	2	0.6
Urban High Density	2	0.5

Note: LAI = Leaf Area Index, Rd = root depth

Topography

The topography data was obtained from the SFWMD Composite Topography Dataset (SWFFS 2005). This dataset has a cell size of 100 feet and it covers the Lower West Coast part of the South Florida Water Management District. It is composited from multiple sources, which include LIDAR (Light Detection and Ranging) data, aerial/photogrammetric data, and USGS contour and spot-elevation data. This dataset was also used in the SWFFS model. The topography data provided by Lee County does not cover the entire model domain, but it matched the SFWMD when both datasets were overlaid. The original 100-ft raster data was resampled by averaging the elevation values to a 750 ft grid and then converted to a dfs2 file for use in the ECM. The resulting map is displayed in **Figure 8**. This topographic map, however, does not contain the bathymetry of mine pits and other water bodies. These features were incorporated into the topographic map during the model development.
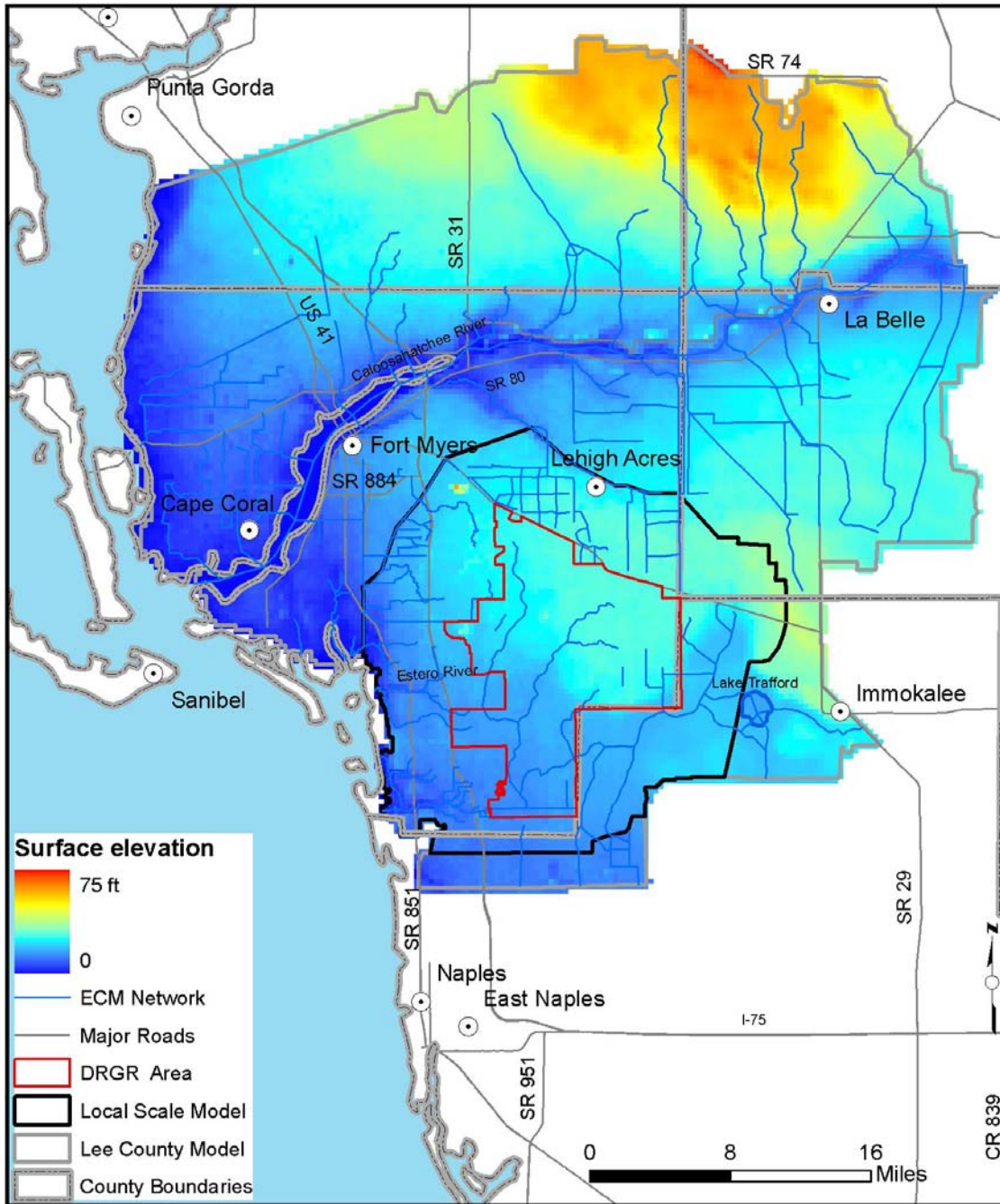
Figure 8. Model Topography in ECM.

Refined Model Topography For LS ECM

New LIDAR topographic data was flown in 2007 and became available in 2009. This updated topographic data was incorporated into the model after calibration of the first version had been completed. The County's goal in undertaking this update was to improve the accuracy of the model.

The 2007 LIDAR topographic data set was delivered by Lee County in a raster format with a grid size resolution of 5 ft by 5 ft. The data covers only Lee County and it was not available for Collier County areas included in the model domain. Thus, the 5-ft resolution topographic data was averaged in a 750-ft resolution raster file and superimposed on the topographic map previously described in order to build the updated topographic map that covers the entire model domain. **Figure 9** shows the resulting 750-ft surface elevation map. The elevations were decreased in mining pits and lakes in accordance with the conceptualization of the water bodies.
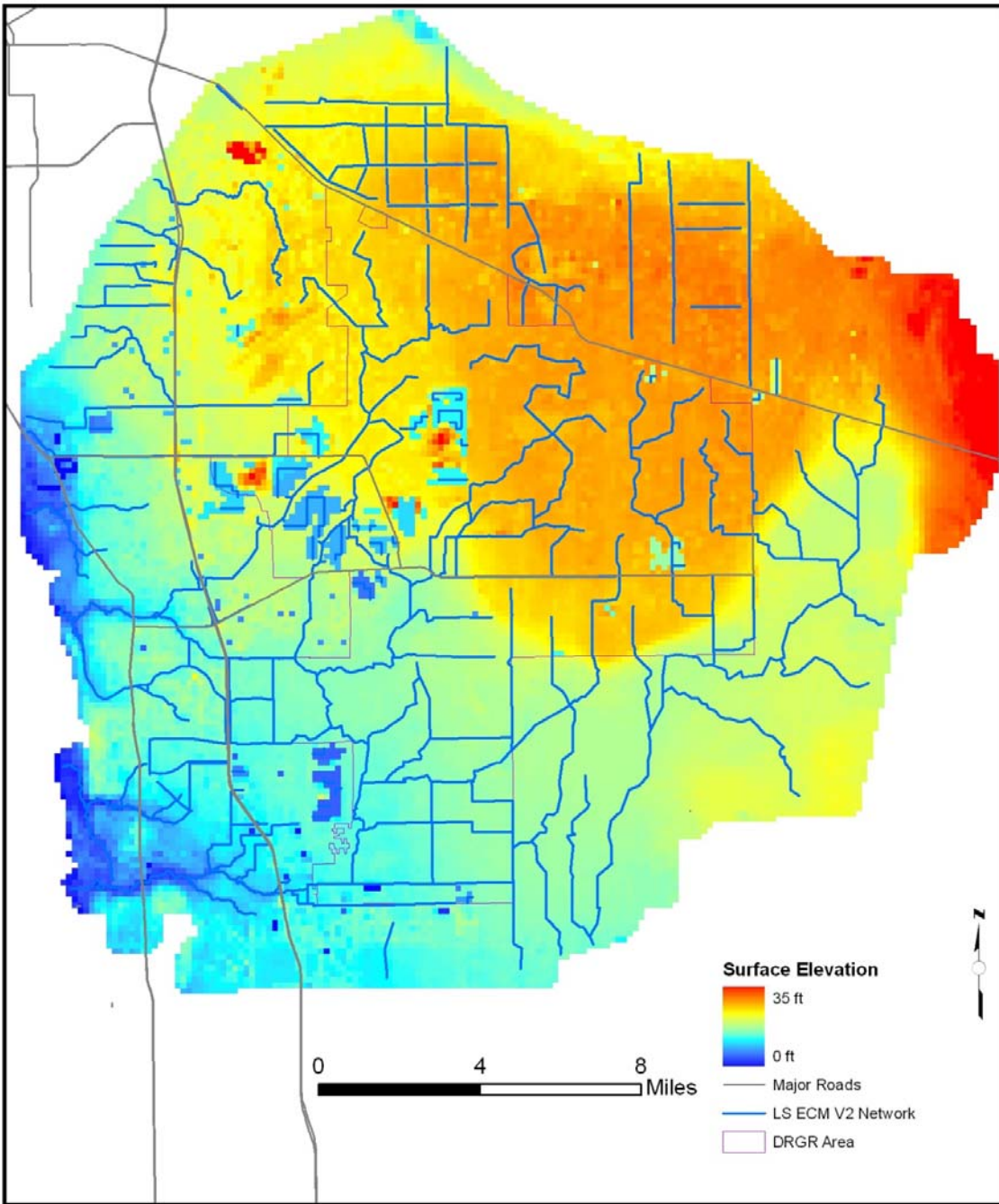
Figure 9. Model Topography in the LS ECM.

Land Use

This study uses several land use/vegetation maps to represent predevelopment, existing, and future conditions. The existing conditions land use represents the period from 2002 to 2006. The land use data for the ECM was developed from three different sources: the SFWMD, the Southwest Florida Water Management District (SWFWMD), and Kevin L. Erwin Consulting Ecologist, Inc. (KLECE). The SWFWMD 2004 land use data was used to fill in the north western portions of the model domain which are not covered by the SFWMD 2004 land use. The 2007 land use map developed by KLECE, which covers DR/GR areal extent, was superimposed on the 2004 land use data.

The land use categories are based on Florida Land Use, Land Cover Classification System (FLUCCS). The FLUCCS codes for each land use map were grouped in more general MIKE SHE land use categories as shown in **Table 5**. Land use based parameters in the model include overland roughness coefficients, detention storage, drainage parameters, and paved runoff coefficients. The land use parameter values used in the final model are presented in **Table 5**. The land use maps were merged and converted into 750-ft and 1500-ft resolution grid files that cover the entire model domain. The 1500-ft model land use map is shown in **Figure 10**. The 750-ft land use map used in the LS ECM is presented in Appendix D.

Table 5. MIKE SHE land use categories and corresponding FLUCCS codes.

Model Land Use Type	Model Code	FLUCCS Code
Citrus	1	220, 221, 222, 223
Pasture	2	165, 210, 2103, 211, 212, 213, 231, 260, 2603, 261, 262, 263
Sugar Cane & Sod	3	2156, 242
Truck (Row) Crops	5	214, 215, 216
Golf Course	6	182, 1821
Bare Ground	7	153, 1603, 161, 162, 163^S, 181, 2302, 740, 7403, 742^S, 743, 744, 747, 8113, 8115, 835
Mesic Flatwood	8	190, 1903, 191, 194, 310, 3102, 320, 321, 323, 330, 3302, 410, 4103, 411, 414, 429, 435, 440, 4403, 441, 442, 443, 7102, 7202, 741
Mesic Hammock	9	420, 4203, 422, 423, 426, 427, 4271, 434, 437, 438, 439
Xeric Flatwood	10	412, 413
Xeric Hammock	11	322, 421, 432
Hydric Flatwood	12	4119, 419, 624, 625
Hydric Hammock	13	329, 424, 425, 428, 433, 610, 6103, 611, 6111, 618
Wet Prairie	14	643, 6439
Dwarf Cypress	15	6219
Marsh	16	6171, 6172, 6403, 641, 6411, 6412, 644, 660
Cypress	17	620, 6203, 621, 6215, 6216, 6218, 629, 745
Swamp Forest	18	613, 614, 615, 616, 617, 619, 6191, 626, 628, 630, 6302, 631
Mangrove	19	612, 642
Water	20	163^D, 166, 184, 254, 5001, 510, 511, 512, 520, 525, 530, 533, 540, 541, 543, 560, 572, 650, 651, 653, 742^D
Urban Low Density	41	110, 1102, 111, 112, 113, 118, 119, 148, 164, 180, 1802, 185, 192, 193, 240, 2403, 241, 243, 245, 246, 247, 250, 2502, 251, 255, 821, 832
Urban Medium Density	42	1009, 120, 1202, 121, 122, 123, 129, 144, 176, 812, 833, 834
Urban High Density	43	130, 1302, 131, 132, 133, 134, 135, 139, 140, 1402, 141, 1411, 142, 1423, 146, 149, 150, 1503, 151, 152, 154, 155, 156, 159, 160, 170, 1702, 171, 183, 187, 252, 810, 8102, 811, 814, 820, 8202, 830, 8302, 8310

Note: The conversion is the same for the SFWMD and DR/GR land use maps, except in two FLUCCS codes that were noticed with super indices "S" and "D", respectively.

Table 6. Vegetation-based global parameters used in the ECM and LS ECM.

MSHE Code	Land Use/Vegetation	OL Manning's (M)	Detention Storage (inches)	Paved Runoff Fraction	Drainage Depth (ft)	Drainage Time Constant (1/day)
1	Citrus	5.88	1.0	0	0.5	0.25
2	Pasture	7.14	1.2	0	0.5	0.25
3	Sugar Cane	5.88	1.0	0	0.5	0.25
5	Truck Crops	5.88	1.0	0	0.5	0.25
6	Golf Course	7.14	1.2	0	1.0	0.25
7	Bare Ground	11.36	1.2	0	0	0
8	Mesic Flatwood	5.00	1.2	0	0	0
9	Mesic Hammock	3.33	1.2	0	0	0
10	Xeric Flatwood	10.00	1.2	0	0	0
11	Xeric Hammock	5.00	1.2	0	0	0
12	Hydric Flatwood	4.00	1.2	0	0	0
13	Hydric Hammock	2.50	1.2	0	0	0
14	Wet Prairie	3.33	1.2	0	0	0
15	Dwarf Cypress	5.00	1.2	0	0	0
16	Marsh	2.33	1.2	0	0	0
17	Cypress	3.33	1.2	0	0	0
18	Swamp Forest	2.50	1.2	0	0	0
19	Mangrove	5.00	1.2	0	0	0
20	Water	16.67	1.2	0	0	0
41	Urban Low Density	7.14	1.0 (0.13)	0.05	0.5 (1.0)	0.25 (0.5)
42	Urban Medium Density	8.33	0.4 (0.13)	0.15 (0.22)	0.75 (1.0)	0.35 (0.5)
43	Urban High Density	9.01	0.13 (0.13)	0.45 (0.70)	1.0 (1.0)	0.5

Note: OL Manning's M is the reciprocal of the conventional Manning's Roughness Coefficient *n*. Values are shown in parenthesis when used differently in the ECM.
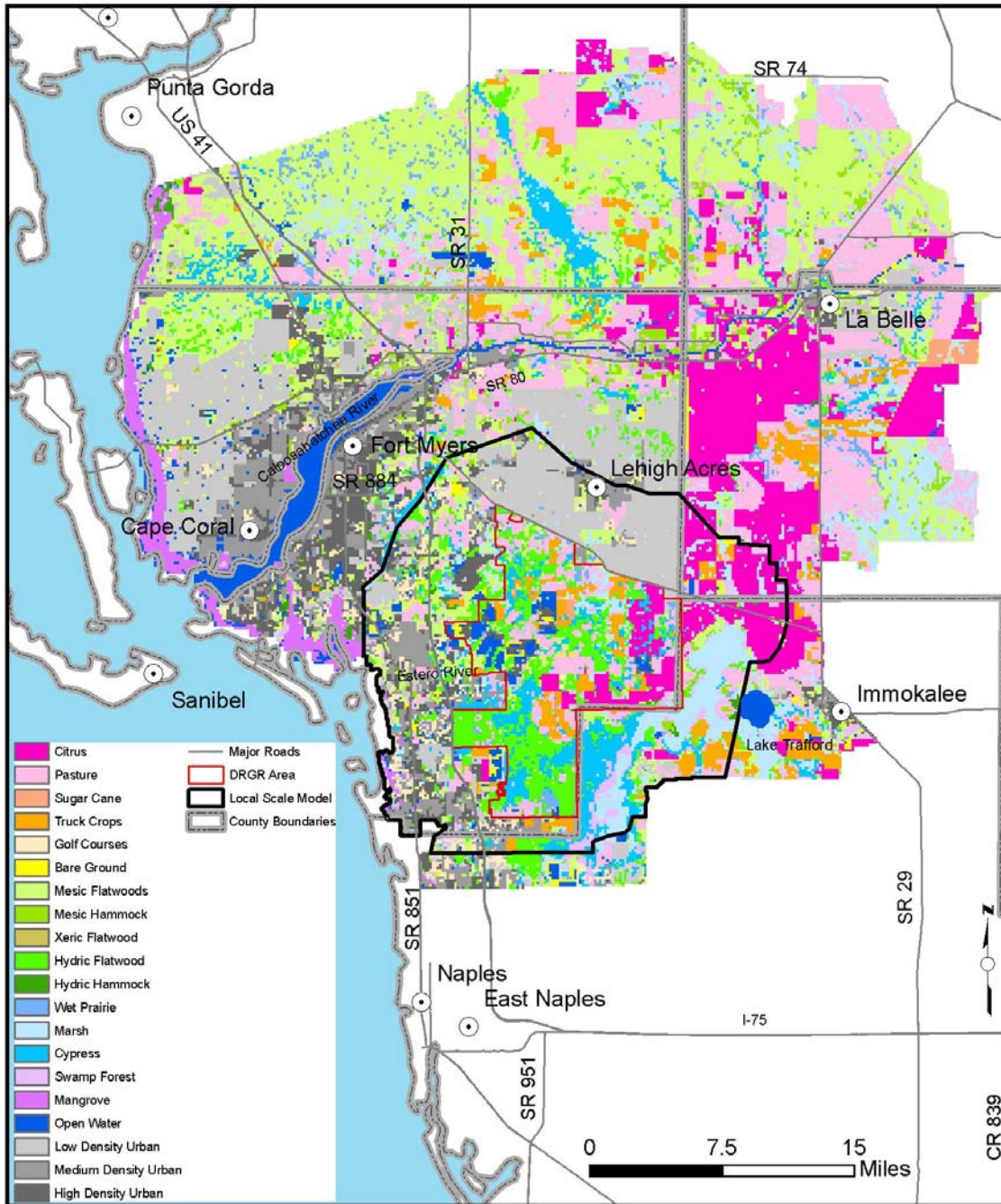
Figure 10. Existing Conditions Land Use Map.

Soils

The unsaturated zone in South Florida is shallow and the soils are sandy and highly permeable, except in wetlands where a surface deposit of fine-grained sediment may be present. Soil porosities are typically high for sandy soils in South Florida and it has been determined in previous MIKE SHE/MIKE 11 models developed in southwest Florida. Those models use the explicit gravity drainage unsaturated zone option, which does not consider the capillary pressure head term, but it is adequate for long-term regional applications. The texture and properties of soils vary on both local and regional scales. Soil types for the SWFFS area were classified into six different hydrologic response groups, shown in **Figure 11**. This soil classification was based on the predevelopment vegetation map prepared by the SFWMD in 2003, and better represents the conditions of the SWFFS area. The soil classification used in the SWFFS area and associated properties are summarized in **Table** 7**.**
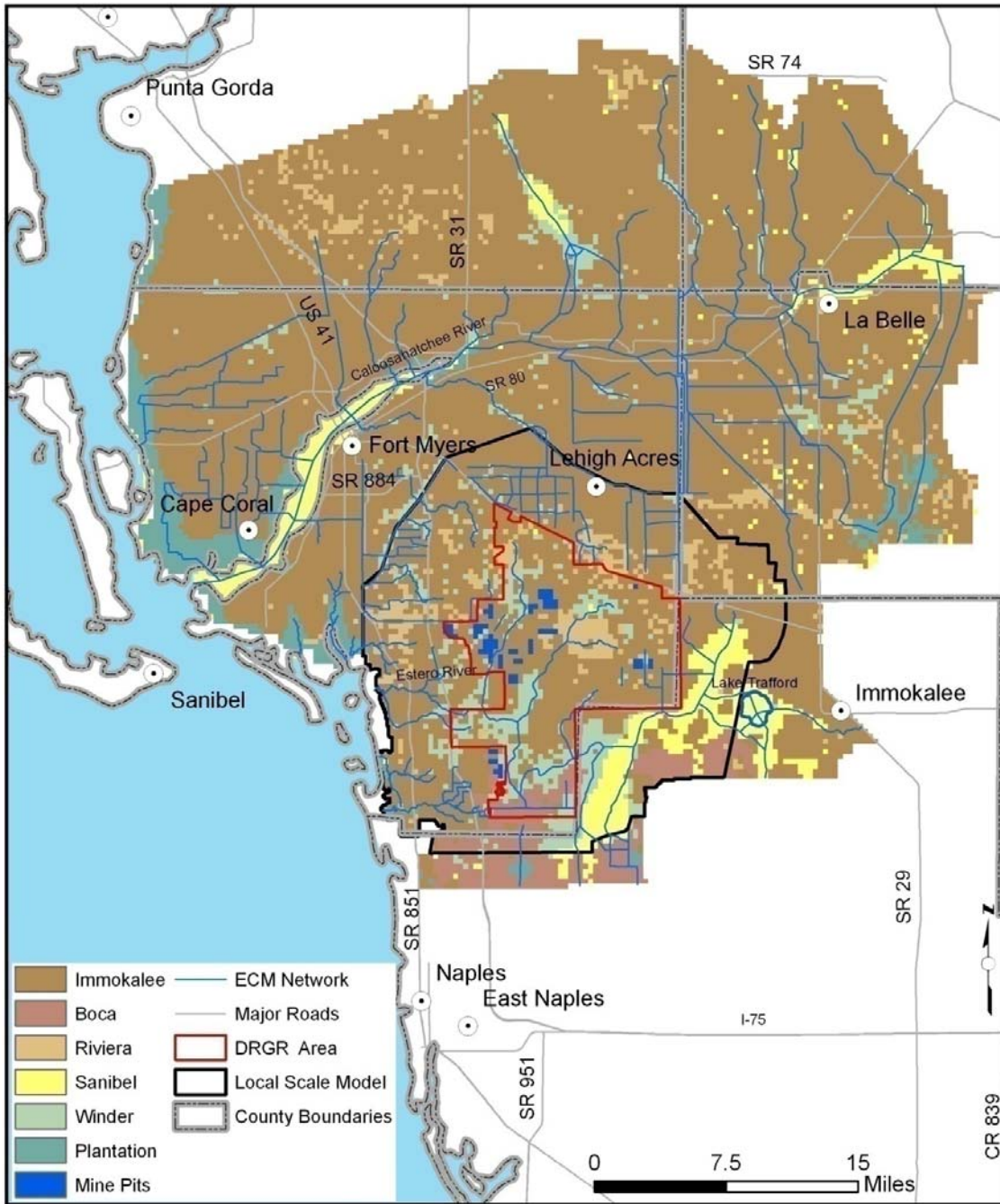
Figure 11. Soils Map.

Table 7. Soil Parameters.

MSHE Code	Soil Type	Depth interval (m)	Saturated Hydraulic Conductivity Ks (m/s)	Saturated Water Content Θ_s	Water Content at Field Capacity Θ_{fc}	Water Content at Wilting Point Θ_w	Residual Water Content Θ_r
1	Immokalee A1	(0.0-0.1)	2.00E-4	0.420	0.15	0.013	0.010
	Immokalee AE	(0.1-0.23)	1.10E-4	0.420	0.15	0.020	0.031
	Immokalee E1	(0.23-0.41)	8.60E-5	0.390	0.14	0.020	0.015
	Immokalee E2	(0.41-0.91)	1.00E-4	0.380	0.14	0.010	0.010
	Immokalee Bh1	(0.91-1.27)	1.20E-6	0.380	0.33	0.057	0.031
	Immokalee Bh2	(1.27-1.4)	6.10E-6	0.380	0.28	0.050	0.043
	Immokalee Bw/Bh	(1.4-30)	7.50E-5	0.380	0.20	0.030	0.020
2	Boca A	(0.0-0.08)	1.10E-4	0.487	0.11	0.040	0.029
	Boca E1	(0.08-0.23)	9.70E-5	0.460	0.11	0.034	0.023
	Boca E2	(0.23-0.36)	8.00E-5	0.408	0.09	0.024	0.015
	Boca Bw	(0.36-0.64)	5.40E-5	0.396	0.10	0.009	0.006
	Boca Btg	(0.64-30)	8.30E-6	0.355	0.33	0.122	0.071
3	Riviera Ap	(0-0.15)	3.64E-5	0.528	0.23	0.049	0.020
	Riviera A	(0.15-0.28)	4.20E-5	0.520	0.22	0.047	0.040
	Riviera E1	(0.28-0.41)	5.00E-5	0.460	0.12	0.022	0.001
	Riviera E2	(0.41-0.64)	5.50E-5	0.400	0.06	0.003	0.001
	Riviera Bw	(0.64-0.74)	3.50E-5	0.380	0.06	0.004	0.001
	Riviera Btg	(0.74-30)	2.50E-7	0.380	0.32	0.102	0.080
4	Sanibel Oa1	(0-0.12)	2.00E-5	0.752	0.72	0.207	0.200
	Sanibel Oa2	(0.12-0.15)	7.80E-5	0.730	0.69	0.205	0.100
	Sanibel A1	(0.15-0.23)	9.40E-5	0.510	0.39	0.025	0.010
	Sanibel A2	(0.23-0.3)	1.70E-4	0.410	0.17	0.013	0.010
	Sanibel C1	(0.3-0.66)	1.40E-4	0.370	0.09	0.013	0.010
	Sanibel C2	(0.66-30)	1.10E-4	0.380	0.08	0.011	0.010
5	Winder A1	(0.0-0.08)	3.60E-5	0.374	0.26	0.024	0.014
	Winder E	(0.08-0.33)	5.00E-5	0.370	0.15	0.008	0.004
	Winder B/E	(0.33-0.41)	1.60E-6	0.328	0.23	0.048	0.027
	Winder Btg	(0.41-0.58)	7.40E-6	0.430	0.40	0.153	0.101
	Winder BCg	(0.58-0.74)	7.40E-6	0.340	0.26	0.050	0.028
	Winder C1	(0.74-0.89)	1.00E-4	0.332	0.27	0.038	0.021
	Winder C2	(0.89-1.04)	5.00E-6	0.347	0.23	0.042	0.024
	Winder C3	(0.89-30)	1.90E-5	0.358	0.31	0.107	0.062
6	Plantation Oap	(0-0.23)	1.00E-4	0.770	0.66	0.200	0.150
	Plantation A/E	(0.23-0.48)	8.40E-5	0.491	0.19	0.029	0.022
	Plantation Bw	(0.48-30)	1.20E-4	0.392	0.10	0.003	0.002

Hydrogeology

The major hydrogeologic units in southern Florida in descending order are: the Surficial Aquifer System (SAS), the Intermediate Aquifer System (IAS), and the Floridan Aquifer System (FAS). According to Missimer and Martin (2001), Lee County has more individual aquifers with unique hydraulic properties within these systems than any other region in Florida, many of these having high transmissivities. The Water Table Aquifer (SAS), the Sandstone Aquifer (IAS), and the Lower Hawthorn Aquifer (FAS) are the aquifers with the highest production zones for public supply and irrigation. The Lee County MIKE SHE model includes the Water Table Aquifer and the Sandstone Aquifer, but excludes the FAS.

Saturated Zone Model

The saturated zone groundwater model in MIKE SHE is fully three-dimensional and thus, allows for the spatial distribution of the hydrogeologic unit thickness, horizontal and vertical hydraulic conductivities, and storage parameters. The geologic model can include both geologic layers and geologic lenses. Geologic layers cover the entire model domain whereas lenses exist in only parts of your model area. Both geologic layers and lenses are assigned the geologic parameters mentioned above. The numerical model, i.e. computational layers, is defined by the user to assign an appropriate vertical discretization for the model. The parameters of the layers and lenses that are part of a single computational layer are interpolated into the numerical grid (DHI 2008).

The geologic characterization in the ECM includes essentially the same hydrogeologic units used for the SWFFS model, plus the addition of a conceptual lens to represent the mining pits. The geologic model consists of three geologic layers and three lenses. The geologic layers are the Holocene-Pliocene, the Lower Tamiami and the Peace River Sandstone units, which correspond to the Water Table Aquifer (SAS), Lower Tamiami Aquifer (SAS), and the Sandstone Aquifer (IAS), respectively. The geologic lenses are the Bonita Spring Marl (SAS) and the Upper Peace River (IAS) confining units. The numerical model is divided initially into three computational layers (see **Figure 12**) defined as:

- Computational Layer 1 – Holocene-Pliocene
- Computational Layer 2 – Bonita Spring Marl confining unit + Lower Tamiami Aquifer
- Computational Layer 3 – Upper Peace River confining unit + Sandstone Aquifer.

The Mining Pit conceptual lens in some cases extends down to the upper portion of computational layer 3. The MIKE SHE preprocessing tool converts all the hydrogeological parameters specified for all the geological layers and lenses into the equivalent parameters for the computational layers.
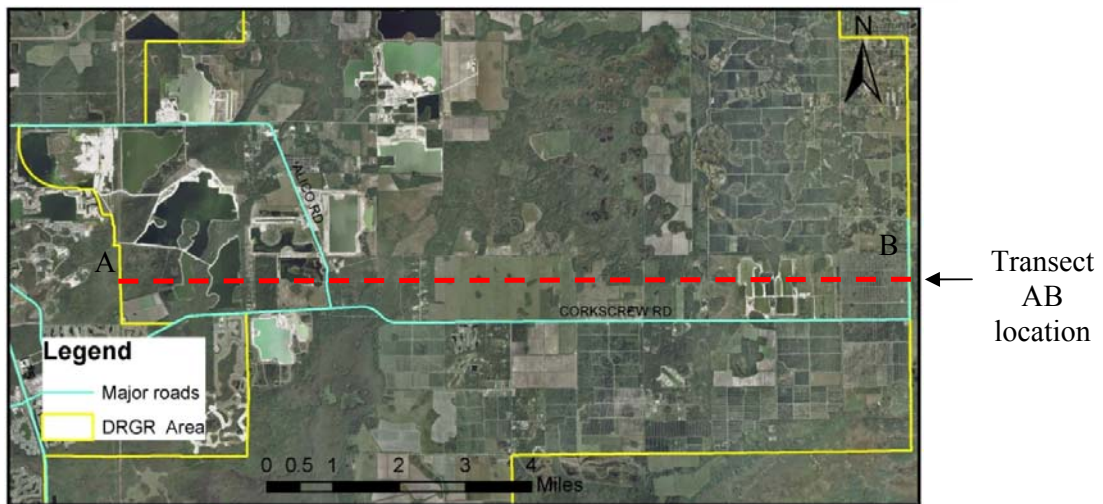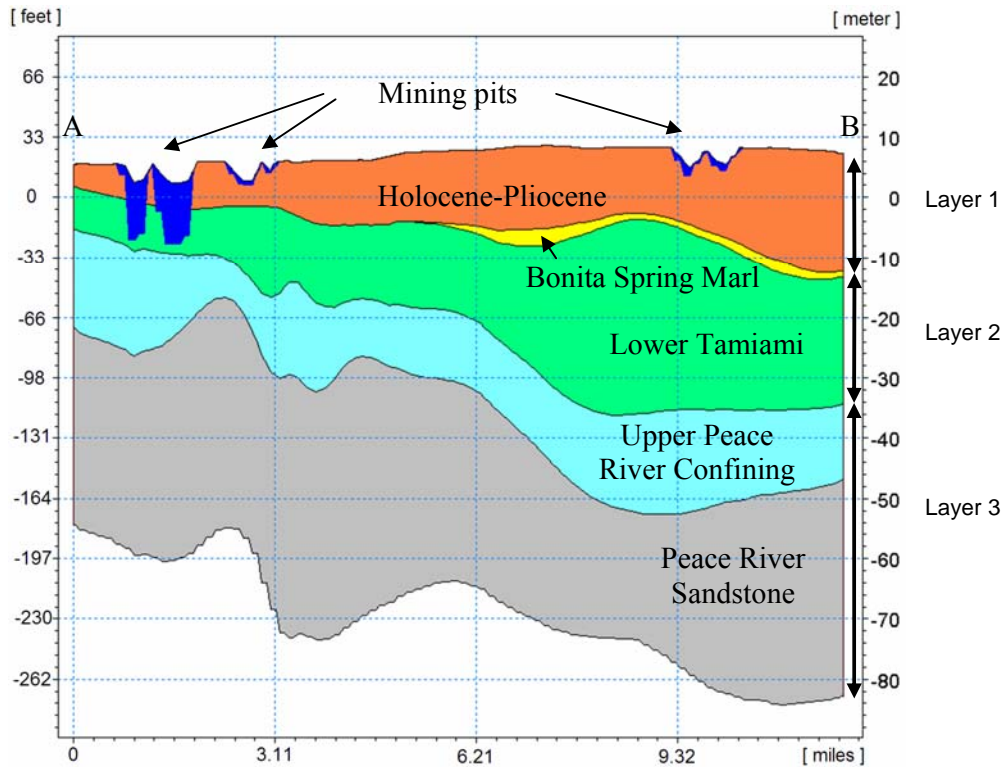
Figure 12. Geologic Model and Computational Layers along a transect in the DR/GR Area.
Note: blue color in above profile corresponds to the extent of the mining pit conceptual lenses and does not include the water above it, which is conceptualized in the overland component of the model.

Groundwater Boundaries

The Local Scale and Lee County model boundaries are shown in **Figure 13**. The boundary conditions in the groundwater layers at the eastern and southern boundaries were extracted from the SWFFS model results for the 1995-1999 simulation period. The time-varying groundwater heads from the SWFFS were used to calculate the averaged heads for every five Julian days for all simulation years in the three groundwater layers. Those averaged heads for a one year period are extended periodically and used for all the years in the ECM simulation period in order to simulate seasonal changes at the eastern and southern boundaries. The northern and western boundaries coincide with the ones in SWFFS model boundaries and thus, the ECM uses the same type of boundary conditions that was used in the SWFFS model. The northern boundary was set as zero-flux boundary and the western (coastal) boundary was set to a constant head value approximate to the mean see level elevation (0 m NAVD88).
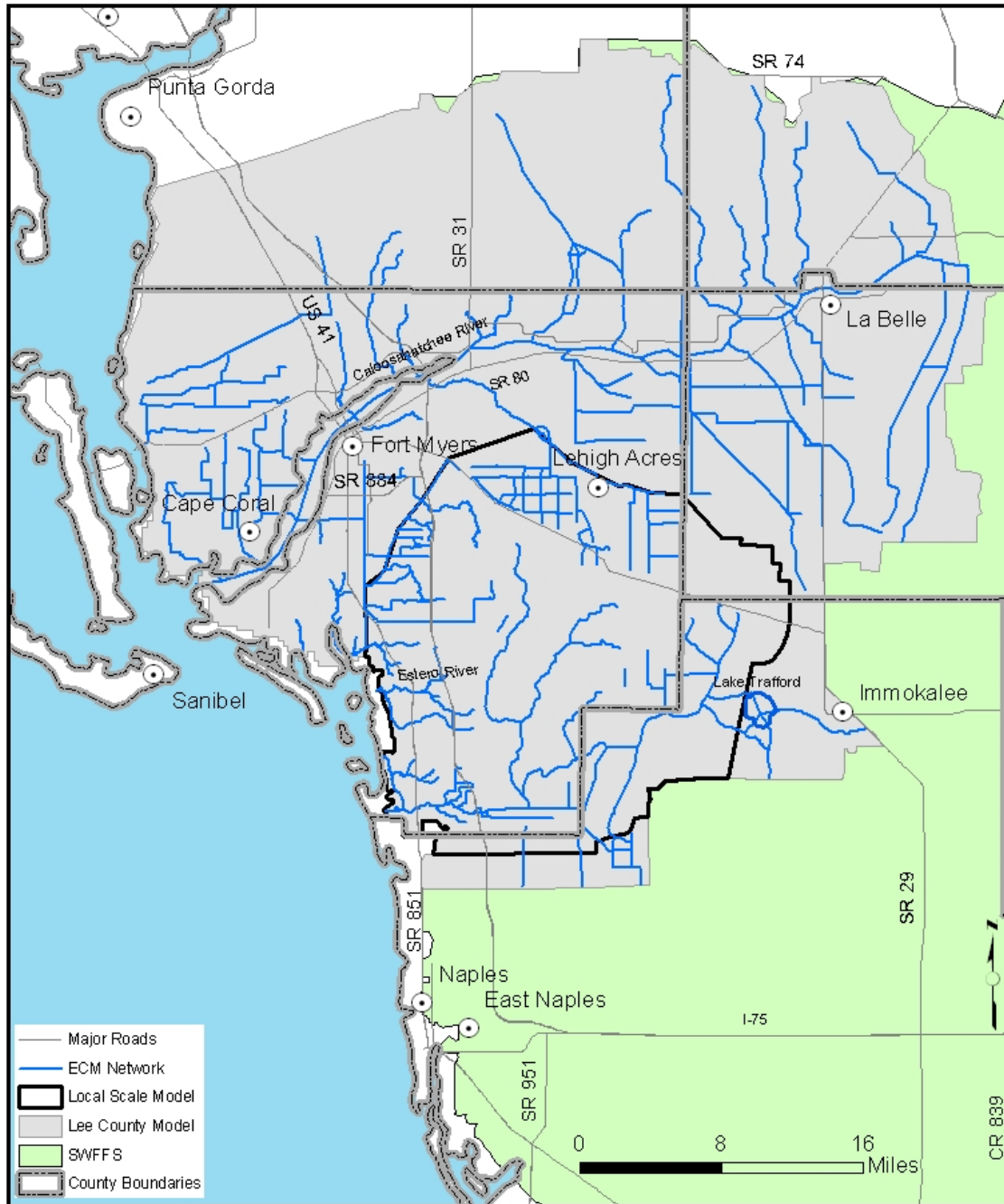
Figure 13. Model Boundaries.

Groundwater Withdrawals

Two types of groundwater extraction wells are included in the model: municipal potable water supply wells and domestic self supply wells. The Pumping Wells Module in MIKE SHE uses a well database in which the location, the depths of the screen interval, and the pumping rates for wells are specified. All of the municipal water supply wells are included in this module. The Irrigation Module, on the other hand, can be used to represent groundwater withdrawals and water from other sources that are applied as irrigation water in the model. The domestic self supply wells are represented in the irrigation module as an irrigation source.

<u>Municipal Water Supply</u>

Lee County provided the most current locations and depths of the potable water supply wells. This information was used to update the well data from the SWFFS model. The deep wells that extract water from the Hawthorn and Floridan aquifers were not added to the well database since these geological layers are not included in the model.

The pumping wells included in the model are listed in **Table 8** and the well locations are shown in **Figure 14**. The monthly extraction rates were obtained from the SFWMD Public Record Office for the period from year 2000 to 2007. The pumping rates for individual wells were used if it was available. If the data was only available for individual wells, the total rate for the well field was used and a fraction of the total pump rate for each well based on the number of wells in a given well field was applied. There was no data reported for individual wells at two well fields (CCI and GES shown in Table 8) and the total pumping rate was distributed uniformly in each well. For the well labeled as WF, the nominal maximum rate in the permit was applied.
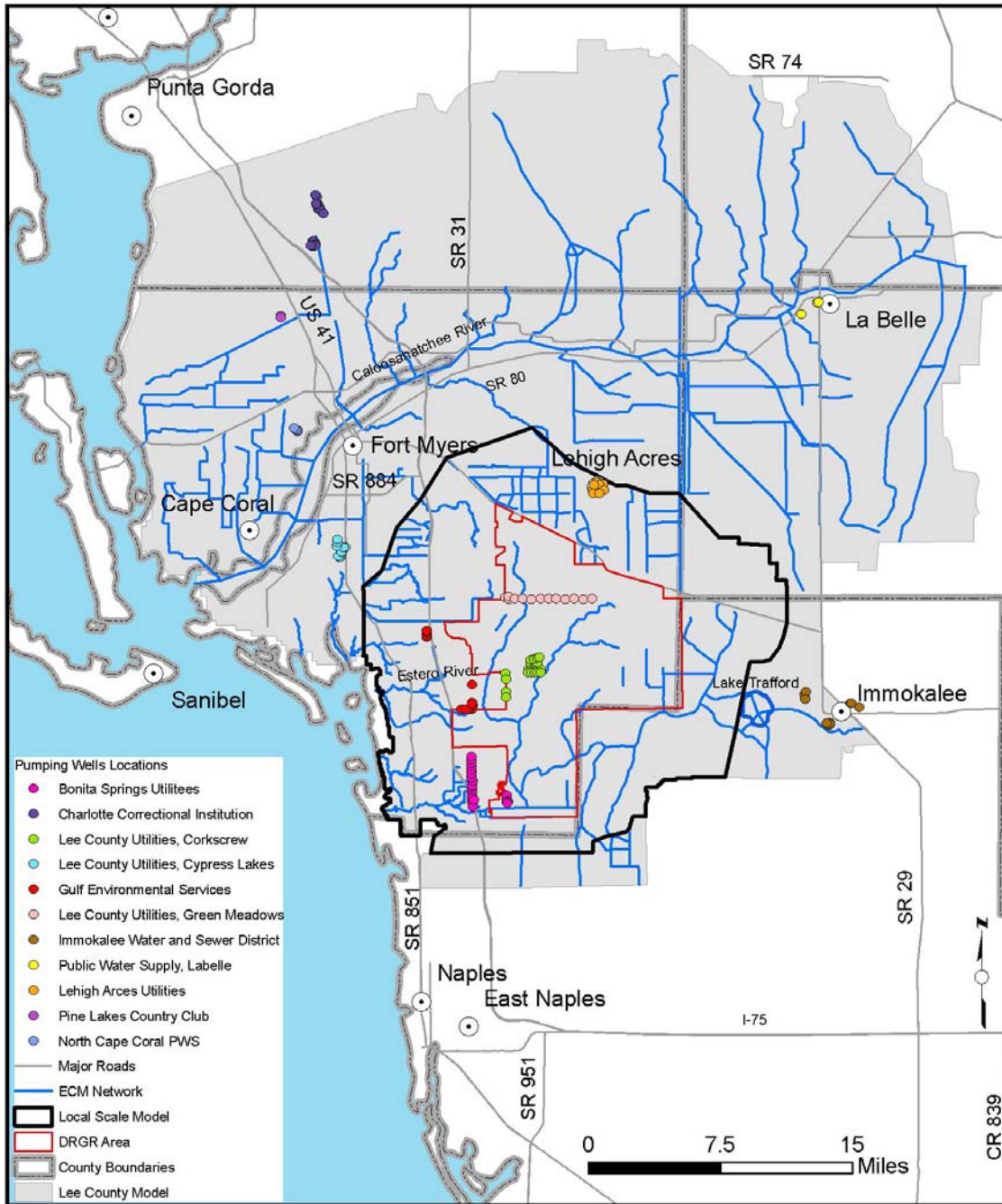
Figure 14. Municipal potable water supply well locations.

Table 8. Municipal potable water supply well included in the MIKE SHE model.

Permit Number	Project Name	ID	Well Numbers
08-00047-W	Charlotte Correctional Institution	CH-	218,219,220,221,222,227,228, 229,230,231,1,2,3,4,5,6,7
11-00013-W	Immokalee Water & Sewer District	IWSD	7,8,9,10,10A,11,12,13, 102,103,104,201,202,203,
26-00105-W	Public Water Supply, Labelle Wellfield	LAB	5,7,10,11
36-00003-W	Lee County Utilities, Green Meadows	GM-	1,1D,2,2A,3,3A,3B,4,4A,5,5A,6, 6A,7,7A,8,8A,9,9A,10,10A, 11,11A,12,12A,13,13A
	Lee County Utilities, Corkscrew	COR	2,3,4,5,6,7,8,9,10,11,12,13,14, 15,16,18,19,20,21,22,23,24,25D,25S,26 D,26S,27D,27S,28D,28S
	Lee County Utilities, Cypress Lakes	CP-	2,3,4,6,7,8,14,15,17
36-00008-W	Bonita Springs Utilities	BSU	1,2,3,4,5,6,7,8,9,10,11,12,13,14,15,16,1 7,18,19,20,21,22,23,24
36-00081-W	Pine Lakes Country Club	PL-	1,2
36-00122-W	Gulf Environmental Services, Pinewoods	GES	1,2,3,4,5,6,7,8,9,10,11,12,19,22
	Gulf Environmental Services, Bartow		13,14,15,16,16A
36-00152-W	Waterway Estates, North Cape Coral PWS	WENCC	1,2,4,12
36-00166-W	Lehigh Acres Utilities, Florida Water Services	LAC	1,2,3,4,5,6,7,8,9A,10,19,20,21
36-02986-W	Waldee Farm	WF-	3

Domestic Self-Supply Wells

The domestic self-supply (DSS) wells were represented in the Irrigation Module. The method used to represent these wells is described below in the urban irrigation section.

Irrigation

The Irrigation Module in MIKE SHE includes two main components: Irrigation Command Areas (ICAs), which is a map that indicates the cells in the model where irrigation is applied, and Irrigation Demand, where the criteria used to start and stop irrigation are specified. For each command area, several sources of irrigation (wells, rivers, external) and types of application (sprinkle, drip, sheet) can be specified. The Irrigation demand is based on "the maximum allowed global deficit" option. Irrigation is activated when the water saturation in the soil is lower than a land-use dependent value between the wilting point and the field capacity of the soil, and it stops when the field capacity is reached. The Irrigation Command Areas for the ECM are shown in **Figure 15**. The ICAs specified in the model are either agricultural or urban areas.
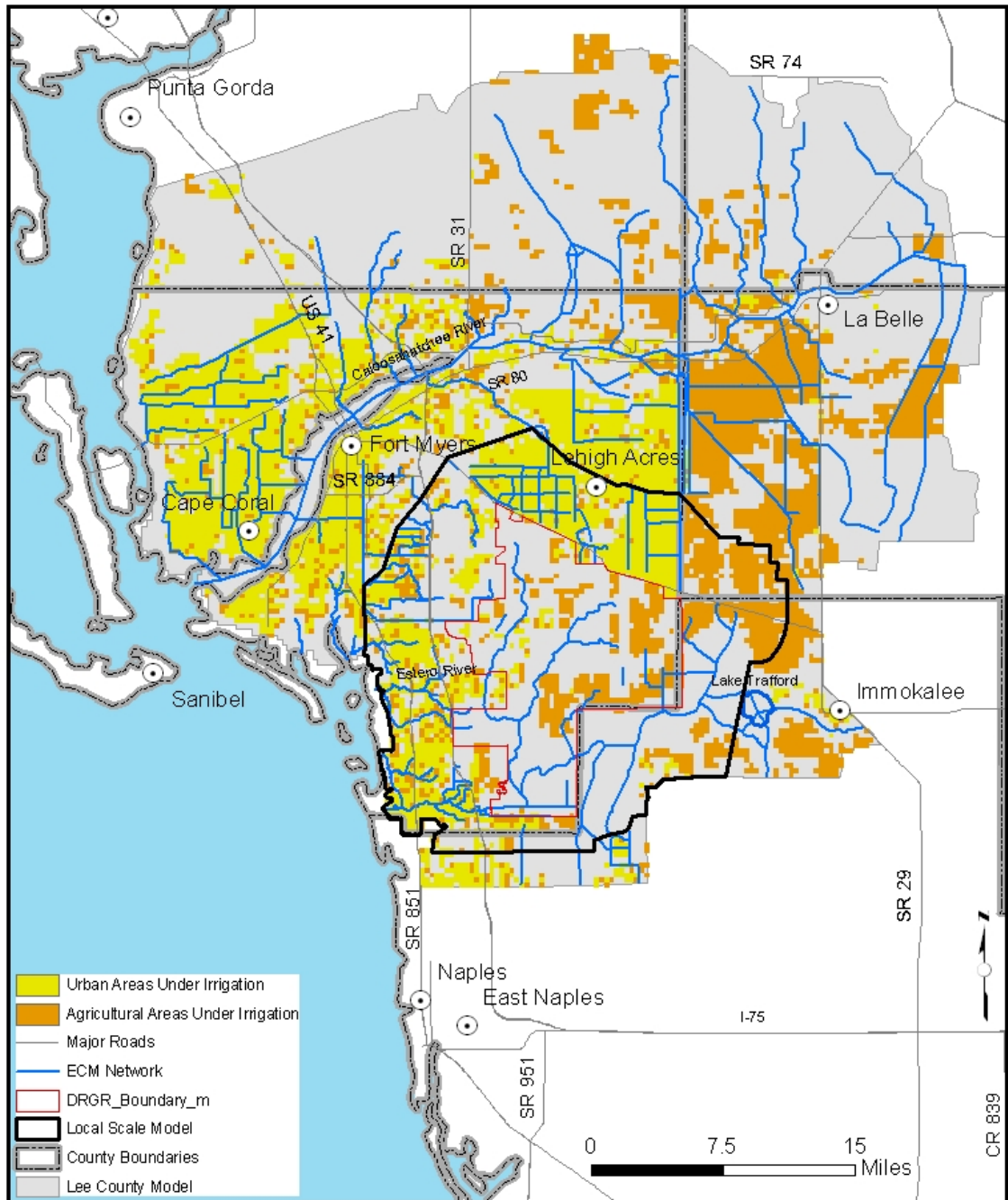
Figure 15. Irrigation Command Areas.

Some of the ECM irrigation setup in the model was taken from the SWFFS model. ICAs that rely primarily upon surface water supply from the C-43 Canal were not modified. These areas are mainly located in the Freshwater Caloosahatchee River Basin portion of the model and upstream of the S-79 structure. Some of the irrigation setup was updated to account for land use changes after year 2000. For example, agricultural irrigation was removed from the model or modified in areas where agricultural uses have converted to other uses.

For the LS ECM, the 1,500-ft resolution map with ICA codes was converted to a 750-ft resolution and the maximum pumping rates per cell for shallow well sources were decreased by four, accordingly.

Agricultural Irrigation

For agricultural lands located within and near the DR/GR Area, the most current permit information was obtained from the Florida Water Management Districts Permitting Portal (http://webapub.sjrwmd.com/agws/permitportal). For the areas where current or active permits were not available, the most recent (expired) permit was used. The permit information was used to update the source of irrigation (usually one groundwater well with a given screened interval) and the maximum pumping rate allowed. The actual amount of irrigation for a given area at a given model time step depends on the calculated soil moisture content. The soil moisture irrigation criteria differ depending of the type of crop.

Many of the row crop farms utilize flood irrigation methods. The drip irrigation method, in which the water is added directly to the ground surface of the irrigation (ICA) cells, was applied for those areas. Although there is a flood (sheet) irrigation method available in MIKE SHE, it is designed for finer grid scale applications where the flood routing can be more accurately represented. For other types of crops and for urban areas, the sprinkle irrigation method is used. The difference of the water applied as sprinkle (which is incorporated to the rainfall component) and as drip (which is placed on the ground surface) is that the former can have vegetative interception losses.

Urban Irrigation

Domestic Self-Supply (DSS) wells were specified in the model as part of the irrigation processes. This method was selected because irrigation makes up approximately 75 percent of total usage for domestic wells. Lee County provided the location of domestic self supply wells, which was used to determine the number of domestic self supply wells in each 1,500-ft grid cell as shown in **Figure 16**. The County also provided the information of the aquifers used by each DSS well that was processed to assign them an appropriate screen interval. DSS wells were grouped according to location and type of well usage. The green

polygons in Figure 16 show the general area of each group of DSS wells included in the model. The ICAs in the model within each area are the grid cells containing wells.

In Figure 16 the information provided by the County about the DSS wells in the City of Cape Coral did not include all wells. However, a large amount of them are deep wells extracting from the Hawthorn Aquifer (outside the model domain).
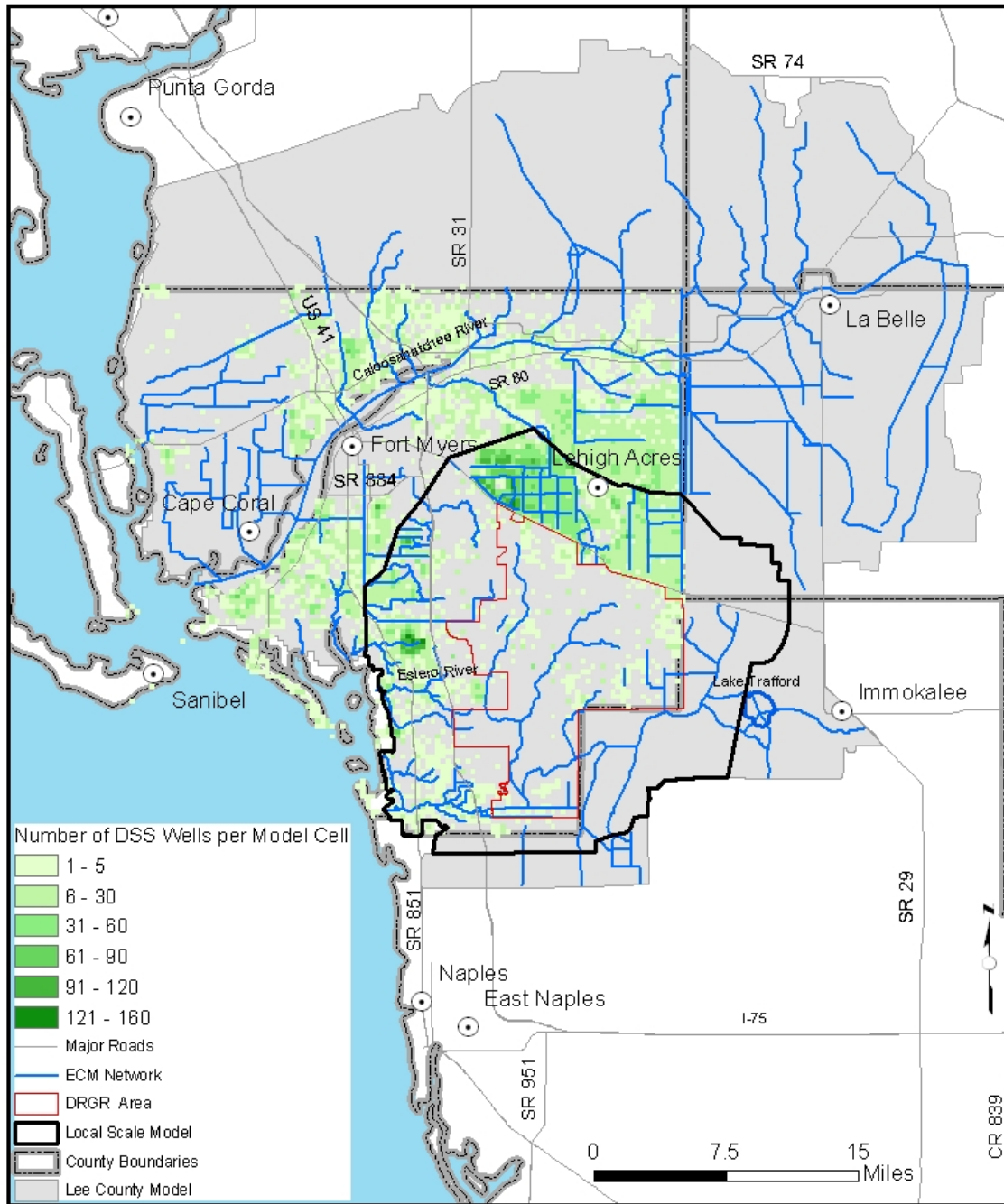
Figure 16. Domestic Self Supply Well Distribution.

A detailed description of the domestic self-supply ICAs defined in the model is provided in **Table 9**.

Table 9. Summary of ICAs defined to represent the water consumption from DSS wells.

ICA code	Total No. DSS wells	No. 1,500-ft cells	Include potable?	Well permitting region	Most used aquifer	Screen interval (ft)
545	58	3	Y	East Lee County	Sandstone	65 - 98
549	108	103	Y	Bonita Springs	Sandstone	65 - 98
551	7	15	Y	Bonita Springs	Lower Tamiami	65 - 98
557	98	1	Y	East Lee County	Sandstone	65 - 98
575	135	3	Y	East Lee County	Sandstone	65 - 98
579	160	213	N	Bonita Springs	Lower Tamiami	65 - 98
602	51	4	Y	East Lee County	Sandstone	80 - 130
606	89	33	Y	East Lee County	Sandstone	65 - 98
607	18	40	N	San Carlos/Estero	Sandstone	65 - 98
610	279	26	N	East Lee County	Sandstone	65 - 98
612	621	116	N	San Carlos/Estero and Bonita Springs (Coastline)	Lower Tamiami	65 - 98
626	69	39	N	San Carlos/Estero	Sandstone	65 - 98
1121	44	72	N	Fort Myers	Sandstone	65 - 98
1140	47	67	N	North Cape Coral	Lower Tamiami	30 - 65
1158	684	18	Y	North Fort Myers	Water Table	0 - 35
1159	286	127	N	Fort Myers and South Fort Myers	Sandstone	65 - 98
1164	3184	335	N	South Fort Myers	Sandstone	65 - 98
1166	479	22	N	Six Mile Cypress	Sandstone	65 - 98
1168	750	77	Y	Fort Myers	Sandstone	80 - 130
1171	1269	67	N	Six Mile Cypress	Sandstone	80 - 130
1172	2714	98	Y	San Carlos/Estero	Sandstone	80 - 130
1173	863	155	Y	North Fort Myers	Mid Hawthorne	160 – 230
1174	106	43	Y	Cape Coral	Mid Hawthorne	160 – 230
1175	15999	379	Y	Lehigh Acres	Sandstone	80 - 130
1178	1168	198	Y	East Fort Myers	Sandstone	80 - 130
1179	11455	674	Y	Lehigh Acres	Sandstone	80 - 130
1180	366	59	Y	North Fort Myers	Mid Hawthorne	160 - 230
1186	708	109	N	Cape Coral	Mid Hawthorne	160 - 230
1190	381	147	Y	Cape Coral	Mid Hawthorne	160 - 230
1193	1216	118	Y	Alva	Sandstone	80 - 130
1194	207	59	N	Cape Coral	Lower Tamiami	30 - 65

The following assumptions have been made in order to obtain an estimate of the average consumption of a domestic self-supply (DSS) well:

I. Maximum irrigation water demand is assumed to be 20 gallons per minute per pumping zone, 4 zones per house and each zone operated for 45 minutes per day. The total irrigation rate per house equals (20*45*4) = 3,600 gallons per house per day. Each house irrigates twice weekly; either Wednesday and Saturday, or Thursday and Sunday in accordance with Lee County regulations. Each house applies 75 percent of irrigation water between 12 am and 6 am; and 25 percent between 6 pm and midnight. The irrigation

pumping rate of one average well is then the average of the two possible schedules, which gives the application of the half rate, four times a week.

II. <u>Potable water demand</u> is assumed to be 100 gallons/per person/per day for uses like cooking, cleaning, and bathing with 3 people per household. The assumed consumption per capita per day is in the range from 100 to 130 reported by (Hammer and Hammer, 2001). The majority of usage (2/3) is assumed to occur in the morning between 6 am and noon while the remainder of usage (1/3) is assumed to occur in the evening between 6 pm and midnight.

Note that the maximum irrigation water demand is equal to or higher than the current irrigation consumption. The current consumption is in general higher during the dry season than during the wet season. The weekly time series for the maximum pumping rate of an average domestic self-supply well obtained from previous assumptions is presented in **Figure 17**. Two cases are considered corresponding to the use of DSS water for all the needs or just for irrigation in areas where the potable water demand is supplied from municipal wells. The weekly period in Figure 17 is then extended over the whole simulation period. The time series created has an average maximum pumping rate from a domestic self-supply well of 1029 gal/day (4.51×10^{-5} m^3/s) for irrigation only and of 1329 gal/day (5.82×10^{-5} m^3/s) including potable water consumption.

The maximum groundwater extraction rates for each ICA are found by multiplying the appropriate extraction time series (irrigation only or irrigation plus potable supply) for one averaged well by the total number of wells within the ICA. The extraction rate (or demand below this limit) is determined automatically by the model based on the soil moisture content.
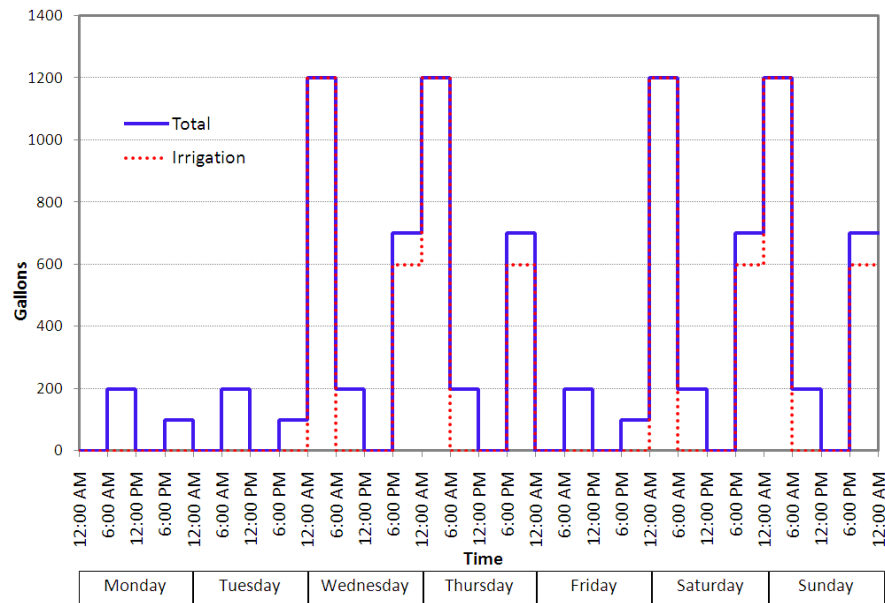
Figure 17. Maximum weekly consumption for a DSS well. The total volume includes irrigation and potable water supply.

Surface Water Model

Surface water is modeled in the overland component of MIKE SHE and in MIKE 11. The Overland Flow component solves the 2-dimensional diffusive wave approximation of the Saint Venant equations and MIKE 11 solves the fully dynamic Saint Venant equations in one dimension. The MIKE SHE overland component routes the surface runoff to the reaches defined in MIKE 11. MIKE SHE also has a drainage component that can route the drainage from urban or agricultural areas to the MIKE 11 canals.

ECM Development

MIKE 11 Model

The surface water model includes an extensive network of primary and secondary canals with many hydraulic structures, natural sloughs, rivers, and lakes. The surface water network is modeled using DHI's one-dimensional hydraulic model, MIKE 11. Inputs for the MIKE 11 model consist of the river network path, channel cross-sections, boundary conditions, and bed resistance. Moreover, structures such as culverts, dams, bridges and control gates that may alter river flows and stages are specified as input to the model. The ECM MIKE 11 network and structures is shown in **Figure 18**.

The network was built using the SWFFS canal network as the starting point and adding secondary canals and structures from the EIC, BCB and TCRB sub-regional models to build the BLM. In addition, secondary canals and structures were added or updated from the

ECWCD model. Finally, the structures in Alico and Corkscrew roads were also updated or included based on the information received from Lee County.
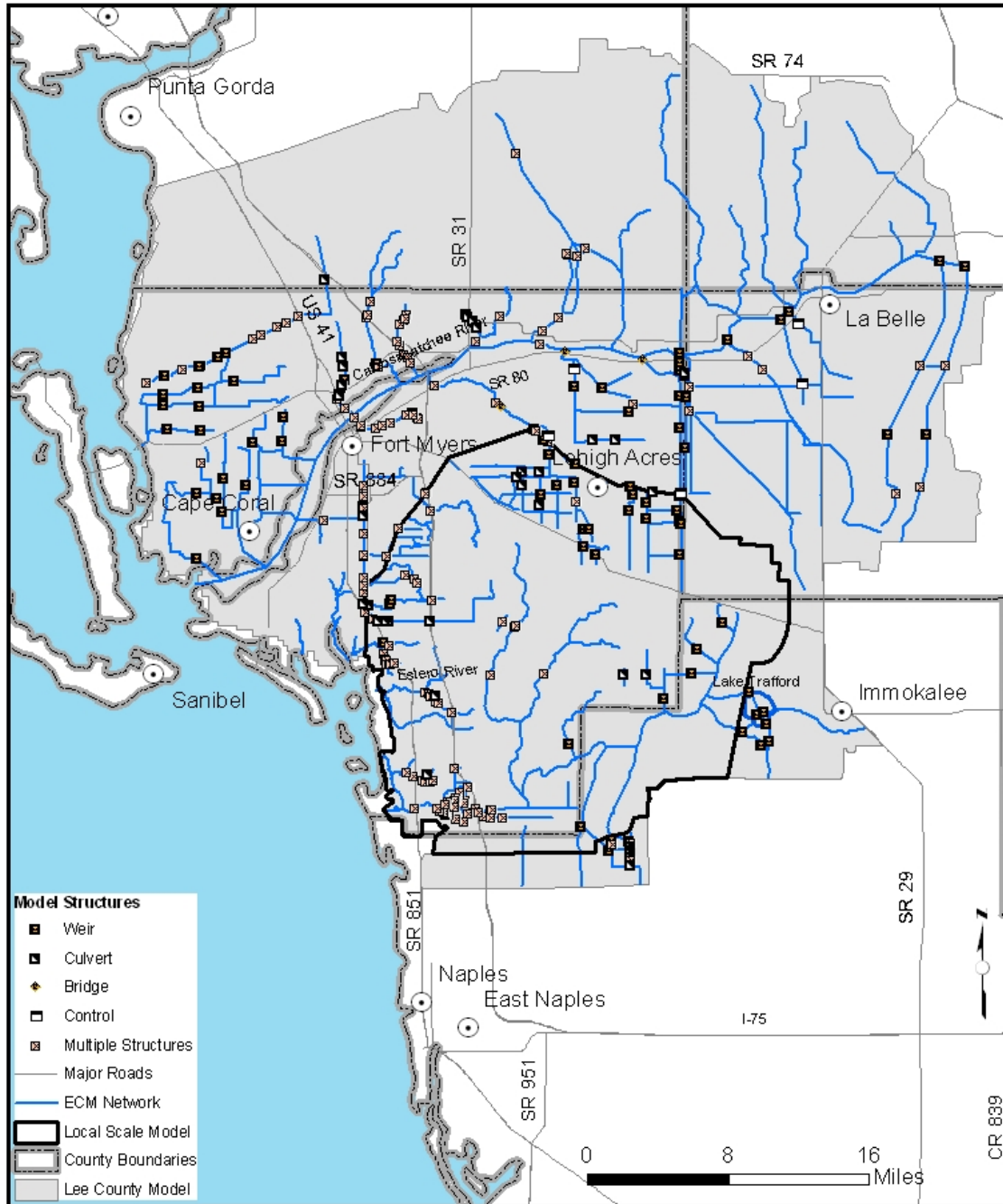
Figure 18. MIKE 11 Network and Structures in the ECM.

<u>MIKE SHE and MIKE 11 Interaction</u>

Water flow is exchanged dynamically between the MIKE 11 hydraulic model and the MIKE SHE hydrologic model. The MIKE 11 canals exchange water with the underlying aquifer, driven by the head gradient and controlled by either the aquifer conductivities or by a river lining leakage coefficient, or a combination of both. Runoff from the MIKE SHE overland surface is driven by topographic gradient and flows into MIKE 11 in places where both the river bank elevations and the water levels are lower than the water elevations in adjacent MIKE SHE cells. MIKE 11 branches also receive water from the drainage component of MIKE SHE.

Flooding from the MIKE 11 rivers, lakes or canals to the overland surface in MIKE SHE is allowed to occur where specified. The flooding method used for the ECM is the flood code mapping option. This method is appropriate for modeling lakes, wide rivers and sloughs. The flood code approach ensures that the volume of water is not double counted in the same spatial location that the branches and the flooded MIKE SHE cells occupy if the extents of the specified flood coded cells are consistent with the cross section widths of the MIKE 11 branches. **Figure 19** shows the flood code map used for the ECM. The flood coded cells are the MIKE SHE cells where the water from MIKE 11 canals is allowed to spill out. The movement of water in flood coded cells along the river direction is controlled by MIKE 11, but this water is also available for all other MIKE SHE processes, such as evaporation, overland flow, and infiltration.
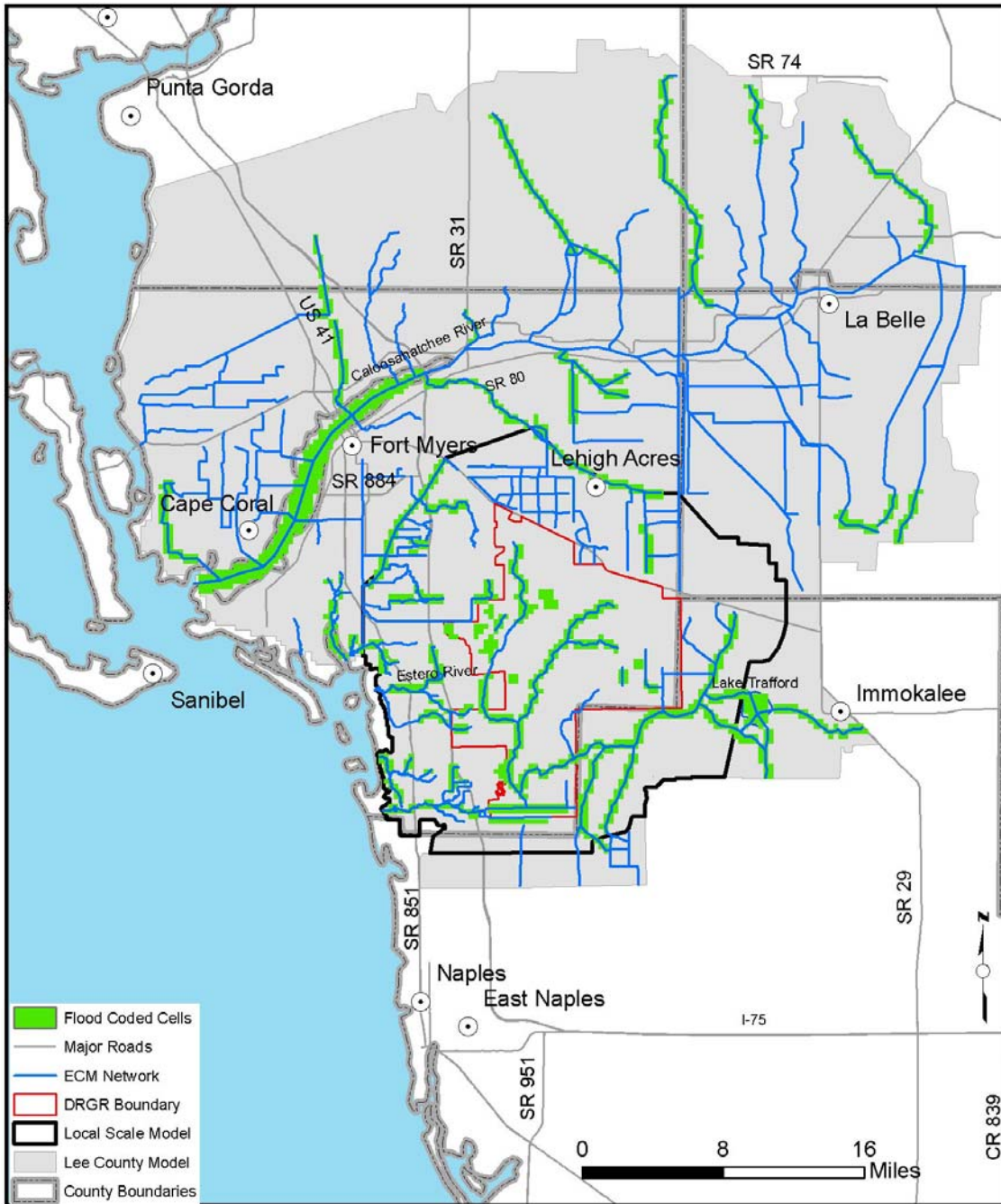
Figure 19. Flood coded cells in the ECM.

<u>Representation of Roads and Berms</u>

Due to the relatively large size of the model cell size (1,500 feet), the elevations of certain features that impede flow between certain areas are not properly represented in the model topography. The separated flow areas are specified in the overland flow module in MIKE SHE to define localized higher topography that would prevent overland flow from naturally occurring from one area to another. For example, an elevated roadway would prevent overland flow except at designated culvert crossings. Another example would include a farm field or mining operation that is bermed on all sides to prevent overland flow from surrounding areas.

Discussions with Lee County staff revealed that Alico and Corkscrew Roads serve as barriers to natural overland flow. Multiple culvert crossings exist along the right-of-ways to allow flow to move towards the south and towards the west. The existing separated overland flow areas defined in the SWFFS model were further subdivided to account for the barriers defined by Alico and Corkscrew Roads. Moreover, additional branches and structures were defined in the MIKE 11 river network to represent the culvert road crossings under these roadways, as stated the previous sections.

Separated flow areas were also defined for the mining pits to represent the surrounding berms. This approach assumes that there is no overland flow between the mine and surrounding properties. In some agricultural or urban areas in the DR/GR Area, separated flow areas were also defined. The separate flow areas map used for the ECM is shown in **Figure 20**.
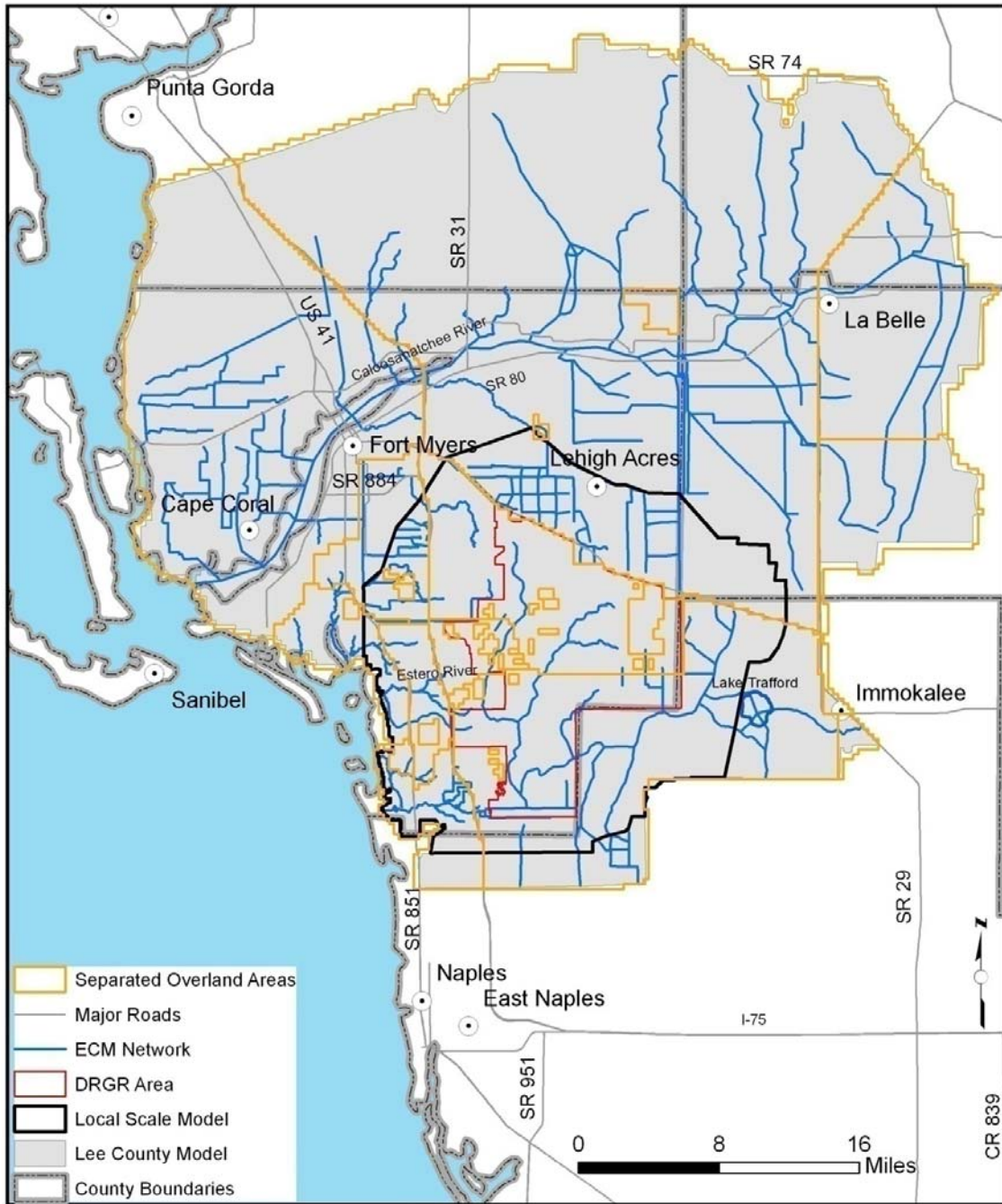
Figure 20. Separated Overland Flow Areas in the ECM.

Representation of Mining Pits

There are several mining pits in and around the DR/GR Area that may alter the water budget in the region. Those mining pits are open water bodies that may have higher ET rates than the pre-developed land. In open water conditions, there is more storage (porosity) than in pre-existing soils, and the amplitude of the changes in the water table level are lower than in subsurface pore water at equal volumetric fluxes from rainfall, ET, infiltration, etc. Moreover, open water bodies represent high hydraulic conductivity areas that flatten the preexisting regional hydraulic gradient and drain upgradient pore water.

The representation of the mining areas includes the following:

1) The Environmental Resource Permits (ERPs) for mines require that at least the 25-year three-day (or, in some cases, the 100-year) storm events are contained. In order to represent the berms, a separate flow area was defined at the boundaries of the mining pit areas. The separate flow areas prevent overland flow to or from surrounding areas. The separate flow areas corresponding to mining pits in the ECM are shown in Figure 20.

2) Dover, Kohl and Partners provided the depth of the mining pits in and around the DR/GR Area from official records. This information was used to assign the bottom elevation of the conceptual mining pit lens at each corresponding grid cell in the model. This approach, which has been used in other groundwater models (May-Chu and Freyberg, 2008), allows lateral exchange from the mining pit to the adjacent groundwater cells. The mining pit lens is set with a high conductivity ($K_h = K_v = 1$ m/s $= 2.8 \times 10^5$ ft/day) and the maximum specific yield (Sy= 1), to mimic open water conditions. Some of the deeper mining pits reach the upper part of the Upper Peace River Confining Unit, which is the third computational layer of the model.

3) A portion of the mining pits were etched in the model topography to ensure that there is ponded water through the simulation. The portion of the mining pit below the level burned in the topography is represented in the groundwater model as a geological lens.

4) After converting the higher resolution land use maps to the model resolution, the maps were modified to ensure that all mining pits were defined using the same code equal to "water". This allows the proper application of land use based parameters for these areas, such as ET parameters to calculate the proper evaporation rate from open water.

Surface Water Boundaries

Measured water levels and flows were used to define the surface water boundary conditions for the ECM. The surface water time-varying boundaries are shown in **Figure 21**. In MIKE 11, boundary conditions are required at the unconnected ends of all branches. The unlabeled unconnected ends in Figure 21 are set as zero-flux (or closed) boundaries. The eastern boundary of the canal network is located at the S-78 structure in C-43 Canal. The measured discharge at the S-78 structure was specified for this location from DBHYDRO.
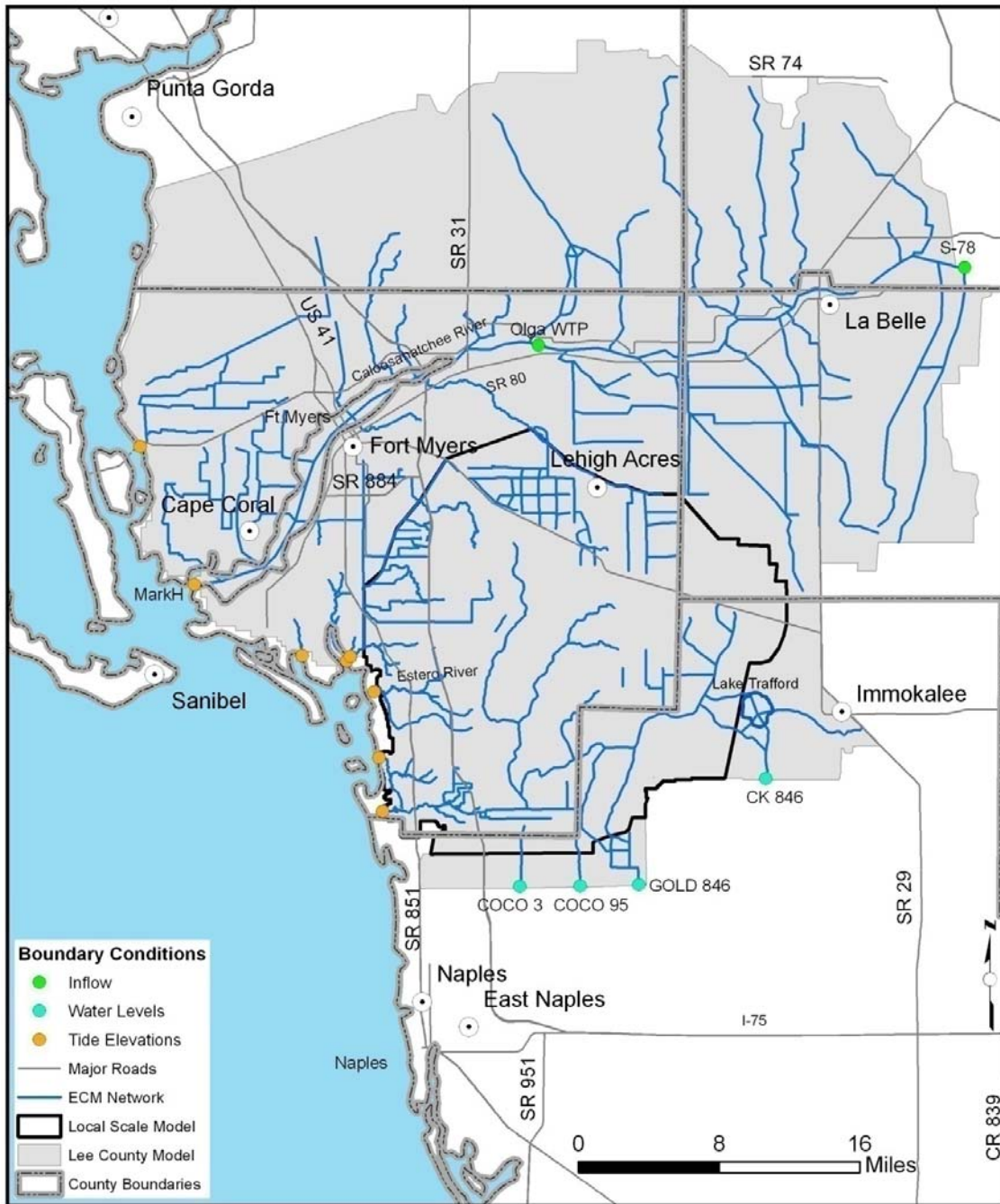
Figure 21. MIKE 11 Time-Varying Boundary Conditions in the ECM.

The south-eastern boundaries consist of the Camp Keais Strand at the CR846 crossing and Immokalee Canal at the intersection with SR29. The available stage data from DBHYDRO for the Camp Keais Strand at the CR846 crossing was applied at this location. A closed (no-flow) boundary was specified for the Immokalee Canal.

The ECM area was extended from its original proposed area in order to reduce boundary effects in the southern part of the DR/GR Area. The new southern surface water boundaries consist of the set of downstream ends of canals that drain to the Cocohatchee Canal. The water level time series from Cocohatchee stations were used as the boundary conditions specified at the southern end of these canals.

The Olga Water Treatment Plant (WTP) at Fort Myers was included as a point source intake from the river network, as in the SWFFS model. The original time series data was updated, with the daily data delivered by Howard S. Wegis, at Lee County Utilities, from April 2001 to December 2007.

The hourly tidal water levels from the NOAA (http://tidesandcurrents.noaa.gov/index.shtml) Naples station were used for all the west coast boundaries. This station was determined the most suitable tidal station for the western area of the model after a comparison was performed between the available tidal data. The two NOAA stations within or close to the model area that have data available for the entire simulation period are: the Fort Myers station (ID: 8725520), which is approximately 13 miles upstream from the coastline at the Caloosahatchee River, and the Naples station (ID: 8725110), which is approximately 10 miles south of the southern boundary of the model domain (see **Figure 22**). The MARKH station from DBHYDRO, located at the downstream end of the Caloosahatchee River, does not have data available for the entire model simulation period. The average hourly and daily data from the Naples and Fort Myers stations were compared to the daily average data from the MARKH station. The recorded values at this station appear to slightly overestimate the daily averages of the other two stations. There are also some differences between the Fort Myers and Naples stations. First, the oscillations of the hourly time series differ in amplitude and phase. Second, the daily averaged elevation at Fort Myers station is slightly higher in general than at the Naples station. These differences are to be expected since the Fort Myers station is farther upstream from the coastline. Thus, it was determined that the Naples station is more representative of the coastal water levels.
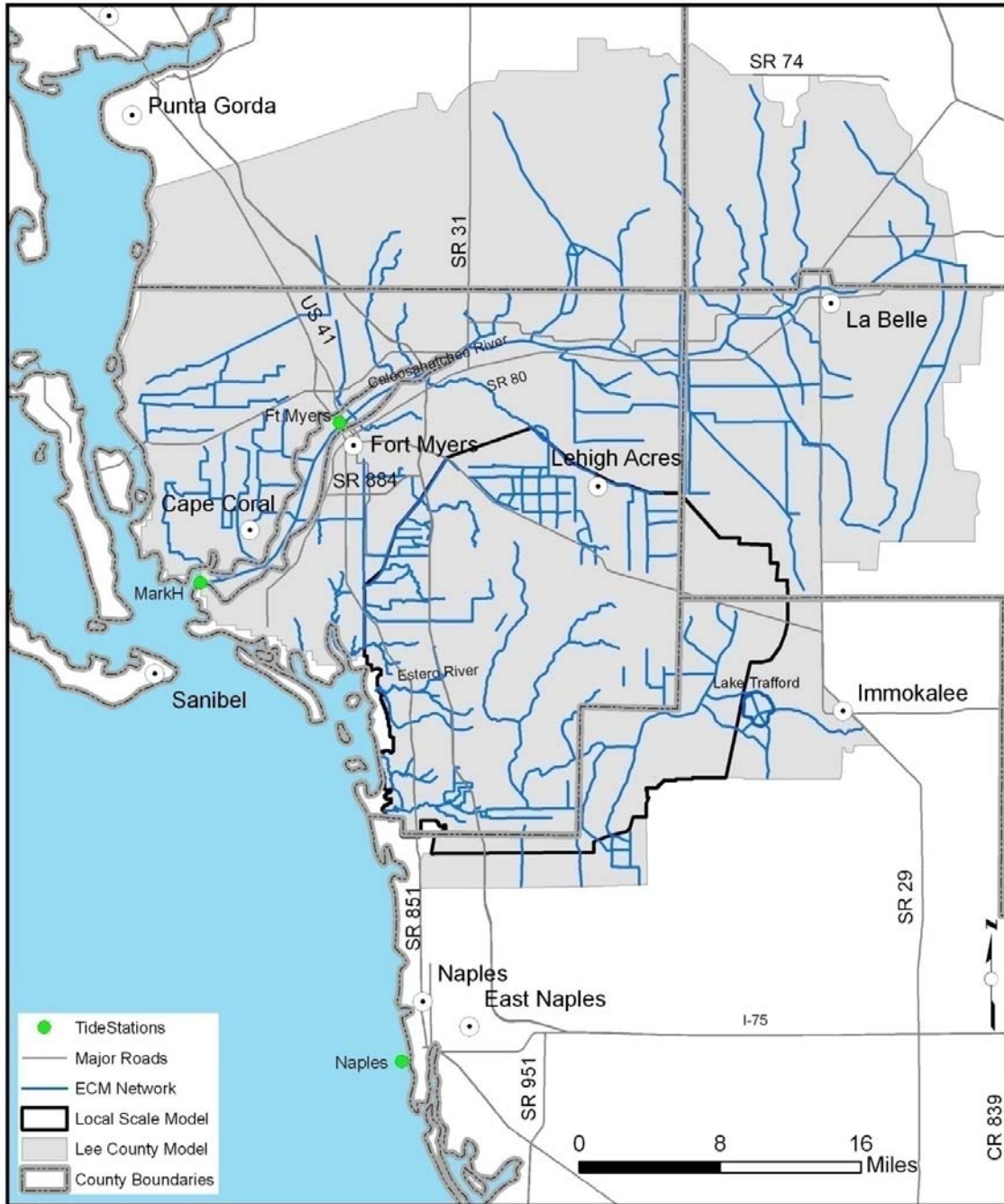
Figure 22. Tidal Stations.

LS ECM Development

Several refinements were made to the surface water component of the LS ECM. Some of the refinements are described below.

- The mining pit coverage was redrawn at 750-ft resolution maps (down from 1500 ft resolution in the ECM) for conceptual lens depth and separated overland flow areas. The separated flow area map with higher resolution was also improved to better represent the road divisions. The drain code map used in the LS ECM was obtained in a similar way as in the ECM from the separated overland flow areas map by setting zero drain codes at mining pits and allowing drainage to the boundaries.

- The 750-ft land use map contains other grid cells classified as water that are not considered as mining pits in the model. Aerial photos reveal in most of those cells well defined open water bodies with sizes from one to several 750-ft grid cells. Those cells are referred to as "shallow lakes" and they were conceptualized in a similar way as mining pit cells. For shallow lakes where the depth was not provided by Dover, Kohl and Partners, a value of 10 ft was assumed.

- The distribution of mining pits and shallow lakes in the LS ECM domain area is shown on **Figure 23**. The representation of the water bodies can be revised in the future, when more information becomes available about the interaction of the water body with the surrounding cells (i.e. presence of berms, drainage system, etc). Also, information about the bathymetry of the water bodies can improve the representation in the model.

- Another improvement in the LS ECM is the representation of contiguous water bodies that are divided by land areas narrower than one grid cell size, like roads for example. As with the ECM, separated overland flow areas were established to prevent communication in the overland component. For the LS ECM, the sheet piling module in the groundwater component was added to the model. Since the separation between the water bodies was less than one grid cell, the model would have shown these water bodies as touching each other without any hydrologic barrier between them. The sheet piling allows for the specification of a hydrologic barrier between these touching water bodies that more closely represents reality. Since mining pits and shallow lakes are represented with a groundwater lens, free communication between contiguous water bodies through the groundwater layer is prevented by introducing conductivity barriers, i.e., artificial sheet pilings. The locations of the flow barriers were found by inspecting aerial photos and assuming the lack of culverts on those divisions. The divisions are shown in Figure 23. A uniform leakage coefficient of 10^{-4} sec^{-1} was assumed by considering divisions of 50 ft wide and a typical conductivity of the Holocene-Pliocene geological layer.

Other improvements and refinements to the surface water system in the LS ECM are described in the following sub-sections.
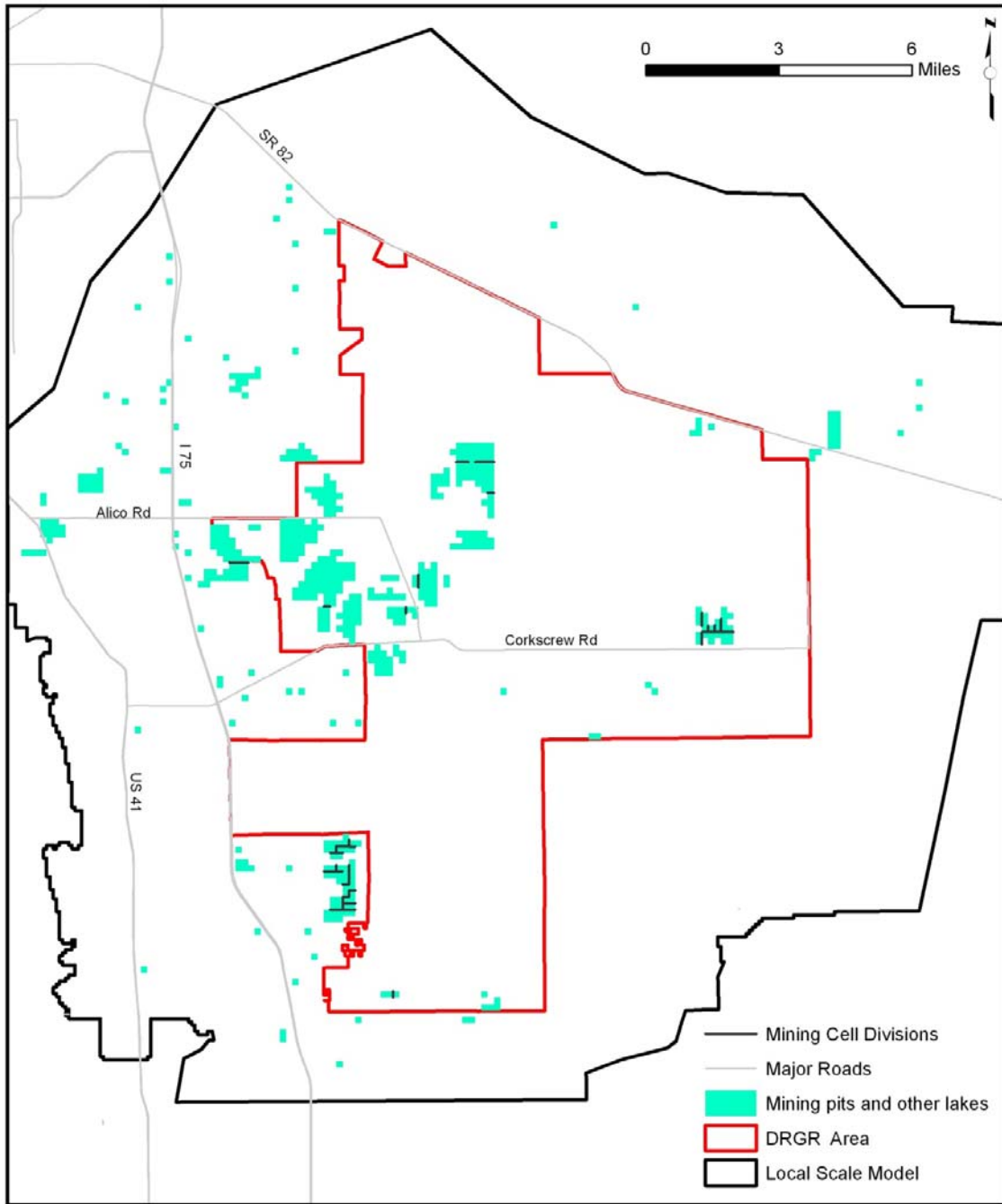
Figure 23. Mining Pits and Shallow Lakes.

Definition of Flow Ways

       The inclusion of all the main flow ways in the MIKE 11 component of the model has advantages over using a combination that alternates channel flow and overland flow. MIKE 11 solves the surface water (channelized) flow problem in a more accurate way since it solves the exact equations in smaller time steps and accounts for the channel geometry (or micro-topography). On the other hand, the overland flow component considers two dimensional flow, which is beneficial for wide flow ways (sloughs, lakes, etc) where the flow across the main path (e.g., toward the center of the slough) may be important. The approach followed by DHI to represent the sloughs and lakes in this model is to create a MIKE 11 branch for the slough center flow with a 750-ft wide cross-section and allocate a flood code to allow full interaction with the overland component that controls the 2D surface water flow in the neighboring areas.

       The definition of new MIKE 11 branches containing the main flow ways was conducted based on the following information:

1. The 5-ft resolution LIDAR topographic map. In this map, the highs (berms and roads) and lows (canals, creeks and sloughs) are clearly visible. Some bridges are removed from flow ways. However, the existence of some culverts is sometimes difficult to determine from this map.

2. Hydroperiod map from KLECE. Natural flow ways like sloughs are likely present in connected natural areas. High and low hydro-periods are useful to delineate flow path ways in some natural areas.

3. Aerial photos from 2007 (and 2004 outside of the DR/GR). They were useful to delineate pathways particularly where there is not LIDAR topographic data.

4. Notes received from Kevin Hill (dated from 5/27/2008). They were useful to delineate flow ways along and across Corkscrew Road.

5. GIS processing of topographic data. The new LIDAR topographic data was averaged to 100 ft resolution and merged into 100-ft SFWMD data from 2004 in order to "fill the gaps" outside the Lee County areas. The resulting 100-ft resolution topographic file was processed in ArcMap to obtain the flow ways. A similar processing was conducted to a 750-ft resolution topographic map obtained from those two topographic data. The flow path ways obtained in both cases cannot be used directly as the existing flow ways (mainly because of the lower resolution that blur canals and creeks and because this processing does not include the culvert information), but they serve as a guide for the more detailed flow ways delineation conducted visually from the previous information.

       The flow ways analysis described above led to a drainage network that was too detailed. That network was later reduced to the coarser MIKE 11 network used in the model.

Figure 24, **Figure 25** and **Figure 26** show the network structures, the flood coded cells and the separate overland areas considered in the new model in conjunction with the new flow ways definition.

ADA Engineering, Inc. [2008] performed some work on the MIKE 11 network in the area between the Estero and Imperial Rivers based on local survey information. The MIKE 11 network of this model was based in part on the MIKE 11 network generated by ADA Engineering, Inc.

While building the MIKE 11 network, considerable effort was made to ensure that all important flow ways were included. However, the network may include flow ways that conduct minimal flow since it is difficult to predict the relevance of all the flow ways considered. Once the network is introduced in the model, the flow rate predicted by the model would allow us to evaluate the importance of each flow way.
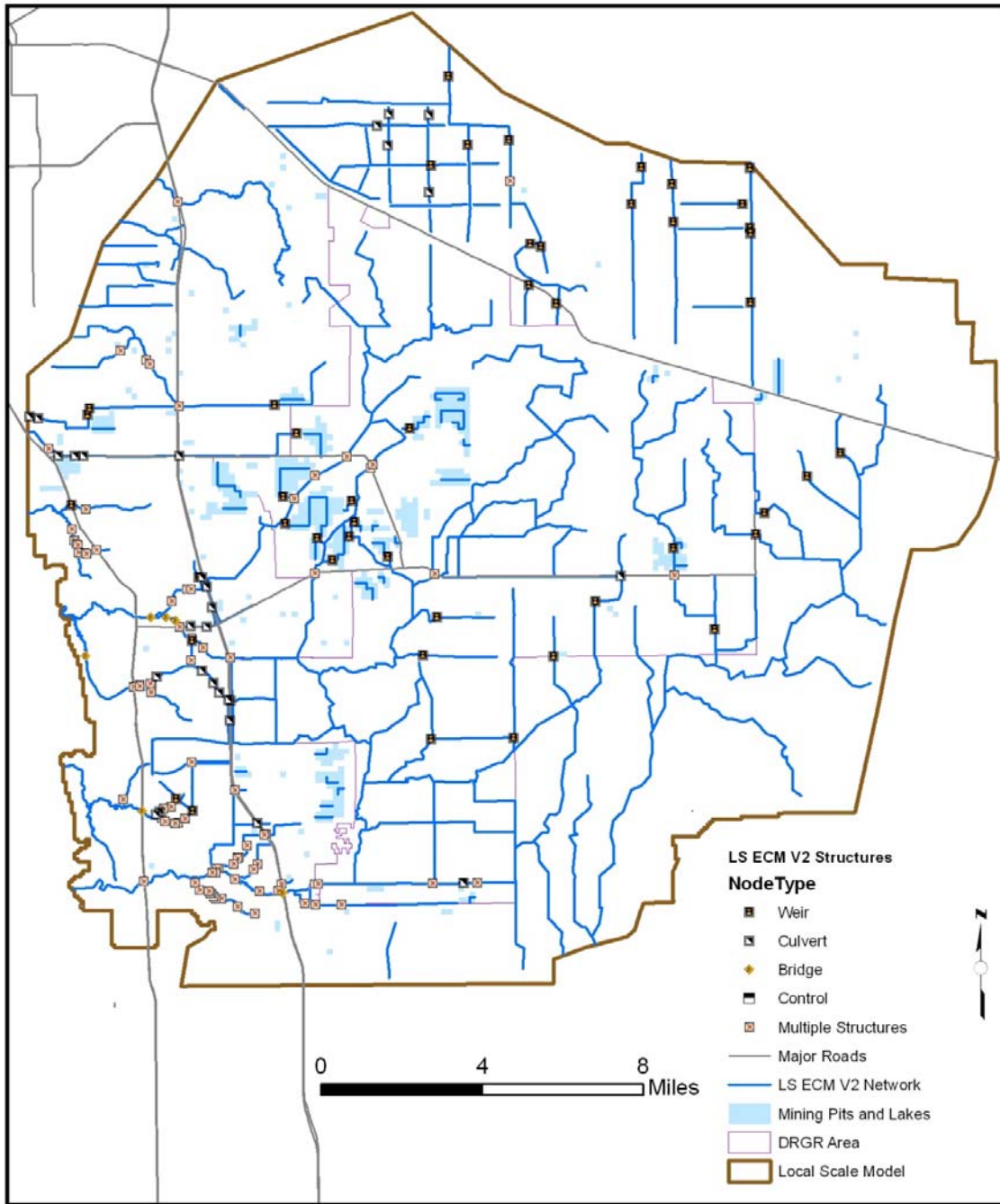
Figure 24. MIKE 11 Network and Structures in the LS ECM.
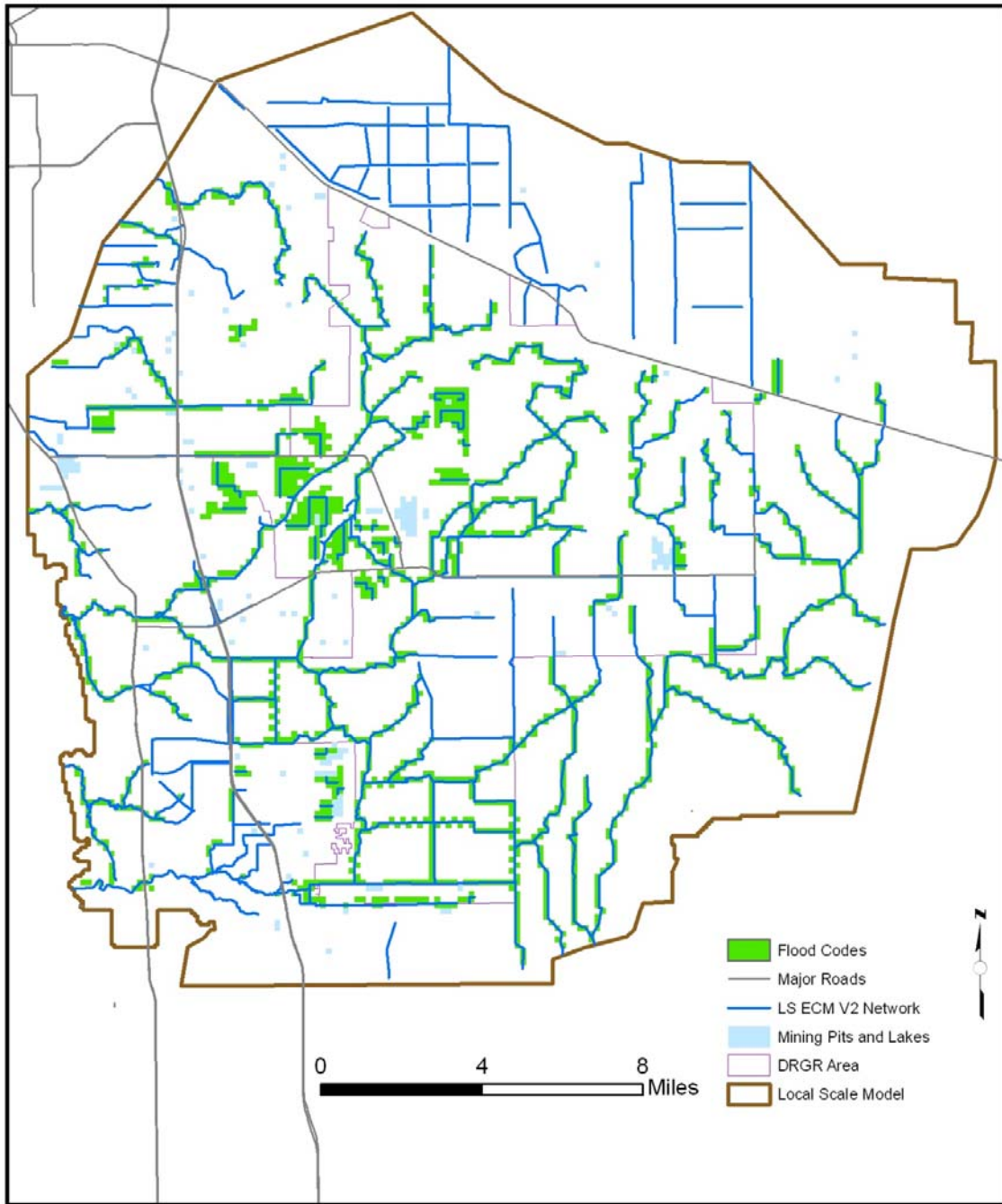
Figure 25. Flood Codes in the LS ECM.
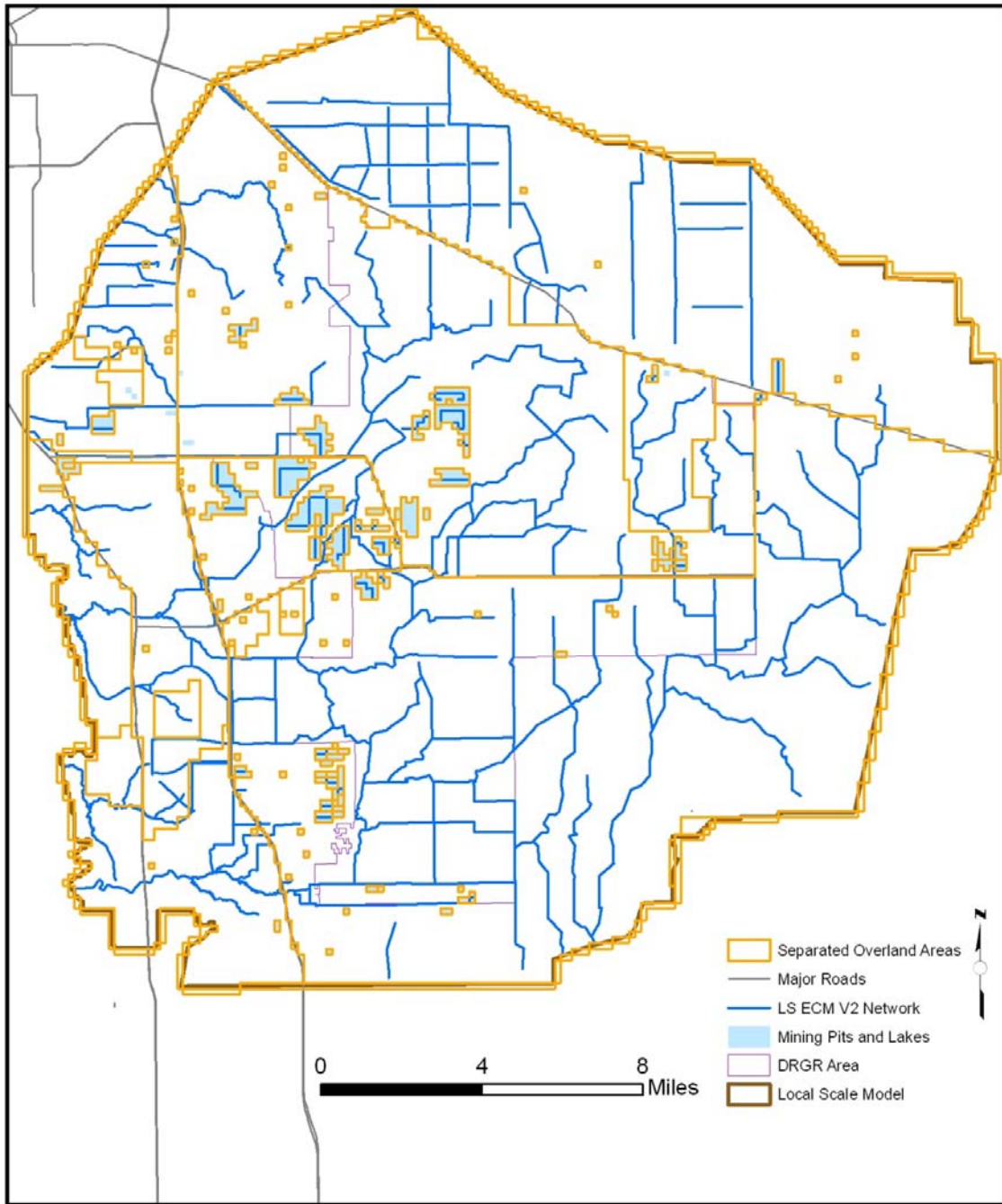
Figure 26. Separated Overland Flow Areas in the LS ECM.

Cross-section Extraction

The cross-section geometry for the MIKE 11 branches was extracted by using the MIKE 11 GIS tool. The 5-ft resolution topographic map was used where available and the SFWMD 100-ft resolution map otherwise. Cross sections were spaced a distance of about two grid cells (~1500 ft). It is recommended to have as many cross-sections as possible to assure a better representation of the channel geometry, but cross-sections spaced less than one grid cell apart may produce instabilities in the model.

In some cases, water in the channel prevented the LIDAR from reaching the channel (or cross-section) bottom. Thus, the cross-sectional geometry of the submerged part was taken from previous surveyed cross-section data. Unfortunately, the LIDAR data was acquired between the months of June and October of 2007 and not at the end of the dry season when the water levels are lower and the bottom of most of the flow ways are dry, which would allow a better estimation of the cross-section geometry from the LIDAR data.

Drainage around Mining Pits

The initial assumption of bermed mining pits used for the ECM is not always the case as revealed following a visual inspection of the high resolution LIDAR topographic map available for the LS ECM development. The fact that some mining pits may be collecting or releasing water from the nearby areas may be relevant to better account for water levels in the mining pits and the discharge rate of nearby flow ways.

The drainage system conceptualized in the MIKE 11 component around some of the mining pits is shown in **Figure 27**. In cases where the mining pit is not fully bermed, a MIKE 11 branch was included to connect the branch that accounts for the standing water at the mining pit and a nearby flow way. A conceptual weir structure is also included in the connecting branch to provide better control of the elevation above which discharge to or from the mining pit occurs.
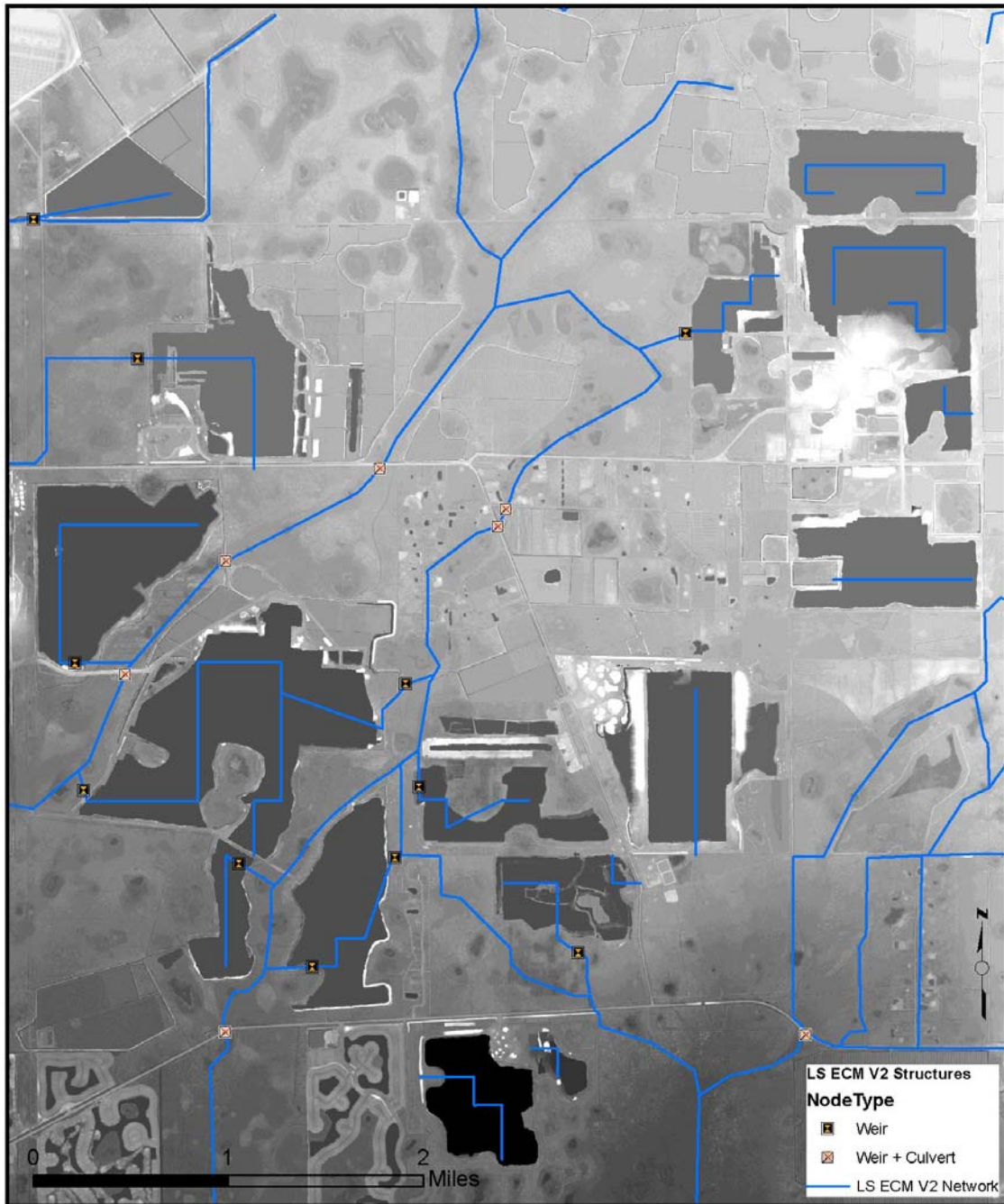
Figure 27. Drainage system around mining pits with a grayscale shaded relief map of LIDAR topographic data in the background.

Note: Lighter areas in the topographic map represent higher elevations, darker represent lower-lying areas.

Model Calibration

Calibration of the ECM and LS ECM was performed for the period of January 1st, 2002 to November 1st, 2007. As part of the model development, considerable effort was spent to improve the representation of certain important features in the model, such as the mining pits and flow ways in the DR/GR Area. Furthermore, a number of model parameters, such as overland flow roughness coefficients, hydraulic conductivities and storage parameters of the geological layers, and subsurface drainage parameters, were tested and varied in order to produce a closer match between model results and observed data. The observation time series data consist of stage and flow time series from surface water stations and of water table levels from observation wells. The surface water data was obtained from DBHYDRO and the groundwater data was obtained from Lee County, DBHYDRO, and the USGS. These data were used to compare the model stages, flows, and groundwater heads at the corresponding locations. For the Lee County Model Area there are a total of 143 groundwater monitoring wells, 31 surface water stage and 10 surface flow stations. Due to the time limitations of this project, DHI and Lee County agreed to focus the calibration of the model on the following areas, listed from highest to lowest priority:

1. The DR/GR Area and the Imperial River Basin.
2. The Orange River basin in the area south of Able Canal.
3. The Six Mile Creek Basin in the area west of the DR/GR.
4. The areas north of Caloosahatchee River and east of the S-79 structure in the freshwater Caloosahatchee River basin.

The calibration was focused primarily on the ECM. However, after extracting the higher resolution model (LS ECM), some additional calibration and improvement efforts continued in both models simultaneously.

After including the changes in the LS ECM derived from the new topographic data, some instability appeared in the MIKE 11 network. Instabilities increase the water balance error and may affect the accuracy of the model results. Moreover, further adjustments were required in the model in order to improve performance at stations where performance had decreased. Thus, a limited-time recalibration was conducted for the LS ECM following the update with the high resolution topographic data.

Model Improvements

As part of the model development, considerable effort was spent to improve the representation of certain important features in the model, such as the mining pits and flow ways in the DR/GR Area. Furthermore, a number of model parameters, such as overland flow roughness coefficients, hydraulic conductivities and storage parameters of the geological layers, and subsurface drainage parameters, were tested and varied in order to produce a closer match between model results to observed data.

ECM

The overall performance of the model was improved by focusing primarily on the DR/GR Area. The most relevant changes in the ECM are summarized below.

1) Some cross-sections and structures in the river network were corrected according to previous sub-regional models. Several cross-section shapes were also modified to meet structure geometry and in other cases to follow the topography. The cross-section widths of flooding branches were adjusted to match the MIKE SHE flood codes. The Manning's roughness coefficients and the leakage coefficient were modified in some of the MIKE 11 branches.

2) The original overland Manning's M (1/n) global values were modified for Hydric Flatwood (3.33 to 4.0), Marsh (1.67 to 2.33) and Cypress (2.5 to 3.33).

3) Additional separated overland flow areas were added to represent flood control features around some agricultural areas in the DR/GR Area. The overland boundary conditions were adjusted in MIKE SHE to represent time-varying conditions.

4) Drain depths and time constants for agricultural areas were decreased to 0.5 ft and 0.25 day^{-1}, respectively; in order to improve the model performance around the DR/GR Area. The drain code map was adjusted to match the separated overland flow areas map in relevant areas. Drainage was set to zero in mining pits. Drain flow was allowed to flow from agricultural and urban areas to the model boundaries.

5) The screen interval and maximum pumping rate in some ICAs were modified based on previous sub-regional models.

6) Mining pits were conceptualized as described in a previous section.

7) The hydraulic conductivities of the different geological layers and lenses were adjusted during the model refinement process. The conductivities for the different geological layers and lenses were taken initially from the SWFFS model. In this model, the conductivity values were recognized as having high uncertainty and they were considered as calibration parameters (CDM, 2006). During an inspection of the resulting conductivity maps, it was found that there were areas with high vertical conductivities in relation to the horizontal conductivities, which may have resulted from these parameters being calibrated independently. In the ECM, the vertical conductivity for the Water Table Aquifer was limited to a value equal to, or lower than the corresponding horizontal conductivity. Also, conductivities of the two confining lenses and the Sandstone Aquifer were considered isotropic. The isotropy assumption is reasonable because in the model the computational layers 2 and 3 are each composed by one lens and one geological layer (Figure 12). The confining units (represented as lenses) are less permeable than the aquifers (represented as geological

layers). Thus, the conductivity of the lens defines mostly the vertical conductivity of the computational layer and the geological layer conductivity defines the horizontal conductivity. The final conductivity maps obtained after the refining process are illustrated in Appendix A.

8) The specific yield in the upper geological layer was changed from 0.2 in most areas to a uniform value of 0.15, as suggested by SFWMD. The results of the model show no significant variation in response to this change.

9) The storage coefficient in the three aquifer layers was changed from a distribution with a mean value of approximately $4*10^{-4}$ ft^{-1} to a uniform value of 10^{-4} ft^{-1}. Seasonal fluctuations in the groundwater head in deep layers were slightly increased by decreasing this coefficient. The storage coefficient in the model could be decreased further to improve the performance of the model in deeper layers. The minimum possible value of the storage coefficient occurs with negligible porous matrix compressibility. Considering the water compressibility is equal to $5.3*10^{-5}$ atm^{-1} and the porosity is equal to 0.2, the minimum possible storage coefficient value is estimated to be $3.1*10^{-8}$ ft^{-1}.

10) A sensitivity test was also performed by splitting the computational layer 3 into two computational layers. With greater vertical resolution (four computational layers), the model took about the same amount of time to run and showed only minor changes in water elevations at observation well stations. Thus, the final ECM has the original three computational layers.

LS ECM

The numerical instabilities were reduced as much as possible in the LS ECM in order to improve the water budget error and the overall model performance.

Most of the instabilities in the MIKE 11 network were observed where the spacing between cross sections is much lower than the MIKE SHE grid cell size (750 ft). When MIKE SHE grid cells interact with the river network, it chooses the cross section location closer to the grid cell center to discharge the water from the drainage and overland components. If the cross sections are not spaced in one grid cell size or higher, MIKE 11 does not have storage assigned for that cross section and a spike in the stage may occur at that point and time while the water is not redistributed through the MIKE 11 branch. This numerical problem is solved by removing cross sections that are spaced too close to each other.

The maximum pumping rate in a few irrigation command areas (ICAs) was refined. This eliminated unrealistic oscillations in the GW head at those locations. The priority scheme in the irrigation module was changed from "none" to "equal shortage", which is more appropriate. Moreover, the ICA code (dfs2) file was filtered in order to remove cells with natural land uses (codes from 7 to 20), which are unlikely irrigated in most of their extent.

Branches in some mining pits were removed to improve the model stability. Also, the hydraulic conductivities (K_h and K_v) in the conceptual mining pit lens were reduced from 1 to 0.1 m/s. All "bed only" leakance in MIKE SHE-MIKE 11 links were changed to "Aquifer + bed", which is more realistic.

For fine-tuning specific areas, the procedure followed to improve model performance varied from one site to another. In general, if there was a MIKE 11 branch involved, the model conceptualization of the area and the model parameters were revised. Typically the model conceptualization was changed and some corrections or adjustments were necessary for cross sectional data, flood codes, Manning roughness coefficients, leakage coefficients and conceptual weir elevations. The conductivity in the groundwater layers was typically adjusted in cases without any close MIKE 11 branches.

The option of "checking water levels before routing" for the case of the paved-area runoff coefficient was enabled to more accurately simulate gravity drainage systems.

Water Table Level in Mining Pits

In order to evaluate the LS ECM performance in mining pits, 62 values of water levels were extracted at different mining pits and lakes in the model domain area from the LIDAR data. Those points correspond to one day of year 2007, in accordance to the LIDAR flight date. The possible flight dates for those locations were June 18, 28 and 29; August 4, 5, and 6; and August 22, 23, and 24.

The mean water table differences between observed values and model predictions at those 62 locations in mining pits and lakes is presented in **Table 10** as computed from different model tests.

- A first intermediate test of the model (identified as LS ECM V1) overpredicts the water table levels on average in mining pits and lakes by 1.0 ft.
    - o This step in the calibration process preceded the introduction of the refined topography or the distributed ET data.
- A second intermediate test of the LS ECM (marked with **) caused an improvement in the first result of 0.3 ft (mean difference of 0.7 ft).
    - o This step uses the refined topographic map, revised flow ways conceptualized in MIKE 11 and drainage in some mining pits. Also uses the same station based ET as the ECM.
- A third intermediate test of the LS ECM (marked with *) caused an improvement of 0.4 ft compared to the second result (mean difference of 0.3 ft).
    - o This step was modified with the new distributed reference ET (RET) data.

- The final version of the model (LS ECM) caused an improvement of 0.3 ft compared to the third step. This gives a net improvement of 1.0 ft, leaving a mean water table difference in mining pits of 0.0 ft. A zero mean difference does not mean that the water levels from the model are exact in all mining pits and lakes, but on average, the over- and under-predictions balance out.
  - In the final version, lake evaporation was modified to a value of RET + 8.0% to be applied in open water cells of the model.

This sequence reveals the importance of the different changes introduced in the model regarding the average water table levels predicted in mining pits, for which the inclusion of the distributed RET and a higher lake evaporation each had about the same impact as the changes caused by the inclusion of the new topography.

In the third test simulation of the model (LS ECM*), which differs from the early version (LS ECM**) due to adjustments during the recalibration, the average water table level differences in mining pits and lakes is less than 0.1 ft (using the absolute differences) for the two lake evaporation values considered of RET + 8.2% and RET + 5.3%, as shown in Table 10. In the final version of the model (LS ECM), obtained after further adjustments, the mean difference (D) is still below 0.1 ft, and the mean absolute difference (DA) is slightly lower than in previous versions.

Table 10. Mean water table differences in mining pits and lakes from several model runs.

Model	ET	LE – ET (% of ET)	D (ft)	DA (ft)
LS ECM V1	SET	0	-1.04	2.68
LS ECM**	SET	0	-0.7	---
	RET	0	-0.3	---
	RET	8.0	0.02	1.68
LS ECM *	RET	5.3	-0.06	1.67
	RET	8.2	0.01	1.66
LS ECM	RET	8.2	-0.07	1.65

Note: "D" stands for mean difference between LIDAR elevation and water level from the model and "DA" for the mean of the absolute differences. The early version of LS ECM is marked with "**" and the preliminary-report version of LS ECM is marked with an "*". See text for details.

Model Performance at Observation Stations

In order to evaluate the model, the performance metrics for groundwater and surface water observation stations were established. The statistical parameters and equations are shown in **Table 11**. Detailed tables and figures with the results at observation stations are presented in Appendix B for the ECM and in Appendix F for the LS ECM. In **Table 12**, the number of stations in three performance level ranges are summarized for different types of observation stations. These metrics are equivalent to those used in the SWFFS regional model for the groundwater stations, but the tolerance levels were reduced for the surface water

stations. A unique indicator of the performance level (PL) per observation station was calculated by averaging the levels of performance (1= high, 2= medium, or 3= low) obtained for each statistical parameter. For example, if the comparison of simulated surface water levels vs. the observed data in a given station results in a correlation value equal to or above 0.8, then the R parameter for this station has a score of 1. The average score for all the parameters in a given station is the PL value for that station.

Table 11. Statistical Parameters used for Calibration of the ECM.

Symbol	Name	Formula
ME	Mean error	$\overline{Obs_i - Calc_i} = \dfrac{1}{n}\sum_{i=1}^{n}(Obs_i - Calc_i)$
MAE	Mean Absolute Error	$\overline{\lvert Obs_i - Calc_i\rvert} = \dfrac{1}{n}\sum_{i=1}^{n}\lvert Obs_i - Calc_i\rvert$
RMSE	Root Mean Square Error	$\sqrt{\overline{(Obs_i - Calc_i)^2}} = \sqrt{\dfrac{1}{n}\sum_{i=1}^{n}(Obs_i - Calc_i)^2}$
R	Correlation Coefficient	$\dfrac{\sigma_{oc}^2}{\sigma_o \sigma_c}$ $\sigma_{oc}^2 = \overline{(Obs_i - \overline{Obs_i})(Calc_i - \overline{Calc_i})}$ $\sigma_o^2 = \overline{(Obs_i - \overline{Obs_i})^2}\quad \sigma_c^2 = \overline{(Calc_i - \overline{Calc_i})^2}$

Table 12. Number of stations for different performance level ranges.

Type of observation point	Model ->	LS ECM		
	PL ->	1.0-1.5	1.6-2.4	2.5-3.0
	Total	Number of stations		
Mining Pits	62	22	24	16
Shallow Wells (Layer=1)	82	48	30	4
Intermediate Wells (Layer=2)	10	6	3	1
Deep Wells (Layer=3,4)	6	0	2	4
Surface Water	23	8	14	1

Note: "PL" stands for average performance level.

For stations where the model was underperforming, a visual inspection of the model results versus the observed data was conducted. This inspection was used to identify potential outliers in the observation files and other possible causes for the differences. Finally, the

average hydroperiod information received from KLECE for the DR/GR Area was utilized to perform a comparative evaluation of the hydroperiod predicted by the model within the DR/GR Area and to adjust the parameters to improve the model performance.

Water Table Elevation

Water table elevation maps predicted by the model are presented at two times of the year in **Figure 28** and **Figure 29**, corresponding to the end of the dry and wet season, respectively. Water table profiles along two transects in the DR/GR mining complex area (see **Figure 30**) are also presented in **Figure 31** to **Figure 34** at those times of the year for different models.

In the transect plots, the lower water table levels in mining pits and surrounding areas predicted from the LS ECM (identified as V2 in the figures) are noticeable with respect to the levels from the V1 model at the end of the dry and wet seasons. This is in accordance with the average 1-ft overprediction of the V1 model in the water table levels in mining pits that was removed through the calibration process (see Table 10). However, the differences in average water table levels between LE equal to 5.3% or 8.2% higher than RET are small, in correspondence with Table 10.
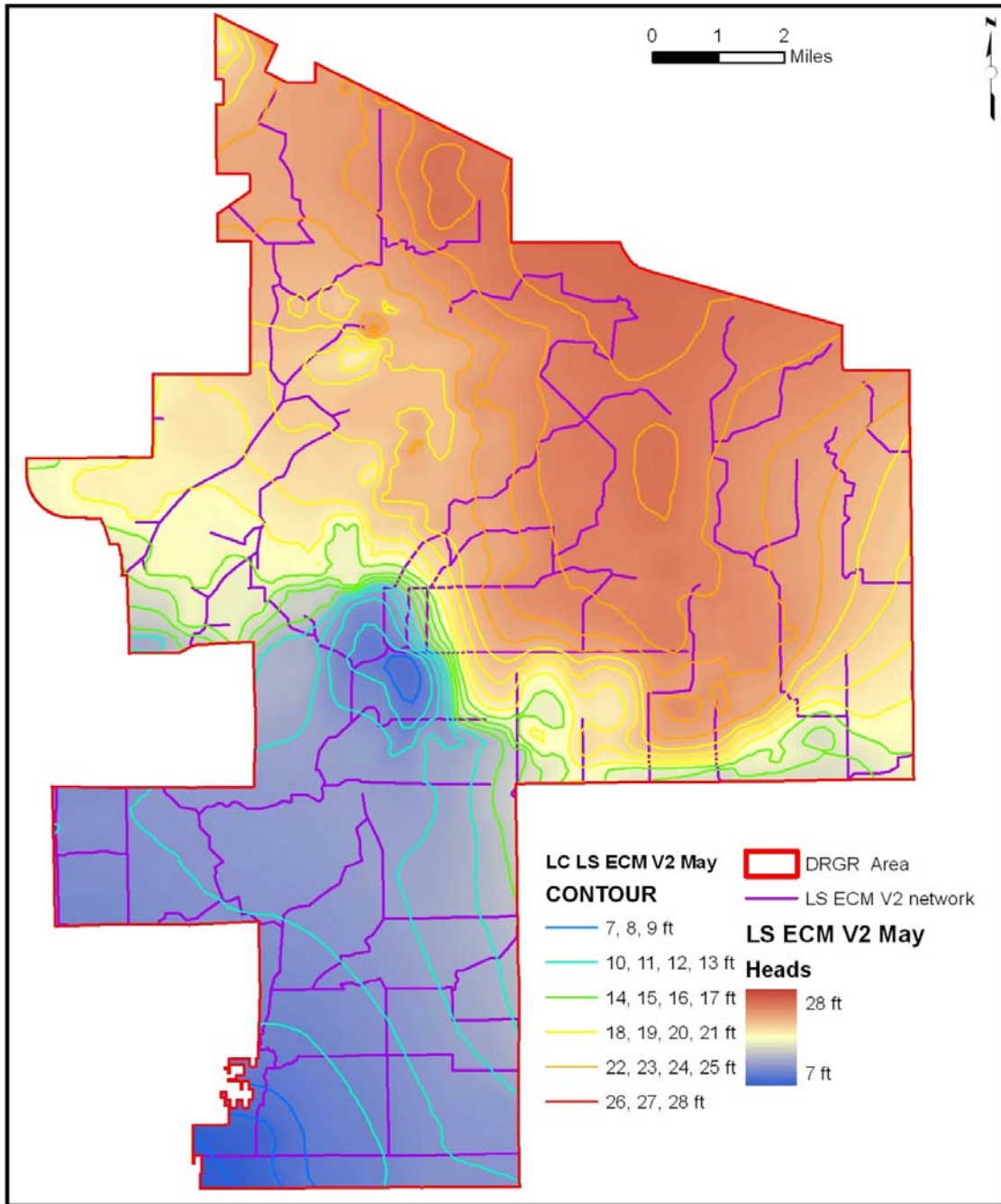
Figure 28. Average water table level map for the DR/GR Area at the end of the dry season as predicted by LS ECM.
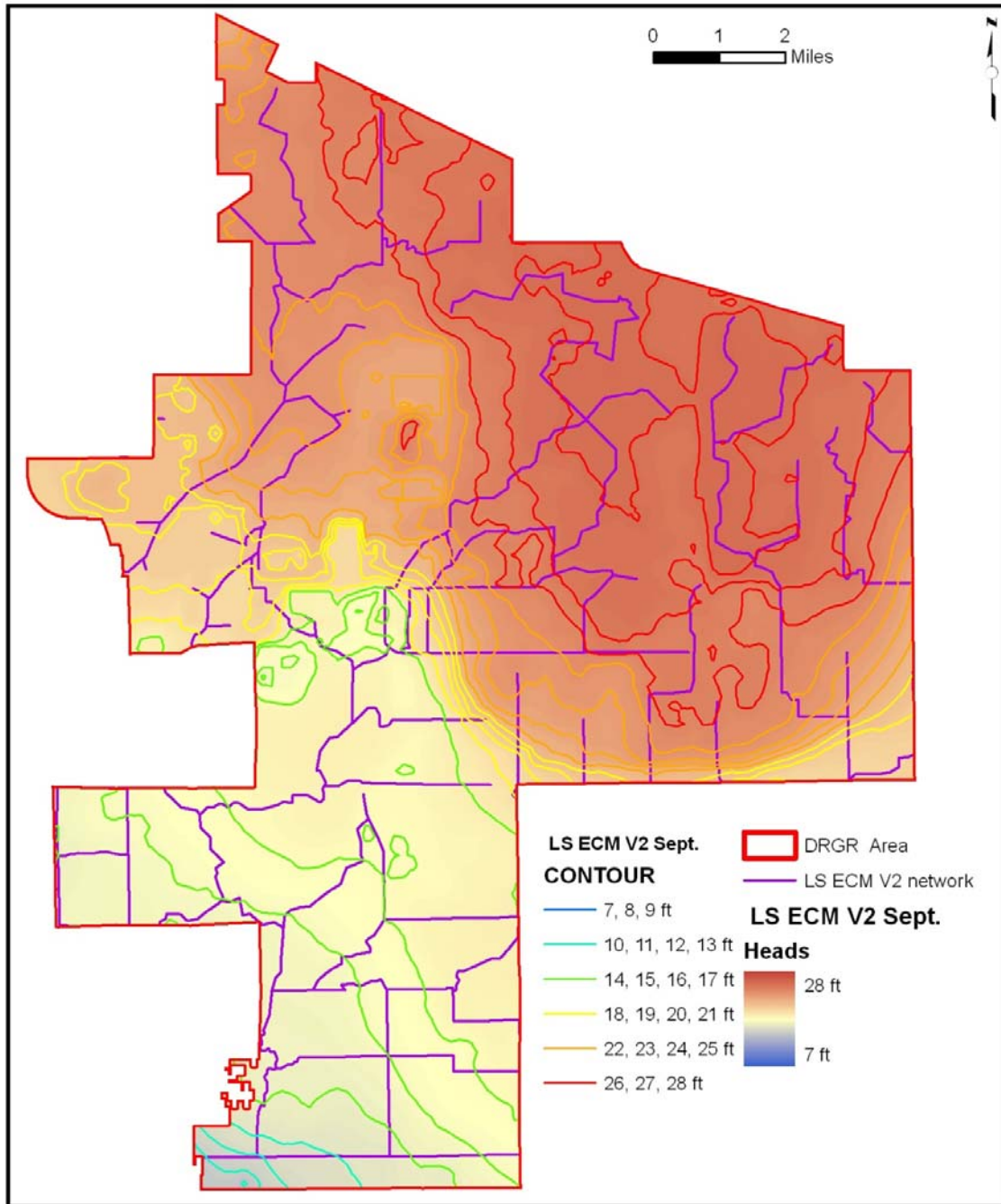
Figure 29. Average water table level map for the DR/GR Area at the end of the wet season as predicted by LS ECM.
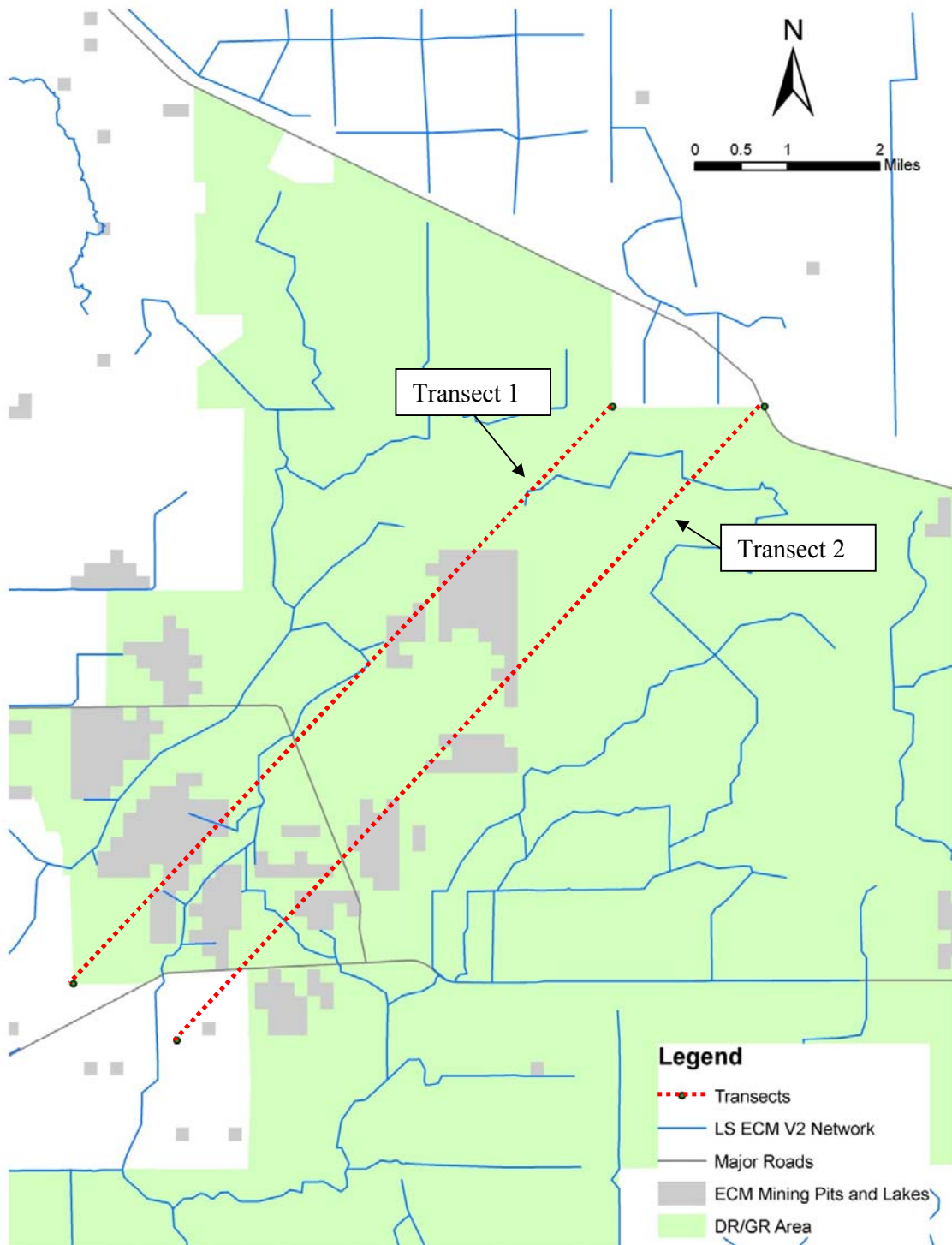
Figure 30. Transects through the mining pit complex area used to generate the water table level profiles presented from Figure 31 to Figure 34.
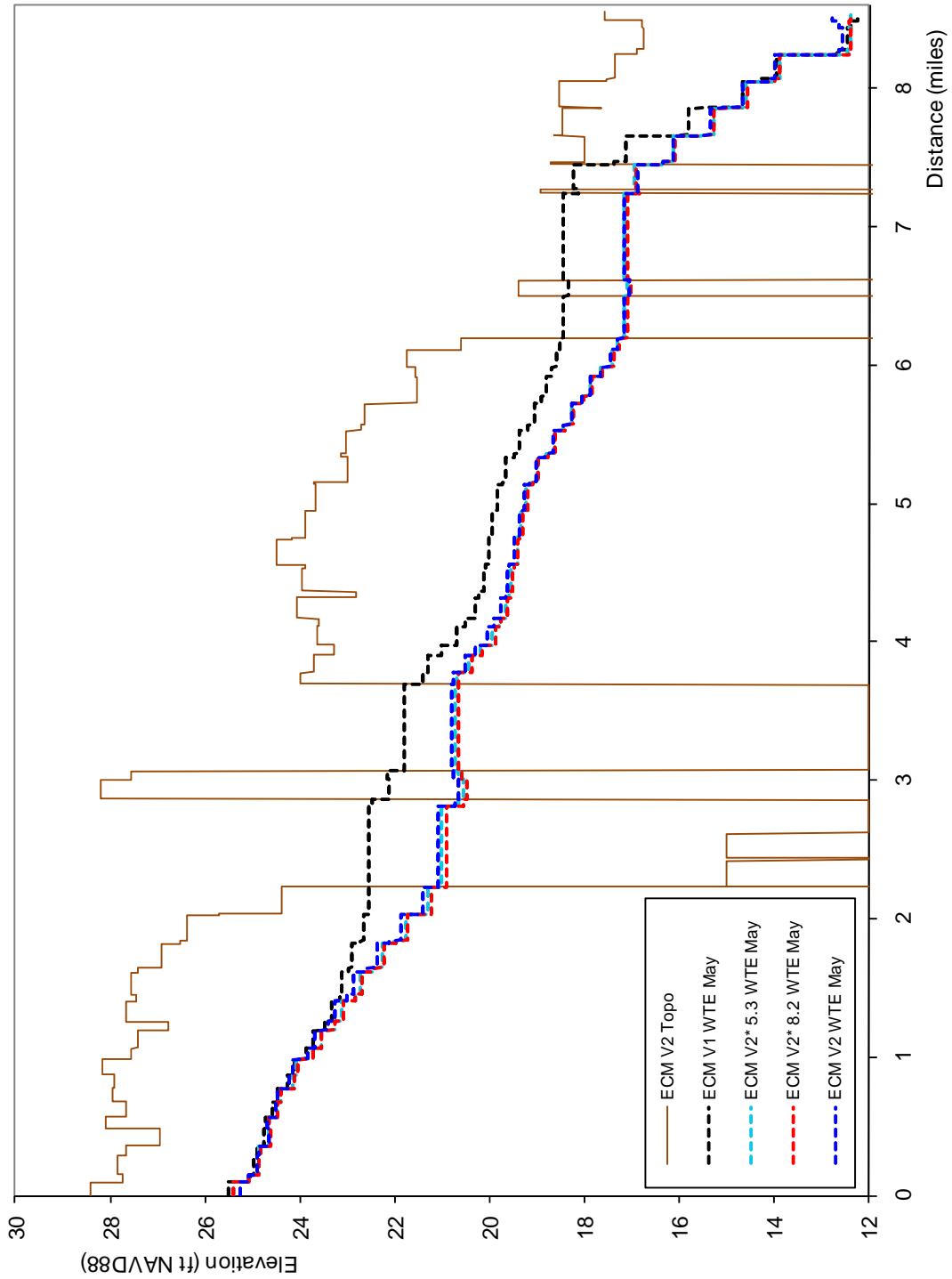
Figure 31. Water table level profile along Transect 1 presented in Figure 30 at the end of the dry season. The numbers 5.3 and 8.2 refer to the value in percent of LE - RET used.
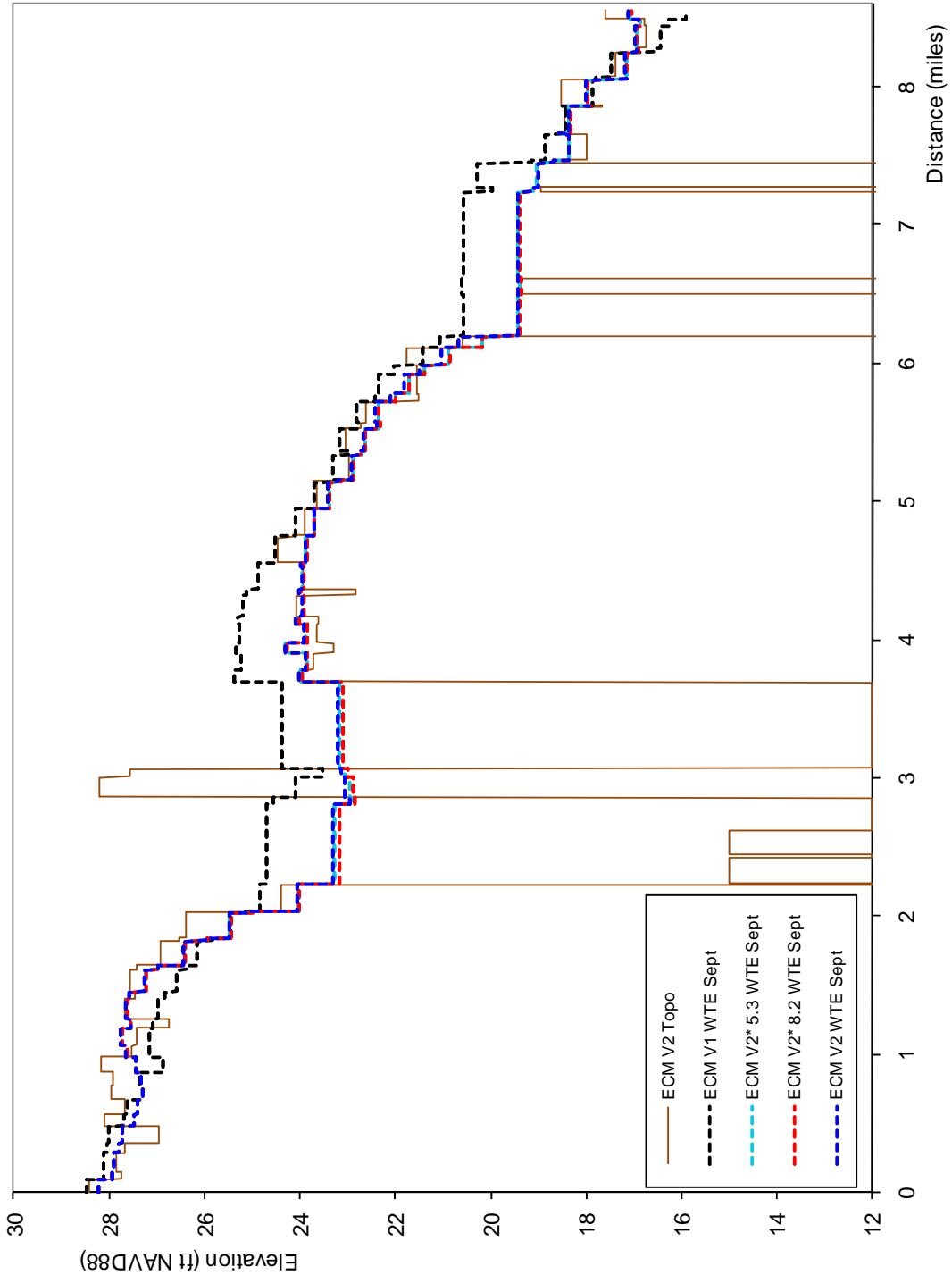
Figure 32. Water table level profile along Transect 1 presented in Figure 30 at the end of the wet season. The numbers 5.3 and 8.2 refer to the value in percent of LE - RET used.
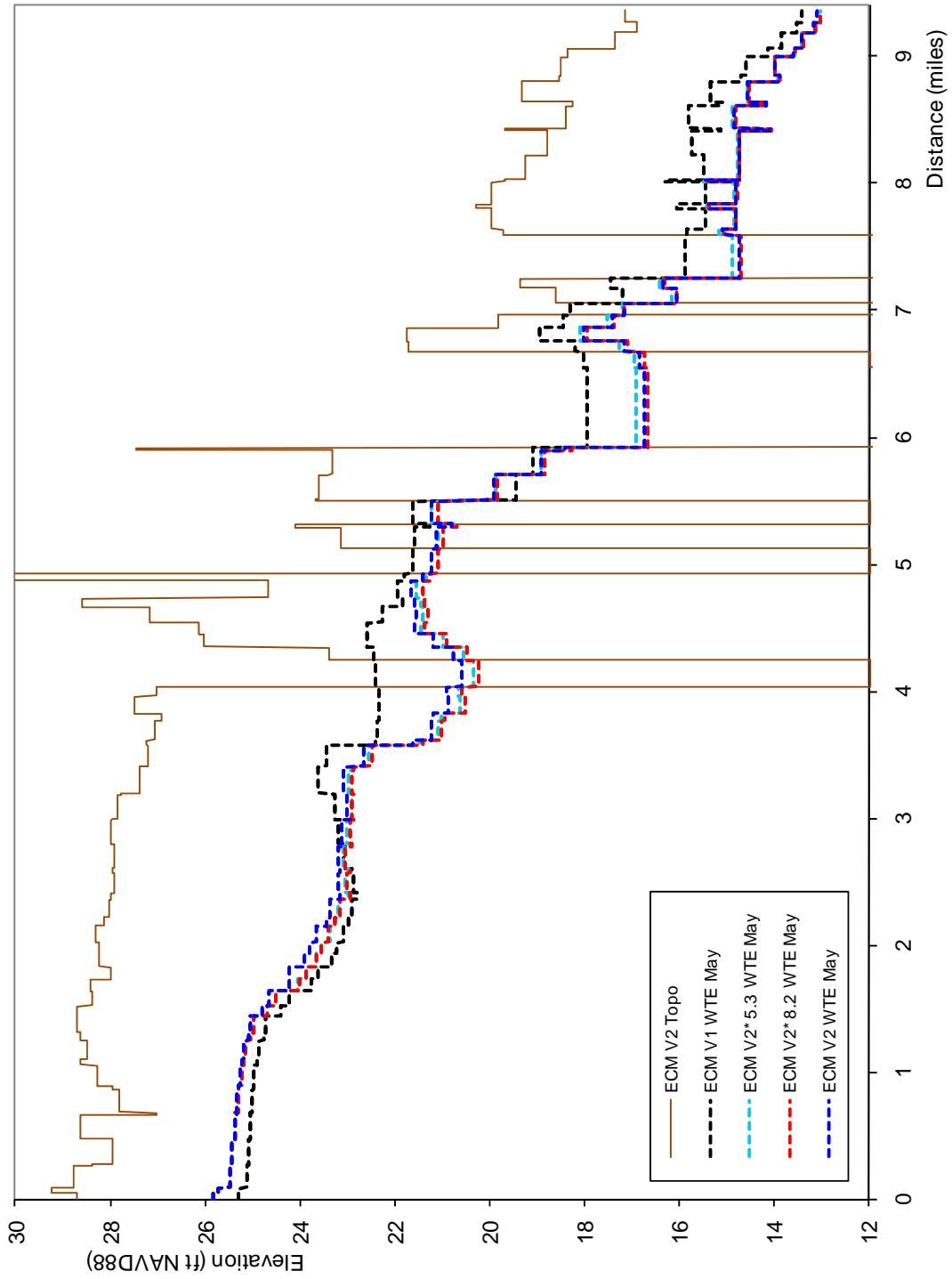
Figure 33. Water table level profile along Transect 2 presented in Figure 30 at the end of the dry season. The numbers 5.3 and 8.2 refer to the value in percent of LE - RET used.
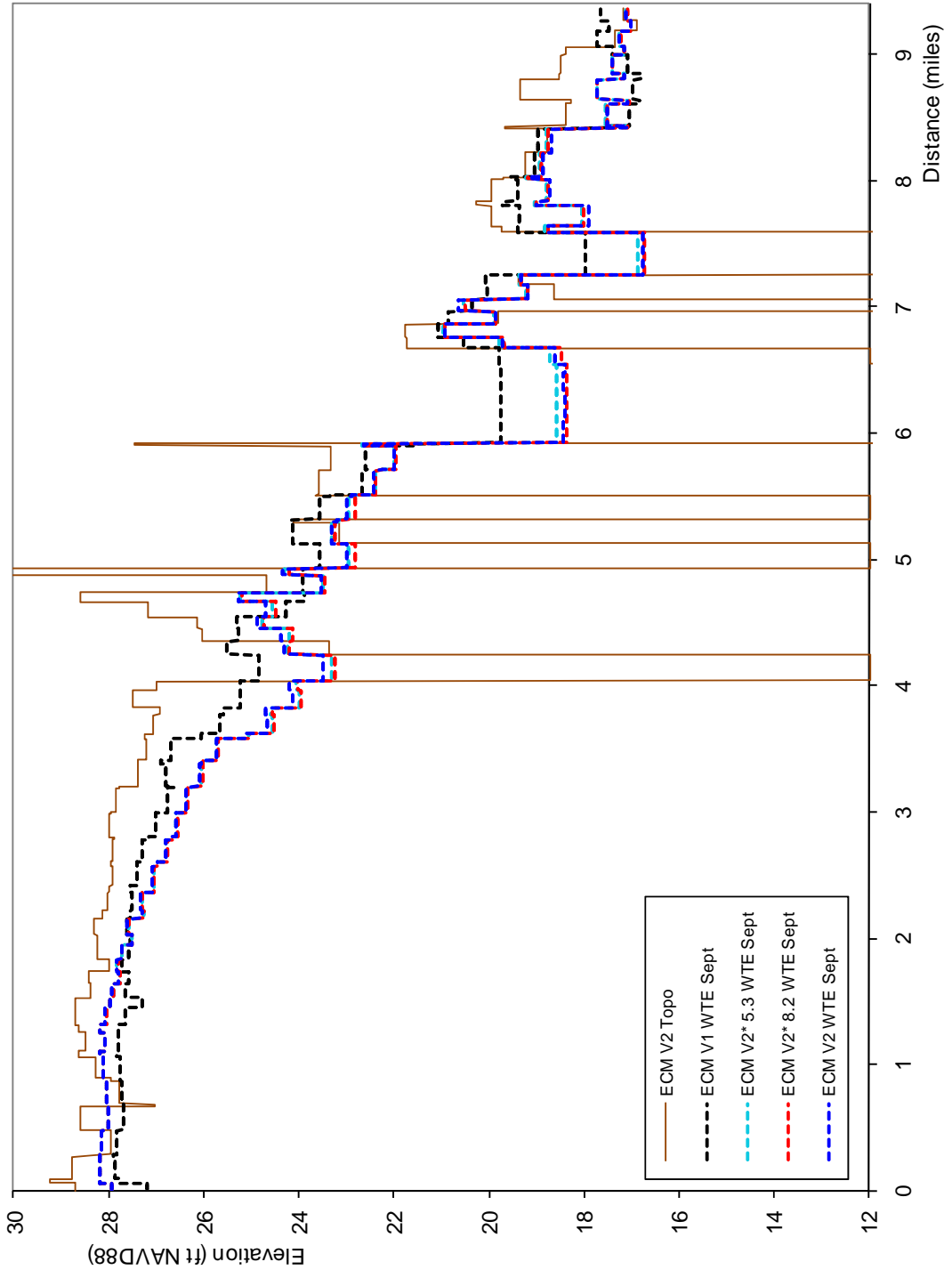
Figure 34. Water table level profile along Transect 2 presented in Figure 30 at the end of the wet season. The numbers 5.3 and 8.2 refer to the value in percent of LE - RET used.

Hydroperiod

The determination of the wetland hydroperiod has been an important indicator used in this study. A wetland hydroperiod has several definitions, but for this evaluation it is defined as the period during which water in the model is at least 1 mm above the topographic surface. The simulated wetland hydroperiod for the DR/GR Area was qualitatively compared with hydroperiod maps generated based on data created by KLECE [2008]. The model follows similar general trends but the comparison is limited due to the coarser resolution of the model in comparison to the map from KLECE data. The scaling limitations are evident when comparing the results of the local higher resolution model hydroperiod map to the KLECE map with higher resolution. Nevertheless, the hydroperiod output of the model together with the water table elevation and the water balance computation provide useful insight into the impact of the land use changes on wetland areas.

The hydroperiod data developed by KLECE is based on the vegetation communities, which have been mapped from GIS data and aerial photographs taken in 2007. This hydroperiod map was generated based on the estimated relationships among vegetation, hydroperiod, and water depth conditions. These are shown in the legend on **Figure 35**. According to KLECE, the estimated water depths and hydroperiods are typical ranges of conditions for unaltered wetland systems in southwest Florida (KLECE 2008). These relationships have not been compared with measured water level data, though. Thus, a quantitative or direct comparison between this hydroperiod map and the one produced by the model is not appropriate.

The hydroperiod map for the DR/GR Area and the corresponding map of mean water depths during the hydroperiod obtained from the model are presented in **Figure 36** and **Figure 37**, respectively. Other related maps can be found in Appendix H.

The hydroperiod map obtained from LS ECM* does not differ visibly when the lake evaporation changes from RET + 5.3 to RET + 8.2 (see maps in Appendix H). The same applies for the water depth maps during the hydroperiod. Thus, the hydroperiod maps do not show visible sensitivity to that change in lake evaporation.
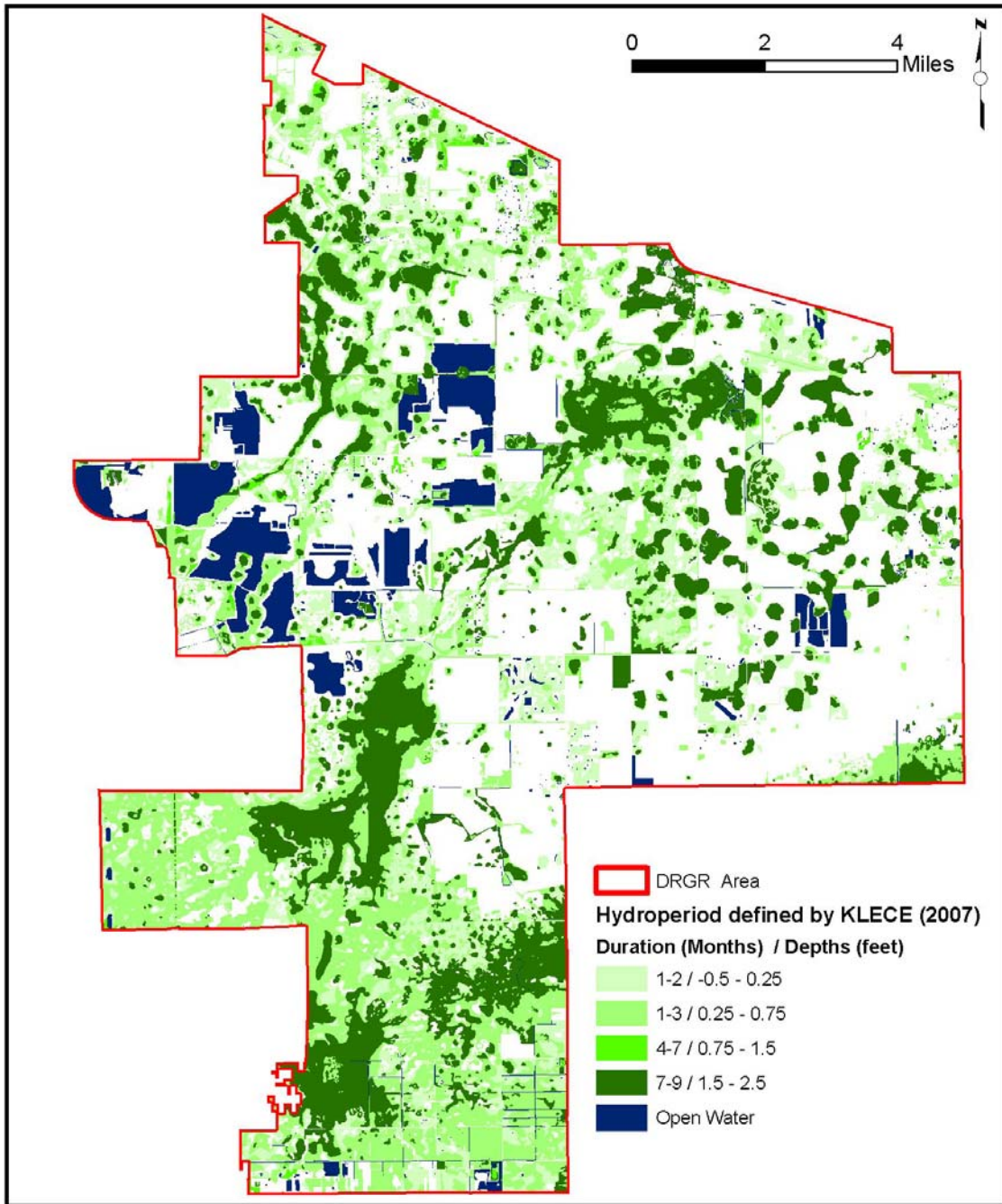
Figure 35. Hydroperiod map generated based on data created by KLECE from 2007 aerial photos.
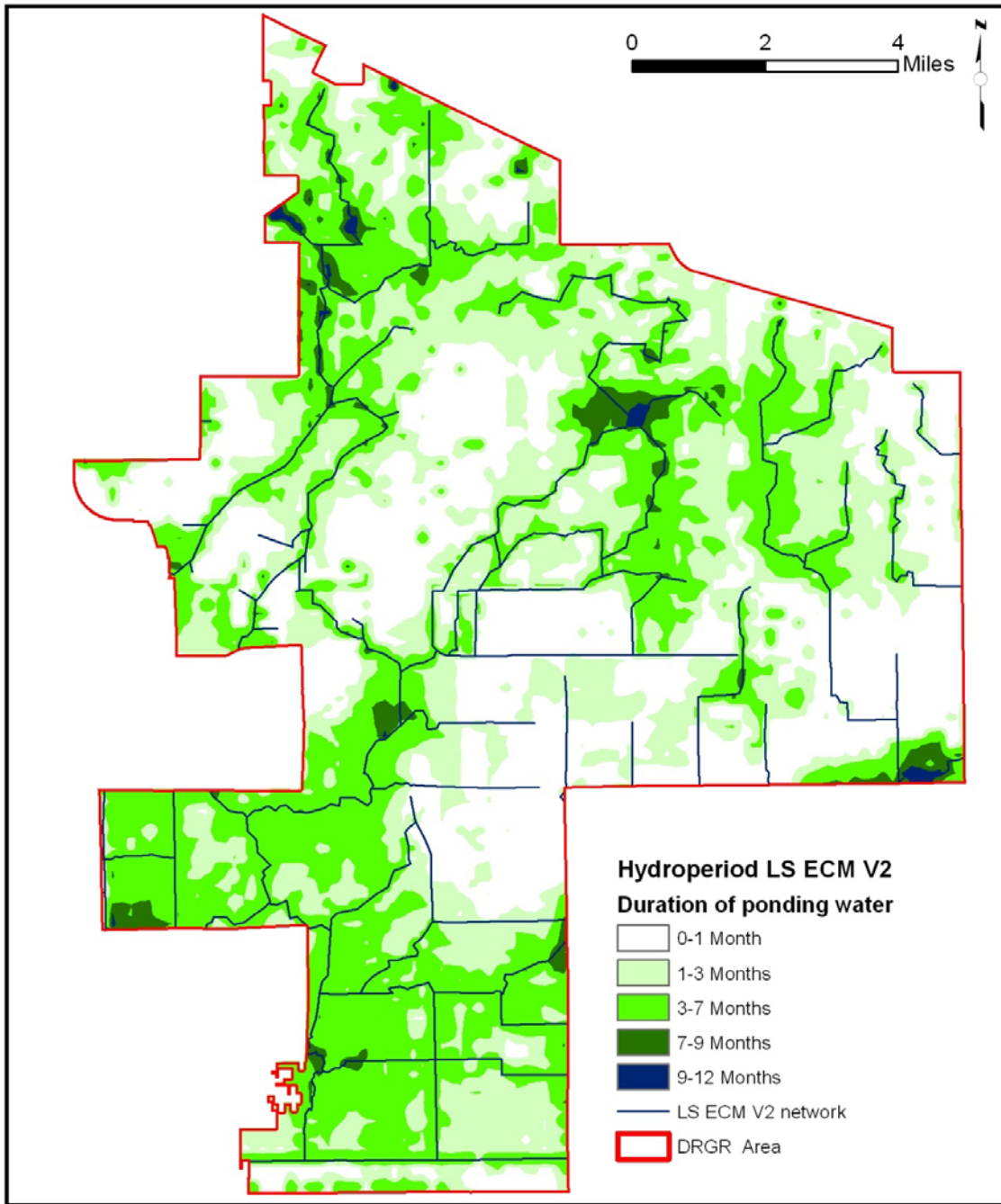
Figure 36. Hydroperiod map obtained from LS ECM.
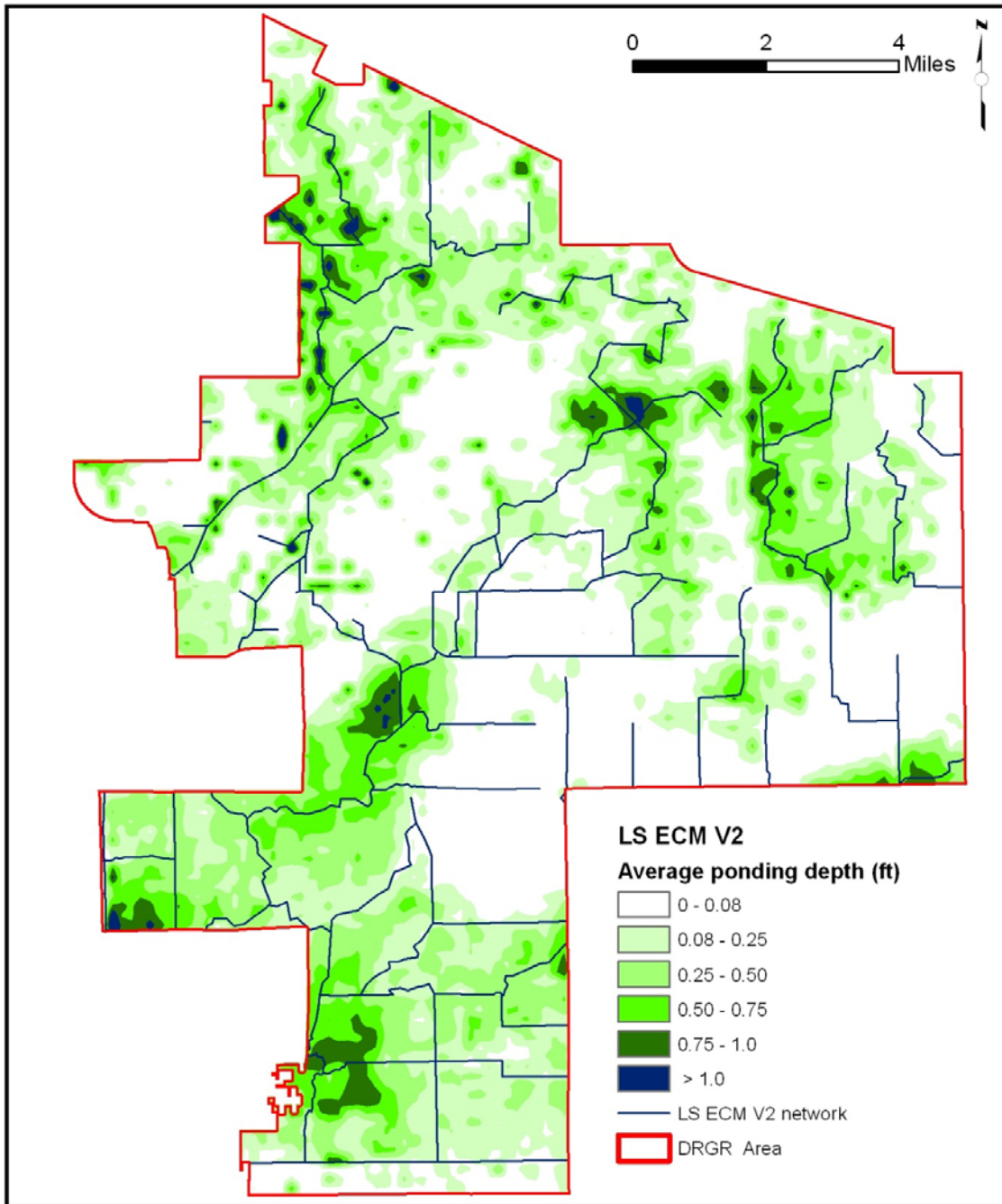
Figure 37. Hydroperiod water depth map obtained from LS ECM.

Water Budgets

A sketch of annual averaged water balance components obtained from the LS ECM in the entire DR/GR Area and in mining pits and shallow water bodies around the DR/GR area is presented in **Figure 38** and **Figure 39**, respectively. In **Table 13**, the water balance components from the final model and two intermediate models are displayed for comparison of the impact the lake evaporation has on the overall water budgets. All those water balance depth rates reported are annual averaged values for the 5-year period from 2002 to 2006.

Naturally, the increased ET rates in the open water bodies decreases the net rainfall (rainfall minus ET) in these areas. In fact, a lake evaporation of RET + 8.2% produces a net rainfall of zero inches per year in mining pits and lakes. Furthermore, the inclusion of a drainage system in some mining pits causes a net surface water outflow from mining pits and lakes in the model. As a result, the model predicts a negative groundwater outflow from the mining pits and open water bodies.

The overall water budget in the DR/GR area indicates that the higher ET rate and other changes made to the model causes a reduced boundary outflow through the groundwater, overland layers, and also through the rivers.
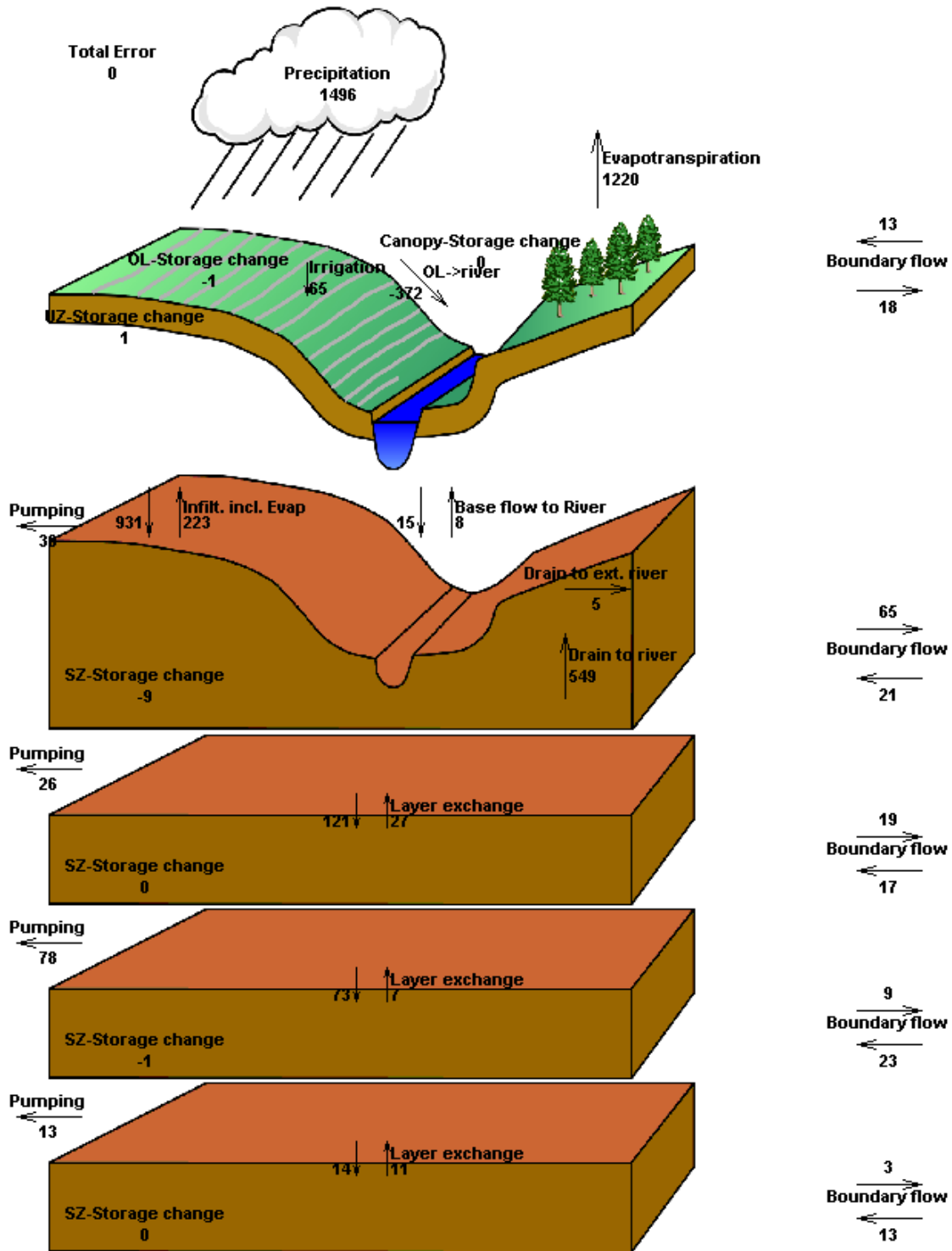
Figure 38. Annual averaged water balance components in mm/yr for the entire DR/GR Area as predicted by the LS ECM.
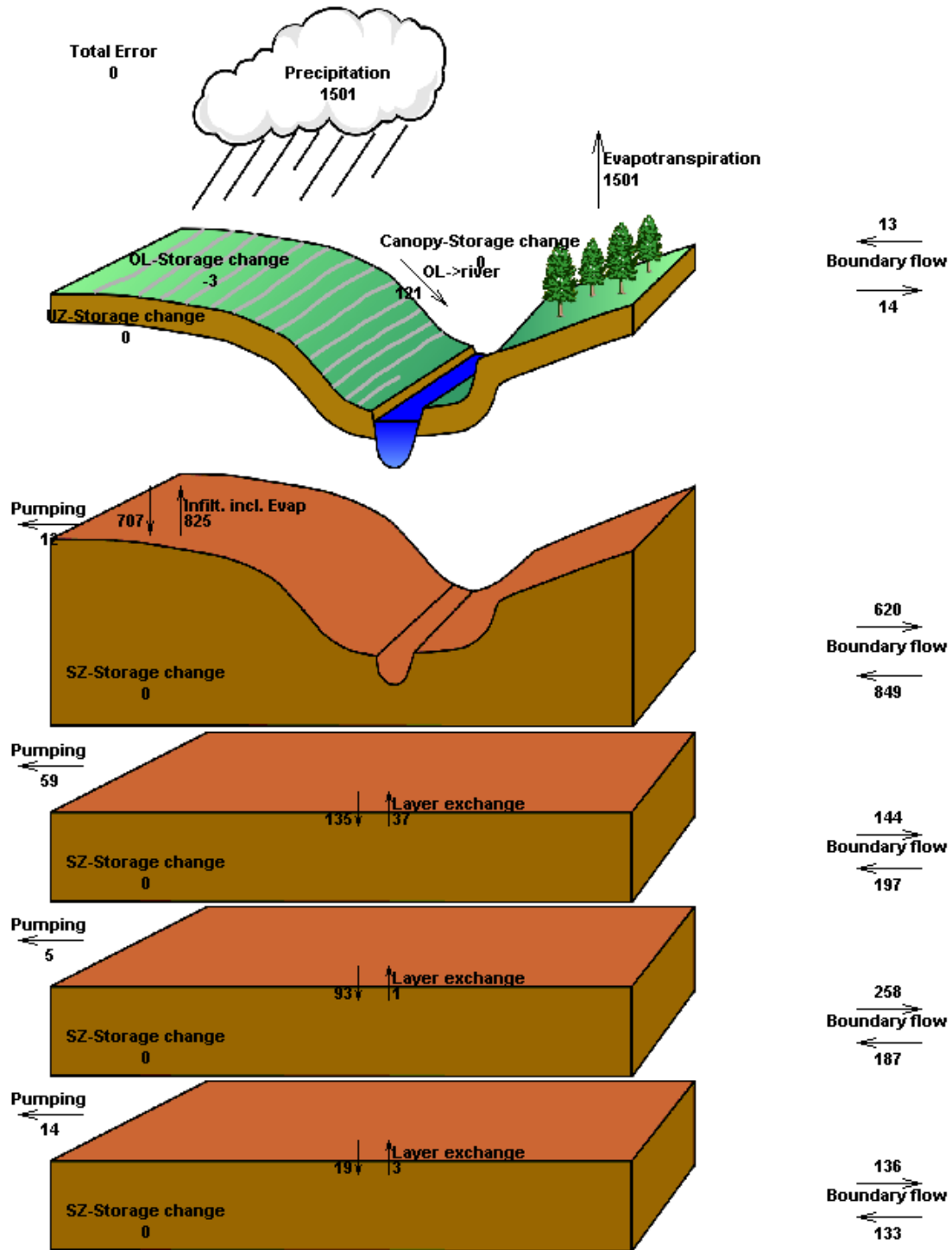
Figure 39. Annual averaged water balance components in mm/yr for the mining pits and other shallow water bodies around the DR/GR Area as predicted by the LS ECM.

Table 13. Annual average depth rates of the water balance components from the different versions of LS ECM, different ET data and in two different areas: in the entire DR/GR and in the Mining Pits and shallow water bodies in and around the DR/GR Area.

Area		DR/GR			Mining Pits		
LS ECM version		ECM*	ECM*	ECM	ECM*	ECM*	ECM
ET		RET	RET	RET	RET	RET	RET
Depth rates (inches/year)	**LE - ET (% of ET)**	**5.3**	**8.2**	**8.2**	**5.3**	**8.2**	**8.2**
Rainfall		58.9	58.9	58.9	59.1	59.1	59.1
ET		48.1	48.1	48.0	57.5	59.1	59.1
Rainfall - ET (A)		**10.8**	**10.7**	**10.9**	**1.6**	**0.0**	**0.0**
OL storage change		0.0	0.0	0.0	-0.2	-0.2	-0.1
UZ Storage change		0.0	0.0	0.0	0.0	0.0	0.0
Total SZ Storage change (BSZ)		-0.4	-0.4	-0.4	0.0	0.0	0.0
Total storage (B)		**-0.4**	**-0.4**	**-0.4**	**-0.2**	**-0.2**	**-0.2**
Net OL Boundary outflow (COL)		0.1	0.1	0.2	0.0	0.0	0.0
Drain to Boundary (CDR)		0.0	0.0	0.0	0.0	0.0	0.0
Net SZ Boundary outflow from SZ1		1.7	1.7	1.7	-8.0	-9.0	-9.0
Net SZ Boundary outflow from SZ2		0.0	0.0	0.1	-2.1	-2.2	-2.1
Net SZ Boundary outflow from SZ3		-0.6	-0.6	-0.5	3.0	2.9	2.8
Net SZ Boundary outflow from SZ4		-0.4	-0.4	-0.4	0.2	0.1	0.1
Net SZ Boundary outflow from all SZ (CSZ)		0.8	0.8	0.9	-7.0	-8.2	-8.2
Total Boundary outflow (C)		**0.9**	**0.9**	**1.1**	**-7.0**	**-8.1**	**-8.2**
Pumping from SZ1		1.5	1.5	1.2	0.6	0.6	0.5
Pumping from SZ2		1.1	1.1	1.0	2.5	2.5	2.3
Pumping from SZ3		3.3	3.3	3.1	0.2	0.2	0.2
Pumping from SZ4		0.5	0.5	0.5	0.6	0.6	0.6
Pumping from all SZ		6.4	6.4	5.8	3.8	3.8	3.6
Irrigation		3.2	3.2	2.5	0.0	0.0	0.0
Pumping-Irrigation (D)		**3.2**	**3.2**	**3.2**	**3.8**	**3.8**	**3.6**
Infiltration from OL to SZ1		27.5	27.4	27.9	-3.2	-4.4	-4.7
Infiltration from SZ1 to SZ2		3.9	3.9	3.7	4.2	4.0	3.9
Infiltration from SZ2 to SZ3		2.8	2.8	2.6	3.8	3.8	3.6
Infiltration from SZ3 to SZ4		0.1	0.1	0.1	0.7	0.7	0.7
OL->river		-13.7	-13.6	-14.7	4.9	4.5	4.8
Drain to river		20.7	20.6	21.6	0.0	0.0	0.0
Drain to ext. river		0.2	0.2	0.2	0.0	0.0	0.0
Base flow to River		-0.2	-0.2	-0.3	0.0	0.0	0.0
Total flow to river (E)		**7.0**	**7.0**	**6.9**	**4.9**	**4.5**	**4.8**
Error (A-B-C-D-E)		0.0	0.0	0.0	0.0	0.0	0.0
Boundary surface outflow (runoff)	COL+CDR+E	7.2	7.1	7.1	5.0	4.6	4.8
	COL+CDR	---	---	---	---	---	---
Net groundwater recharge	A-(B-BSZ)-(C-CSZ)-E= BSZ+CSZ+D	3.6	3.6	3.7	-3.2	-4.4	-4.7
	A= B+C+D+E	---	---	---	---	---	---

Note: the preliminary version of LS ECM is marked with an "*".

Surface Water Flow

Figure 40 shows the annual average flow rate in the MIKE 11 network as predicted with the LS ECM from year 2002 to 2006. Primary flow ways are the ones having higher averaged flow rates. The sudden changes in color in the branches primarily indicate the interaction with the overland component of MIKE SHE, i.e., locations where water is flowing between the rivers and the flood plains. The annual average flow map suggests that the MIKE 11 network generated following incorporation of the high resolution LIDAR data into the LS ECM more accurately represents the main flow ways in the DR/GR Area compared to its performance prior to the reanalysis of the flow ways. Further refinement in the network can be conducted by removing branches with negligible flow (that are not visible in Figure 40) and by checking the path and cross section geometry in locations with high interaction with overland flow.

A closer look to the annual average flow rate through the conceptual weirs around mining pits (that were introduced to represent the drainage system) is presented in **Figure 41**. Single sided arrows are used to represent the net flow direction and double sided arrows are used where there are important flows in both directions. The instantaneous flow rates at some of those weirs are plotted in **Figure 42**. According to the model, mining pits with conceptual weirs at locations D and G may serve as reservoirs, collecting water during the rainy season and releasing it early in the dry season. Mining pits with conceptual weirs at locations E-F and I-J may serve to route surface water in the southwest direction. A positive or negative net annual flow rate into a mining pit may indicate whether the specific mining pit is contributing to the groundwater recharge or discharge, respectively. The drainage system around the mining pits is based on LIDAR data elevations and other model assumptions. Observation data to compare and validate those model results were not available at that time.
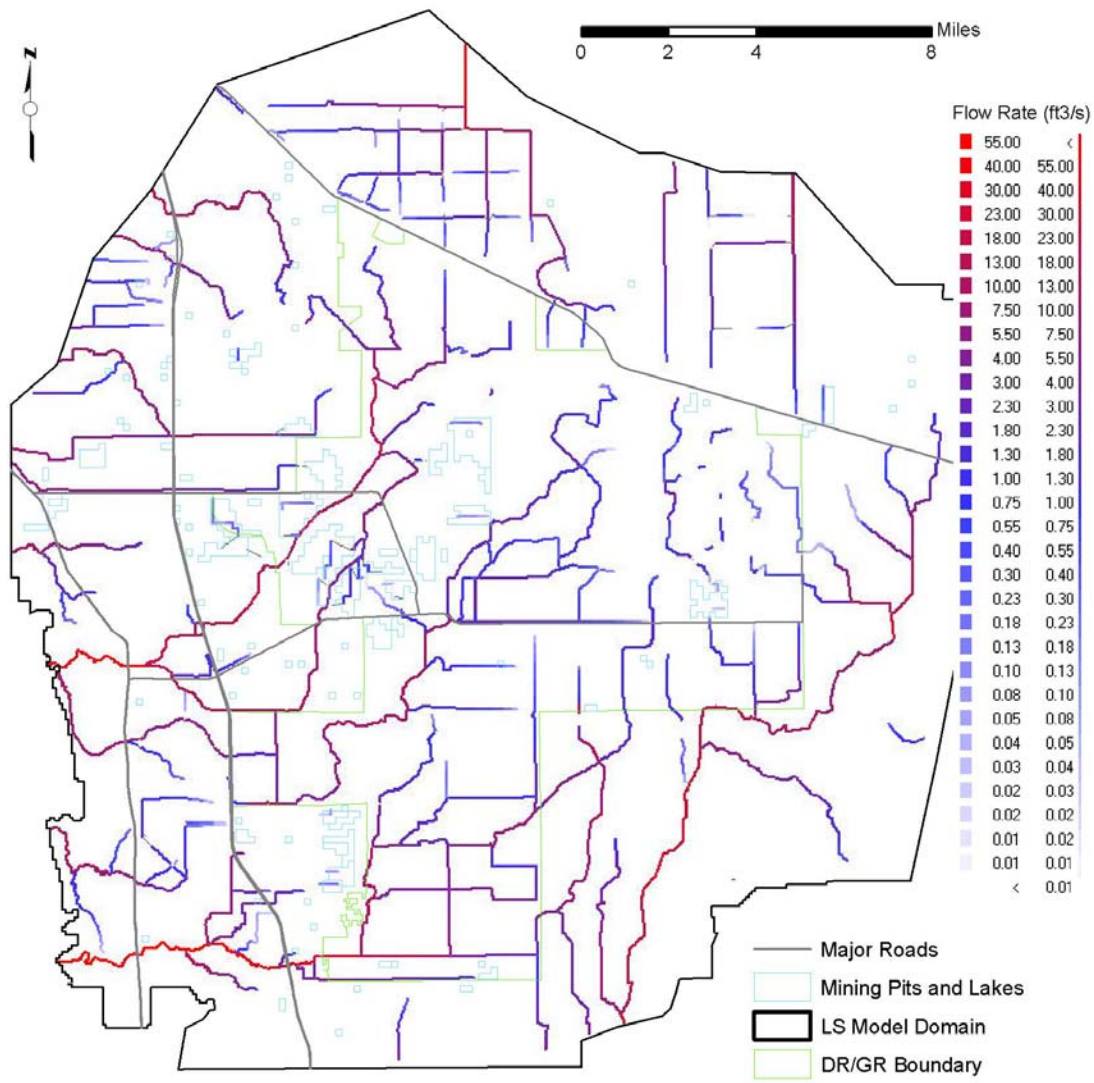
Figure 40. Annual averaged flow rates obtained at the river network from the LS ECM**.**
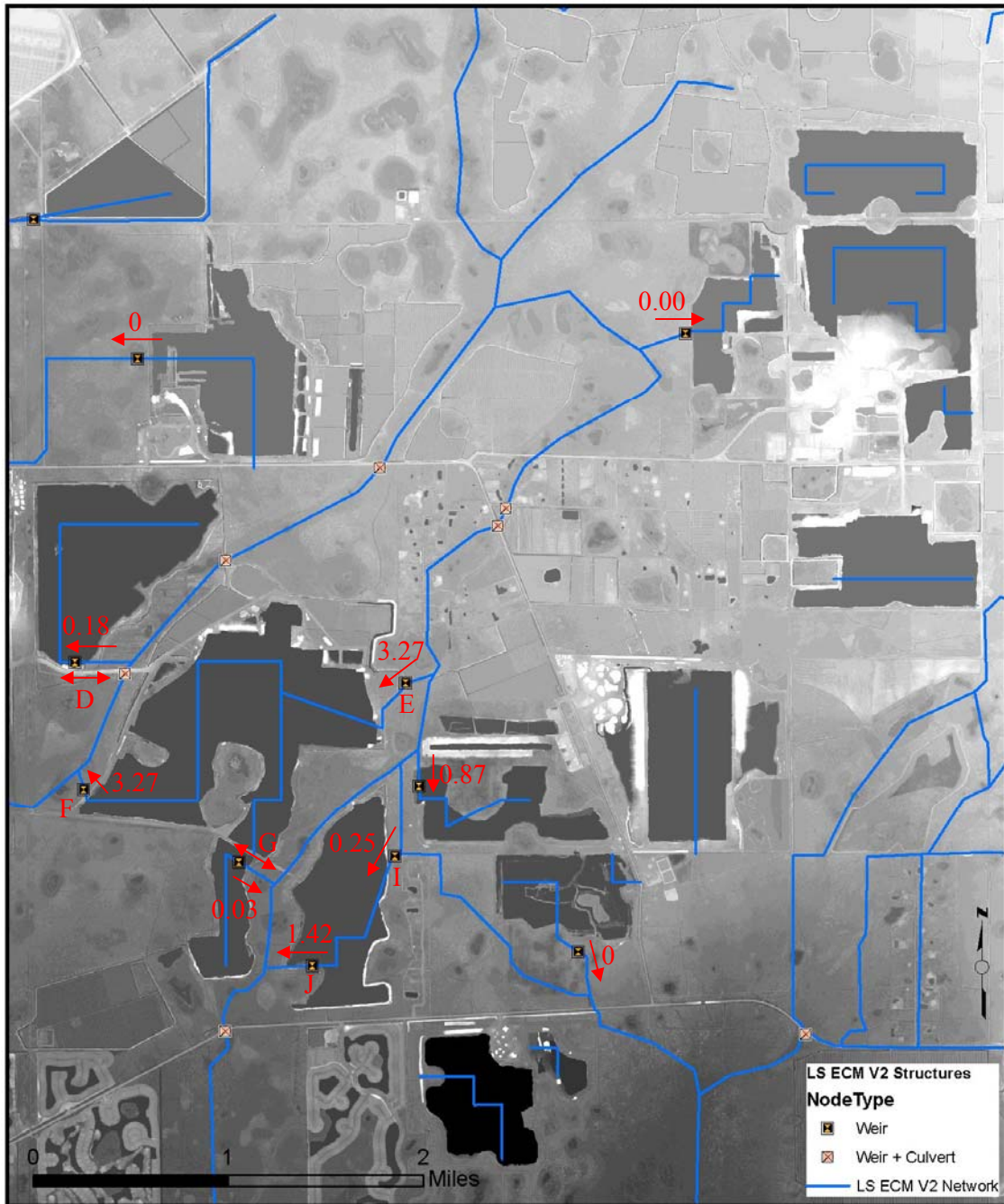
Figure 41. Annual averaged flow rates (in ft³/s) in the drainage system around mining pits as obtained from the LS ECM.
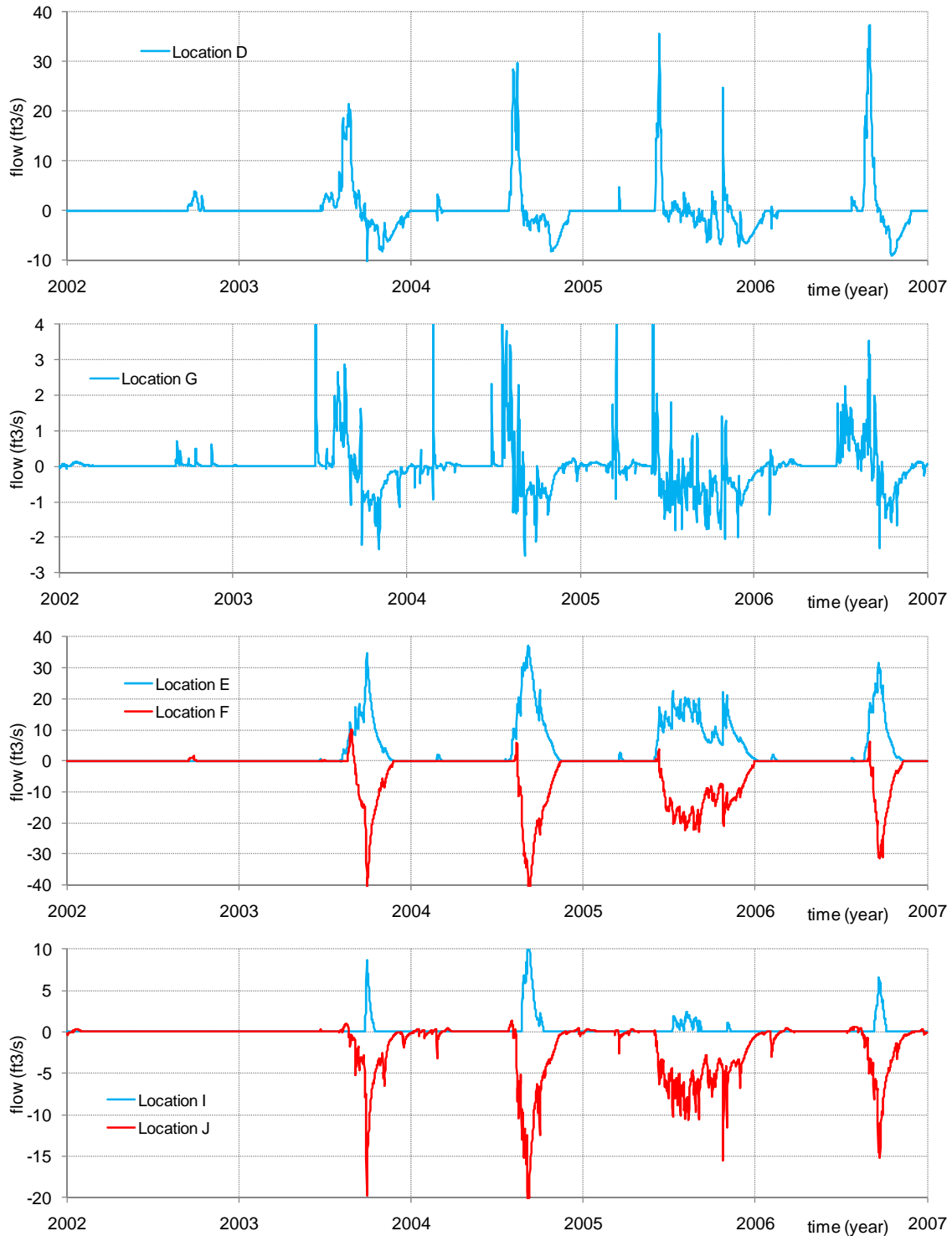
Figure 42. Flow rates at some conceptual weirs around mining pits presented on Figure 41.
Note: solid blue and red lines are used when positive flow is toward and away from the mine, respectively**.**

Land Use Scenarios

In order to evaluate the hydrological effects of land use changes in the DR/GR Area, four Future Conditions Models (FCMs) were developed. The results of these models were analyzed by using relative measures, such as differences in hydroperiod, water table elevations, and overall water budget.

Development of Future Land Use Alternatives

The future land use scenarios consist of four alternatives in the DR/GR Area provided by Lee County (see land use maps in Appendix D). The land use changes are of three types: creation of urban areas, expansion or creation of mining pits and restoration of agricultural lands into wetlands. Land use alternative 1 (FCM1) is conceptually similar to Scenario 1 in "Prospects for Southeast Lee County" [Dover, Kohl & Partners, July 2008]. Mining would be limited to already-approved mining pits plus some new pits north of Alico Road near the airport (but fewer pits than in Scenario 1). A broad westerly flow way to Corkscrew Swamp would be restored southward from the Imperial Marsh. Land use alternative 2 (FCM2) is conceptually similar to Scenario 2 in the Dover Kohl report. Mining would be limited to already-approved pits plus a major expansion to the Green Meadows Mine. A broad flow way to Corkscrew Swamp would be restored southward from the east end of Corkscrew Road in Lee County. Land use alternative 3 (FCM3) is conceptually similar to Scenario 3 in the Dover Kohl report. Mining would be limited to already-approved pits plus proposed new pits that were in the application process in September 2007, including pits along Corkscrew Road east of the Flint Pen Strand. Both flow ways to Corkscrew Swamp would be restored to whatever extent is still possible after significant portions of each were mined. Land use alternative 4 (FCM4) is conceptually similar to an alternative scenario that emerged favorably during public meetings after release of the Dover Kohl report. Mining would be limited to already-approved pits plus a moderate expansion to the Green Meadows Mine. Both flow ways to Corkscrew Swamp would be restored in full. The extent of the restored areas in all scenarios is less than originally proposed in the Dover Kohl report.

The new urban areas added in the future conditions land use map were exactly the same in all four alternatives. The increase of new mining areas from smallest mining area to largest mining area is: FCM1, FCM4, FCM2, and FCM3. The mining area in FCM3 is nearly double the amount of mining area in FCM1. The amount of mining area in FCM2 and FCM4 are approximately the same, and these scenarios fall in between FCM3 and FCM1, with respect to mined area. The total amount of newly restored areas increases monotonically from FCM1 to FCM4. FCM3 is a unique case in that its restored areas are imbedded with mining pits. Figures and tables in Appendix D show more details of the land use changes for all scenarios.

All land use based parameters in the model (e.g., overland roughness Manning's coefficient, detention storage, paved runoff fractions, drainage depths and drainage time constants) were modified to correspond to the new land use maps, but the relationship between land use type and parameters remained consistent with the ECM. The same meteorological and boundary conditions data utilized in the ECM were used in the four FCMs. The irrigation setup

in the future conditions model was modified to reflect future land use changes. For example, irrigation areas were removed in areas where the land use was converted from urban or agricultural to mining or wetland areas. For new urban areas, irrigation was added in those close to the northern DRGR boundary. The monthly groundwater withdrawal rates of the most recent year of available groundwater withdrawal data were repeated for every year in the FCM simulation period (2002-2007). In some cases, the 2007 withdrawal rates were used if available, but in others the 2006 rates were used. The same groundwater withdrawal rates for public water supply were used for the four future conditions scenarios. The domestic self supply rates vary according to land use changes.

Initial Conditions

Special effort was conducted to obtain initial conditions that are representative of "average" or "steady state" conditions in the LS FCMs, as in the final version of the LS ECM. The SFWMD technical staff recommends a warming period of several months in the model (including an entire rainy season) in order to make the model results independent of the initial condition assumed. However, in the DR/GR model, there are two slow processes that need more than one year in order to remove the long term "drift" caused by assuming inaccurate initial conditions. They are the head in the deepest layer (sandstone aquifer) and the water level in mining pits.

Three to five iterations (running the model for three years and taking the results from September 1, 2004 as initial conditions for the next run) were necessary to assure that the differences in water elevation in mining pits between iterations is less than 10 cm.

Assuming "average" or "steady state" initial conditions in the FCMs means that the model is evaluating the water resources at some time long after the land use changes. In other words, the period of time during which those land use changes are being made are not simulated in the model.

Results

The results shown in this section demonstrate the potential effect of land use alternatives on the water resources of the DR/GR Area. Water table levels at specific locations (where changes in land use occur) were plotted for the different scenarios to compare the water table level changes throughout the five year simulation period. Averaged water table elevation maps were created for all land use alternatives for two times of the year: at the end of the dry season (end of May) and at the end of the wet season (end of September). Hydroperiod maps and maps of the mean water depth during the hydroperiod were also produced for all scenarios. Water table level and hydroperiod map differences between the FCMs and the ECM are also presented.

The water budget for the entire DR/GR Area was calculated to determine what hydrologic components were affected by the different alternatives. Finally, changes in surface water flow were calculated at specific locations for each scenario.

Water Table Plots

Figure 43 to **Figure 46** illustrate the specific locations where the changes in water table elevation were compared for all land use alternatives throughout the 5-year simulation period. The water table elevation plots are shown in **Figure 47** to **Figure 69**. The following results arise from those comparative plots:

- In all the locations converted to mining pits (M2, M6, M7, M8, M12, and M15), the seasonal amplitude of the water table oscillation is reduced, which is an expected consequence of increased open-water storage in mining pits.
- The model results in locations M1, M2 and M3 (see **Figure 70**) predict that the mine is acting like a groundwater reservoir, i.e., releasing water (collected during the rainy season) into the aquifers during the dry season. As a result, the seasonal amplitude of the water table oscillation around the mine pit is reduced, and particularly, the water table level during the dry season is higher. This effect is an expected consequence of the higher open-water storage than in the neighboring porous media. In the Water Budget section, further analysis of this proposed mine is conducted by computing the water balance components.
- Locations M4, M5, M6 and M7 are upstream of a mining pit complex in the DR/GR Area, and locations M8, M9 and M10 are downstream. As predicted by the model, larger and more closely spaced mining pits in the FCM create a larger flattening effect over the regional water table gradient. Specifically, the dry-season water table level decreases up gradient and increases down gradient. This effect was also observed on a smaller scale around single mining pits in locations with steeper slopes at locations M11 and M13. The areal extent of zones with lower and higher water table levels can be seen in the maps presented in the following section.
- In two of the three locations converted to wetlands (W2 and W3), the dry-season water table elevation increases. In the case of location W3, that increase is higher when it is close to new mining pits (in FCM3).
- Most of the new urban locations (U1, U2, and U3) showed a slight decrease in the wet-season water table elevation, which is likely a consequence of the new urban drainage. An increase in the dry-season water table elevation is observed in most of the new urban locations (U1, U3, and U4), which is likely related to a reduction in the ET losses (see more details in the water budget section).
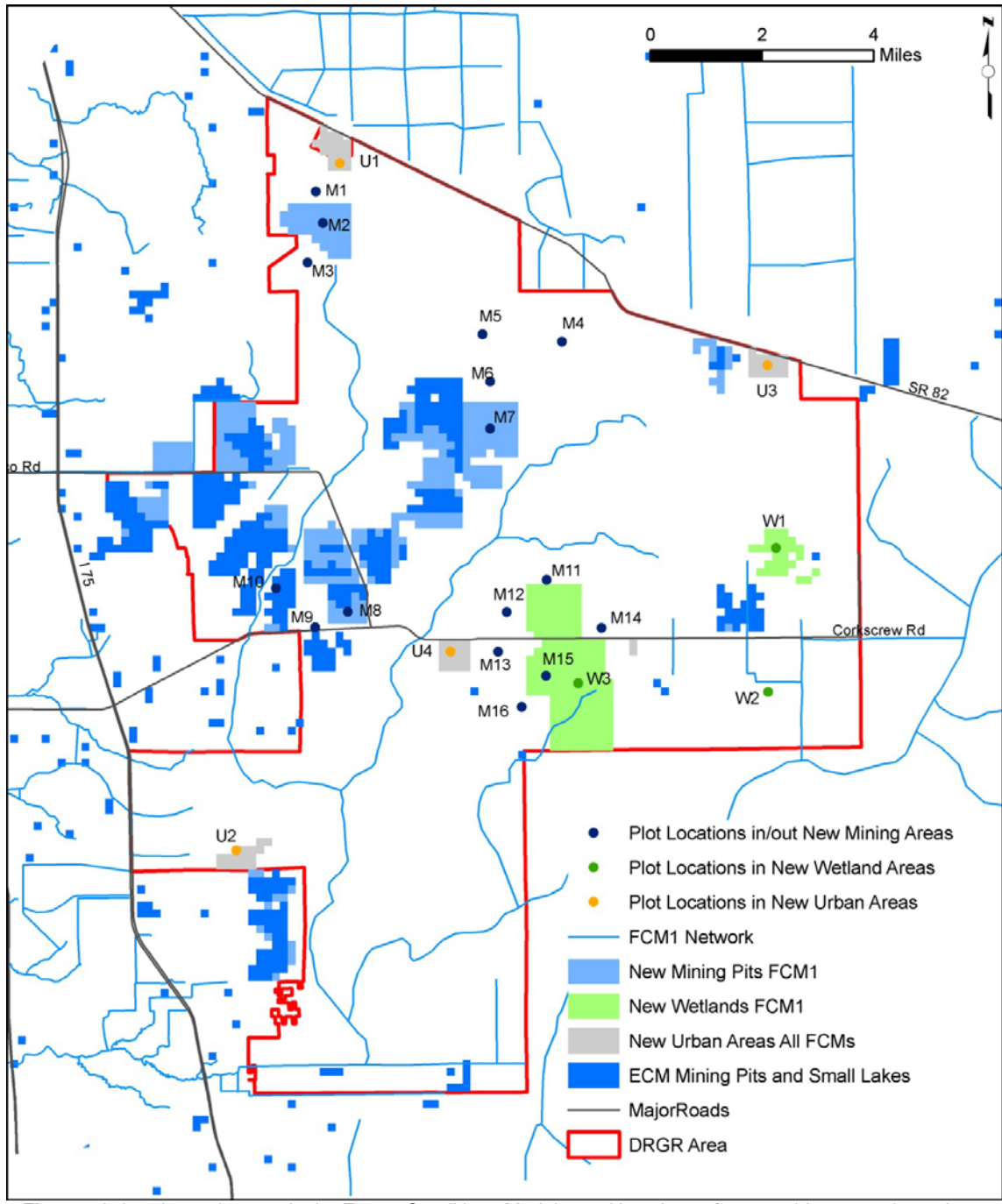
Figure 43. Land use changes in the Future Conditions Model 1 and locations of water table comparison plots.
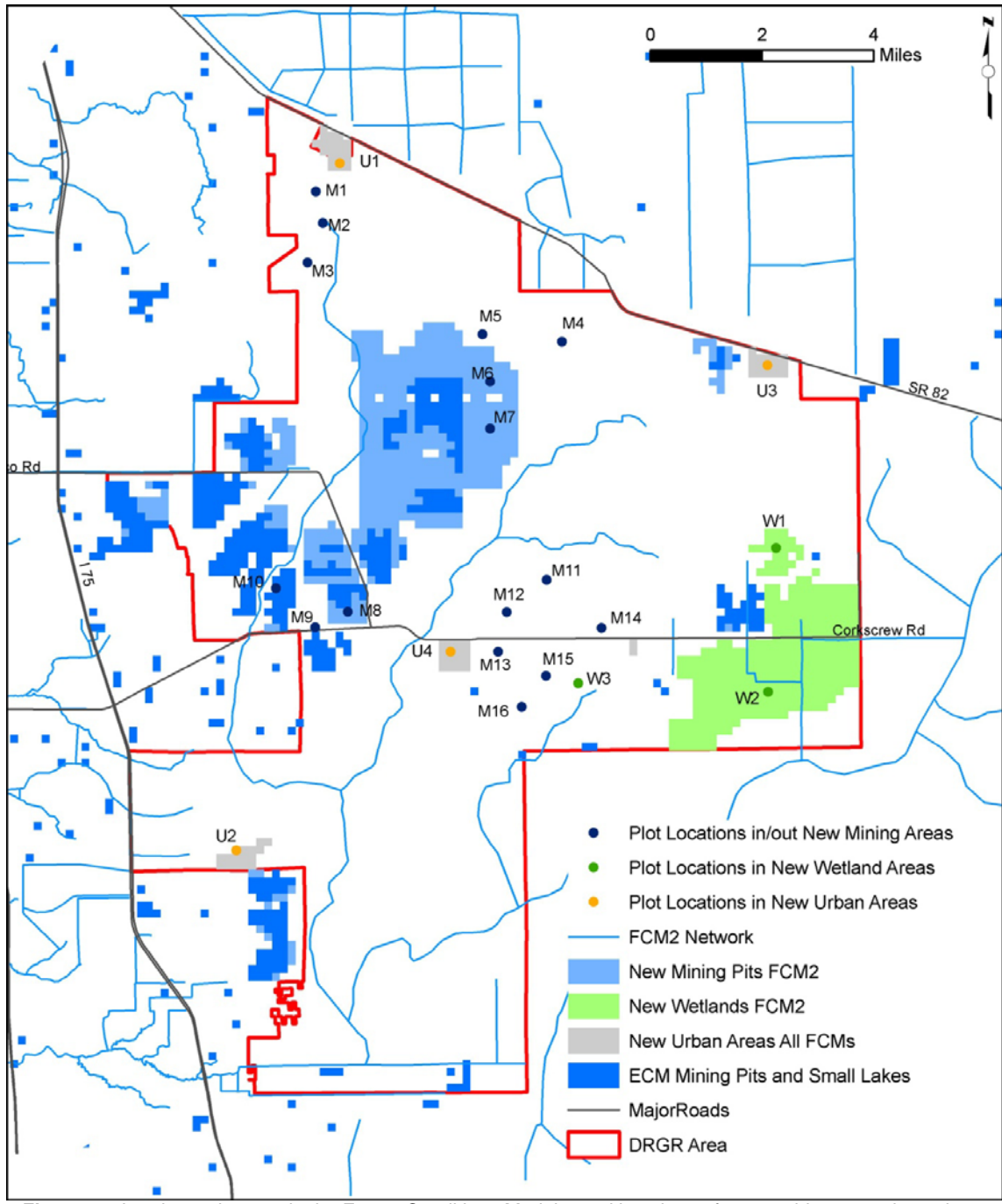
Figure 44. Land use changes in the Future Conditions Model 2 and locations of water table comparison plots.
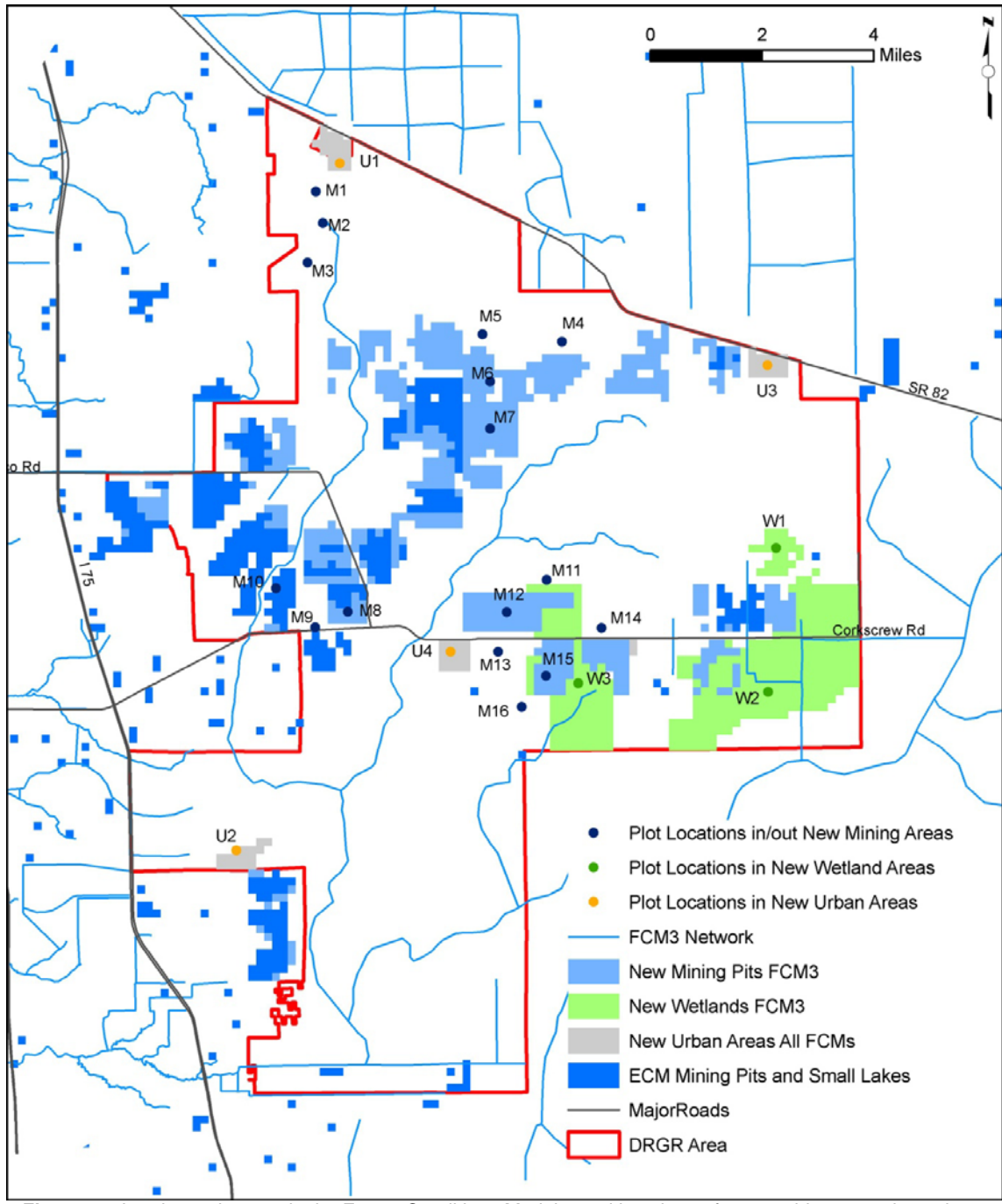
Figure 45. Land use changes in the Future Conditions Model 3 and locations of water table comparison plots.
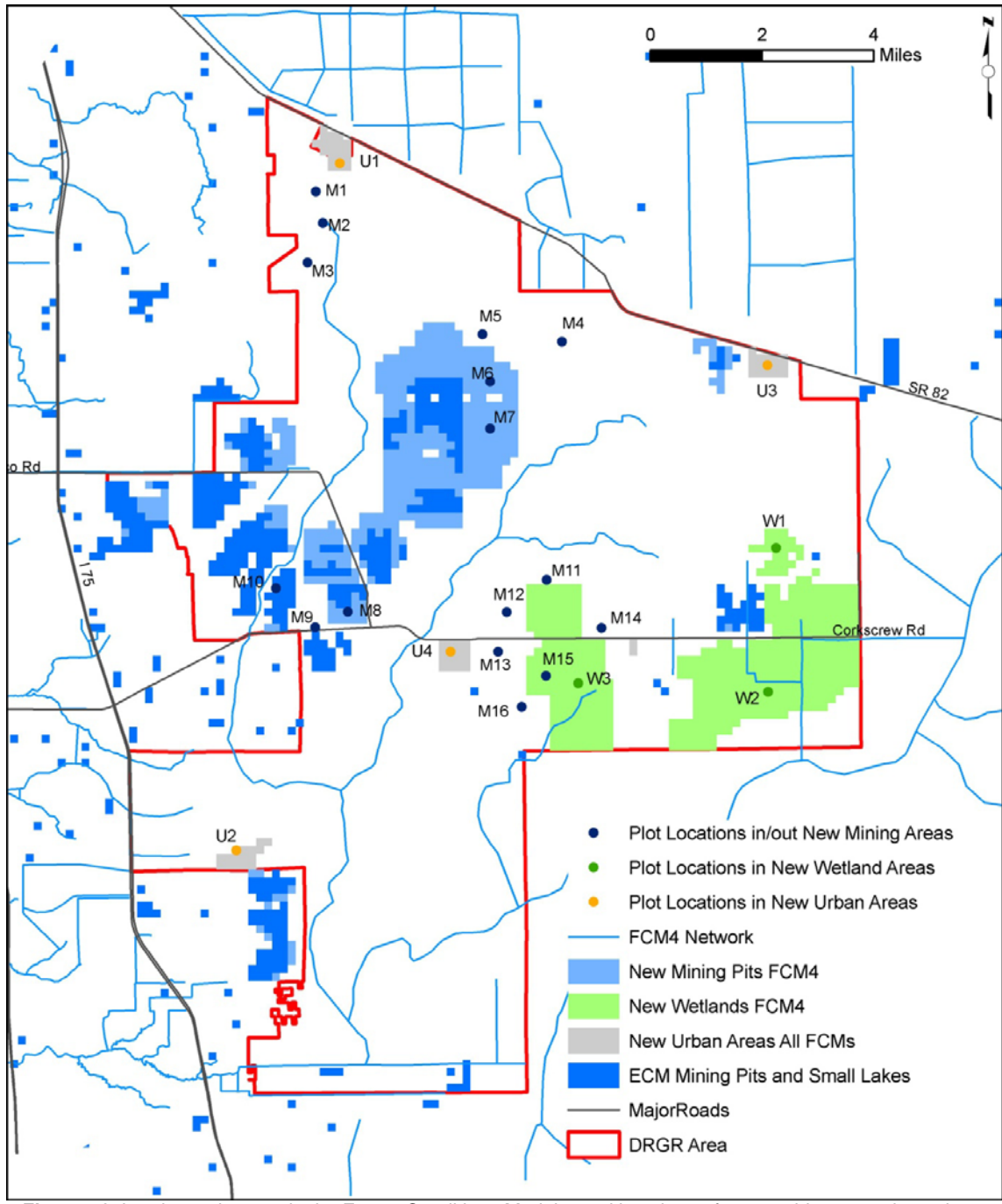
Figure 46. Land use changes in the Future Conditions Model 4 and locations of water table comparison plots.
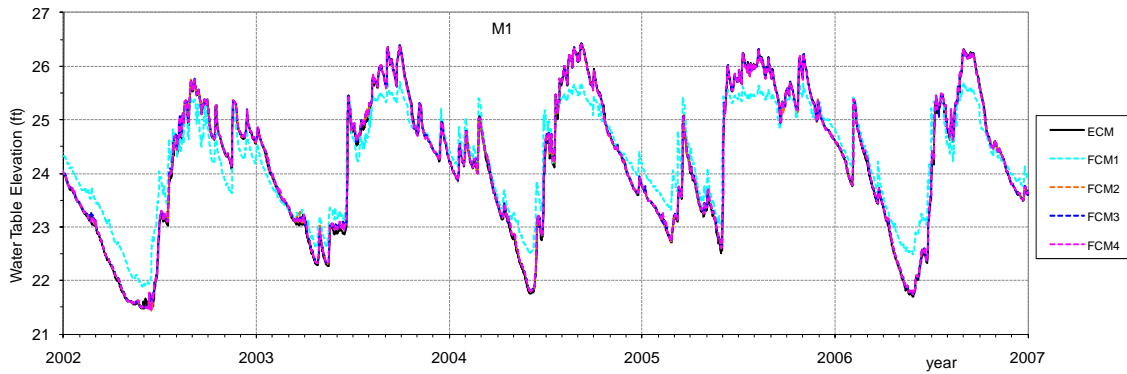
Figure 47. Water table elevations at land use change location M1.
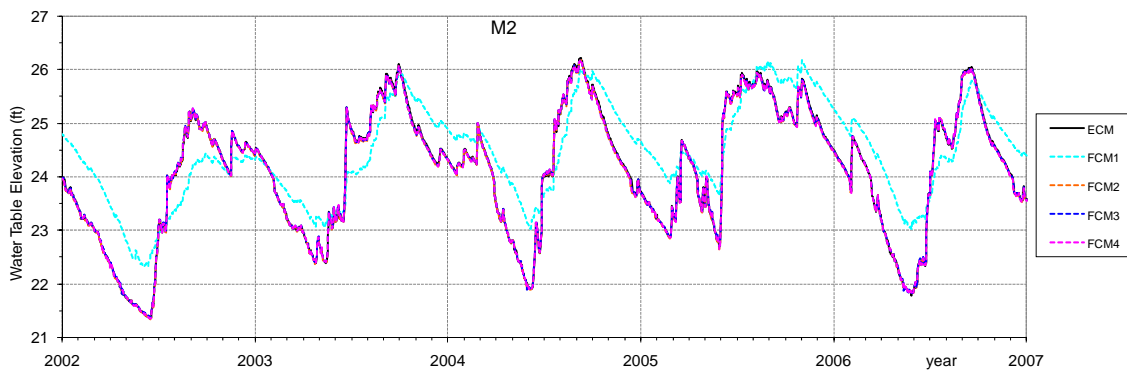
Figure 48. Water table elevations at land use change location M2.
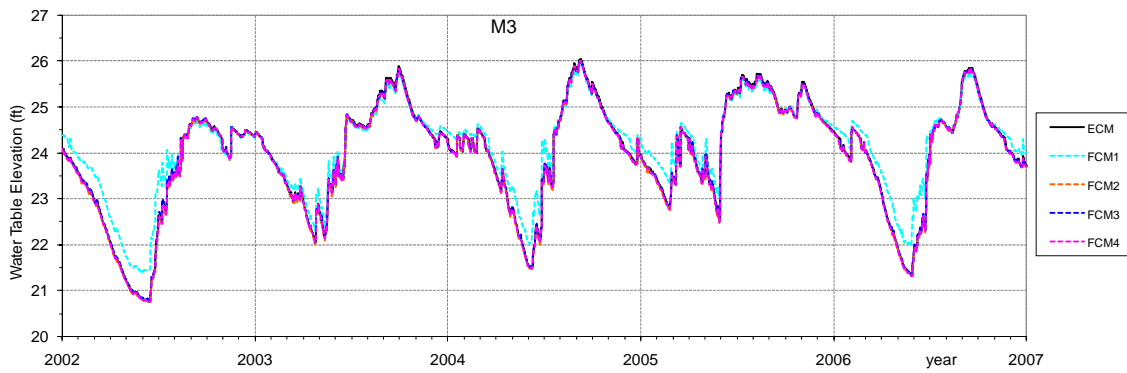
Figure 49. Water table elevations at land use change location M3.

<u>Note:</u> Locations M1 and M3 are close to a new mining pit included in FCM1 and location M2 is inside it. The model predicts that this mining pit recharges the groundwater such that the water table elevation (WTE) in neighboring areas increases during dry periods compared to the ECM. WTE oscillation in location M2 shows a reduction in the seasonal amplitude when located in a mining pit. The corresponding seasonal averaged plots are shown in Figure 70.
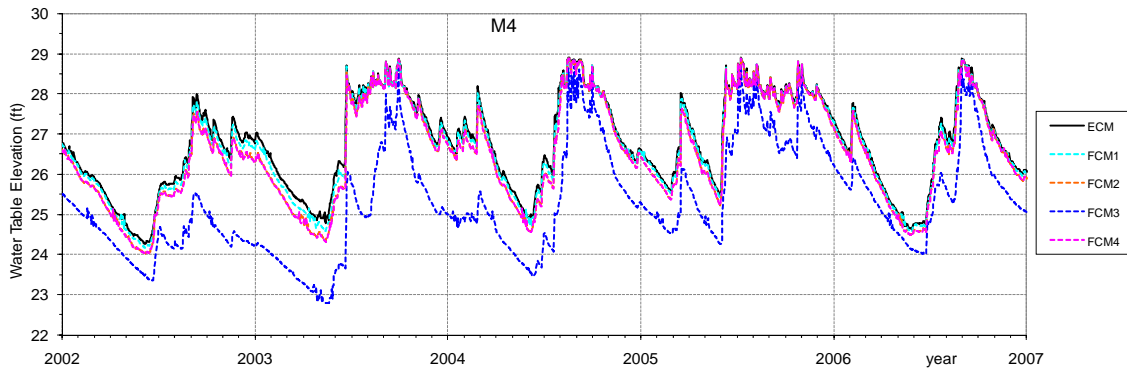
Figure 50. Water table elevations at land use change location M4.
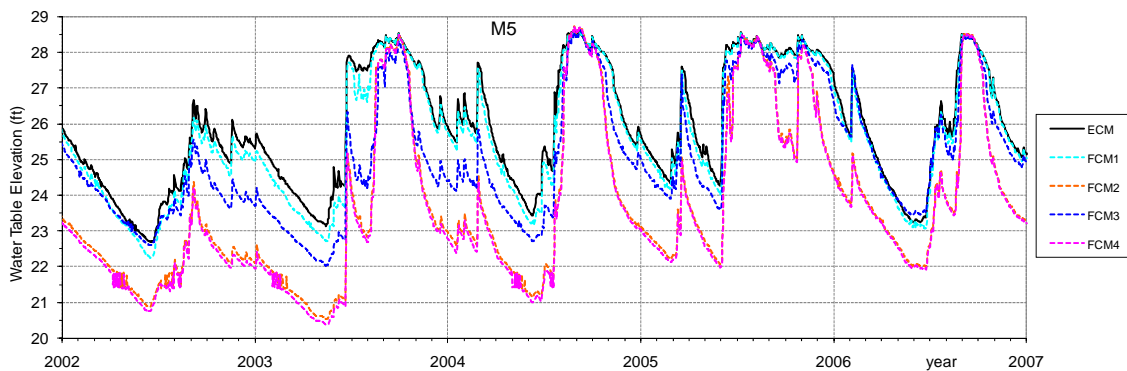
Figure 51. Water table elevations at land use change location M5.
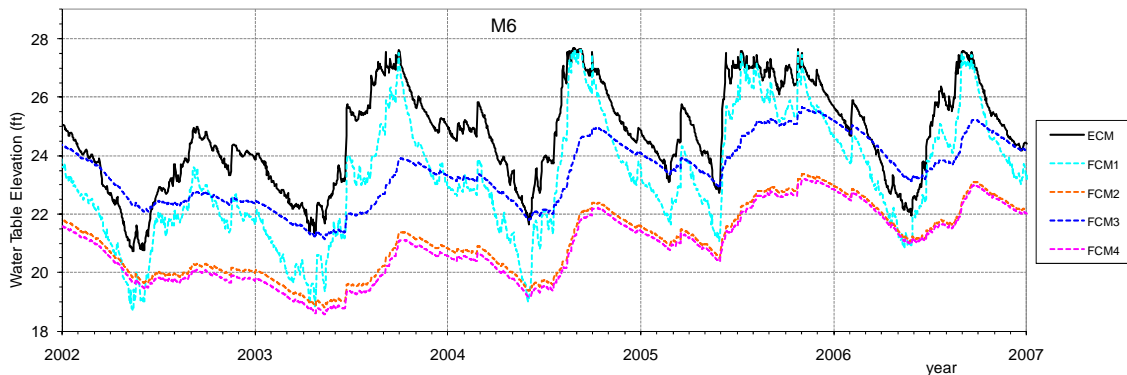
Figure 52. Water table elevations at land use change location M6.

Note: Locations M4, M5, M6 and M7 show that the new mining pit area in the FCMs generally causes a WTE decrease in the northern–central part of the DR/GR Area. This area is up gradient of the large mining pit complex area. WTE oscillation in locations M6 and M7 indicate a reduction in the seasonal amplitude when they become part of a mining pit.
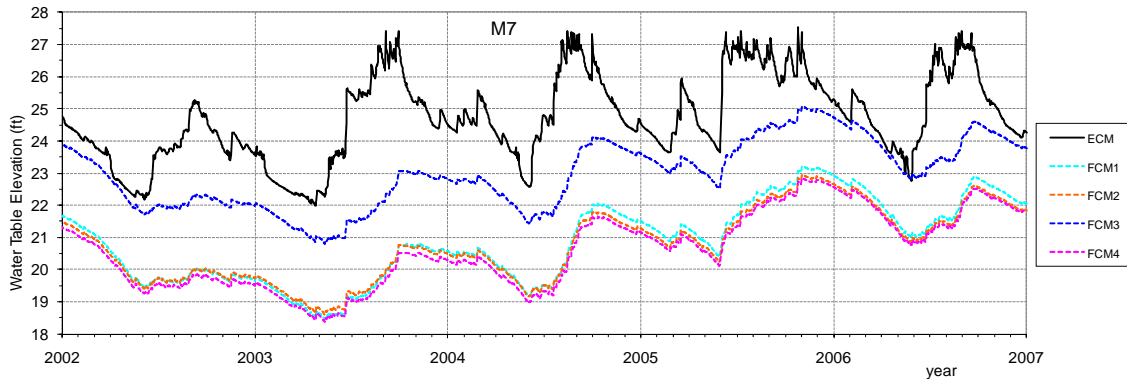
Figure 53. Water table elevations at land use change location M7.
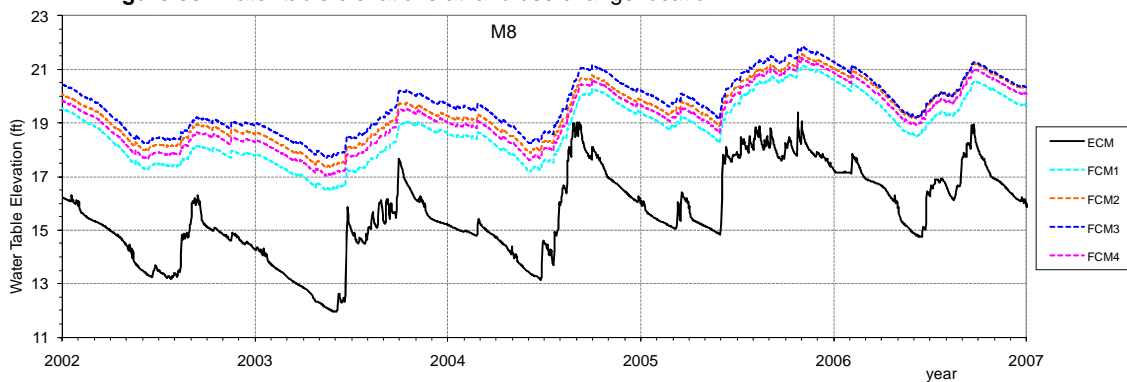
Figure 54. Water table elevations at land use change location M8.
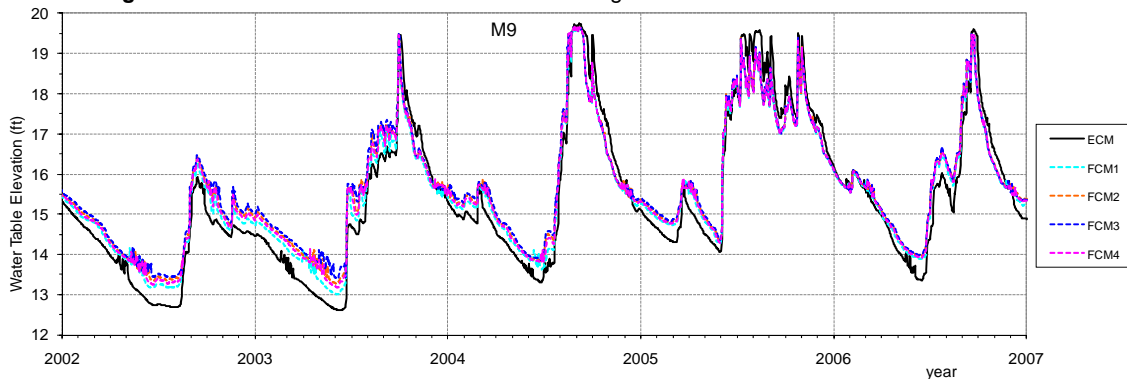
Figure 55. Water table elevations at land use change location M9.

<u>Note:</u> Locations M8, M9, and M10 show that the new mining pit area in the FCMs generally cause a WTE increase in the western-central part of the DR/GR Area. This area is down gradient of the large mining pit complex area. The WTE oscillation in location M8 is reduced in seasonal amplitude when it becomes part of a mining pit.
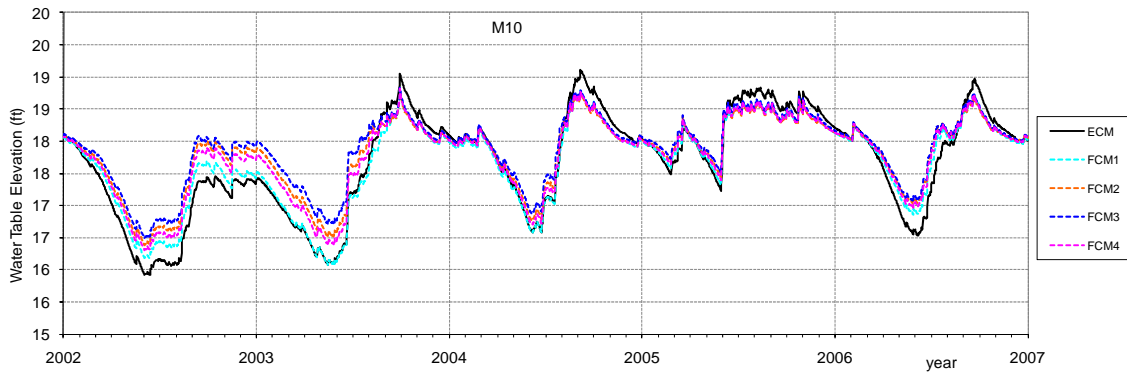
Figure 56. Water table elevations at land use change location M10.
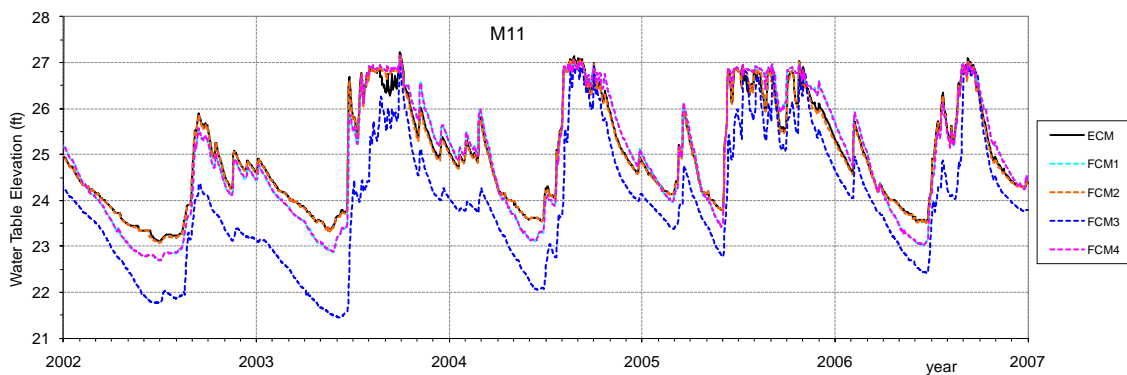
Figure 57. Water table elevations at land use change location M11.
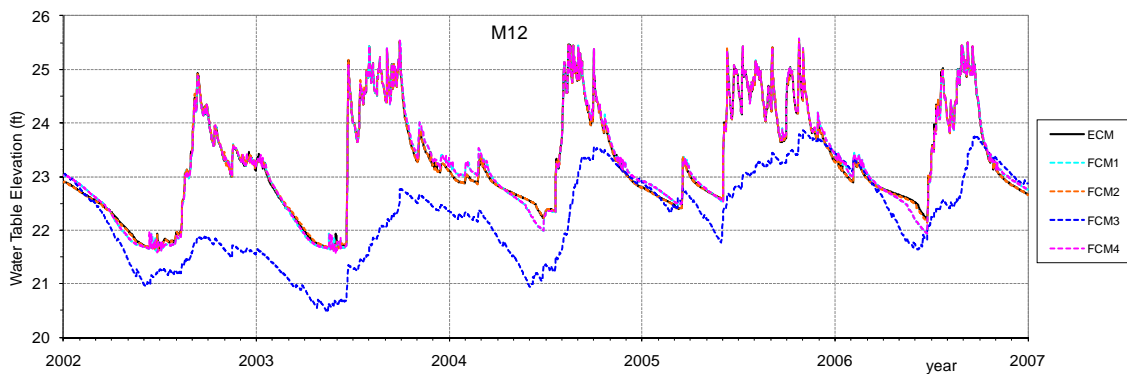
Figure 58. Water table elevations at land use change location M12.

<u>Note</u>: Location M11 shows a dry-season WTE oscillation decrease in FCM3. This is likely due to the mining pit down gradient of this location. M12 has a reduction in seasonal WTE oscillation amplitude when it becomes part of the mining pit in FCM3.
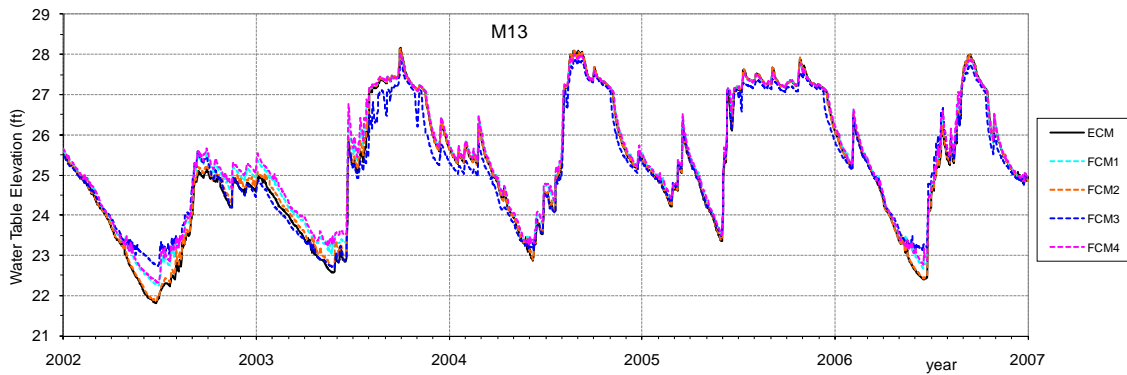
Figure 59. Water table elevations at land use change location M13.
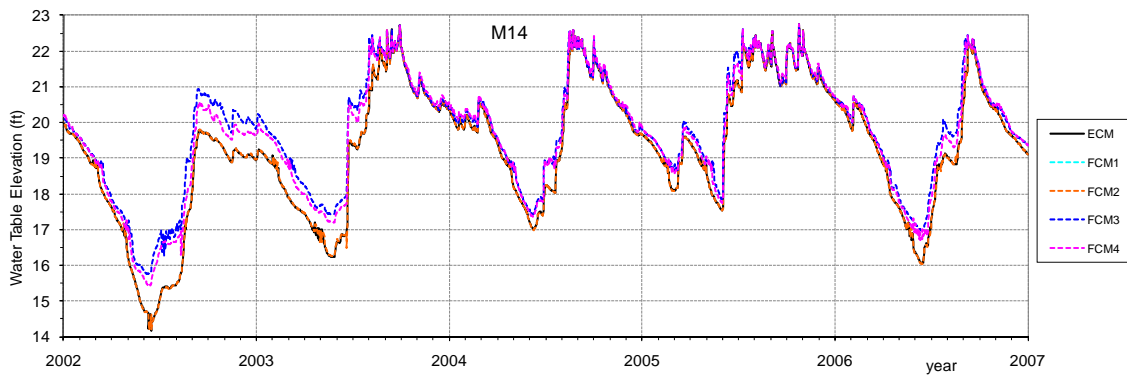
Figure 60. Water table elevations at land use change location M14.
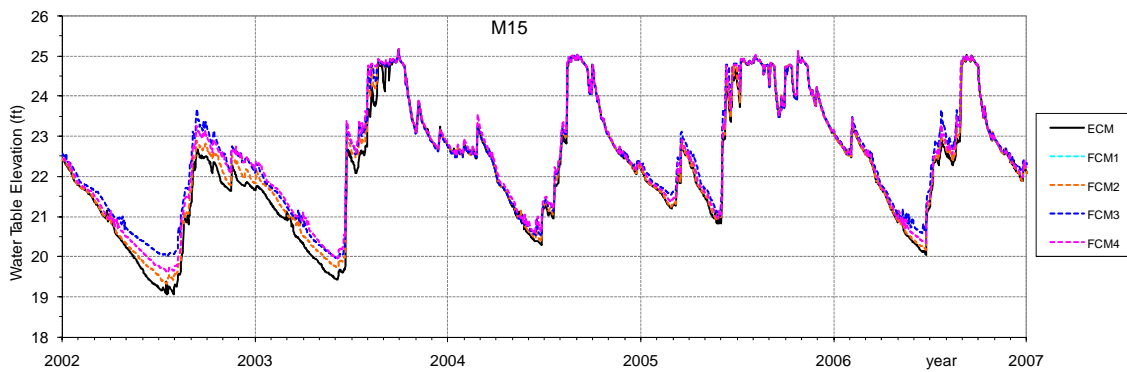
Figure 61. Water table elevations at land use change location M15.

<u>Note</u>: Locations M13, M14, M15 and M16 show a dry-season WTE increase in FCM3 due to the combined effects of the new mining pit and wetland areas. There is also a dry-season WTE increase in FCM1 and FCM4 due to new wetland areas. M15 shows a reduction of the seasonal oscillation amplitude when it becomes part of the mining pit in FCM3.
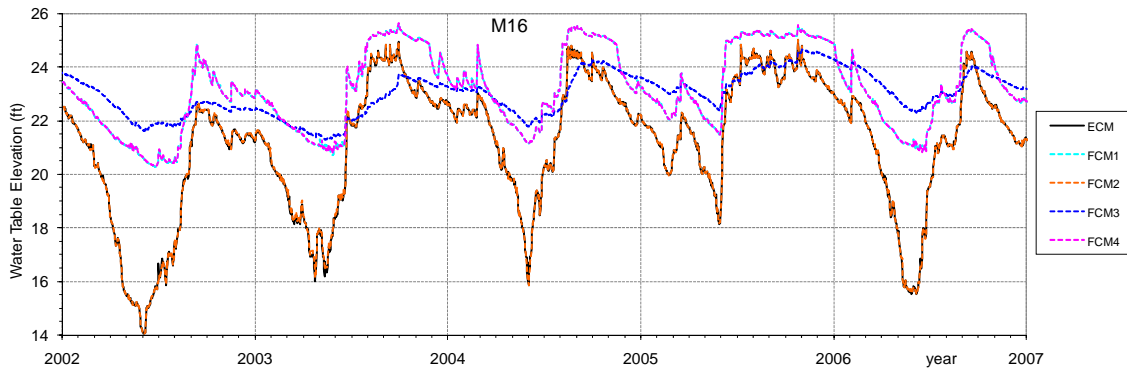
Figure 62. Water table elevations at land use change location M16.
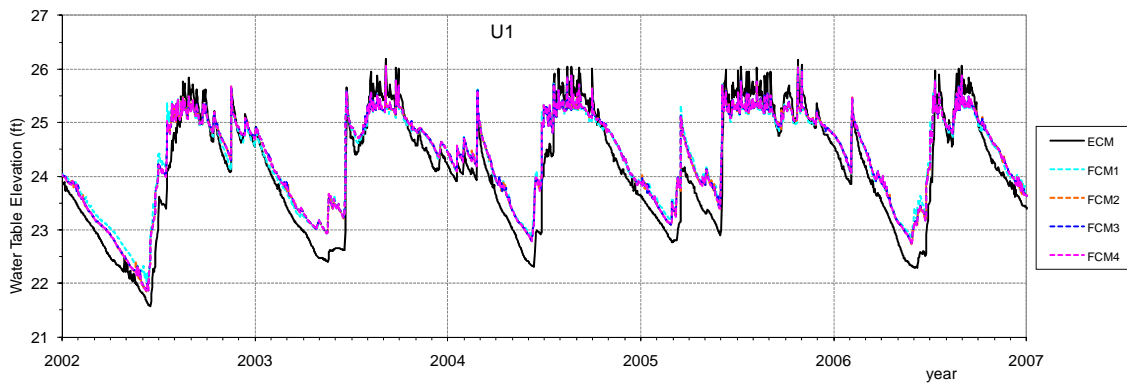
Figure 63. Water table elevations at land use change location U1.
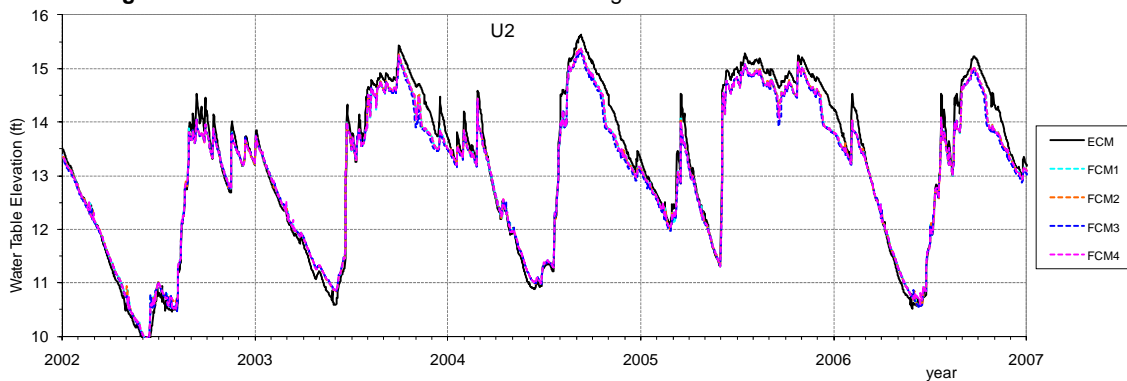
Figure 64. Water table elevations at land use change location U2.

<u>Note</u>: Locations U1, U2, and U3 show a decrease in wet-season WTEs, likely due to the new urban area drainage.
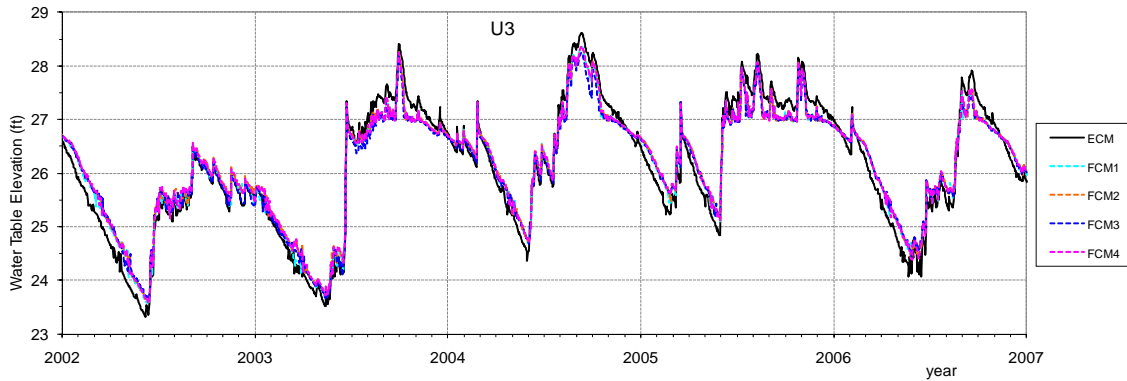
Figure 65. Water table elevations at land use change location U3.
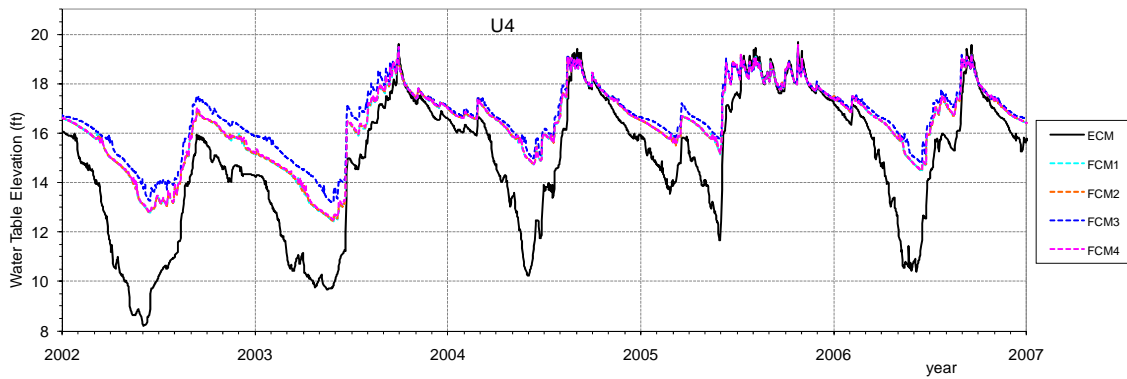
Figure 66. Water table elevations at land use change location U4.
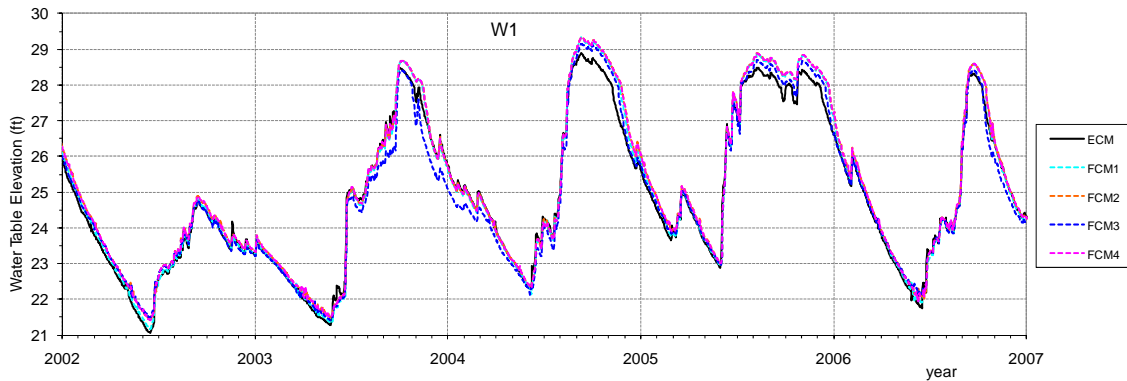
Figure 67. Water table elevations at land use change location W1.

Note: Locations U1, U3, and U4 show a dry-season WTE increase in all FCMs.. Location W1 shows small WTE differences after the small wetland area was added in all FCMs.
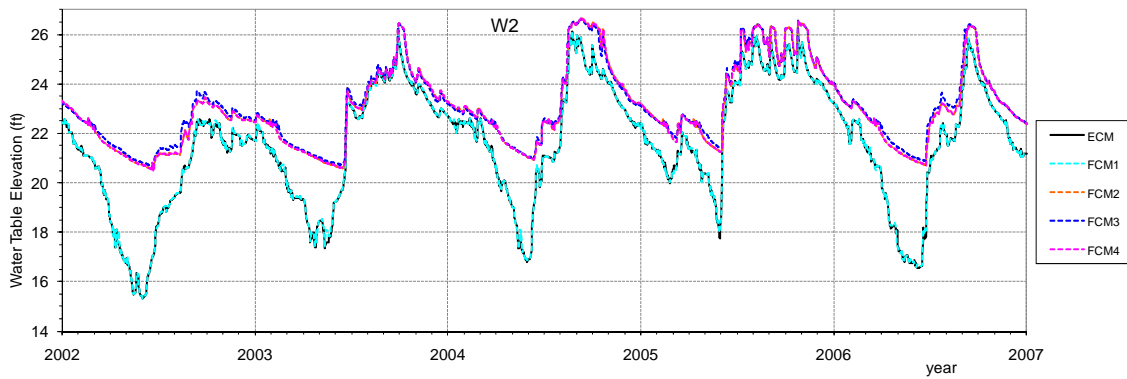
Figure 68. Water table elevations at land use change location W2.
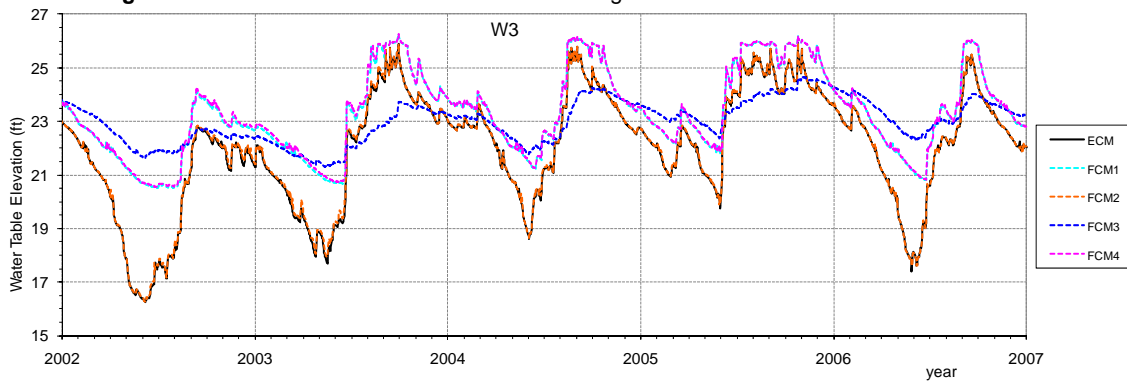
Figure 69. Water table elevations at land use change location W3.

Note: Location W2 shows a dry-season WTE increase due to new wetland areas added in FCM2, FCM3, and FCM4. Location W3 shows a dry-season WTE increase due to new wetland areas added in FCM1 and FCM4, and the combination of new mining pit and wetland areas in FCM3.
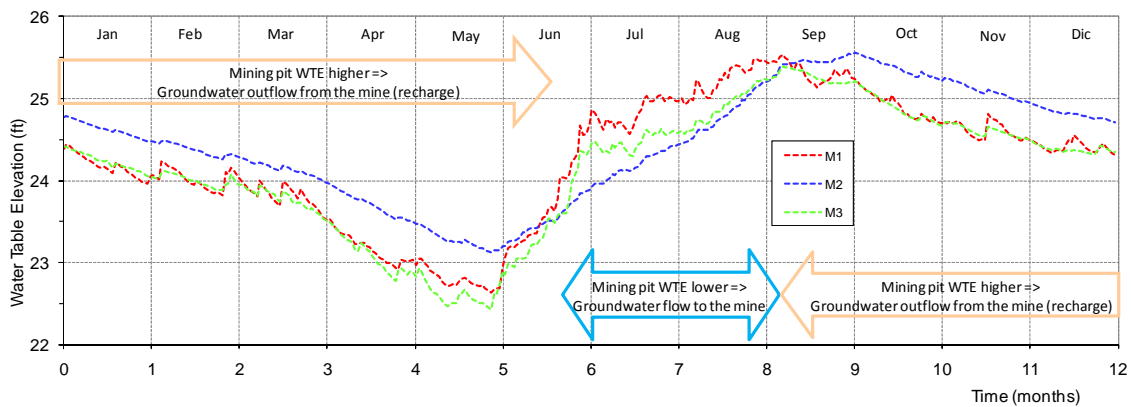
Figure 70. Seasonal averaged water table elevation at locations M1, M2 and M3 in FCM1.

Water Table Maps

Water table elevation maps obtained from all the FCMs are presented in Appendix G. Those maps are extracted from the different models at the end of the dry and the wet season (i.e., the ten last days of May and the ten last days of September, respectively). **Figure 72** to **Figure 79** show water table difference maps for all future condition scenarios in relation to the LS ECM for both the wet and dry seasons.

The most significant changes in the water table are observed in the large mining pit complex of the DR/GR Area. In the future conditions scenarios, the area occupied by mining pits increases, the distance between neighboring mining pits decreases, and they become more hydrologically connected (i.e. via groundwater). Consequently, the water table elevation decreases in up-gradient areas and increases down gradient. The down gradient effect is bigger in the dry season than in the wet season.

A conceptual model of the flattening effect of a single mining pit on the water table elevation is sketched in **Figure 71**. The model predicts that the mine flattens the water table commonly causing a decrease in groundwater levels up gradient with respect to the pre-mining conditions. Down gradient of the mining pits, this effect may produce either an increase or a decrease in groundwater levels, depending on the local hydrologic conditions, the time of the year, etc. These effects in the upstream and downstream areas are more pronounced in the model in areas with steeper topographic slopes and for larger area mine footprints.
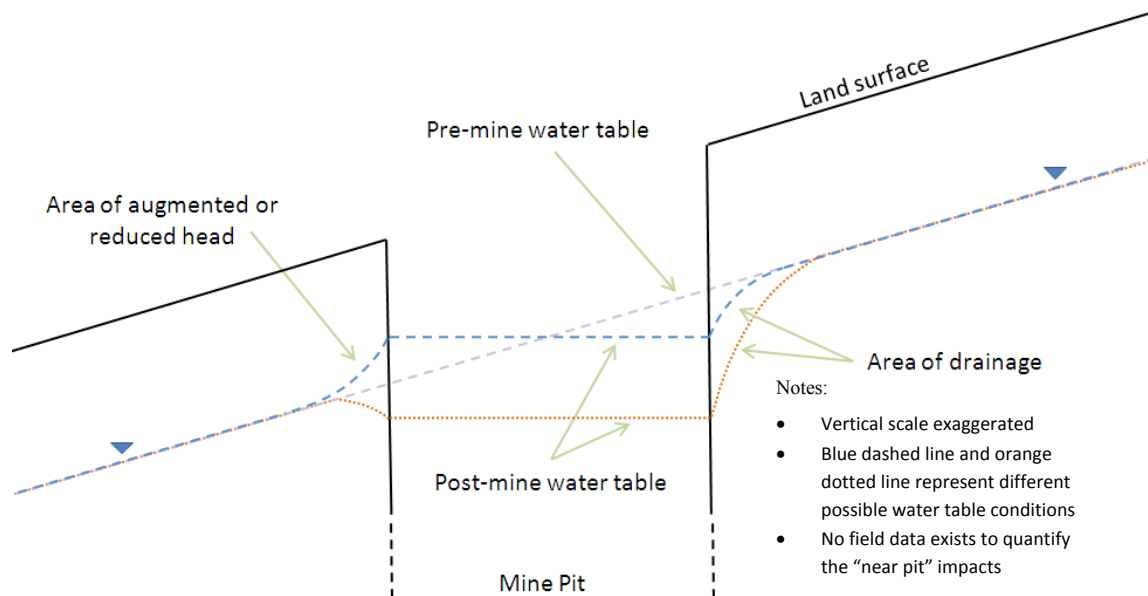
Figure 71. Sketch of the flattening effect on the water table elevation of a mining pit in the presence of a regional gradient.

In the case of the large mining pit complex of the DR/GR Area, there are several mines that are hydrologically connected to some extent. The water table profiles from **Figure 80** through **Figure 83** show that the flattening effect in the water table of the entire mining pit complex area becomes more important in the future condition scenarios as the groundwater connectivity between mines increases. In other words, the groundwater connectivity between mines and therefore the flattening effect increases once land between existing pits is also mined.

The flattening effect was also noticeable at a mine proposed in FCM3 at the central part of the DR/GR Area (see Figure 76 and Figure 77). In this case, the mining pit length is smaller than the length of the mining pit complex, but it was located in an area with a steep water table gradient, as can be seen in Figure 28 and Figure 29. The upstream decrease in the WTE is also observed at location M11 presented in Figure 57.

The mine proposed in the FCM1 at the north-western corner of the DR/GR Area does not cause a flattening effect because it is located in a relatively flat area. In this case, the model predicts that the mining pit maintains a higher water table elevation at the end of the dry season around the pit perimeter (see Figure 72). The higher water table elevation here is presented with respect to the LS ECM, where there are not any pits present. This result cannot be extrapolated to mines in other areas in the DR/GR since the rainfall rate in that mine area is much higher than the average rainfall rate in the entire DRGR (see Water Budget section).

The water table in the new wetland areas increases, in general, due to the removal of the drainage system from when it was an agricultural area. Differences in the water table in the new wetland areas are in general greater at the end of the dry season.

The water table in the new urban areas is usually higher at the end of the dry season compared to the existing conditions. This is likely related to a reduction in the ET losses (see more details in the water budget section).
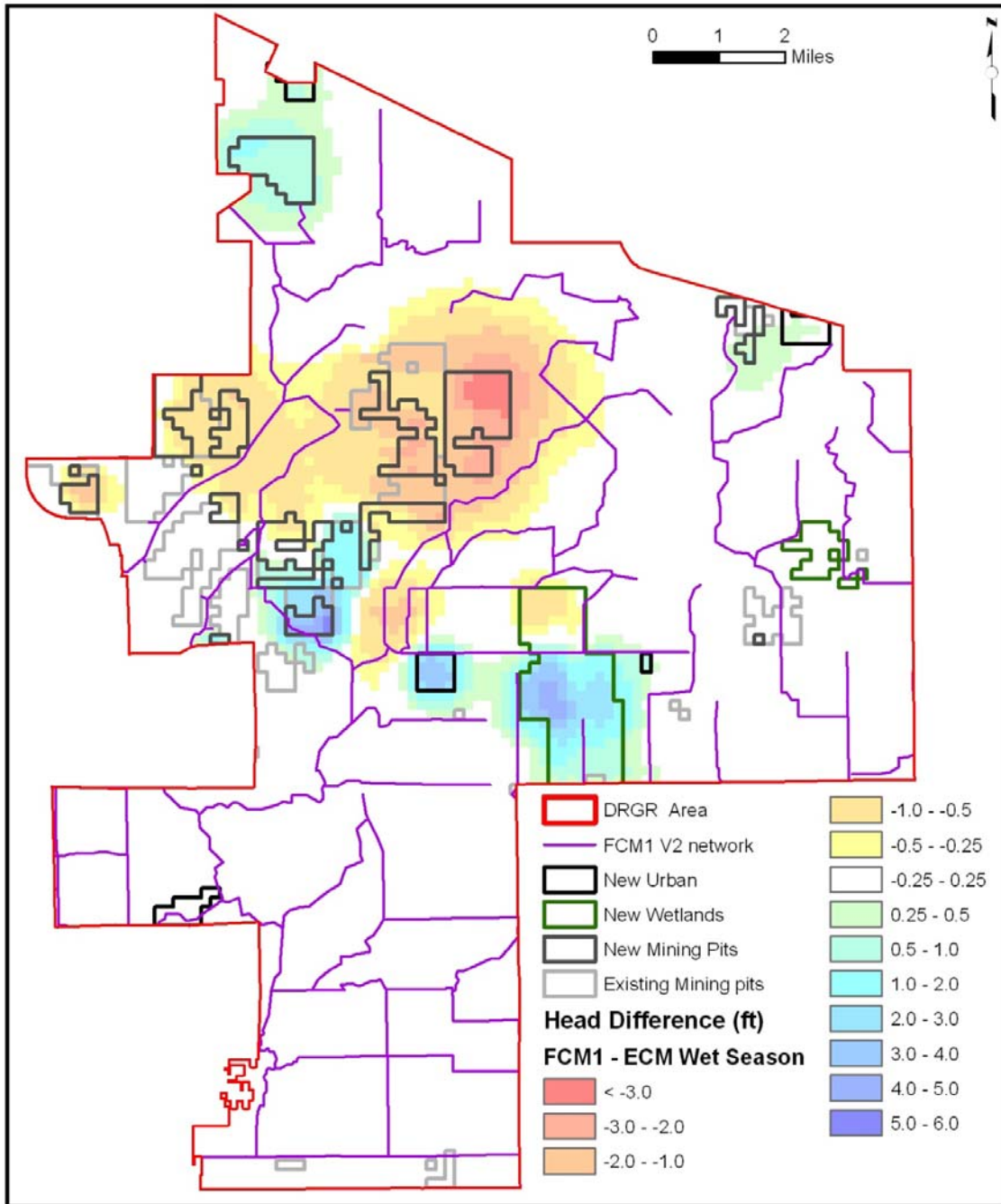
Figure 72. Difference in dry season water table in FCM1 in relation to the LS ECM (Positive values indicate increase in water table elevation in the FCM1).
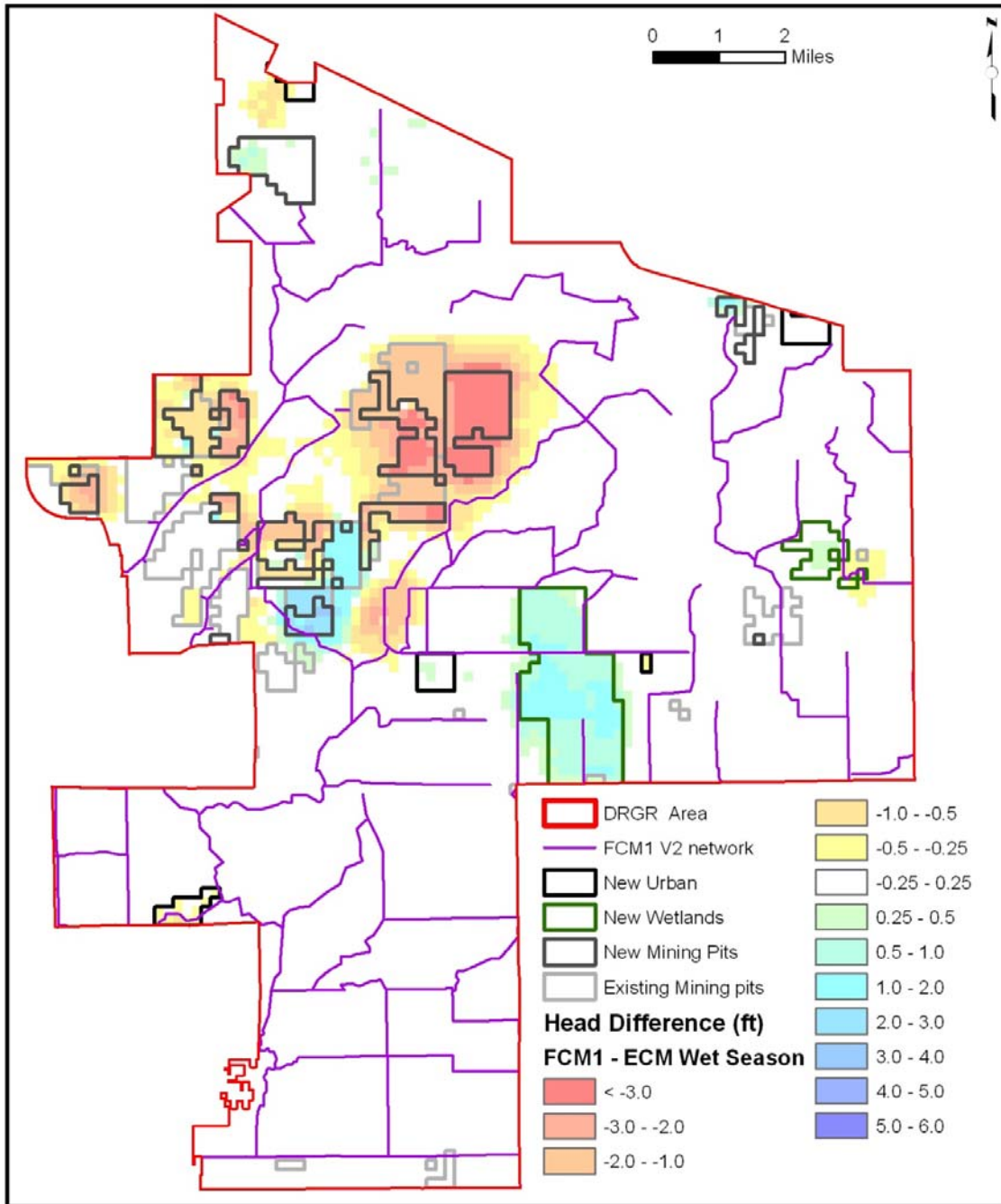
Figure 73. Difference in wet season water table in FCM1 in relation to the LS ECM (Positive values indicate increase in water table elevation in the FCM1).
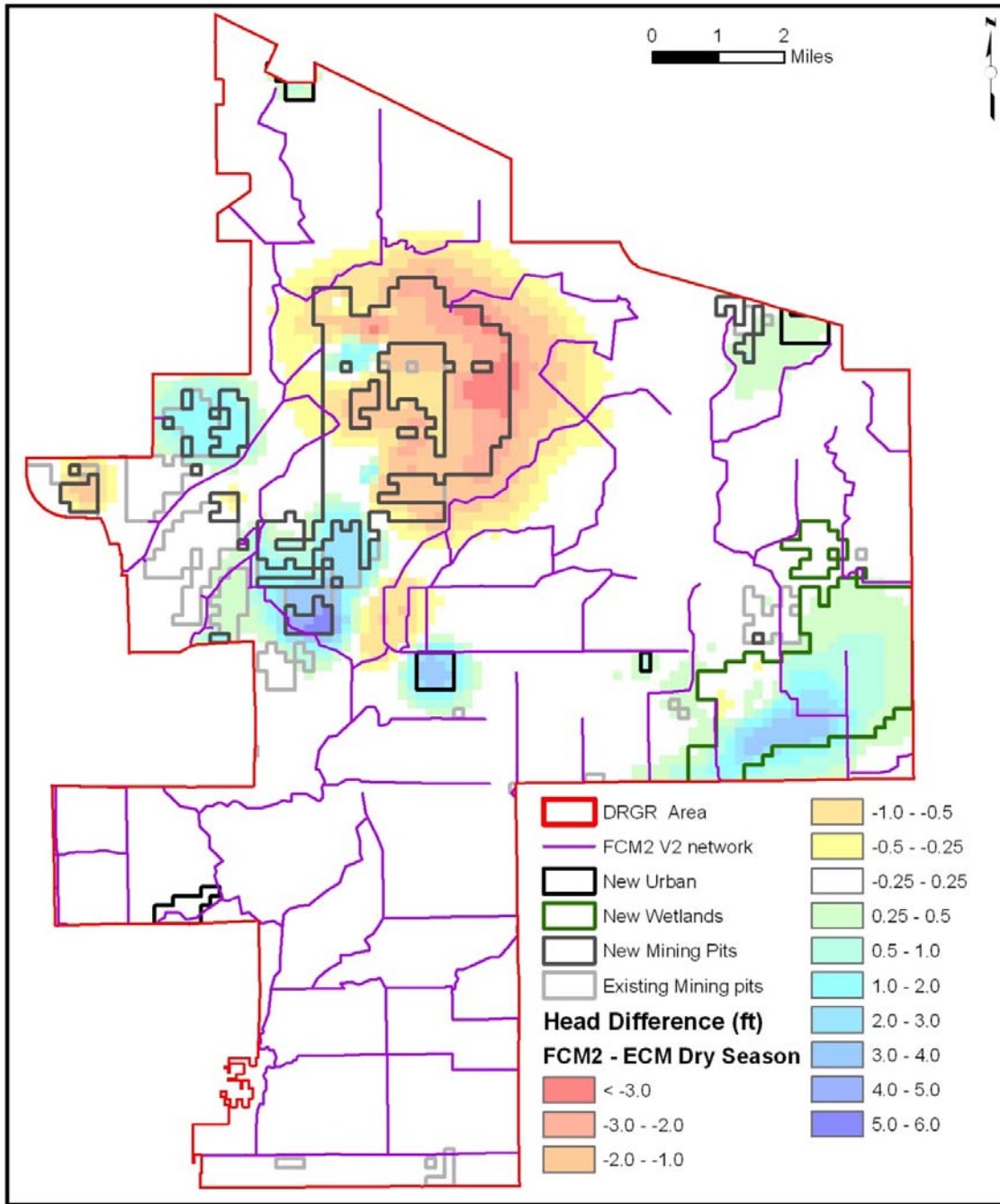
Figure 74. Difference in dry season water table in FCM2 in relation to the LS ECM (Positive values indicate increase in water table elevation in the FCM2).
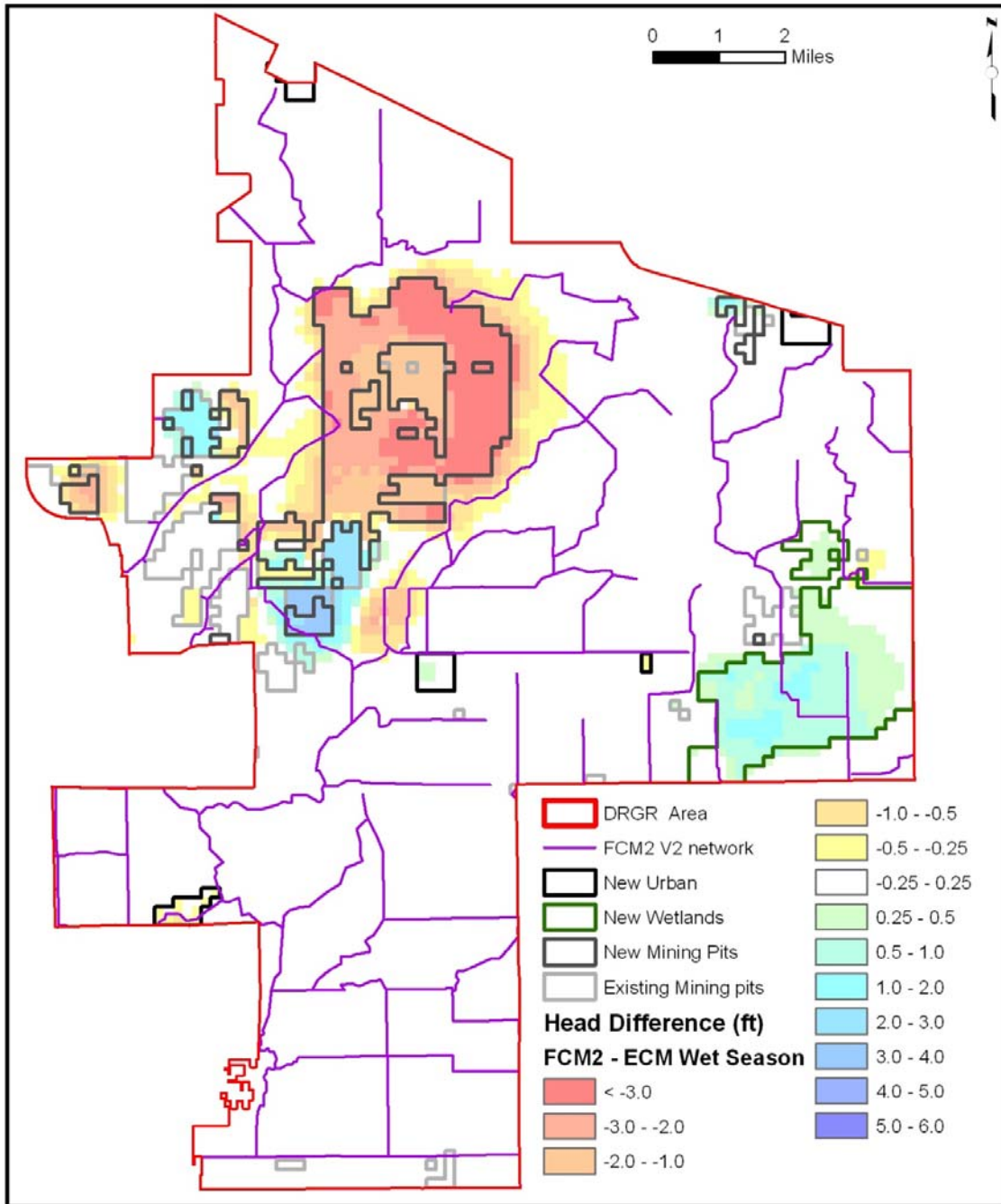
Figure 75. Difference in wet season water table in FCM2 in relation to the LS ECM (Positive values indicate increase in water table elevation in the FCM2).
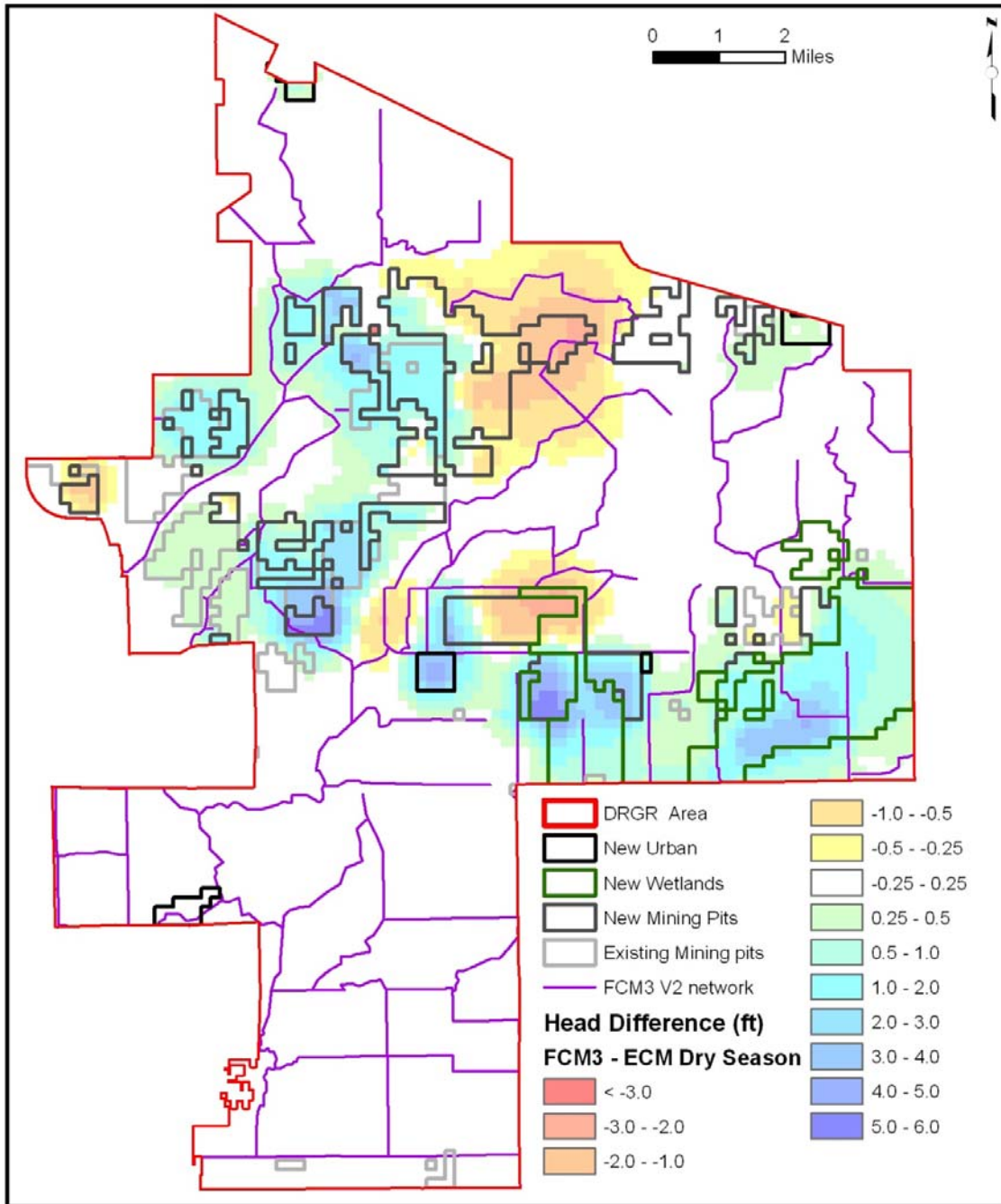
Figure 76. Difference in dry season water table in FCM3 in relation to the LS ECM (Positive values indicate increase in water table elevation in the FCM3).
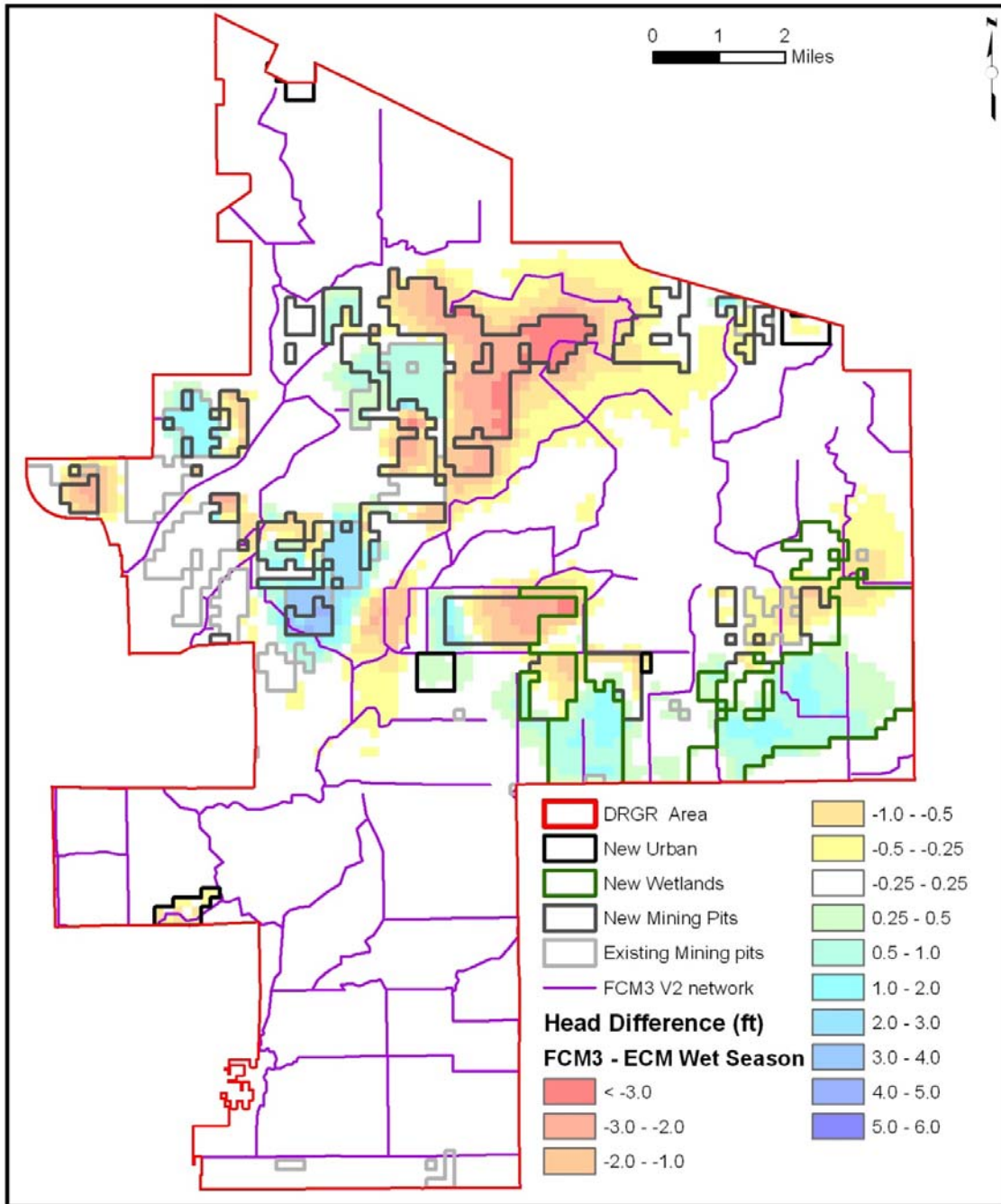
Figure 77. Difference in wet season water table in FCM3 in relation to the LS ECM (Positive values indicate increase in water table elevation in the FCM3).
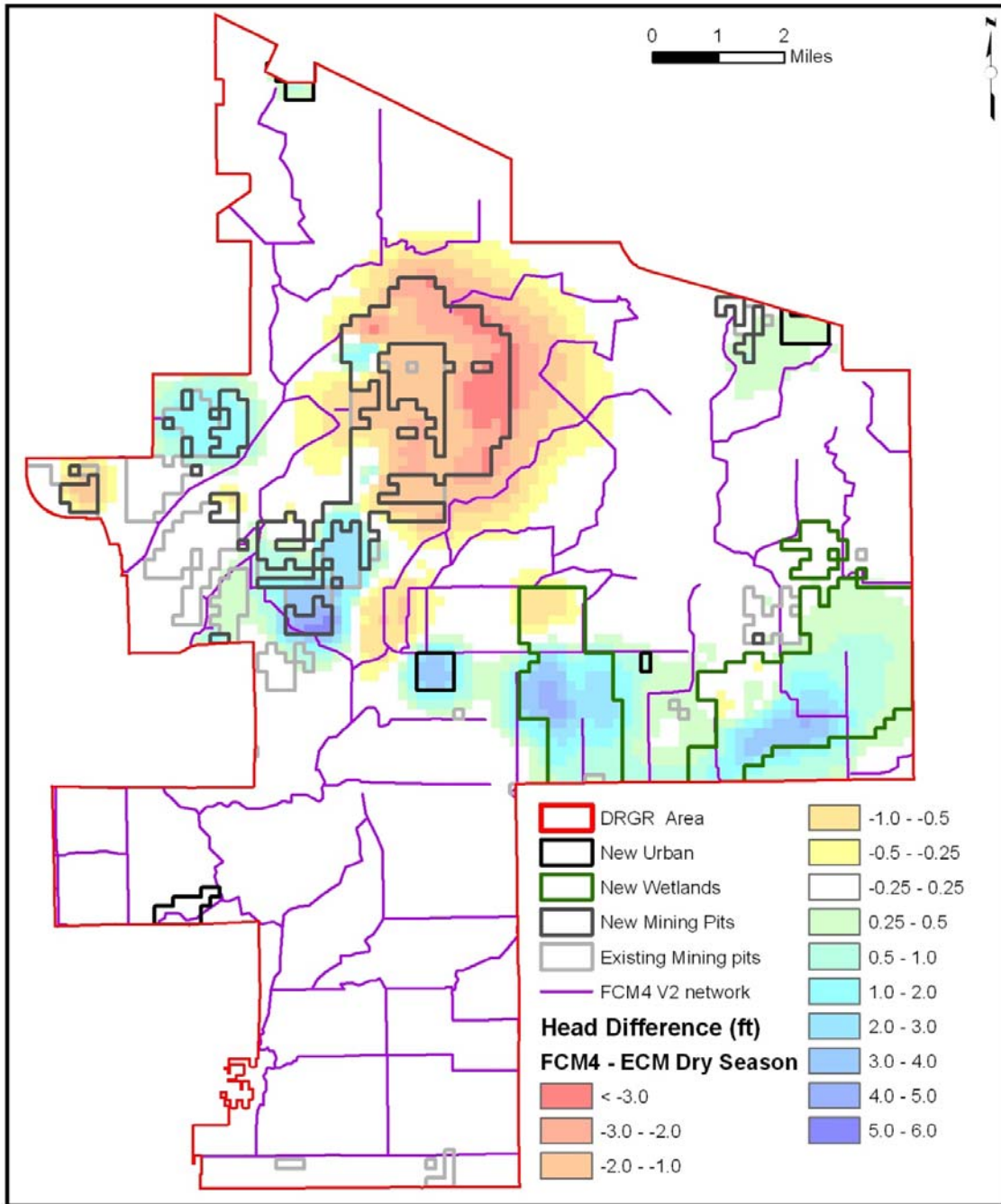
Figure 78. Difference in dry season water table in FCM4 in relation to the LS ECM (Positive values indicate increase in water table elevation in the FCM4).
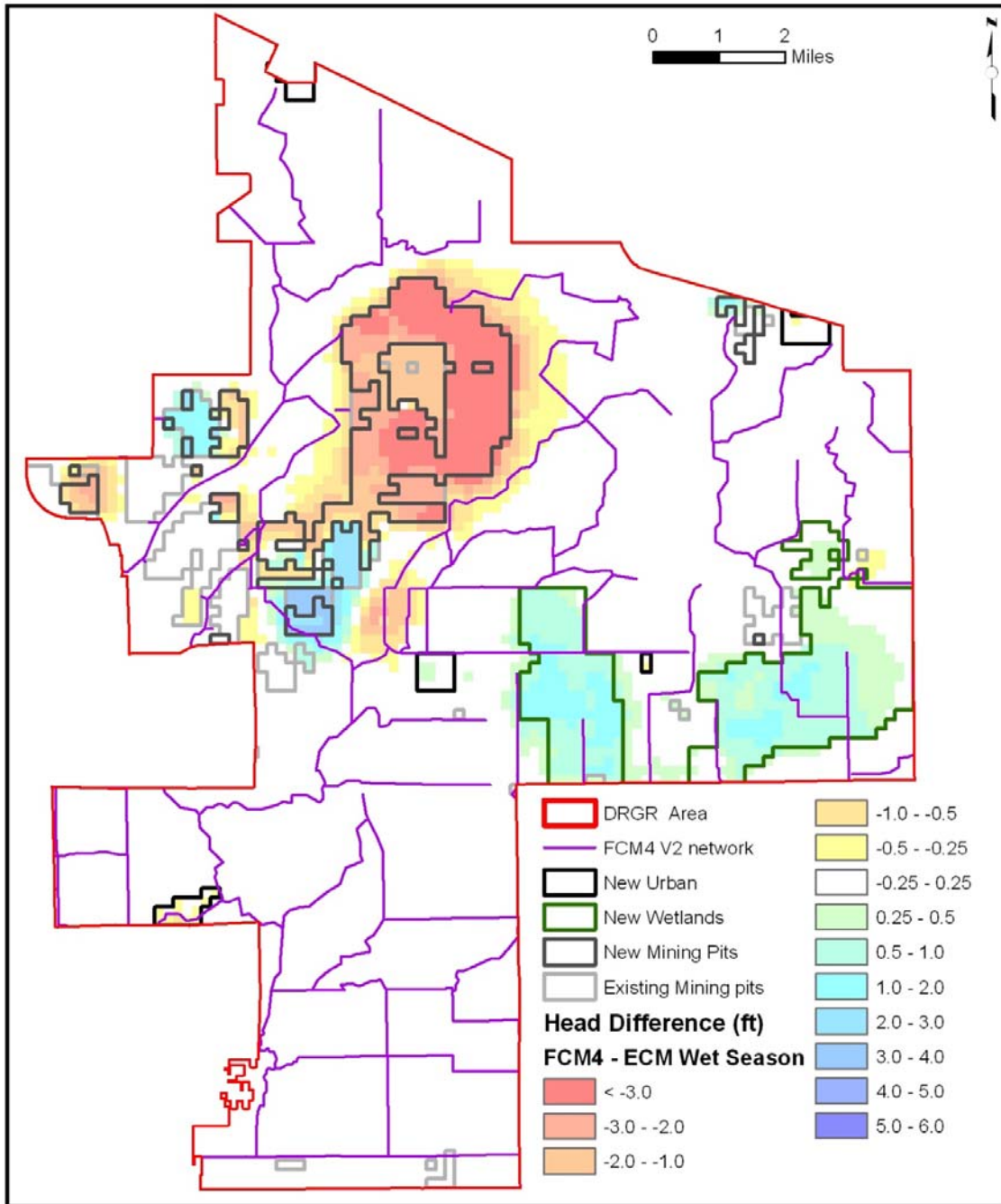
Figure 79. Difference in wet season water table in FCM4 in relation to the LS ECM (Positive values indicate increase in water table elevation in the FCM4).
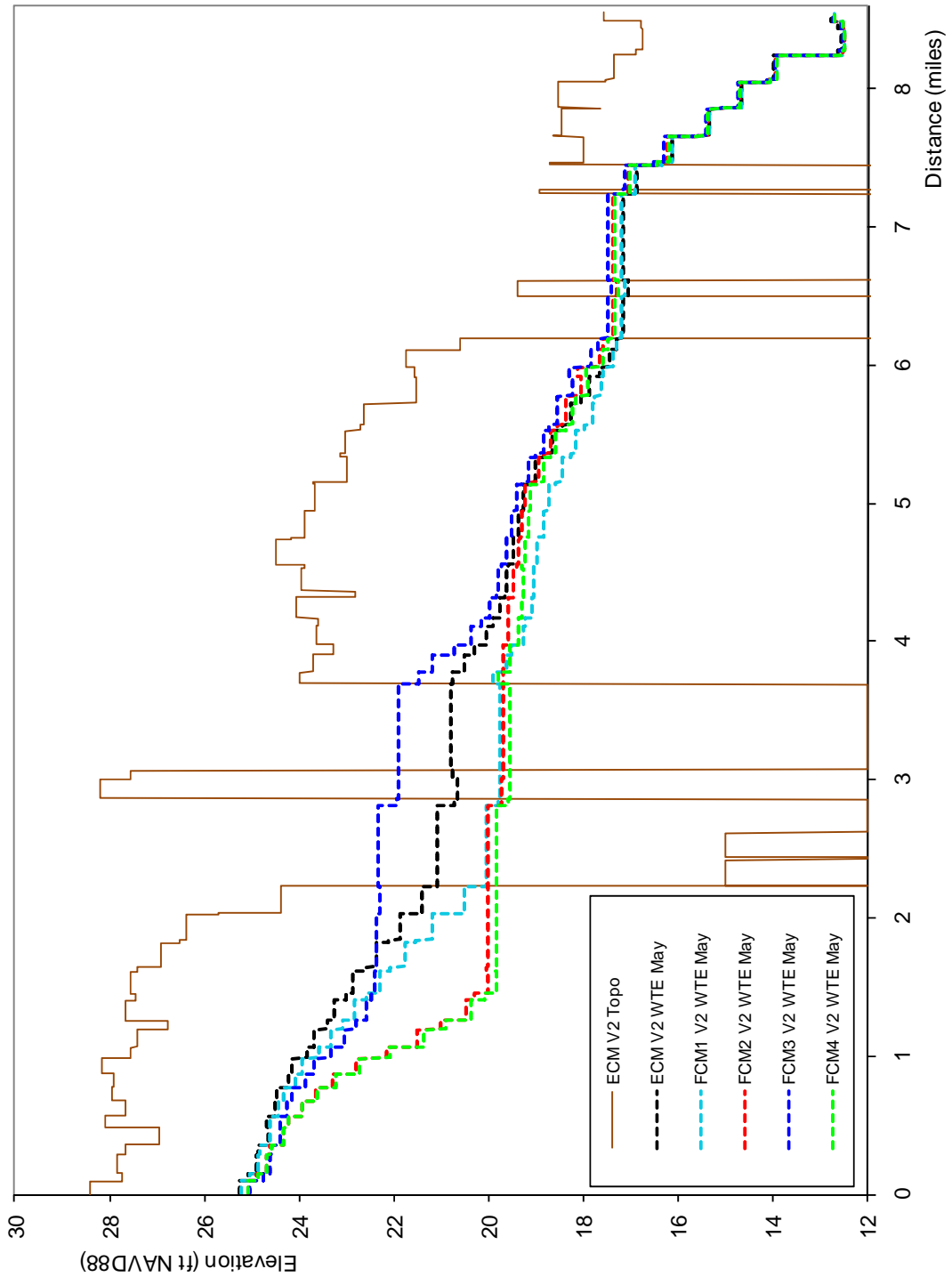
Figure 80. Water table level profile along Transect 1 presented in **Figure 30** at the end of the dry season.
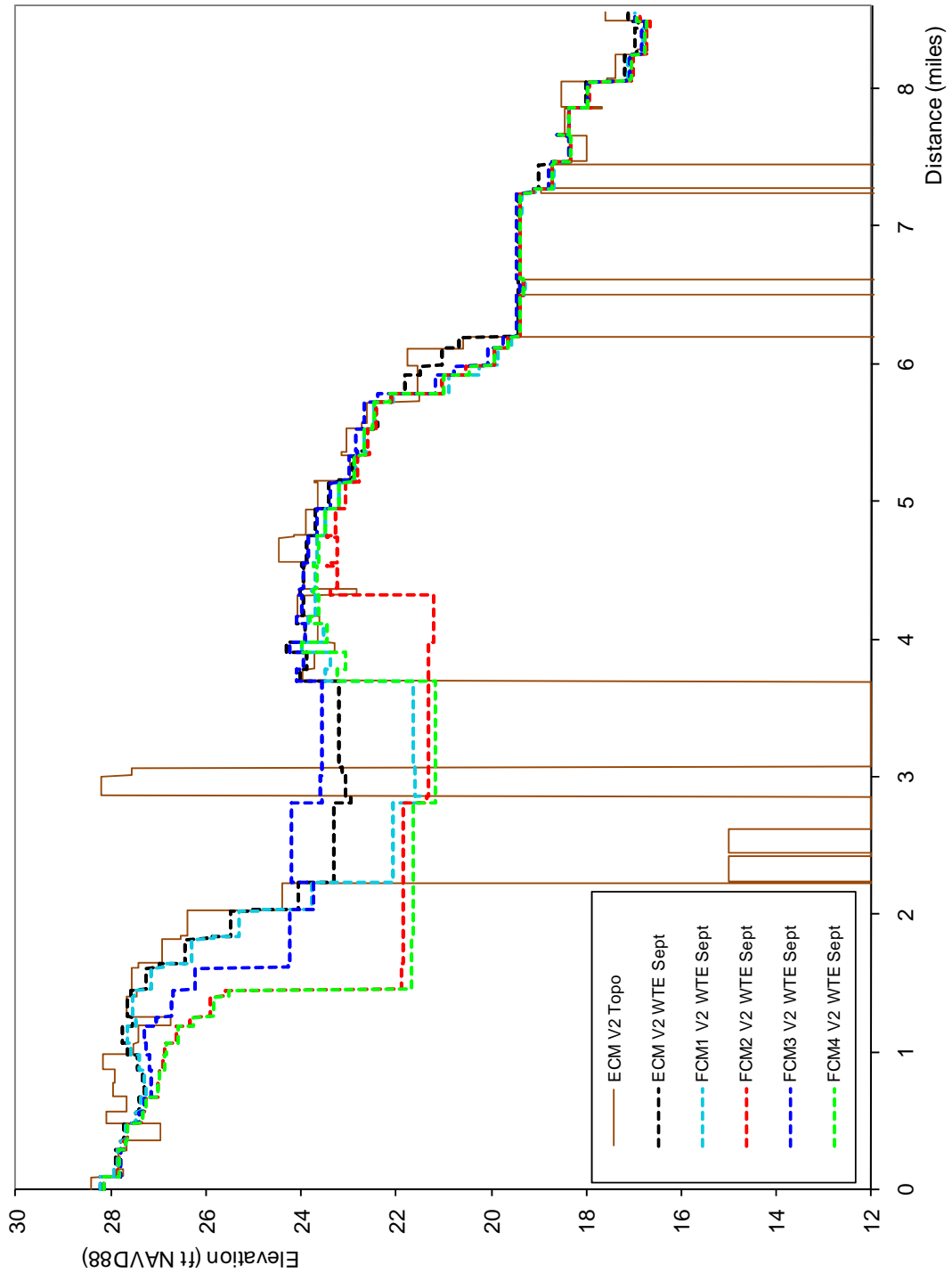
Figure 81. Water table level profile along Transect 1 presented in Figure 30 at the end of the wet season.
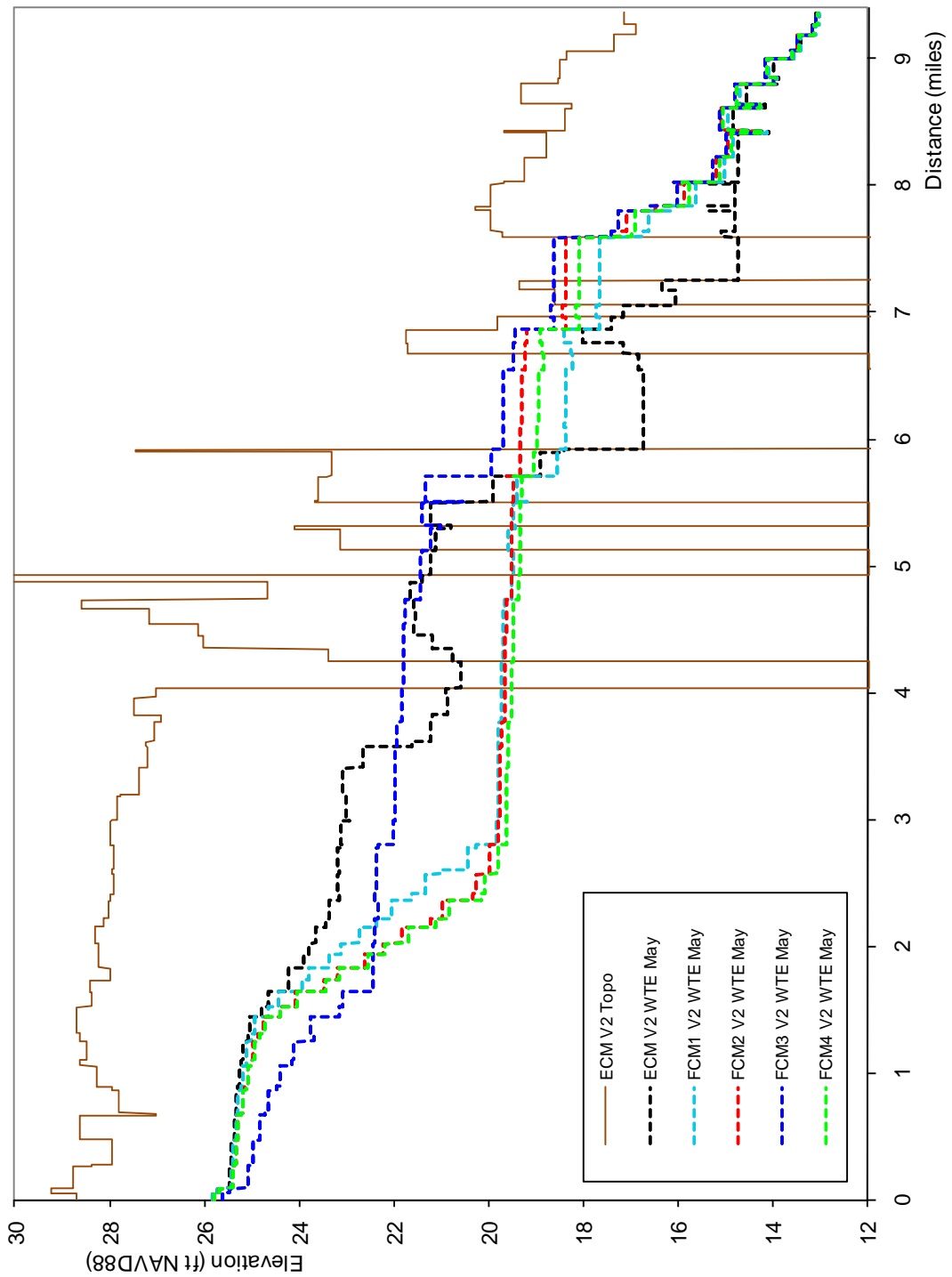
Figure 82. Water table level profile along Transect 2 presented in Figure 30 at the end of the dry season.
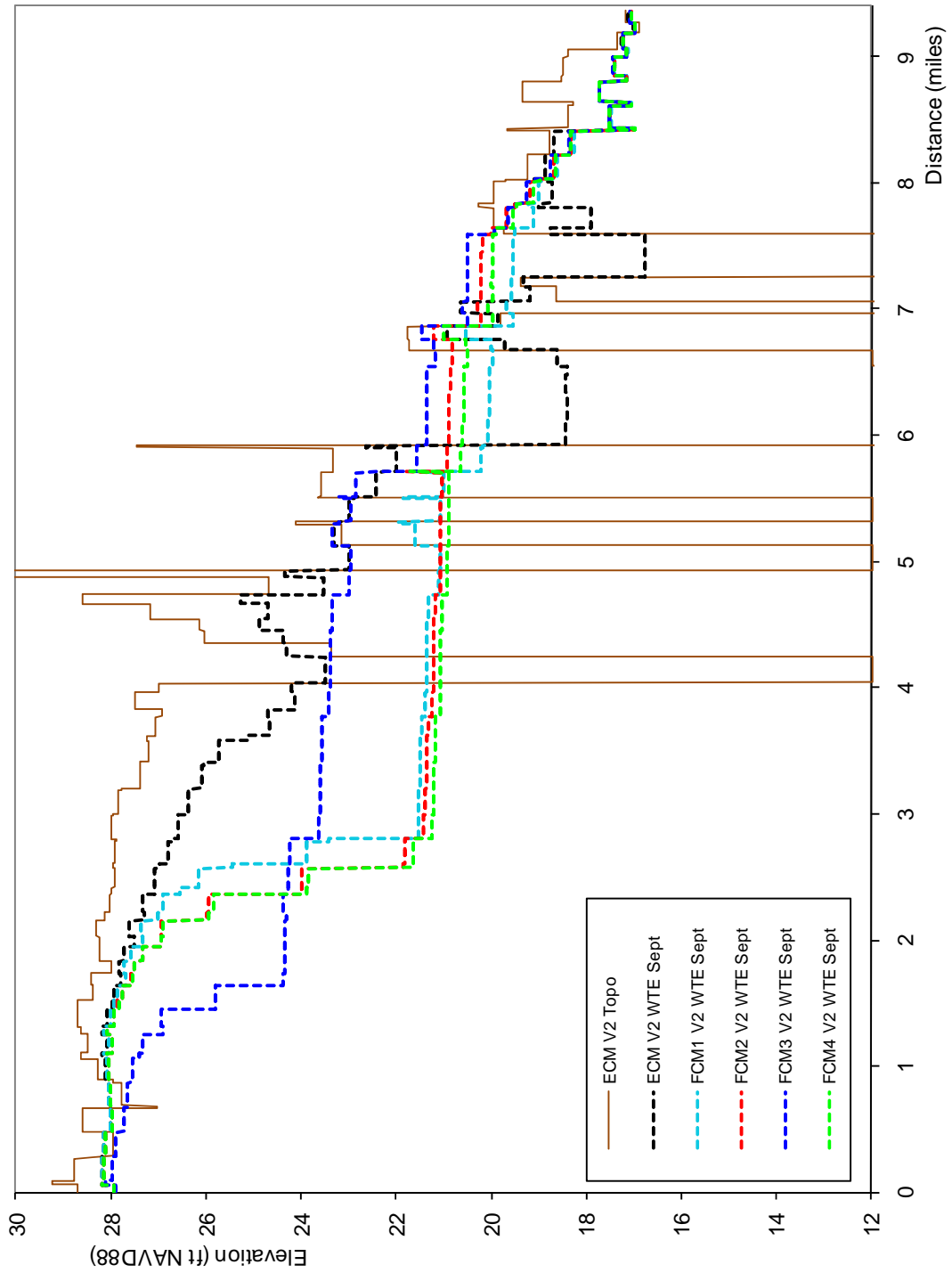
Figure 83. Water table level profile along Transect 2 presented in Figure 30 at the end of the wet season.

Water Table Maps Statistical Analysis

A statistical analysis of the water table difference maps (Figure 72 to Figure 79) was performed by considering grid model cells inside the DR/GR Area that are classified as "natural" land uses (land use codes from 7 to 19). From those grid cells, an average difference was computed. Additionally, the differences were divided into classes matching those shown in the legend of those figures. The number of grid cells that were wetter (positive differences) minus the number of drier grid cells (negative differences) was calculated. The result of this processing is shown in **Table 14**.

The DR/GR Area has been dried out through the years with respect to the predevelopment (natural system) conditions. Thus, it is desirable to increase the water table levels in natural areas inside the DR/GR Area. Consequently, a higher average difference in water table levels (corresponding to wetter conditions at those locations) may be considered a desirable net impact and lower average water table levels could be considered as a negative impact. A higher number of wetter minus drier cells may also be an indication of a desirable net impact. In the former case, the impact is referred to as a net water level change, and in the second case as a net areal extent of wetter conditions. Usually, a net positive impact from a FCM is shown in both water level and areal extent.

According to this statistical processing for natural areas remaining in the DR/GR Area, the dry-season water table elevation differences are highest in the FCM3 and lowest in the FCM1. In the case of the wet-season water table elevation differences, they are highest in the FCM4 and lowest in the FCM3.

Table 14. Statistical processing of the water table difference maps.

FCM Maps	Statistical parameter	FCM1	FCM2	FCM3	FCM4
Water Table Level differences at the end of the dry season (May)	spatial average (ft)	0.010	0.033	0.178	0.096
	Number of wetter minus drier 750-ft grid cells	-216	16	736	256
Water Table Level differences at the end of the wet season (September)	spatial average (ft)	-0.037	-0.030	-0.054	0.012
	Number of wetter minus drier 750-ft grid cells	82	48	6	372

Hydroperiod Maps

Hydroperiod maps obtained from all the FCMs are presented in Appendix H. **Figure 84** through **Figure 87** illustrate the hydroperiod differences between the various scenarios and the existing conditions model (ECM) inside the DR/GR Area. Those maps are a complementary indicator to measure the impact of the land use changes on natural wetland areas.

The hydroperiod results are consistent with water table results previously displayed. The areas that show hydroperiod differences in the Future Condition Models (FCMs) in

general correspond to the areas that show differences in water table elevations at the end of the wet season.

Increasing the areal coverage of mining pits in the large mining pit complex of the DR/GR Area causes differences in the hydroperiod in surrounding areas. In general, the hydroperiod decreases with decreased water table levels up gradient of the mining pits and increases with increased water table levels down gradient of the mining pits. The flow ways north of Corkscrew Road experienced the largest negative effect on hydroperiod in the case of the FCM3.

In general, the hydroperiod increases in restored areas (converted from agricultural to wetland). This is a consequence of removing the drainage system of the agricultural area, which tends to lower the water table during the wet season.
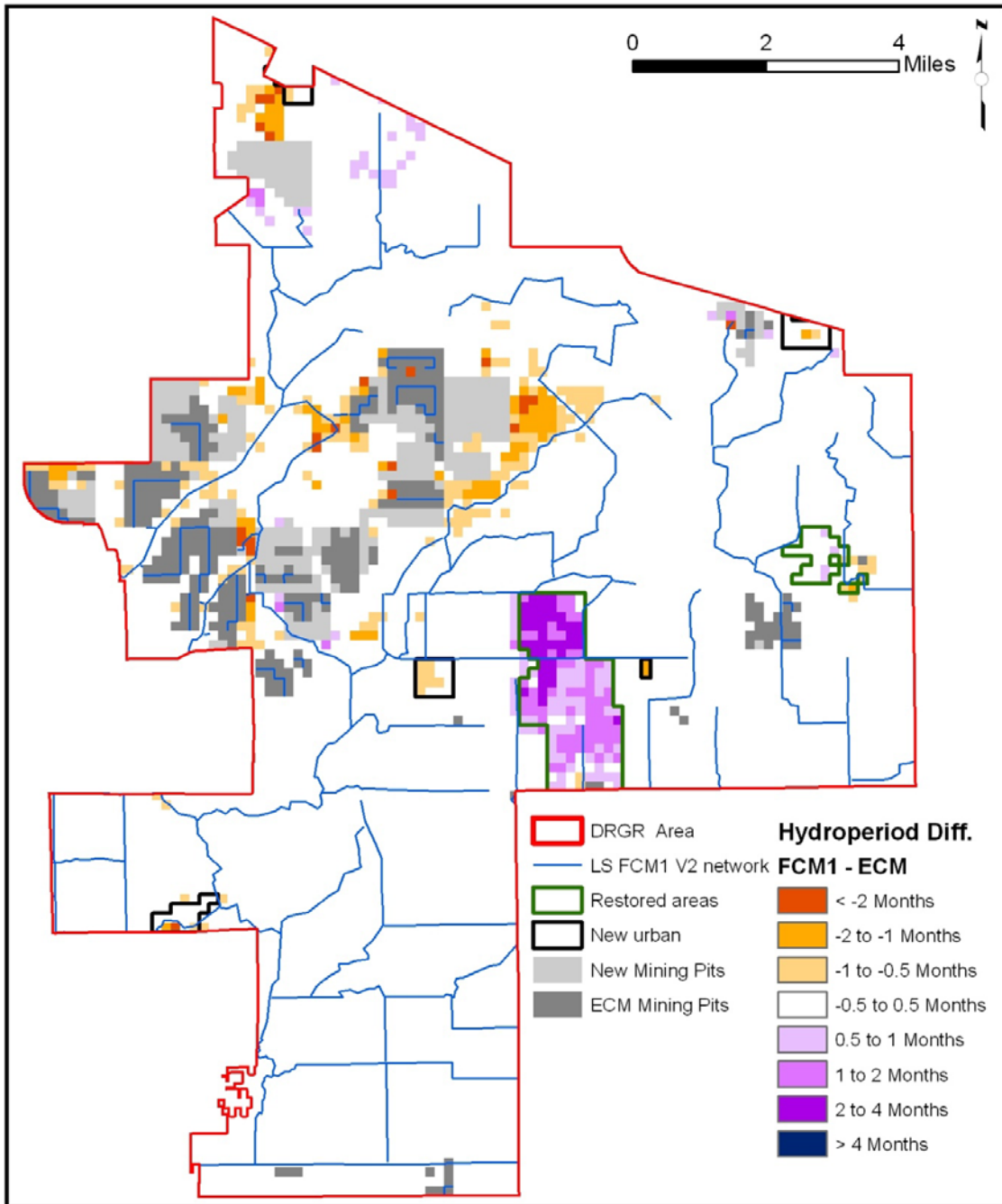
Figure 84. Difference in hydroperiod in FCM1 in relation to the LS ECM (Positive values indicate greater duration of water ponding in FCM1).
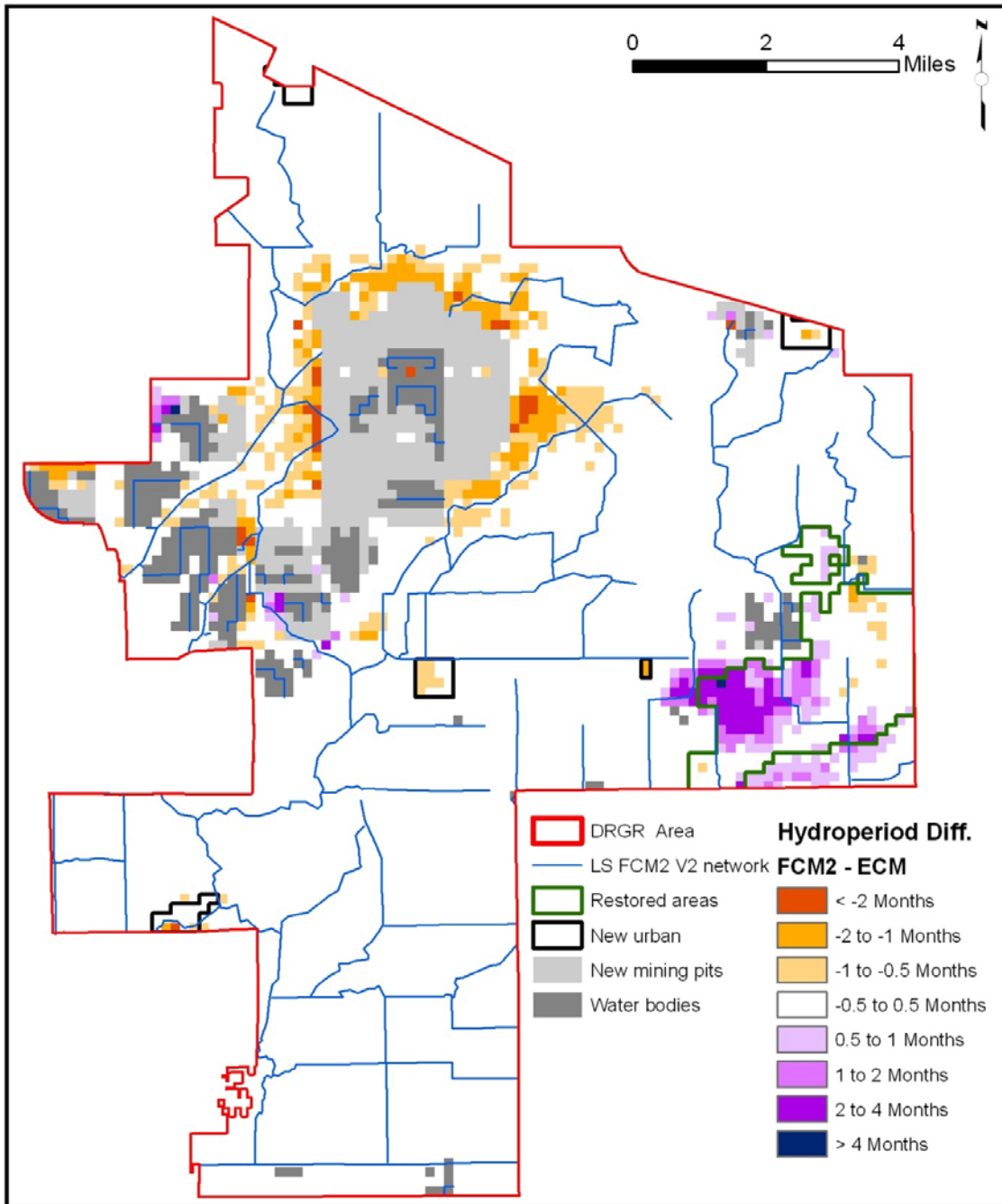
Figure 85. Difference in hydroperiod in FCM2 in relation to the LS ECM (Positive values indicate greater duration of water ponding in FCM2).
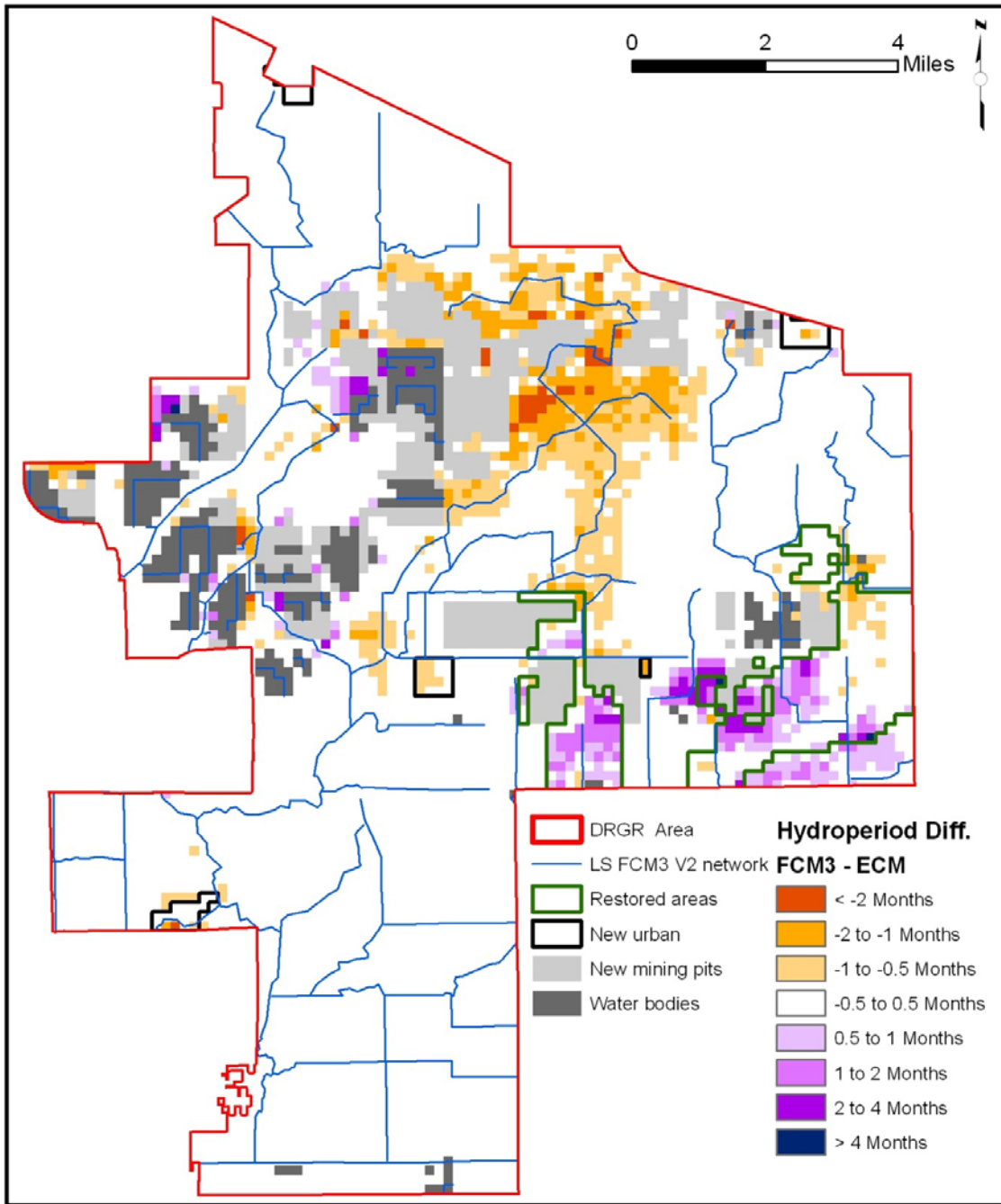
Figure 86. Difference in hydroperiod in FCM3 in relation to the LS ECM (Positive values indicate greater duration of water ponding in FCM3).
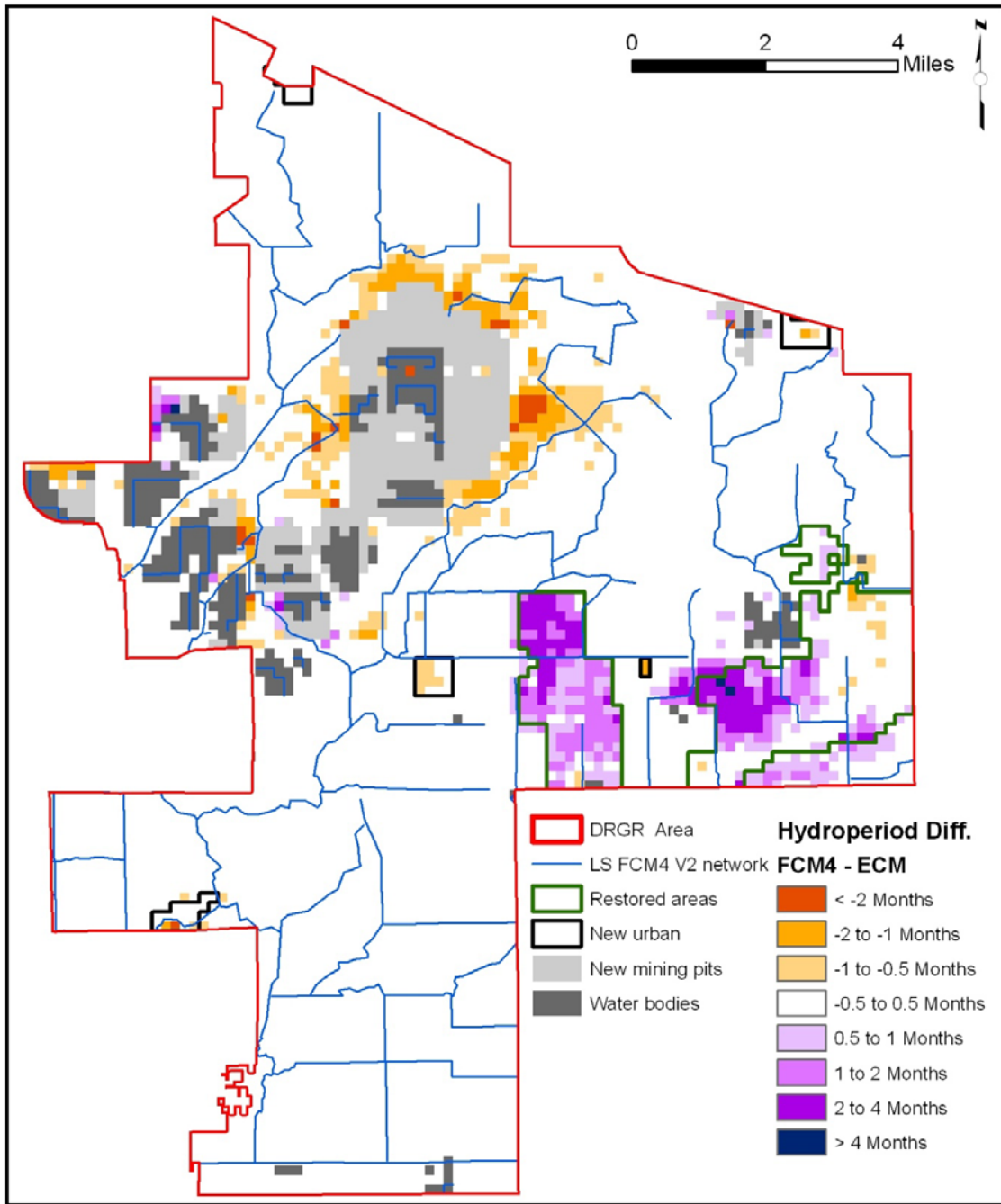
Figure 87. Difference in hydroperiod in FCM4 in relation to the LS ECM (Positive values indicate greater duration of water ponding in FCM4).

A statistical analysis of the hydroperiod difference maps (Figure 84 to Figure 87) as well as the water depth differences during the hydroperiod (included in Appendix H) was performed by considering grid model cells inside the DR/GR Area that are classified as "natural" land uses (land use codes from 7 to 19). From those grid cells, an average difference was computed. Additionally, the differences were divided into classes matching those shown in the legend of those figures. The number of grid cells that were wetter (positive differences) minus the number of drier grid cells (negative differences) was calculated. The result of this processing is shown in **Table 15**.

An average positive difference in hydroperiod and water depth during the hydroperiod (corresponding to wetter conditions at those locations) may be considered a desirable net impact. A negative average hydroperiod and water depth difference during the hydroperiod could be considered as a negative impact. A higher number of wetter minus drier cells may also be an indication of a desirable net impact. In the former case, the impact is referred to as a net hydroperiod or water depth change, and in the second case as a net areal extent of wetter conditions. Usually, a net positive impact from a FCM is shown in both water level and areal extent.

According to this statistical processing for natural areas remaining in the DR/GR Area, the hydroperiod differences and the water depth differences during the hydroperiod are highest in the FCM4 and lowest in the FCM3.

Table 15. Statistical processing of the hydroperiod difference maps.

FCM Maps	Statistical parameter	FCM1	FCM2	FCM3	FCM4
Hydroperiod differences	spatial average (month)	-0.05	-0.07	-0.11	0.01
	Number of wetter minus drier 750-ft grid cells	-72	-214	-446	160
Water depth differences during hydroperiod	spatial average (in)	-0.08	-0.07	-0.26	0.00
	Number of wetter minus drier 750-ft grid cells	166	136	-614	352

A natural systems model (NSM) was constructed using the intermediate ECM. This model was intended to be used to help determine future scenarios that most closely returned areas of the DR/GR to their natural states. However, the revised topography changed the hydroperiod prediction significantly and the NSM based on that intermediate step was not accurate enough to be useful for such analyses.

In lieu of the NSM evaluation, a comparison of the hydroperiod maps based on KLECE data for existing conditions (Figure 35) and for the historic conditions (**Figure 88**)

was conducted. For the comparison, the hydroperiod (in the mean of the class interval) from those polygon shape file maps was discretized to 750-ft resolution raster maps.

The map with the difference between the existing and the historical mean hydroperiods is shown in **Figure 89**. From that, a map showing the areas where the hydroperiod was increased or decreased was also obtained as shown in **Figure 90**. The area where the hydroperiod has been decreased from the historical conditions is larger, which indicates the DR/GR Area is drier today than it was in the past.

Unfortunately, a direct comparison between the KLECE data (Figure 89) and the modeled maps (Figure 84 to Figure 87) is not possible since the hydroperiod magnitudes reported by KLECE do not correspond exactly to the hydroperiod magnitudes obtained from the model, as discussed in previous sections.

In order to have a semi-quantitative estimation of how close the FCM hydroperiods are with respect to the historical conditions, the following statistical analysis was conducted. FCM hydroperiod difference maps (Figure 84 to Figure 87) were grouped in three classes as was done in Figure 90, i.e., increased (greater than 0.5 months), decreased (lower than negative 0.5 months) and unchanged (otherwise). Then, the grouped FCM hydroperiod differences in natural area (land use codes from 7 to 19) grid cells in the DR/GR Area were compared with the differences in Figure 89. The results are summarized in **Table 16**.

Table 16. Statistical processing of the model- and KLECE-based hydroperiod-grouped-difference maps.

(1) Existing – historical (based on KLECE)	(2) FCM – ECM (based on modeling)	(3) FCM – historical (combined)	(4) FCM direction with respect to historical	(5) Number of natural 750-ft grid cells in the DR/GR Area			
				FCM1	FCM2	FCM3	FCM4
increased	decreased	undefined	neutral	39	37	70	39
increased	unchanged	increased	neutral	412	410	367	404
increased	increased	increased	neutral	35	30	46	64
unchanged	decreased	decreased	negative	91	138	223	118
unchanged	unchanged	unchanged	neutral	1355	1289	1204	1319
unchanged	increased	increased	neutral	53	63	85	100
decreased	decreased	decreased	negative	96	150	217	146
decreased	unchanged	decreased	neutral/negative(*)	1478	1498	1477	1534
decreased	increased	undefined	positive	101	124	153	215
Positive- minus negative-direction grid cells		case (*) as neutral		-86	-164	-287	-49
		case (*) as negative		-1564	-1662	-1764	-1583

Table 16 shows the combined hydroperiod difference between future and historical conditions also classified as increased, unchanged and decreased. A class labeled as undefined was added to account for areas with the combination of decreased plus increased where the net result of this combination is unknown.

This table also includes a column to classify the direction of changes in future conditions hydroperiod with respect to the historical conditions (see column (4)). Changes are considered to be in the "negative" direction when the FCM predicts the hydroperiod decreases with respect to the ECM and the existing hydroperiod from KLECE decreases or does not change with respect to the historical. It may be considered to be "neutral" or "negative", when the FCM predicts no changes in hydroperiod with respect to the ECM and the existing hydroperiod from KLECE decreases with respect to the historical. A change is considered to be in the "positive" direction in this column, when the FCM predicts a hydroperiod increase with respect to the ECM and the existing hydroperiod from KLECE decreases with respect to the historical. Other combinations labeled as "neutral" are assumed to produce no changes in that direction. Even when an increase in the future condition hydroperiod with respect to the ECM may be an indication of some mitigation effort, it is not considered as "positive" in the direction toward the historical conditions, if this occurs in a cell that has the same or higher hydroperiod in the existing conditions with respect to the historical conditions, i.e., increasing the period of the ponded water in an area that already has the historical hydroperiod is not considered "positive".

An overall measure of the direction of the hydroperiod changes with respect to the historical conditions is computed in the last row of Table 16 by subtracting the number of cells with hydroperiod changes in the "negative" direction (in the "FCM direction with respect to historical" column) to the ones in the "positive" direction (in that same column). Two choices are shown by considering the combination "decreased" in column (1) and "unchanged" in column (2) as "neutral" or "negative". As a result, FCM3 is the scenario with the highest areal extent where the hydroperiod is shorter than in the historical conditions (i.e. it has the most negative number). FCM1 and FCM4 have the lowest areal extent where the hydroperiod is shorter than in the historical conditions (i.e. their results are closest to positive values in the last row of the table).
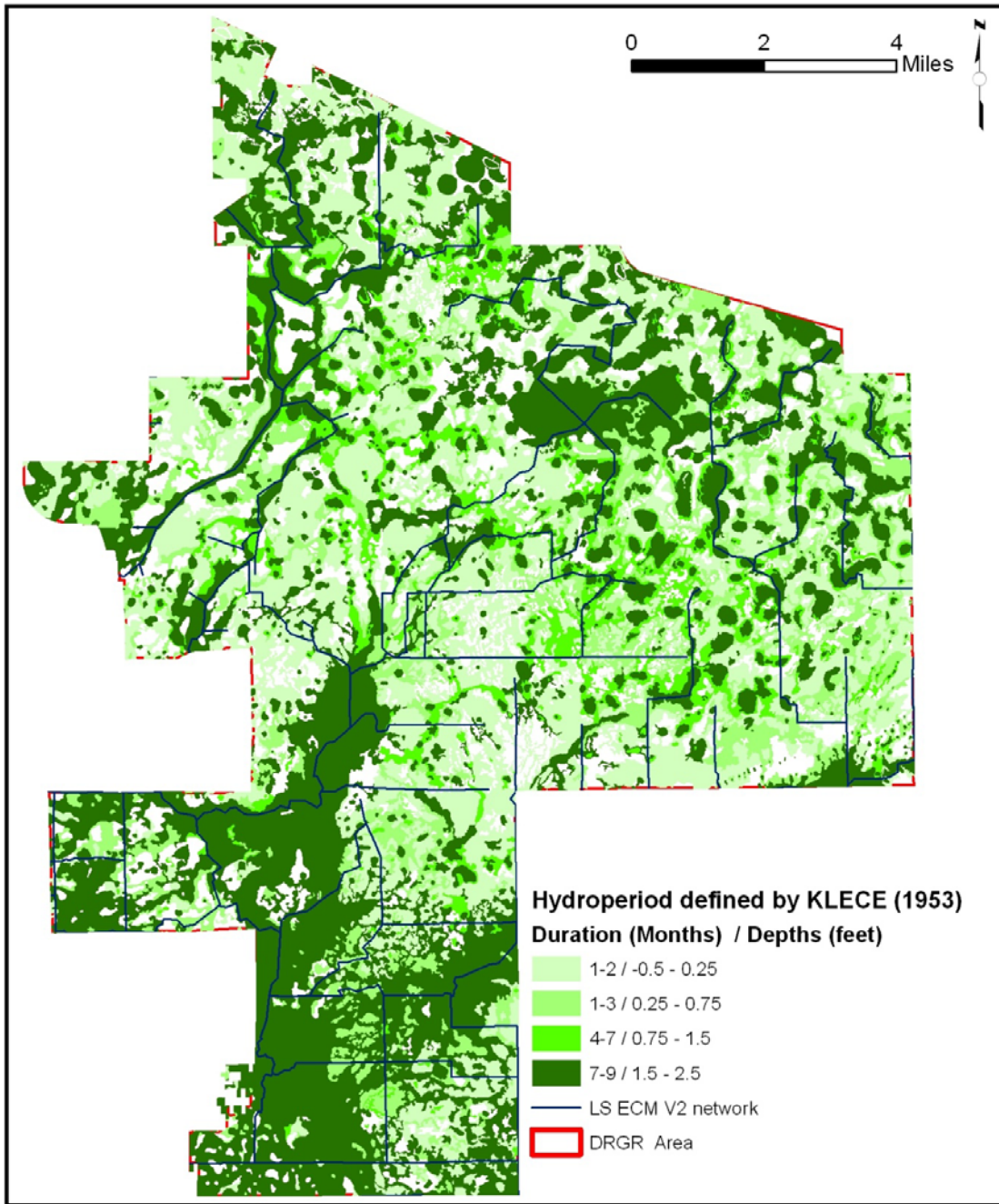
Figure 88. Hydroperiod map generated based on data created by KLECE from 1953 aerial photos.
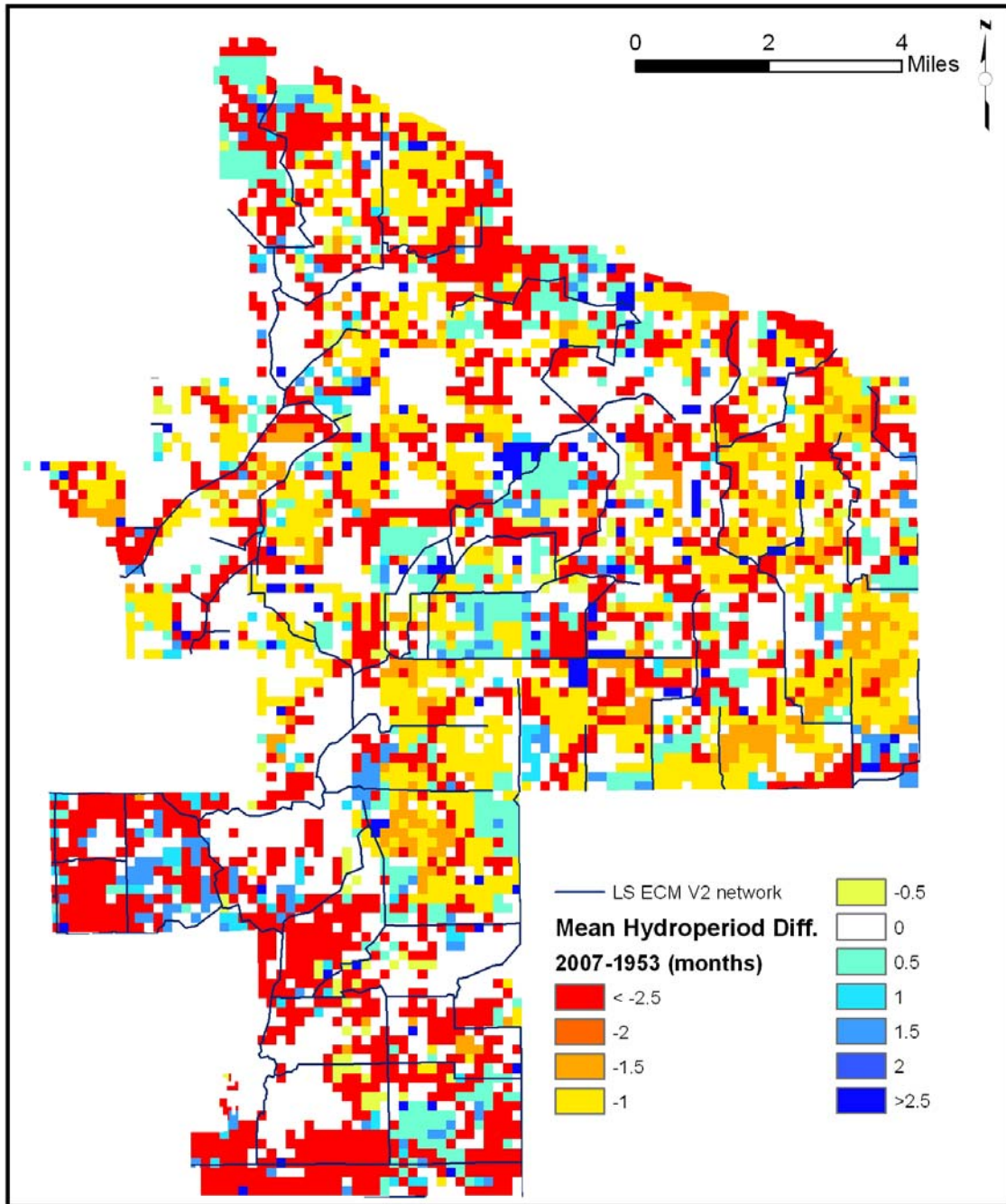
Figure 89. Mean hydroperiod map differences (existing minus historical) based on data created by KLECE from aerial photos.
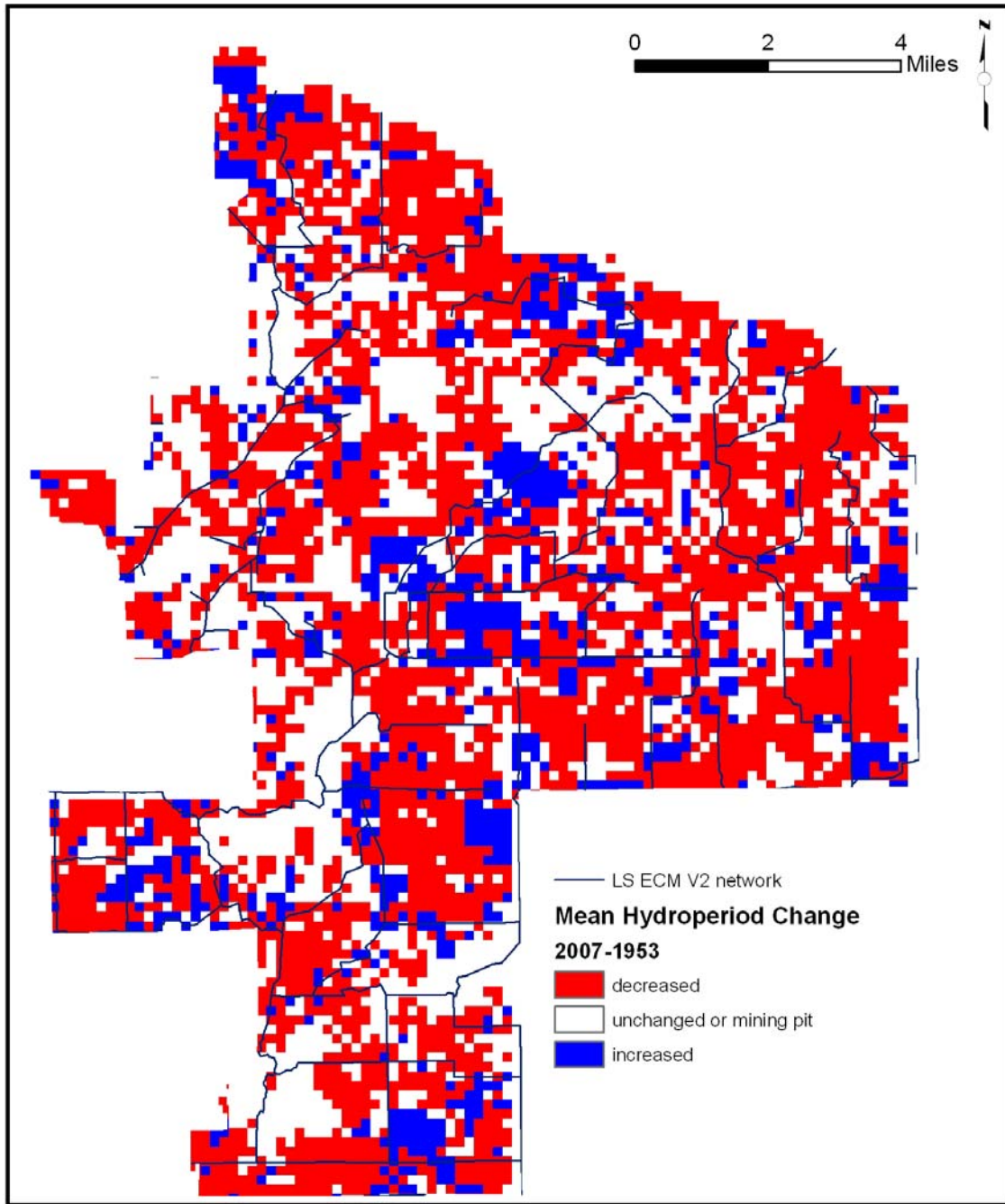
Figure 90. Map of hydroperiod changes after processing the data created by KLECE from aerial photos.

Water Budgets

Water budget calculations conducted for different areas of the models are presented in the following subsections.

DR/GR Area

A detailed water budget component breakdown for the DR/GR Area is presented in **Table 17**, which are annually averaged for all scenarios. More detailed charts for all the scenarios are included in Appendix I. Some of the main components are plotted as a function of the mining pit areal extent in the DR/GR Area and as a function of the area containing mining pits and natural land use in **Figure 91**. A red line is superimposed to highlight the trend of those depth rates with respect to the mining pit area and the mining pit plus natural areas.

The results from the LS ECM and the FCMs indicate, in general, that increased coverage of mining pits and natural areas in a scenario leads to higher evapotranspiration (ET) rates and, therefore, to lower net rainfall (i.e., rainfall - ET) rates. In other words, higher ET rates are found in scenarios where there is a larger area of water ponded or close to the ground surface (i.e., area of mining pits and wetlands).

The annual-averaged surface water outflow (runoff) rates from the DR/GR Area were about 1.1 inch/year lower for the future scenarios with respect to the LS ECM. The correlation in this case with the mining pit areal extents and with the area containing mining pits and natural land use is not as clear in the plot as in the case of the ET. Decreased runoff when more mining pits are present is expected from the higher open-water storage in mining pits and the subsequent absence of runoff from them. A linear extrapolation of the surface water outflow rates in Figure 91 reaches a value of zero at about 45 % areal extent of mining pit coverage. This may be an indication that the mining pits also reduce the surface water flow in neighboring areas and interrupt pre-developed flow ways.

There is a higher pumping rate assumed in the FCMs of about 0.4 inches/year for the entire DRGR area with respect to the LS ECM. This is about one third of the reduction in the SW outflow rate and may be partially contributing to the SW outflow reduction.

The groundwater outflow from the DR/GR Area (labeled as CSZ in Table 17) is an indicator of groundwater recharge in the DR/GR Area. The model results generally show slightly higher groundwater outflow rates from the DR/GR (about 0.2 inches/year) for the future scenarios with respect to the LS ECM. The correlation in this case with the mining pit areal extents and with the area containing mining pits and natural land use is not as clear in the plot as in the case of the ET.

Table 17. Annual average depth rates of the water balance components for the entire DR/GR Area as predicted from different models.

Depth rates (inches/year)	Model	ECM	FCM1	FCM2	FCM3	FCM4
Rainfall		58.88	58.88	58.88	58.88	58.88
ET		48.02	48.53	48.66	48.74	48.48
Rainfall - ET (A)		**10.86**	**10.35**	**10.22**	**10.14**	**10.40**
OL storage change		-0.03	-0.03	0.01	-0.11	0.02
UZ Storage change		0.04	0.04	0.04	0.03	0.04
Total SZ Storage change (BSZ)		-0.38	-0.37	-0.36	-0.34	-0.36
Total storage (B)		**-0.37**	**-0.36**	**-0.31**	**-0.42**	**-0.31**
Net OL Boundary outflow (COL)		0.19	0.17	0.16	0.18	0.21
Drain to Boundary (CDR)		0.00	0.00	0.00	0.00	0.00
Net SZ Boundary outflow from SZ1		1.74	2.00	1.80	1.75	1.81
Net SZ Boundary outflow from SZ2		0.06	0.09	0.08	0.11	0.11
Net SZ Boundary outflow from SZ3		-0.54	-0.59	-0.46	-0.43	-0.46
Net SZ Boundary outflow from SZ4		-0.38	-0.41	-0.36	-0.34	-0.35
Net SZ Boundary outflow from all SZ (CSZ)		0.87	1.10	1.06	1.09	1.11
Total Boundary outflow (C)		**1.06**	**1.26**	**1.22**	**1.26**	**1.32**
Pumping from SZ1		1.18	0.99	0.86	0.68	0.75
Pumping from SZ2		1.02	0.81	0.85	0.73	0.75
Pumping from SZ3		3.09	3.31	2.96	2.89	2.92
Pumping from SZ4		0.50	0.57	0.57	0.56	0.57
Pumping from all SZ		5.79	5.67	5.25	4.87	4.99
Irrigation		2.54	2.09	1.67	1.28	1.41
Pumping-Irrigation (D)		**3.25**	**3.58**	**3.58**	**3.59**	**3.58**
Infiltration from OL to SZ1		27.86	24.16	22.41	19.71	22.42
Infiltration from SZ1 to SZ2		3.70	3.74	3.60	3.48	3.50
Infiltration from SZ2 to SZ3		2.63	2.84	2.69	2.65	2.65
Infiltration from SZ3 to SZ4		0.11	0.14	0.20	0.21	0.21
OL->river		-14.66	-11.90	-10.73	-8.38	-10.87
Drain to river		21.62	17.64	16.42	14.01	16.63
Drain to ext. river		0.21	0.30	0.20	0.22	0.21
Base flow to River		-0.25	-0.18	-0.16	-0.13	-0.16
Total flow to river (E)		**6.92**	**5.86**	**5.73**	**5.71**	**5.81**
Error (A-B-C-D-E)		0.01	0.00	0.00	0.01	0.01
Boundary surface outflow (runoff)	COL+CDR+E	7.11	6.03	5.89	5.88	6.02
	---	---	---	---	---	---
Net groundwater recharge	A-(B-BSZ)-(C-CSZ)-E= BSZ+CSZ+D	3.73	4.30	4.27	4.33	4.33
	---	---	---	---	---	---
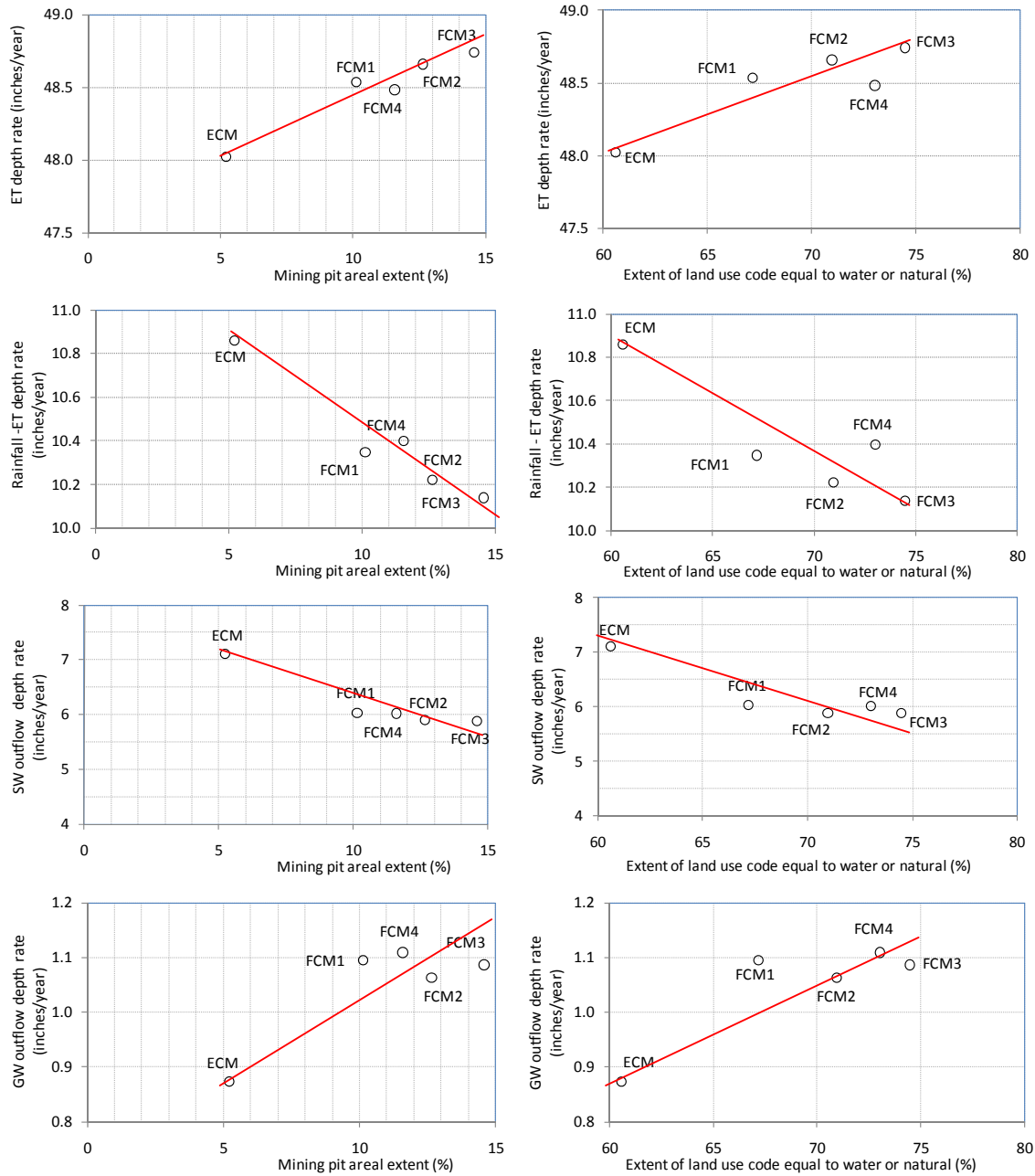
Figure 91. Annual averaged Water Balance Components in the DR/GR Area from all Models.

The seasonal oscillation of the main water balance components is shown in **Figure 92** through **Figure 95**. Daily ET rates are higher from April to September due to the higher temperatures. The daily net rainfall rate is positive from mid May to mid October (rainy season), which approximately matches the period of positive surface water outflow from the DR/GR Area. The surface water outflow rate peaks during the months of August and September (late wet season). Groundwater outflows are higher from August to November.

Different land use scenarios show slight differences in seasonal patterns, which cause the differences in the annual averaged values presented in Table 17. ET and groundwater outflow rate differences are lower in the wet months and higher in drier months. Conversely, surface water outflow rate differences are lower in drier months and higher in wet months.
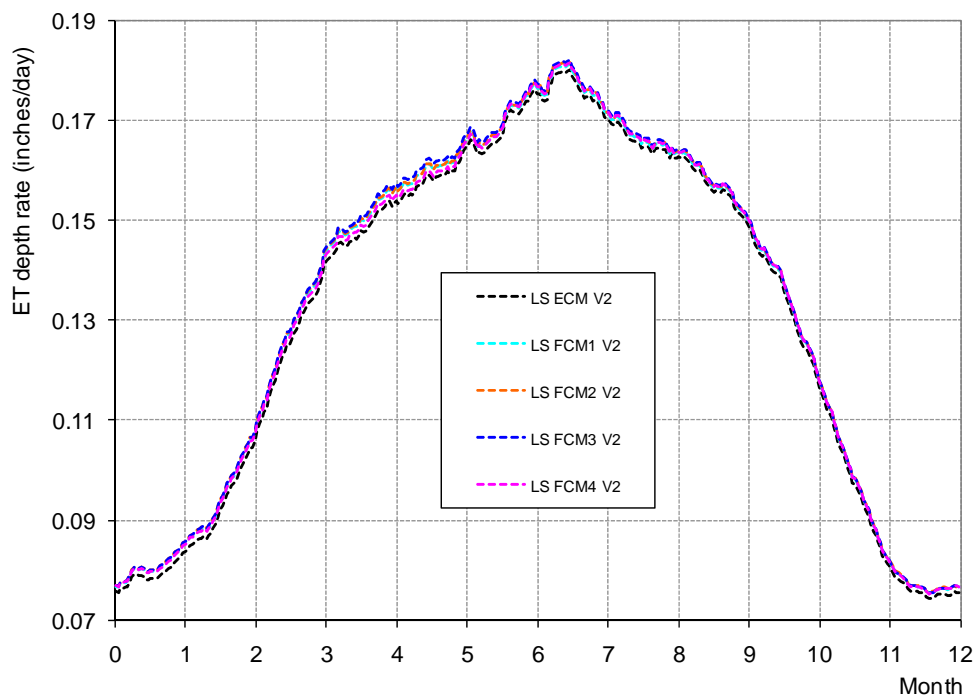
Figure 92. Seasonal averaged evapotranspiration in the DR/GR Area for all scenarios.
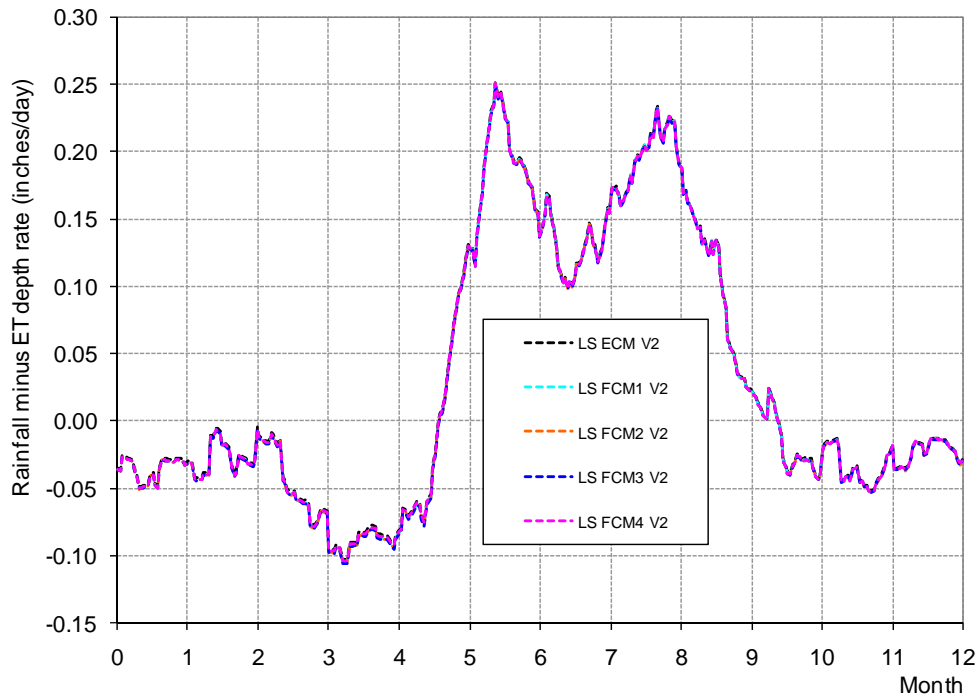
Figure 93. Seasonal averaged net rainfall in the DR/GR Area for all scenarios.
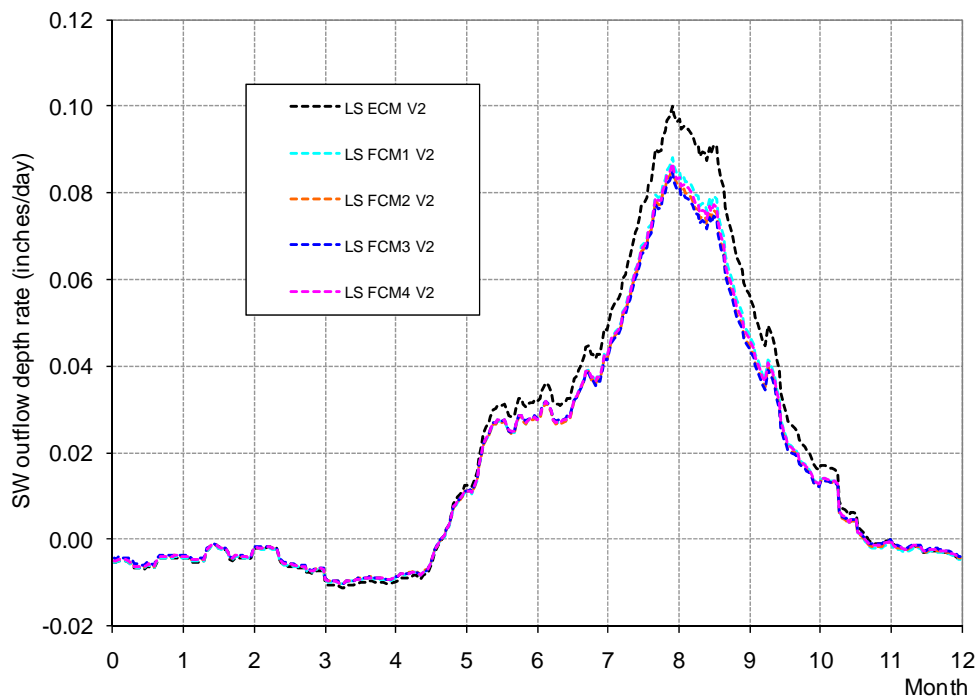
Figure 94. Seasonal surface water outflow from the DR/GR Area for all scenarios.
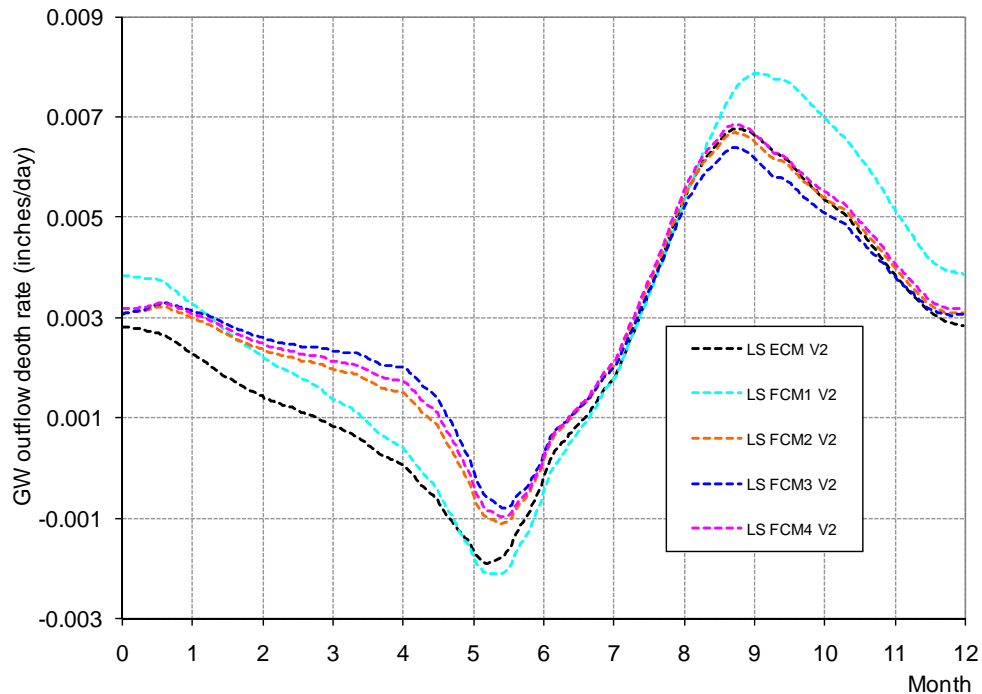
Figure 95. Seasonal groundwater outflow from the DR/GR Area for all scenarios.

Mining Pits and Lakes

A detailed water budget component breakdown for mining pits and shallow water bodies around the DR/GR area is presented in **Table 18**. Notice that the average ET depth rate in the water bodies does not differ significantly from the one in the ECM. Thus, the ET volumetric rate is approximately proportional to the area covered by the water bodies, and this supports the linear correlation between the ET depth rate for the entire DR/GR and the mining pit areal coverage shown previously in Figure 91.

As previously observed when discussing the ECM results in Table 8, the net rainfall (rainfall minus ET) in mining pits and lakes is approximately zero inches per year. Moreover, a positive outflow from the drainage system around mining pits is predicted from the model. As a result, the aquifers need to supply water to the mining pits (negative net groundwater recharge) approximately equal to the amount that is lost through the drainage system (3.8 to 7.0 inches/year).

Observation data, other than the LIDAR, for modeling the drainage system around the mining pits was not available, and there may be inaccuracies. However, if these outflows from mines are verified in the field, the construction of flow barriers (berms, flow structures, etc.) in those locations may reduce the outflow (negative recharge) from the aquifers.

Table 18. Annual average depth rates of the water balance components for mining pits and lakes around the DR/GR area as predicted from different models.

Depth rates (inches/year)	Model	ECM	FCM1	FCM2	FCM3	FCM4
Rainfall		59.10	59.59	59.23	58.81	59.00
ET		59.09	59.14	59.04	58.98	59.02
Rainfall - ET (A)		0.00	0.46	0.19	-0.17	-0.02
OL storage change		-0.13	-0.15	0.21	-0.54	0.24
UZ Storage change		0.00	0.00	0.00	0.00	0.00
Total SZ Storage change (BSZ)		-0.02	-0.02	-0.01	-0.03	-0.01
Total storage (B)		-0.15	-0.17	0.19	-0.57	0.23
Net OL Boundary outflow (COL)		0.03	0.01	0.01	0.17	0.01
Drain to Boundary (CDR)		0.00	0.00	0.00	0.00	0.00
Net SZ Boundary outflow from SZ1		-9.02	-10.89	-9.75	-8.10	-10.18
Net SZ Boundary outflow from SZ2		-2.08	-0.49	-0.57	-0.17	-0.66
Net SZ Boundary outflow from SZ3		2.79	3.45	3.68	2.99	3.64
Net SZ Boundary outflow from SZ4		0.10	0.41	0.74	0.35	0.63
Net SZ Boundary outflow from all SZ (CSZ)		-8.20	-7.51	-5.91	-4.94	-6.57
Total Boundary outflow (C)		-8.17	-7.50	-5.90	-4.77	-6.56
Pumping from SZ1		0.48	0.01	0.00	0.01	0.00
Pumping from SZ2		2.33	0.67	0.83	0.74	0.90
Pumping from SZ3		0.18	0.12	0.17	0.15	0.18
Pumping from SZ4		0.56	0.36	0.48	0.42	0.52
Pumping from all SZ		3.55	1.16	1.49	1.32	1.60
Irrigation		0.00	0.00	0.00	0.00	0.00
Pumping-Irrigation (D)		3.55	1.16	1.49	1.32	1.60
Infiltration from OL to SZ1		-4.67	-6.38	-4.44	-3.64	-4.98
Infiltration from SZ1 to SZ2		3.87	4.50	5.31	4.45	5.20
Infiltration from SZ2 to SZ3		3.62	4.32	5.05	3.89	4.96
Infiltration from SZ3 to SZ4		0.65	0.76	1.21	0.76	1.14
OL->river		4.77	6.97	4.41	3.85	4.71
Drain to river		0.00	0.00	0.00	0.00	0.00
Drain to ext. river		0.00	0.00	0.00	0.00	0.00
Base flow to River		0.00	0.00	0.00	0.00	0.00
Total flow to river (E)		4.77	6.97	4.41	3.85	4.71
Error (A-B-C-D-E)		0.00	0.00	0.00	0.00	0.00
Boundary surface outflow (runoff)	---	---	---	---	---	---
	COL+CDR	0.03	0.01	0.01	0.17	0.01
Net groundwater recharge	A-(B-BSZ)-(C-CSZ)-E= BSZ+CSZ+D	-4.67	-6.37	-4.44	-3.64	-4.98
	A= B+C+D+E	0.00	0.45	0.19	-0.17	-0.02

An isolated mine in a relatively flat area located in the northwest corner of the DR/GR Area was considered in future condition model 1 (FCM1). The water table plot in locations M1, M2, and M3, presented in previous sections, showed that the mine is acting like a groundwater reservoir, i.e., releasing water (collected during the rainy season) into the aquifers during the dry season. This may be a unique characteristic of this mine. All the mines in the other scenarios experience too much influence from surrounding mines to determine whether or not they also act as reservoirs.

A water balance calculation was conducted in the proposed mining pit area from the LS ECM and the FCM1 results. The annual averaged rates from 2002 to 2006 are presented in **Table 19**.

The annual averaged net groundwater recharge from that mining pit presented in Table 19 went from -3.7 inches in the ECM to 7.2 inches in the FCM1. This positive increase in the groundwater recharge, however, is accompanied by an increase in the annual ET depth of 10.4 inches and a decrease in the surface water outflow (runoff) of 20.4 inches. In summary, this new proposed mine would increase the groundwater recharge by retaining the pre-mined runoff, but at the cost of losing about half of it as ET.

A comparison between Table 13 and Table 19 reveals that the average annual rainfall in that mining pit area is about 7.4 inches higher than in the entire DR/GR Area and in the entire mining pits and lakes area. The monthly rainfall time series is compared in **Figure 96** for both areas. It is not clear if that higher rainfall rate is due to local climatic conditions or due to the statistical fluctuations expected when analyzing a smaller area. In any case, that mining pit with an annual rainfall that exceeds RET by 19.6% is not representative of the entire DR/GR area where annual rainfall exceeds RET on average by about 8%.
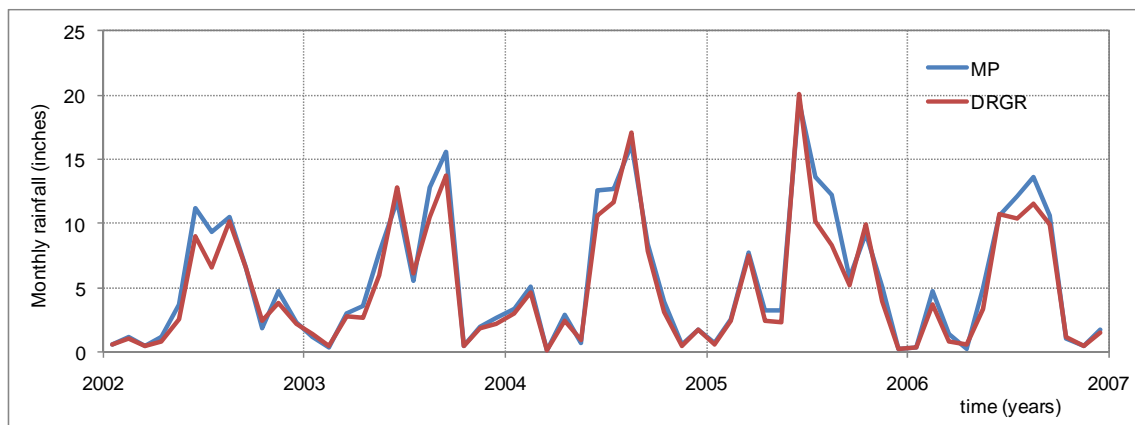
Figure 96. Monthly rainfall in the mining pit area (MP) containing site M2 in Figure 43 compared to the averaged monthly rainfall in the DR/GR Area.

Table 19. Annual average depth rates of the water balance components in a mining pit area located in the northwest corner of the DR/GR Area in the FCM1.

Depth rates (inches/year)		Model	LS ECM	LS FCM1
Rainfall			66.4	66.4
ET			49.8	60.1
Rainfall - ET (A)			**16.7**	**6.3**
OL storage change			0.0	-0.9
UZ Storage change			0.0	0.0
Total SZ Storage change (BSZ)			-0.3	-0.1
Total storage (B)			**-0.3**	**-1.0**
Net OL Boundary outflow (COL)			-9.6	0.0
Drain to Boundary (CDR)			0.0	0.0
Net SZ Boundary outflow from SZ1			-4.5	6.0
Net SZ Boundary outflow from SZ2			0.0	0.0
Net SZ Boundary outflow from SZ3			1.3	1.4
Net SZ Boundary outflow from SZ4			-0.1	-0.1
Net SZ Boundary outflow from all SZ (CSZ)			-3.4	7.3
Total Boundary outflow (C)			**-13.0**	**7.3**
Pumping from SZ1			0.0	0.0
Pumping from SZ2			0.0	0.0
Pumping from SZ3			0.0	0.0
Pumping from SZ4			0.0	0.0
Pumping from all SZ			0.0	0.0
Irrigation			0.0	0.0
Pumping-Irrigation (D)			**0.0**	**0.0**
Infiltration from OL to SZ1			82.2	7.2
Infiltration from SZ1 to SZ2			1.1	1.2
Infiltration from SZ2 to SZ3			1.1	1.2
Infiltration from SZ3 to SZ4			-0.2	-0.2
OL->river			-56.0	0.0
Drain to river			82.2	0.0
Drain to ext. river			4.5	0.0
Base flow to River			-0.8	0.0
Total flow to river (E)			**29.9**	**0.0**
Error (A-B-C-D-E)			0.0	0.0
Boundary surface outflow (runoff)	COL+CDR+E		20.4	0.0
	---		---	---
Net groundwater recharge	A-(B-BSZ)-(C-CSZ)-E= BSZ+CSZ+D		-3.7	7.2
	A= B+C+D+E		---	6.3

New Urban Areas

A water budget calculation was performed in four new urban areas corresponding to the sites labeled from U1 through U4 in Figure 43. The comparison of the annual rates between the ECM and the FCMs are presented in **Table 20**. The differences between the scenarios were small, and just the averaged rate from the four scenarios is displayed.

In general, the modeling predicts that new urban areas have lower ET rates with respect to the existing conditions. This is consistent with the low values of LAI and Rd assumed for this land use classification (see Table 4). Moreover, the absence of irrigation systems assumed in the new urban areas at sites U2 and U4, may contribute to the reduction of the ET losses in those areas. The lower actual ET rate is likely the main reason of why the dry-season water table levels in the new urban areas are in general higher than in the ECM.

Table 20. Annual average depth rates of the water balance components in new urban areas.

Depth rates (inches/year)	Model	U1 ECM	U1 FCMs	U2 ECM	U2 FCMs	U3 ECM	U3 FCMs	U4 ECM	U4 FCMs
Rainfall		64.6	64.6	57.5	57.5	57.5	57.5	56.2	56.2
ET		46.9	45.8	47.9	41.6	52.5	43.1	52.9	35.9
Rainfall - ET (A)		**17.7**	**18.8**	**9.7**	**16.0**	**5.0**	**14.4**	**3.2**	**20.3**
OL storage change		0.0	0.0	0.0	0.0	0.0	0.0	0.0	0.0
UZ Storage change		-0.1	0.0	0.1	0.0	0.0	0.1	0.0	0.0
Total SZ Storage change (BSZ)		-0.4	-0.3	-0.2	-0.2	-0.5	-0.6	-0.3	-0.2
Total storage (B)		**-0.4**	**-0.3**	**-0.1**	**-0.1**	**-0.5**	**-0.4**	**-0.3**	**-0.2**
Net OL Boundary outflow (COL)		-2.6	-5.7	-2.9	-28.7	-41.3	-55.5	-0.6	-0.9
Drain to Boundary (CDR)		0.0	0.0	0.0	0.0	0.0	0.0	0.0	0.0
Net SZ Boundary outflow from SZ1		-5.0	-3.6	8.7	-14.1	-24.2	-39.3	-9.0	0.8
Net SZ Boundary outflow from SZ2		0.0	0.0	0.9	-1.6	0.0	0.0	-0.1	-0.1
Net SZ Boundary outflow from SZ3		5.7	-1.6	0.9	0.9	-10.3	-9.5	5.5	8.4
Net SZ Boundary outflow from SZ4		-0.7	-1.0	0.3	0.4	-0.6	-0.5	1.5	1.9
Net SZ Boundary outflow from all SZ (CSZ)		0.0	-6.2	10.8	-14.4	-35.1	-49.2	-2.1	11.1
Total Boundary outflow (C)		**-2.6**	**-11.9**	**7.9**	**-43.1**	**-76.3**	**-104.8**	**-2.7**	**10.2**
Pumping from SZ1		0.0	0.0	0.1	0.0	0.7	0.0	13.5	0.0
Pumping from SZ2		0.0	0.0	0.0	0.0	0.0	0.1	0.0	0.0
Pumping from SZ3		0.4	8.1	0.0	0.0	13.5	12.5	0.0	0.0
Pumping from SZ4		0.0	0.0	0.0	0.0	0.0	0.0	0.0	0.0
Pumping from all SZ		0.4	8.1	0.1	0.0	14.3	12.5	13.5	0.0
Irrigation		0.4	8.1	0.5	0.0	7.1	5.3	13.5	0.0
Pumping-Irrigation (D)		**0.0**	**0.0**	**-0.4**	**0.0**	**7.2**	**7.2**	**0.0**	**0.0**
Infiltration from OL to SZ1		20.8	32.4	100.0	339.5	53.2	75.1	17.2	21.1
Infiltration from SZ1 to SZ2		5.3	5.4	2.1	-0.2	2.6	2.5	6.9	10.2
Infiltration from SZ2 to SZ3		5.3	5.4	1.2	1.3	2.6	2.4	7.0	10.3
Infiltration from SZ3 to SZ4		-0.8	-1.0	0.3	0.4	-0.6	-0.5	1.5	1.9
OL->river		0.0	0.2	-87.0	-294.8	0.0	0.0	0.0	0.0
Drain to river		0.0	0.0	90.1	323.6	0.0	0.0	6.3	10.3
Drain to ext. river		20.7	30.8	0.0	32.0	74.5	112.4	0.0	0.0
Base flow to River		0.0	0.0	-0.8	-1.5	0.0	0.0	-0.1	-0.1
Total flow to river (E)		**20.7**	**31.0**	**2.3**	**59.2**	**74.5**	**112.4**	**6.2**	**10.2**
Error (A-B-C-D-E)		0.0	0.0	0.0	0.0	0.0	0.0	0.0	0.0

Surface Water Flows

Figure 97 shows a map of locations that were selected for comparison of surface water flow rates among different model scenarios. The annual averaged flow rates presented in **Table 21** show that the flow rate in the main pathways of the DR/GR decreases in the future condition scenarios. This is consistent with the reduction of the total surface outflow rate from the DR/GR Area in the FCMs, as discussed in the previous section.

Table 21. Annual average flow rates at selected pathway locations.

Flow Location	Flow (%)	Flow percentage differences regarding ECM			
	ECM	FCM1	FCM2	FCM3	FCM4
AL	18.6	-4.7	-8.1	-3.9	-6.5
CSa	22.5	-9.7	-10.1	-7.6	-9.6
CSb	3.9	0.0	0.2	-0.6	0.2
CSc	4.9	0.0	-1.8	-2.3	-1.8
CSd	55.0	-7.2	-9.6	-4.5	-7.1
I-75a	35.6	-9.1	-9.3	-10.0	-9.2
I-75b	27.7	-7.3	-6.8	-14.6	-7.8
I-75c	13.3	-2.2	-2.1	-2.7	-2.2
I-75d	100.0	-0.6	-0.8	-2.2	-0.1

Note: A flow of 100 % corresponds to 37.4 ft^3/s.
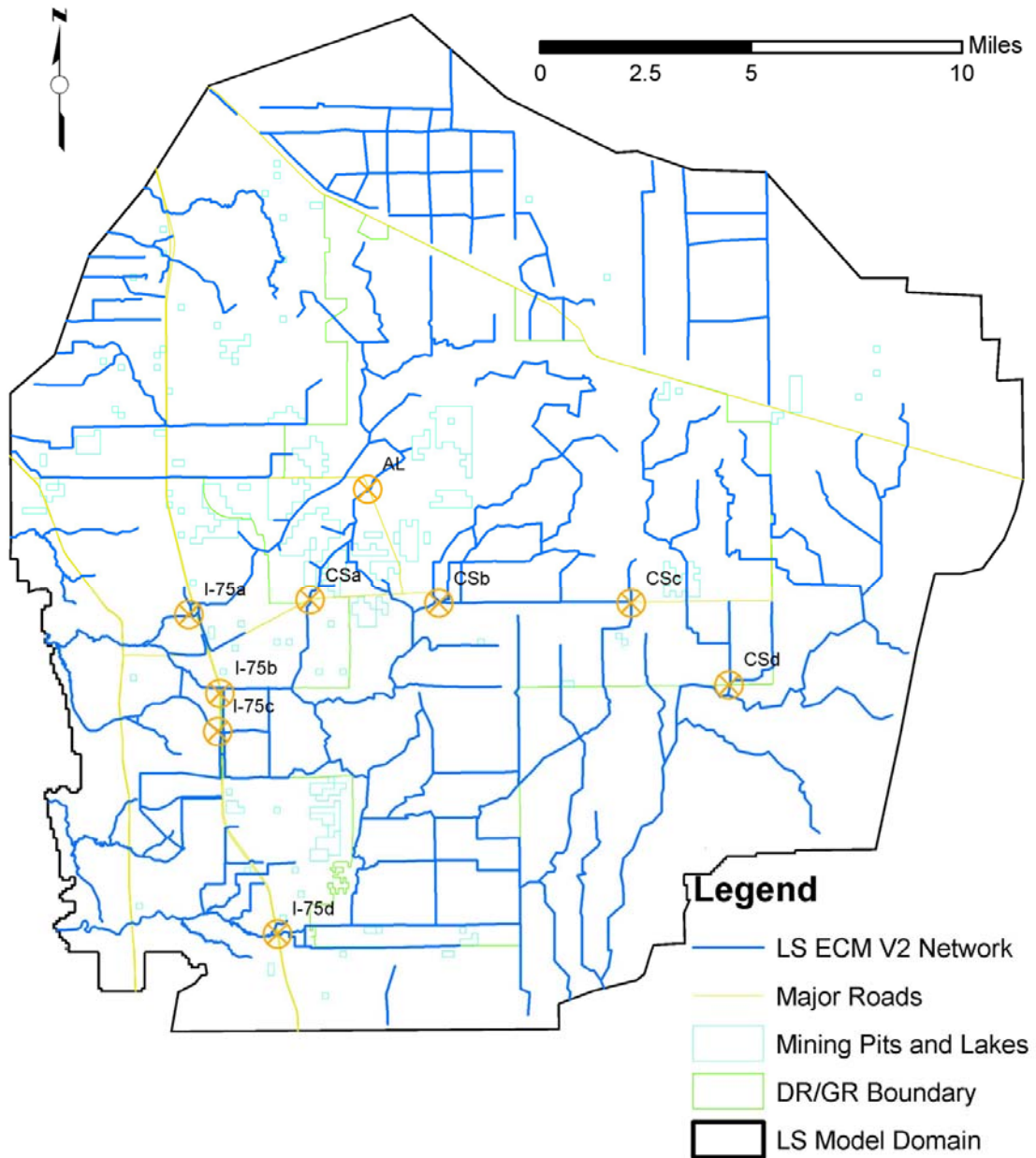
Figure 97. Selected flow comparison locations.

Conclusions

General Findings

The model results from the different land use scenarios indicate several concepts that may be useful during the planning process.

- Wetland areas converted from agricultural areas in the future condition alternatives help to increase the water table elevations during the dry season and to extend the period of time that those areas are wet (hydroperiod).

- The conversion of natural and agricultural areas to urban development slightly lowers the water table during the wet season due to the new urban drainage system. The water table in the new urban areas is usually higher at the end of the dry season compared to the existing conditions, which is likely related to a reduction in the ET losses.

- The water budget in all mines and lakes around the DR/GR Area suggests that the annual net rainfall (rainfall minus evaporation) is about zero on average. This is a consequence of the open water evaporation rate, which is commonly higher than the annual ET rate in pre-mined conditions. The model also predicts that the drainage system around some mines produces a positive net water outflow from the mines. As a result, the aquifers need to supply water to the mining pits (negative net groundwater recharge) in about the amount that is lost through the drainage system.

- This modeling has indicated, in general, that the annual averaged ET rates from the DR/GR Area would be higher with greater areal coverage of mining pits. The surface water outflow rate (runoff) from the DR/GR Area was lower in all the scenarios compared to the ECM, which is likely related to the greater mining pit coverage. These results are expected due to the higher ET losses and the lower runoff from mining pits and its effect on the surface water flow in neighboring areas.

- Mining pits cause a flattening in the water table that affects the pre-developed water table gradient. This often implies a decrease in the water table elevation on the up-gradient side of the pits and an increase on the down-gradient side. On the down gradient side, there may also be a decrease in some situations. The most pronounced flattening effect is seen towards the end of the dry season. This also has an effect on the hydroperiod by shortening the up-gradient hydroperiod and increasing (or sometimes also decreasing) the down-gradient hydroperiod. The flattening effect of mine development on the water table is larger in areas with steeper water table gradients, in larger mine pits, and in the case of a number of mining pits that are closer and therefore more hydrologically connected (i.e. via groundwater).

The expected qualitative effects of the different land use changes listed above are based on general model predictions generated by this study. In the future, uncertainty associated with these model results can be improved as more field data becomes available. In particular, as groundwater level data near the mining pits becomes available in the future, the model calibration will improve and the results around mining pits will be more representative of observed field data. Furthermore, the combined effect of the land use changes on water table elevation and hydroperiod may vary from one location to another and also from year to year. Thus, it is important to observe the results obtained from the different models at specific areas and times.

Recommendations for the Planning Process

The evaluation of the performance of the four future condition scenarios was based on several performance indicators extracted from the water table, hydroperiod and water budget sections. They are normalized in the interval (0, 1), where "0" represents the driest and "1" the wettest conditions from the four scenarios. The normalized indicators are shown in **Table 22**. The value of the indicator for the LS ECM was also estimated by using a mean difference of zero before normalizing. Water budget indicators for the LS ECM were not considered since they were far from the FCM range. In the case of the groundwater outflow from the ECM, it is not appropriate since it may be affected by the use of a different pumping rate in the FCMs with respect to the LS ECM. An average indicator (or score) for each scenario was computed by assuming a uniform weighting between them. Scenarios that are better for the water resources score higher average indicator values, and scenarios that are worse for the area water resources score lower average indicator values. From the average indicator, the FCM4 is the best scenario due to a variety of factors which includes a smaller number of mining pits compared to the acreage of restored land. These factors actually make FCM4 wetter on average than the LS ECM. Scenario FCM3 is the driest followed by FCM2.

Table 22. Normalized indicators to evaluate the scenario performance.

Section	Indicator (normalized)	ECM	FCM1	FCM2	FCM3	FCM4
Water Table Maps (Table 14)	Dry season water table level mean difference	-0.06	0.00	0.14	1.00	0.51
	Wet season water table level mean difference	0.82	0.26	0.37	0.00	1.00
Hydroperiod maps (Table 15)	Hydroperiod mean difference	0.91	0.54	0.35	0.00	1.00
	Water depth mean difference during hydroperiod	1.01	0.68	0.72	0.00	1.00
Water Budget (Table 17)	Annual averaged ET losses	---	0.80	0.32	0.00	1.00
	Annual averaged GW outflow	---	0.71	0.00	0.50	1.00
	Average indicator	0.67	0.50	0.32	0.25	0.92
Land use Changes	New mining pit area in DRGR (%)	0.00	4.90	7.42	9.35	6.35
	Restored area in DRGR (%)	0.00	3.11	5.14	6.28	7.81
	Restored minus new mining pit area in DRGR (%)	0.00	-1.79	-2.28	-3.07	1.46

The areal extent of the land use changes is also presented in Table 22 for the new mining pit and restored areas. In **Figure 98**, the average indicator is plotted as a function of the difference between newly restored minus new mining pit area. In this graph, the difference between the newly restored land and new mining pit areas comes from the new mining pit area and restored area rows in Table 22. As the percent of new mining pit area decreases, the resulting difference will be more and more positive. In the graph shown in Figure 98, this will correspond to the data point moving toward the right along the x-axis, which corresponds with an increasing average indicator value (or score) within the known data domain.

The almost perfect correlation in this graph may be helpful for the planning process. This correlation indicates that the restored (mitigated) area should be about equal to the new mining pit area in order to maintain, on average, the water table levels, hydroperiod and water budget in the entire DR/GR area. If the restored areal extent is greater than the new mining pit areal extent (which is the case in FCM4), this relationship suggests that scenario should be wetter than the ECM. The smaller the areal extent of the restored areas with respect to the areal extent of the new mining pit areas, the drier this relationship predicts the scenario to be.

The correlation shown in Figure 98 also enables the estimation of the performance of new scenarios based on one of the four FCMs. The impact of adding new restoration areas or mining pit areas can be quickly estimated from this graph, without a need to develop a new MIKE SHE model. However, these correlations are only valid within the range of values that have been simulated to date. Also, these are only valid for restoration areas or mining pit areas in the vicinity of those modeled to date. Therefore, the new mining pit areas and restored areas should be limited to the locations simulated in the four FCMs, and also in the range of areal extents considered.
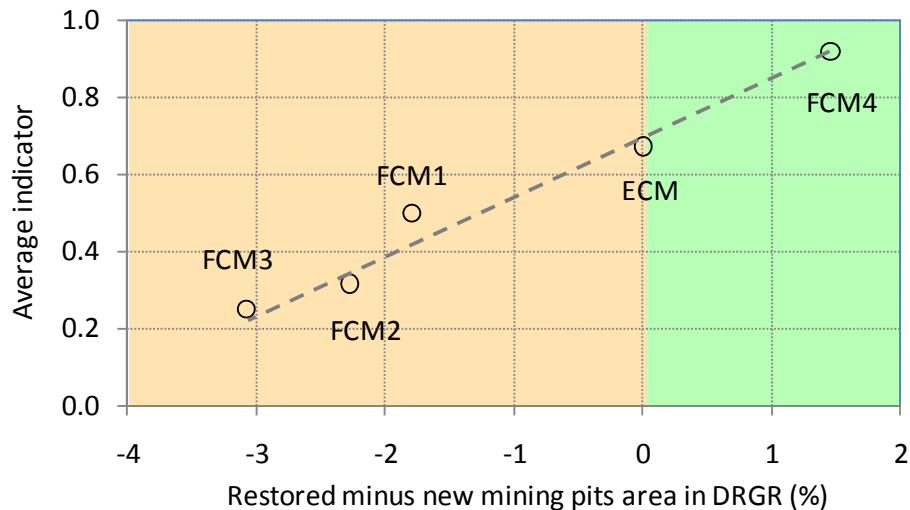
Figure 98. Correlation between the average indicator (score) of each scenario and the land use changes for the DR/GR Area.

Another recommendation for the planning process arising from this work is related to where to locate the new mining pits. In order to avoid mining impacts to water table levels and hydroperiods with respect to the current conditions, the flattening effect mentioned above should be minimized. There are two requirements to this, as demonstrated in the modeling results. One is to locate the mining pits in areas with flat topography (and flat water table, assumed to mimic the land surface). The second is to separate the mining pits by some critical distance in order to minimize their hydrologic connectivity. It is acknowledged that both of these requirements may not be achievable due to prior approvals granted for mine pits that are on sloping topography and/or are not adequately separated to minimize hydrologic connectivity. This study did not explore the critical gradient slope or critical spacing between mining pits, though.

Model Limitations and Recommended Future Work

The MIKE SHE model was developed based on the best available data at the time with a state of the art, fully integrated modeling package. However, as with any other model, there may be some opportunities for improvement.

1. **Revision of pumping data.** Pumping data is a source of uncertainty in all hydrologic models. The pumping rates and the pumping depths are not well known, in general. However, production rates can have a tremendous influence on groundwater heads. In this work, the time to collect that information was limited and its review is recommended in any future work.
2. **Revision of the hydro-geologic data.** The vertical extent of the geologic layers and lenses in the model were extracted from the SWFFS model, as indicated in the project

scope. The hydraulic conductivity, specific yield, and storage coefficient were also taken originally from the same model, and modified during the calibration process. All hydrogeologic parameters could be reviewed from the information available in DBHYDRO.

3. **Inclusion of the Hawthorn Aquifer in the model.** Because of the intensive pumping from the Hawthorn Aquifer and the poor prediction of the heads in the Sandstone Aquifer, the evaluation of the introduction of deeper layers in the model is recommended.

4. **Revision of the drainage system around mining pits.** The drainage system around some mining pits was introduced in the model based on available LIDAR data. However, the incoming and outgoing flows predicted by the model at mining pits could not be verified with observation data. Since those flows are important for the water budget and the surface flow reliability of the model, the review of the drainage system around mining pits is recommended as data become available.

Note that even with the proposed improvements listed above, the model has limitations related to the grid cell size (750 ft). For local studies that require a higher resolution, the construction of a new model with a smaller model domain area and grid cell size is recommended.

References

Abtew, W. 1996. *Evapotranspiration measurements and modeling for three wetland systems in South Florida*. Water Resources Bulletin **32** (3), 465-473.

Abtew, W., Huebner, R.S., and Ciuca V., 2005. *Hydrology of the South Florida Environment*. Chapter 5 in 2005 South Florida Environmental Report.

ADA Engineering, Inc., 2008. *South Lee County Watershed Plan Update Work Order C-4600000791 WO01-R1 90% Draft Deliverable 1C. Task 1 – Survey Cross Sections and Model Update.* 35 p.

Allen, R. G., L. S. Periera, D. Raes, and M. Smith. 1998. *Crop evapotranspiration: Guidelines for computing crop requirements*. Irrigation and Drainage Paper No. 56. Rome, Italy: FAO. Available at http://www.fao.org/docrep/X0490E/X0490E00.htm

CDM, 2006. *Southwest Florida Feasibility Study: Hydrologic Model Development – Big Cypress Basin*. Final Report, May 5, 2006.

DHI, 2008. *MIKE SHE User Manual, Volume II: Reference Guide*.

Dover, Kohl & Partners, July 2008. *Prospects for Southeast Lee County. Planning for the Density Reduction / Groundwater Resource Area (DR/GR)*.

Hammer, M. J. and Hammer, M.J. Jr., 2001. *Water and Wastewater Technology Upper Saddle River*: Prentice Hall Fourth Edition.

Jacobs, J., J. Mecikalski, S. Paech, 2008. *Satellite-based solar radiation, net radiation, and potential and reference evapotranspiration estimates over Florida*. Technical Report July 2008.

KLECE, 2008. *Ecological Memorandum of The Density Reduction/Ground-water Resource Area (DR/GR)*. Prepared for Dover, Kohl & Partners.

Lee, T. M., and Swancar, A., 1997. *Influence of evaporation, ground water, and uncertainty in the hydrologic budget of Lake Lucerne, a seepage lake in Polk County, Florida*. U.S. Geological Survey Water-Supply Paper 2439, 61 p.

May-Chu, T. F. and D. L. Freyberg, 2008. *Simulating a Lake as a High-Conductivity Variably Saturated Porous Medium*, Groundwater 46 (5), pp 688.

McLane Environmental LLC,, May 2007. *Review and Summary of Studies Containing Information Relating to the Density Reduction / Groundwater Resource (DRGR) Lands Southeastern Lee County, Florida.*

Missimer, T. M. and Martin, W. K., 2001. *The Hydrogeology of Lee County, Florida, in Geology and Hydrology of Lee County Florida* by T.M Missimer and T.M Scott (editors) Florida Geological Survey Special Publication No. 49.

Sacks, L. A., T. M. Lee, M. J. Radell, 1994. *Comparison of energy-budget evaporation losses from two morphometrically different Florida seepage lakes*. Journal of Hydrology **156**, 311-334.

Southwest Florida Feasibility Study Composite topography for SW Florida, 100-ft. (September 2005)

Swancar, A., T. M. Lee, and T. M. O'Hare, 2000. *Hydrogeologic Setting, Water Budget, and Preliminary Analysis of Groundwater Exchange at Lake Starr, a Seepage Lake in Polk County, Florida*. U.S. Geological Survey Water-Resources Investigations Report 00-4030.